

# Evaluation of Altering the Hydrogen Concentration for Mitigation of Primary Water Stress Corrosion Cracking





# **Evaluation of Altering the Hydrogen Concentration for Mitigation of Primary Water Stress Corrosion Cracking**

**1015017**

Final Report, December 2007

EPRI Project Managers  
C. Libby  
K. Fruzzetti

THIS DOCUMENT WAS PREPARED BY THE ORGANIZATION(S) NAMED BELOW AS AN ACCOUNT OF WORK SPONSORED OR COSPONSORED BY THE ELECTRIC POWER RESEARCH INSTITUTE, INC. (EPRI). NEITHER EPRI, ANY MEMBER OF EPRI, ANY COSPONSOR, THE ORGANIZATION(S) BELOW, NOR ANY PERSON ACTING ON BEHALF OF ANY OF THEM:

(A) MAKES ANY WARRANTY OR REPRESENTATION WHATSOEVER, EXPRESS OR IMPLIED, (I) WITH RESPECT TO THE USE OF ANY INFORMATION, APPARATUS, METHOD, PROCESS, OR SIMILAR ITEM DISCLOSED IN THIS DOCUMENT, INCLUDING MERCHANTABILITY AND FITNESS FOR A PARTICULAR PURPOSE, OR (II) THAT SUCH USE DOES NOT INFRINGE ON OR INTERFERE WITH PRIVATELY OWNED RIGHTS, INCLUDING ANY PARTY'S INTELLECTUAL PROPERTY, OR (III) THAT THIS DOCUMENT IS SUITABLE TO ANY PARTICULAR USER'S CIRCUMSTANCE; OR

(B) ASSUMES RESPONSIBILITY FOR ANY DAMAGES OR OTHER LIABILITY WHATSOEVER (INCLUDING ANY CONSEQUENTIAL DAMAGES, EVEN IF EPRI OR ANY EPRI REPRESENTATIVE HAS BEEN ADVISED OF THE POSSIBILITY OF SUCH DAMAGES) RESULTING FROM YOUR SELECTION OR USE OF THIS DOCUMENT OR ANY INFORMATION, APPARATUS, METHOD, PROCESS, OR SIMILAR ITEM DISCLOSED IN THIS DOCUMENT.

ORGANIZATION(S) THAT PREPARED THIS DOCUMENT

**Dominion Engineering, Inc.**

<p><b>NOTICE:</b> THIS REPORT CONTAINS PROPRIETARY INFORMATION THAT IS THE INTELLECTUAL PROPERTY OF EPRI. ACCORDINGLY, IT IS AVAILABLE ONLY UNDER LICENSE FROM EPRI AND MAY NOT BE REPRODUCED OR DISCLOSED, WHOLLY OR IN PART, BY ANY LICENSEE TO ANY OTHER PERSON OR ORGANIZATION.</p>
---

## **NOTE**

For further information about EPRI, call the EPRI Customer Assistance Center at 800.313.3774 or e-mail [askepri@epri.com](mailto:askepri@epri.com).

Electric Power Research Institute, EPRI, and TOGETHER...SHAPING THE FUTURE OF ELECTRICITY are registered service marks of the Electric Power Research Institute, Inc.

Copyright © 2007 Electric Power Research Institute, Inc. All rights reserved.

# CITATIONS

---

This report was prepared by

Dominion Engineering, Inc.  
11730 Plaza America Drive #310  
Reston, VA 20190

Principal Investigator  
C. Marks

This report describes research sponsored by the Electric Power Research Institute (EPRI).

The report is a corporate document that should be cited in the literature in the following manner:

*Evaluation of Altering the Hydrogen Concentration for Mitigation of Primary Water Stress Corrosion Cracking.* EPRI, Palo Alto, CA: 2007. 1015017.



# REPORT SUMMARY

---

This report evaluates altering the hydrogen concentration for mitigation of primary water stress corrosion cracking (PWSCC).

## Background

For several years, EPRI has investigated the possible benefits of changes to the hydrogen concentration in the reactor coolant system (RCS) with regard to ameliorating the occurrence of PWSCC of nickel-base alloys. This issue also has been under investigation by several other organizations that have made many of their findings available to EPRI. Since changes in hydrogen concentration might affect many other aspects of the plant, such as fuel performance and shutdown radiation fields, these other aspects also are being evaluated. A recent milestone in this effort was the Hydrogen Management Workshop conducted in January 2007, which was attended by representatives of EPRI's Materials Reliability Program (MRP), Fuel Reliability Program (FRP), and Chemistry Program as well as representatives of vendors, including nuclear steam supply system (NSSS) vendors, and consultants.

## Objectives

To provide an overall assessment of the entire EPRI program that addresses both benefits and possible drawbacks of operating current generation plants at alternative (high or low) hydrogen concentrations (for example, outside of the current EPRI Primary Water Chemistry Guidelines range of 25- to 50-cc/kg hydrogen).

## Approach

These four specific inputs to EPRI's overall hydrogen management program were identified:

- A Babcock and Wilcox Canada (BWC) report on the general feasibility of operating at lower or higher hydrogen concentrations than are already encompassed by industry experience
- An assessment by Westinghouse of the feasibility of operating Westinghouse and CE design plants with high or low hydrogen concentrations
- An FRP report addressing issues related to the compatibility of high hydrogen concentrations and fuel reliability
- An MRP assessment of the relationship between hydrogen concentration and PWSCC of nickel-base alloys and weld metals

These four sources, along with numerous other references, meetings, and communications with EPRI project managers and original researchers, were synthesized into the current document, providing a summary of the overall EPRI effort. Since mitigation of PWSCC is the motivation

for considering alternative hydrogen concentrations, only plants with PWSCC susceptible materials are considered.

## Results

In general, evaluations in this report suggest that operation at a moderately increased hydrogen concentration (for example, cycle average of 50 cc/kg with a limit of 55 or 60 cc/kg to accommodate reasonable fluctuations about this set point) will provide modest but significant mitigation of PWSCC without causing problems with other plant systems and components. Additional benefits of increasing hydrogen concentrations beyond this level will have diminishing returns, based on current understanding. Furthermore, the effect on other systems requires significantly more review to ensure adverse effects are unlikely. Operation below the current limit of 25 cc/kg is not recommended for the current generation of plants.

The recommended path regarding elevated hydrogen has two parallel groups of activities in the near term. These are as follows:

- Generic tests and analyses to address high-priority items, including the following:
  - Confirm that effects of hydrogen concentration on modern fuel cladding are negligible
  - Review the literature on the effect of hydrogen concentration on stainless steels
- Plant-specific analyses at candidate plants, including the following:
  - Review safety-analyses regarding explosive gas mixtures
  - Evaluate the effect of hydrogen concentration on the adequacy of plant programs to prevent/identify gas pocket formation in safety-related systems
  - Evaluate volume control tank (VCT) pressure limits related to reactor coolant pump (RCP) seals and verify that these limits do not impact the choice of hydrogen concentration within the limits under consideration (up to 80 cc/kg)
  - Evaluate pressure limits in other low-pressure systems and verify that these will not impact the choice of hydrogen concentration

Lower priority issues are identified for resolution on a generic or plant-specific basis.

## EPRI Perspective

This report provides a summary of numerous programs within EPRI to support utility efforts to manage materials aging issues. Specific evaluations investigating the effect of alternative hydrogen concentrations in the RCS on fuels and PWSCC mitigation can be found in EPRI reports 1013522 and 1015288, respectively. The conclusions indicate that chemical mitigation of PWSCC through optimization of hydrogen concentration in the primary coolant is a viable path for reducing costs associated with component degradation and inspection. These results and all further assessments will be considered for application to the next revision of the *PWR Primary Water Chemistry Guidelines*.

## Keywords

Pressurized water reactor  
Hydrogen optimization

Primary water stress corrosion cracking  
Alloy 600

Mitigation of cracking

## ACKNOWLEDGMENTS

---

The author wishes to acknowledge his debt to the many researchers, project managers, and utility personnel who have contributed to the understanding of the effects of hydrogen on primary water chemistry and reactor coolant system materials. In particular, the following people, who were participants in the Hydrogen Management Workshop, are thanked for their contributions:

AECL

Dave Guzonas  
Craig Stuart

Duke

Ken Johnson

EPRI

Al Ahluwalia  
Jeff Deshon  
Keith Fruzzetti  
Aylin Kucuk  
Cara Libby  
David Perkins

AREVA NP, Inc.

Ken Baity  
Paul Sherburne

Dominion Engineering, Inc.

Jeff Gorman

NWT Corporation

Steve Sawochka

Babcock and Wilcox

John Jevec  
Peter King  
Revi Kizhatil  
Jianguo Yu

Exelon

David Morey

Westinghouse

Richard Jacko  
Nicole Vitale

Finally, the author also wishes to thank Peter Andresen (GE-GRC) for his work in quantifying the benefits of elevated hydrogen and for his thorough answers to many questions regarding testing of PWSCC crack growth rates.



# CONTENTS

---

<b>1 INTRODUCTION AND OVERVIEW .....</b>	<b>1-1</b>
<b>2 CONCLUSIONS AND RECOMMENDATIONS .....</b>	<b>2-1</b>
2.1 Introduction .....	2-1
2.2 Summary of Expected PWSCC Mitigation .....	2-1
2.3 Areas of Concern .....	2-2
2.3.1 High Priority Issues.....	2-3
2.3.1.1 Fuel Performance and Integrity.....	2-4
2.3.1.2 Explosive Gas Mixtures .....	2-4
2.3.1.3 Radiolysis.....	2-4
2.3.1.4 Acceleration of PWSCC.....	2-5
2.3.1.5 Hydrogen Embrittlement .....	2-5
2.3.1.6 Safety-Related System Operability .....	2-5
2.3.1.7 RCP Seal Flow .....	2-5
2.3.1.8 Pressure Limits in Low Pressure Systems.....	2-5
2.3.2 Other Generic Issues.....	2-6
2.3.3 Plant-Specific Issues .....	2-7
2.4 Additional Research and Analysis.....	2-7
2.4.1 Issues Currently Being Investigated .....	2-7
2.4.1.1 Mixed Metal Oxide Solubilities .....	2-7
2.4.1.2 Interaction of Hydrogen and Zinc.....	2-8
2.4.1.3 Incorporation of Hydrogen Effects Into Comprehensive PWSCC Models .....	2-8
2.4.2 Issues Not Currently Under Investigation by EPRI.....	2-8
2.4.2.1 Relevance of the Nickel-Nickel Oxide Transition .....	2-8
2.4.2.2 Effects of Material Condition on Mitigation by Hydrogen Optimization .....	2-9
2.4.2.3 Hydrogen Effects on Other Materials.....	2-9
2.4.2.4 Compilation of Initiation and Propagation Data.....	2-9
2.4.2.5 Hydrogen Effects on Modern Fuel Cladding Alloys .....	2-10

2.4.2.6 Hydrogen Effects in Corrosion and Corrosion Product Transport and Deposition .....	2-10
2.4.2.7 Assessment of Effects of RCS Hydrogen Concentration on LTCP.....	2-11
2.5 Overall Conclusions and the Path Forward.....	2-11
<b>3 FUNDAMENTAL ELECTROCHEMISTRY .....</b>	<b>3-1</b>
3.1 Units of Measure .....	3-1
3.1.1 Ideal Gas Behavior of Hydrogen .....	3-1
3.1.2 Volume-Based Units (cc/kg) .....	3-2
3.1.3 Fugacity .....	3-3
3.2 Henry's Law.....	3-3
3.3 Hydrogen Diffusion in Metal .....	3-7
3.3.1 Basic Diffusion Model for Loss of Hydrogen Through SG Tubes .....	3-7
3.3.2 Permeability of Hydrogen in SG Tube Alloys .....	3-9
3.3.3 Sources of Variability and Uncertainty.....	3-11
3.4 Metal — Metal Oxide Transitions .....	3-11
3.4.1 Nickel.....	3-11
3.4.2 Other Metals .....	3-12
3.5 Nickel Solubility .....	3-13
3.6 Iron Solubility.....	3-15
3.7 Simultaneous Concentrations of Oxidizers and Reducers .....	3-18
3.8 Areas for Further Research.....	3-21
<b>4 EFFECTS OF HYDROGEN CONCENTRATION ON PWSCC.....</b>	<b>4-1</b>
4.1 Introduction .....	4-1
4.2 Fundamental Observation.....	4-1
4.2.1 PWSCC Initiation.....	4-3
4.2.1.1 Laboratory Data .....	4-3
4.2.1.2 Plant Data .....	4-5
4.2.1.3 Conclusions Regarding Initiation .....	4-5
4.2.2 PWSCC Propagation.....	4-5
4.3 Specific Parameter Values .....	4-9
4.4 Factors of Improvement for Specific Changes .....	4-12
4.5 Areas for Further Research.....	4-28
4.5.1 Relevance of the Nickel-Nickel Oxide Transition.....	4-28

4.5.2 Effect of Material Condition .....	4-28
4.5.3 Other Alloys .....	4-29
4.5.4 Interaction With Zinc.....	4-30
4.5.5 Incorporation Into More Comprehensive Models.....	4-30
4.5.6 Data Compilation .....	4-30
4.6 Conclusions.....	4-30
<b>5 EFFECTS OF ELEVATED DISSOLVED HYDROGEN ON FUEL INTEGRITY .....</b>	<b>5-1</b>
5.1 Introduction .....	5-1
5.2 Hydrogen Pickup and Hydriding.....	5-2
5.2.1 Full Power Operation.....	5-3
5.2.2 Startup .....	5-5
5.3 Recommendations of the Fuel Reliability Program .....	5-7
5.3.1 Autoclave Testing .....	5-8
5.3.2 Out-Reactor Loop Testing .....	5-8
5.3.3 In-Reactor Loop Testing .....	5-8
5.3.4 Plant Demonstrations .....	5-8
5.3.5 FRP Recommended Schedule .....	5-9
5.4 Possible Effects of Low Hydrogen Concentrations .....	5-10
5.5 Conclusions.....	5-10
<b>6 EFFECT OF HYDROGEN ON CORROSION, CORROSION PRODUCT TRANSPORT, AND CORROSION PRODUCT DEPOSITION.....</b>	<b>6-1</b>
6.1 Introduction .....	6-1
6.2 Effect of Hydrogen on Steam Generator General Corrosion.....	6-1
6.3 Effect of Hydrogen on Corrosion Product Release .....	6-2
6.4 Effect of Hydrogen on Corrosion Products in the Reactor Coolant.....	6-5
6.5 Effect of Hydrogen on Deposition of Corrosion Products on Fuel Cladding.....	6-6
6.5.1 Gravitational Deposition .....	6-6
6.5.2 Inertial Deposition.....	6-7
6.5.3 Diffusive Deposition.....	6-7
6.5.4 Boiling Deposition.....	6-8
6.5.5 Thermophoretic Deposition .....	6-8
6.5.6 Electrophoretic Deposition.....	6-8
6.5.7 Crystallization Deposition .....	6-10

6.5.8 Overall Effect of Hydrogen on Deposition .....	6-10
6.6 Conclusions.....	6-11
<b>7 EFFECT OF HYDROGEN ON LTCP .....</b>	<b>7-1</b>
7.1 Introduction .....	7-1
7.2 Summary of Laboratory Observations.....	7-2
7.2.1 Internal Hydrogen Embrittlement.....	7-2
7.2.1.1 General Mechanism.....	7-2
7.2.1.2 Operational Applicability .....	7-3
7.2.1.3 Test Data .....	7-3
7.2.2 Hydrogen Environment Embrittlement.....	7-5
7.2.2.1 General Mechanism.....	7-5
7.2.2.2 Operational Applicability .....	7-5
7.2.2.3 Test Data .....	7-6
7.3 Summary of on-Going and Future Work .....	7-10
7.4 Conclusions.....	7-10
7.4.1 Effect of Elevated Hydrogen on Internal Hydrogen Embrittlement .....	7-11
7.4.2 Effect of Elevated Hydrogen on Hydrogen Environment Embrittlement.....	7-11
7.4.3 Recommendations for Further Analysis and Testing.....	7-11
7.5 Slow Cracking in Air at Room Temperature .....	7-12
<b>8 HYDROGEN CONCENTRATIONS AND RADIOLYSIS.....</b>	<b>8-1</b>
8.1 Introduction .....	8-1
8.2 Full Power Operation.....	8-2
8.2.1 Bulk Equilibrium.....	8-2
8.2.2 Sensitivity to Model Inputs.....	8-4
8.2.3 Variations Along a Fuel Assembly.....	8-4
8.2.4 The Effects of Boiling.....	8-5
8.2.5 Metal Ion Effects.....	8-7
8.2.6 Surface Effects .....	8-7
8.2.7 Restricted Flow Areas .....	8-8
8.3 Reduced Power Operation .....	8-8
8.4 Conclusions.....	8-10

<b>9 OPERATIONAL AND SAFETY ISSUES.....</b>	<b>9-1</b>
9.1 Introduction .....	9-1
9.2 Priority Concerns.....	9-1
9.2.1 Formation of Explosive Gas Mixtures.....	9-1
9.2.2 Effects of Hydrogen Concentration on Fuel Performance and Integrity .....	9-2
9.2.3 Avoidance of Radiolysis .....	9-2
9.2.4 Acceleration of PWSCC .....	9-2
9.2.5 Hydrogen Embrittlement.....	9-3
9.2.6 Safety-Related Systems Inoperability.....	9-3
9.2.7 Effect on RCP Seals and Seal Performance .....	9-3
9.2.8 Pressure Limits in Low Pressure Systems .....	9-3
9.3 Additional Issues .....	9-4
9.3.1 Gas Pocket Formation.....	9-4
9.3.2 Secondary Side Conditions .....	9-4
9.3.3 Cavitation.....	9-5
9.3.4 Waste Gas Handling.....	9-5
9.3.5 Degassing During Shutdown .....	9-6
9.3.6 Tritium Generation.....	9-6
9.3.7 Corrosion Product Removal During Shutdown.....	9-6
9.3.8 Control During Water Transfers.....	9-6
9.3.9 Control During Hydrogen Transients .....	9-6
9.3.10 Flow Rates Returning to the VCT .....	9-7
9.3.11 Resin Degradation.....	9-7
9.3.12 Radiocobalt Behavior .....	9-7
9.3.13 Interaction With Elevated Lithium .....	9-7
9.3.14 Non-Technical Issues .....	9-7
9.4 Distribution Modeling.....	9-7
9.4.1 Accumulation in the Pressurizer .....	9-8
9.4.2 Required VCT Pressures.....	9-8
9.4.3 Effect of Hydrogen on Saturation Pressure (Voiding).....	9-10
9.5 Conclusions.....	9-14

<b>10 OPERATING EXPERIENCE .....</b>	<b>10-1</b>
10.1 Introduction.....	10-1
10.2 Normal Operating Experience Base.....	10-1
10.3 Early Off-Normal Operating Experience and Test Reactor Experience .....	10-3
10.3.1 Obrigheim .....	10-3
10.3.2 Belgian Reactor 3 .....	10-3
10.3.3 Turkey Point 4 .....	10-3
10.3.4 Unidentified CE Plants.....	10-3
10.3.5 Trojan and Beaver Valley Comparison.....	10-4
10.3.6 Saxton .....	10-4
10.3.7 Shippingport .....	10-5
10.3.8 Halden .....	10-5
10.3.9 Belleville .....	10-5
10.4 Specific Plant Events.....	10-5
10.4.1 RHR/ECCS Common Piping Gas Pockets.....	10-5
10.4.2 Charging Pump Gas Binding .....	10-6
10.4.3 Valve Failures.....	10-7
10.4.4 Voiding in the Letdown Ion Exchange Beds .....	10-7
10.5 Conclusions.....	10-8
 <b>11 ONGOING EPRI RESEARCH .....</b>	 <b>11-1</b>
11.1 Introduction.....	11-1
11.2 Fuel Reliability Program .....	11-1
11.3 Materials Reliability Program.....	11-1
11.3.1 Crack Growth Rate Testing .....	11-1
11.3.2 Low-Temperature Crack Propagation .....	11-2
11.4 Chemistry .....	11-2
11.4.1 Solubility of Nickel Metal in Reducing Environments.....	11-3
11.4.2 Nickel/Nickel Oxide Transition.....	11-3
11.4.3 Nickel Ferrite Solubility Estimation .....	11-4
11.4.4 Development of an EPRI Thermodynamic Model for Nickel/Nickel Oxide/ Nickel Ferrite Systems.....	11-5

<b>12 COMPLEMENTARY MITIGATION STRATEGIES.....</b>	<b>12-1</b>
12.1 Introduction.....	12-1
12.2 Zinc Injection .....	12-1
12.3 Mechanical Mitigation.....	12-2
12.4 Replacement .....	12-2
12.5 Conclusions.....	12-2
 <b>13 REFERENCES .....</b>	 <b>13-1</b>
 <b>A TABULATED FACTORS OF IMPROVEMENT .....</b>	 <b>A-1</b>



## LIST OF FIGURES

Figure 3-1 Henry's Law Constant as a Function of Temperature, Correlation Validation .....	3-5
Figure 3-2 High Temperature Henry's Law Constant as a Function of Temperature, Correlation Validation .....	3-6
Figure 3-3 Low Temperature Henry's Law Constant as a Function of Temperature, Correlation Validation .....	3-6
Figure 3-4 Curves of Constant Liquid Hydrogen Concentration in the Pressure- Temperature Plane .....	3-7
Figure 3-5 Permeability as a Function of Temperature .....	3-9
Figure 3-6 Nickel Metal – Nickel Oxide Transition: Hydrogen Concentration as a Function of Temperature .....	3-12
Figure 3-7 Nickel Solubility at 50 cc/kg Hydrogen [21] .....	3-13
Figure 3-8 Nickel Solubility at 25 cc/kg Hydrogen [21] .....	3-14
Figure 3-9 Iron Solubility From Nickel Ferrite as a Function of Hydrogen [22] .....	3-16
Figure 3-10 Iron Solubility From Nickel Ferrite as a Function of Hydrogen at 325°C [22] .....	3-17
Figure 3-11 Iron Solubility From Nickel Ferrite as a Function of Hydrogen at 285°C [22] .....	3-17
Figure 3-12 Oxygen and Hydrogen Concentrations, Callaway Startup After RF08 .....	3-19
Figure 3-13 ECP on SS304 in Environments Containing Oxygen, Hydrogen, or Both [25] .....	3-20
Figure 3-14 In-Pile ECP of Stainless Steel [24] .....	3-21
Figure 4-1 Crack Growth Rates of Corrosion Resistant Alloys Over a Wide Range of Potentials [27] .....	4-2
Figure 4-2 Effect of Hydrogen Concentration on Characteristic Life [6] .....	4-3
Figure 4-3 Effect of Hydrogen Concentration on Crack Initiation Time [34] .....	4-4
Figure 4-4 Crack Growth Rates: Alloy 600, Pure Water, 338°C [36] .....	4-6
Figure 4-5 Crack Growth Rates: Alloy 600, Pure Water, 338°C [37] .....	4-8
Figure 4-6 Crack Growth Rates: Alloy 600, 1200 ppm B, 2.2 ppm Li, 330°C [34] .....	4-9
Figure 4-7 Crack Growth Rates: Weld Metal EN82H, Pure Water, 338°C [4] .....	4-10
Figure 4-8 Crack Growth Rates: Alloy X-750 HTH, Pure Water, 360°C [36] .....	4-11
Figure 4-9 Crack Growth Rates: Alloy X-750 AH, Pure Water, 338°C [4] .....	4-12
Figure 4-10 Quadrants in the New versus Old Hydrogen Concentration Plane (343°C) .....	4-14
Figure 4-11 Quadrants in the New versus Old Hydrogen Concentration Plane (325°C) .....	4-15
Figure 4-12 Quadrants in the New versus Old Hydrogen Concentration Plane (290°C) .....	4-16
Figure 4-13 Factors of Improvement, EN82H, 343°C (log-log plot) .....	4-17
Figure 4-14 Factors of Improvement, EN82H, 343°C (linear plot) .....	4-18

Figure 4-15 Factors of Improvement, EN82H, 325°C (log-log plot) .....	4-19
Figure 4-16 Factors of Improvement, EN82H, 325°C (linear plot) .....	4-20
Figure 4-17 Factors of Improvement, EN82H, 290°C (log-log plot) .....	4-21
Figure 4-18 Factors of Improvement, EN82H, 290°C (linear plot) .....	4-22
Figure 4-19 Factors of Improvement versus 35 cc/kg, EN82H (log plot) .....	4-24
Figure 4-20 Factors of Improvement versus 35 cc/kg, EN82H (linear plot) .....	4-25
Figure 4-21 Factors of Improvement versus 35 cc/kg, Alloy 600 (log plot) .....	4-26
Figure 4-22 Factors of Improvement versus 35 cc/kg, Alloy 600 (linear plot) .....	4-27
Figure 4-23 Crack Growth Rates: Alloy 600, Pure Water, 338°C [37] .....	4-29
Figure 5-1 Hydrogen Pickup as a Function of Coolant Hydrogen, Zircaloy 2 and Zircaloy 4 [43] Autoclave Exposure for 14 days at 343°C .....	5-3
Figure 5-2 Hydrogen Pickup as a Function of Coolant Hydrogen, Zr <sub>2.5</sub> Nb [44] Autoclave Exposure at 300°C .....	5-4
Figure 5-3 Hydrogen Pickup as a Function of Coolant Hydrogen (Discharge Fuel) (Zircaloy-2, Zircaloy-4, ZIRLO™, and M5™) .....	5-5
Figure 5-4 Hydrogen Pickup as a Function of Coolant Hydrogen, Zr <sub>2.5</sub> Nb [44] Autoclave Exposure at 300°C, Mechanically Embedded Nickel .....	5-7
Figure 6-1 Effect of Hydrogen of General Corrosion of Alloy 600 [51] .....	6-2
Figure 6-2 Calculated Release Fractions, Plants With Alloy 600 Tubing [49] .....	6-3
Figure 6-3 Release Rate From Alloy 690TT at 300°C [53] .....	6-4
Figure 6-4 Release Rate From Alloy 690TT at 325°C [53] .....	6-4
Figure 6-5 Effect of Hydrogen Concentration on Corrosion Product Morphology [54] Alloy 600, 1000 hrs, 320°C, 500 ppm B, 2.0 ppm Li .....	6-5
Figure 6-6 Comparisons of the Zeta Potential of Stainless Steel and Nickel Ferrite, High B [55] .....	6-9
Figure 6-7 Comparisons of the Zeta Potential of Stainless Steel and Nickel Ferrite, Low B [55] .....	6-9
Figure 7-1 Effect of Hydrogen Pre-Charging on Fracture Toughness, X-750 HTH at 25°C [65] .....	7-4
Figure 7-2 Effect of Hydrogen Pre-Charging on Fracture Toughness, X-750 HTH at 93°C [68] .....	7-4
Figure 7-3 Effect of Hydrogen Pre-Charging on Fracture Toughness, X-750 BH at 93°C [68] .....	7-5
Figure 7-4 Effect of Hydrogen w/o Pre-Charging on Fracture Toughness, Weld Metal 182 at 54°C [63] .....	7-7
Figure 7-5 Effect of Hydrogen w/o Pre-Charging on Tearing Modulus, Weld Metal 182 at 54°C [63] .....	7-7
Figure 7-6 Effect of Hydrogen w/o Pre-Charging on Fracture Toughness, Weld Metal 152 at 54°C [63] .....	7-8
Figure 7-7 Effect of Hydrogen w/o Pre-Charging on Tearing Modulus, Weld Metal 152 at 54°C [63] .....	7-8

Figure 7-8 Effect of Hydrogen w/o Pre-Charging on Fracture Toughness, Weld Metal 52 at 54°C [63] .....	7-9
Figure 7-9 Effect of Hydrogen w/o Pre-Charging on Tearing Modulus, Weld Metal 52 at 54°C [63] .....	7-9
Figure 8-1 Effect of Hydrogen Concentration on Oxidizing Radiolysis Product Concentration 1800 ppm B, $\text{pH}_{300^\circ\text{C}} = 6.9$ [6] .....	8-3
Figure 8-2 Effect of Hydrogen Concentration on Oxidizing Radiolysis Product Concentration 0 ppm B, $\text{pH}_{300^\circ\text{C}} = 7.4$ [6] .....	8-3
Figure 8-3 Sensitivity of Radiolysis Model to Variations in Inputs [72] .....	8-4
Figure 8-4 Hydrogen Concentrations Along a High Power Fuel Assembly [74] .....	8-5
Figure 8-5 $\text{H}_2$ , $\text{H}_2\text{O}_2$ , and $\text{O}_2$ Concentrations Near an Expanding Steam Bubble 344°C, 40 cc/kg Bulk $\text{H}_2$ [72] .....	8-6
Figure 8-6 The Effect of Bulk $\text{H}_2$ on $\text{H}_2\text{O}_2$ Concentrations Near an Expanding Steam Bubble (344°C) [72] .....	8-7
Figure 8-7 The Effect of Power Reduction and Accompanying Temperature Change on Radiolysis [6] .....	8-9
Figure 8-8 The Effect of Temperature Reduction at Zero Power on Radiolysis [6] .....	8-9
Figure 8-9 The Effect of Temperature on Radiolysis at High and Low Hydrogen Concentrations [6] .....	8-10
Figure 9-1 Hydrogen Concentrations Resulting From VCT Hydrogen Partial Pressures .....	9-9
Figure 9-2 VCT Partial Pressures of Hydrogen Required for Various Hydrogen Concentrations .....	9-10
Figure 9-3 Partial Pressure of Hydrogen and Total Pressure as a Function of Temperature: 50 cc/kg .....	9-11
Figure 9-4 Partial Pressure of Hydrogen and Total Pressure as a Function of Temperature: 50 cc/kg Low Temperatures .....	9-12
Figure 9-5 Total Pressure Required to Prevent Voiding .....	9-13
Figure 10-1 Recent Trends in Coolant Hydrogen Concentrations [93] .....	10-2
Figure 10-2 Distribution of Current Coolant Hydrogen Concentrations [93] .....	10-2
Figure 10-3 Lines of Constant Hydrogen Concentration as a Function of Temperature .....	10-8
Figure A-1 Use of FOI Tables .....	A-1



## LIST OF TABLES

---

Table 2-1 High Priority Issues .....	2-3
Table 2-2 Other Generic Issues.....	2-6
Table 2-3 Plant-Specific Issues .....	2-7
Table 3-1 Implied Permeability From Westinghouse Plant Tests [15] .....	3-10
Table 4-1 SCC Parameter Values for Various Materials [27] .....	4-9
Table 4-2 Example Factors of Improvement.....	4-31
Table 5-1 FRP Recommended Research Program [42] .....	5-9
Table 7-1 Mills Classification System [69] .....	7-10
Table A-1 Factors of Improvement for EN82H (Part 1).....	A-3
Table A-2 Factors of Improvement for EN82H (Part 2).....	A-4
Table A-3 Factors of Improvement for Alloy 600 (Part 1) .....	A-5
Table A-4 Factors of Improvement for Alloy 600 (Part 2) .....	A-6
Table A-5 Factors of Improvement for Alloy X-750 HTH (Part 1) .....	A-7
Table A-6 Factors of Improvement for Alloy X-750 HTH (Part 2) .....	A-8
Table A-7 Factors of Improvement for Alloy X-750 AH (Part 1).....	A-9
Table A-8 Factors of Improvement for Alloy X-750 AH (Part 2).....	A-10



# 1

## INTRODUCTION AND OVERVIEW

---

For several years EPRI has had a program to investigate the possible benefits of changes to the hydrogen concentration in the reactor coolant system (RCS) with regard to ameliorating the occurrence of primary water stress corrosion cracking (PWSCC) of nickel-base alloys. This issue has also been under investigation by several other organizations that have made many of their findings available to EPRI. Since changes in hydrogen concentration might affect many other aspects of the plant, such as fuel performance and shutdown radiation fields, these other aspects are also being evaluated. A recent milestone in this effort was the Hydrogen Management Workshop conducted in January 2007, which was attended by representatives of EPRI's Materials Reliability Program (MRP), Fuel Reliability Program (FRP), and Chemistry Program as well as representatives of vendors, including NSSS vendors, and consultants. At this meeting, the following four specific inputs to EPRI's overall hydrogen management program were identified:

- A report by Babcock and Wilcox Canada (BWC) on the general feasibility of operating at lower or higher hydrogen concentrations than are already encompassed by industry experience
- An assessment by Westinghouse of the feasibility of operating Westinghouse and CE design plants with high or low hydrogen concentrations
- An FRP report addressing issues related to the compatibility of high hydrogen concentrations and fuel reliability
- An MRP assessment of the relationship between hydrogen concentration and PWSCC of nickel-base alloys and weld metals

The purpose of this report is to provide an overall assessment of the entire EPRI program that addresses both the benefits and possible drawbacks of operating current generation plants at alternative (high or low) hydrogen concentrations. Since mitigation of PWSCC is the motivation for considering alternative hydrogen concentrations, only plants with PWSCC susceptible materials are considered. The items listed above, feedback from the workshop, and several other sources were consulted in compiling this report.

Based on the assessment of the current state of knowledge regarding primary coolant hydrogen concentrations, a path forward is recommended for the near term and the long term.



# 2

## CONCLUSIONS AND RECOMMENDATIONS

---

### 2.1 Introduction

This report attempts to capture all issues related to operation at elevated or reduced hydrogen concentrations. The purpose of this chapter is to give a brief summary of the major conclusions reached in regard to each issue considered. Of principal interest is an assessment of the benefits likely to be gained from changes to higher or lower hydrogen concentrations, especially with regard to PWSCC. Section 2.2 summarizes the conclusions reached in Chapter 4, which discusses this issue at length.

Chapter 9 addresses safety and operational issues which have been identified for further consideration. These issues are summarized in Section 2.3, which references specific sections of Chapter 9 as well as other sections of the report where these issues are discussed.

In performing this review of prior and ongoing investigations, a number of areas have been identified in which additional research might prove useful. These are summarized in Section 2.4, with references to the sections of this report where particular issues are discussed in depth.

Finally, Section 2.5 provides overall conclusions based on the currently available information.

### 2.2 Summary of Expected PWSCC Mitigation

Experimental data on PWSCC crack propagation and initiation were reviewed to evaluate the effect of hydrogen concentration. An extensive body of data indicates that crack growth rates (CGRs) correlate to the difference between the actual hydrogen concentration and the hydrogen concentration at which nickel metal and nickel oxide are in equilibrium. The farther from the nickel-nickel oxide transition the lower the CGR, with reductions being roughly log-symmetric about the transition in terms of hydrogen concentration (normal-symmetric in terms of electrochemical potential). The effect on PWSCC initiation is less well characterized, but from the data available it is reasonable to conclude that the dependence of initiation rates on hydrogen concentration is similar to that of crack growth rates. The following conclusions are based on calculated factors of improvement (FOI) for crack growth rate:

- Calculated factors of improvement indicate modest mitigation of PWSCC (FOI~1.6 for EN82H) at high-temperature locations (325-343°C) for increases in hydrogen from a current typical operating concentrations (35-40 cc/kg) to about the upper limit of the current operating band (50 cc/kg). For a hydrogen increase to 80 cc/kg from 35 cc/kg, the FOI for EN82H is predicted to be 2.4 (325°C) or 3.2 (343°C). Therefore, the incremental benefit from 50 cc/kg to 80 cc/kg is an FOI of 1.5 (325°C) and 2 (343°C).

### *Conclusions and Recommendations*

- Calculated factors of improvement for Alloy 600 for the same increases in hydrogen concentration are typically smaller than for Alloy 182/82, except at very low temperatures (290°C) where it is similar.
- At lower temperatures, increases in hydrogen concentration above current typical operating concentrations of 35-40 cc/kg have a smaller mitigative effect on PWSCC.
- Reductions in hydrogen concentration that do not go below 5 cc/kg are predicted to increase PWSCC rates relative to current operating conditions at most RCS temperatures (290-325°C). At very high temperatures (343°C) there is modest mitigation with an FOI ~ 2.5 (for EN82H) at 5 cc/kg relative to 25 cc/kg and FOI ~ 1 (for all materials) at 5 cc/kg relative to 50 cc/kg.

In general, conclusions in the literature regarding the effect of hydrogen on PWSCC initiation are limited by one of the following factors:

- Conclusions regarding the existence of a maximum initiation rate at the transition between nickel and nickel oxide have been based on data that contain too much scatter to draw firm conclusions.
- Conclusions regarding a monotonic increase in initiation rates as hydrogen increases have generally been based on data sets that do not extend significantly above the hydrogen concentrations associated with the transition from nickel to nickel oxide.

Although initiation data do not clearly show as strong a correlation to hydrogen concentration as do PWSCC growth rate data, the results of most investigations are not inconsistent with trends observed in crack growth rates.

Chapter 4 is devoted to a review of the available data on the effect of hydrogen on PWSCC and provides additional details regarding the methods of calculating these FOI. Appendix A provides tabular values of FOIs for various materials at different temperatures for the changes in hydrogen concentration under consideration.

## **2.3 Areas of Concern**

Chapter 9 provides an extensive discussion of safety and operability concerns associated with changes in hydrogen concentration. Many issues are discussed at length in this report while others are mentioned only briefly. These issues have been divided into three categories:

- High priority issues that could potentially be “show stoppers” and prevent the application of changes in hydrogen concentrations
- Other, lower priority, issues that can probably be dispositioned on a generic basis
- Additional issues that are plant-specific

These are briefly summarized in the following sections which provide references to sections of this report where these issues are discussed more fully.

Note that this review has not been specifically cast in the context of a CFR50.59 safety evaluation. It is anticipated that the technical discussion in this report and additional research as recommended in Section 2.4 will provide a nearly complete basis for performing a safety evaluation. However, it is possible that additional issues may be identified in a safety evaluation.

### 2.3.1 High Priority Issues

High priority issues are discussed throughout this report, and a concise listing is given in Section 9.2. The sections below briefly summarize the issues and suggest a course of action to address the concerns. A summary of the high priority issues is provided in Table 2-1.

**Table 2-1**  
**High Priority Issues**

Issue	Section Discussed	Action to Be Considered
Fuel Performance and Integrity	Section 2.3.1.1 Chapter 5 Chapter 6 Chapter 8 Section 9.2.1 Section 9.4.2	Confirm limited impact on modern zirconium alloys through laboratory and reactor loop testing
Explosive Gas Mixtures	Section 2.3.1.2 Section 9.2.2	Plant-specific safety analyses
Radiolysis	Section 2.3.1.3 Chapter 8 Section 9.2.3	None
Acceleration of PWSCC	Section 2.3.1.4 Chapter 4 Section 9.2.4	Do not adopt a reduced hydrogen concentration program
Hydrogen Embrittlement	Section 2.3.1.5 Section 2.4.2.3 Section 9.2.5	Perform literature review of the effects of hydrogen on stainless steels Consider PWSCC testing of stainless steels
Safety-Related System Inoperability	Section 2.3.1.6 Section 9.2.6 Section 9.3.2 Section 9.4.3 Section 10.4.1	Evaluate current plant programs to prevent/detect gas pocket formation in safety-related systems
RCP Seal Flow	Section 2.3.1.7 Section 9.2.7 Section 9.4.2	Evaluate plant-specific VCT pressure limits related to RCP seals against desired operating pressures in proposed hydrogen program
Pressure Limits in Low Pressure Systems	Section 2.3.1.8 Section 9.2.8 Section 9.4.2	Evaluate plant-specific pressure limits in low pressure systems connected to the RCS/CVCS

### 2.3.1.1 Fuel Performance and Integrity

Several effects of altered hydrogen concentration have been postulated, including the following:

- Changes in hydriding and other corrosion phenomena in Zr-base fuel cladding (Chapter 5)
- Changes in corrosion product deposition rates on fuel cladding (Chapter 6)
- Changes in boiling rates (Section 9.4.3)
- Increases in oxidant concentrations (for decreases in hydrogen concentrations) (Chapter 8)

These issues are extensively discussed in the sections of this report noted in the above list and are not discussed further here. Although these issues pose significant concerns, they do not appear to prevent the safe application of elevated or decreased hydrogen concentrations based on current knowledge. However, additional work is needed to demonstrate this with acceptable confidence.

The most significant issue is the absence of data on the effect of hydrogen concentrations on hydriding of modern zirconium alloys. Research to address this issue is discussed in Section 2.4.2.5.

### 2.3.1.2 Explosive Gas Mixtures

A major consideration in the use of hydrogen is the potential for the formation of explosive gas mixtures in vapor phase regions (for example, in the pressurizer or the volume control tank). This is discussed in Section 9.2.1.

It is likely that this issue will need to be addressed on a plant specific basis before implementation of an elevated hydrogen program. Generic evaluations which could be used to support such an effort are already available.

### 2.3.1.3 Radiolysis

Radiolysis is discussed in Chapter 8. At the concentrations under consideration (5 – 80 cc/kg) there appears to be no significant risk of increased radiolysis as long as the target hydrogen concentration is maintained. This conclusion considers several secondary factors including temperature, boiling, variations along the fuel assembly, and input uncertainty. Analysis of the ability to control concentrations at 5 cc/kg (i.e., verification that concentrations will not go significantly below 5 cc/kg) is very plant specific, although generally use of low concentrations of hydrogen is considered to increase risks associated with operational events, such as loss of letdown flow or addition of aerated makeup water, that could cause further reductions in hydrogen and inadvertent entry into undesirable oxidizing conditions.

#### 2.3.1.4 Acceleration of PWSCC

As discussed in Section 4.4, some specific changes in hydrogen concentration could result in accelerated PWSCC. For lower temperature locations (325°C to 290°C) all changes to hydrogen concentrations to the range of 5 – 25 cc/kg are expected to accelerate PWSCC of nickel-base alloys and weld metals (regardless of the specific material).

Since numerous susceptible components are at temperatures in this range, lowering coolant hydrogen concentrations would increase the risk of pressure boundary degradation. For this reason, it is considered highly unlikely that decreased hydrogen concentrations can be considered desirable (or even feasible).

#### 2.3.1.5 Hydrogen Embrittlement

As indicated in Section 9.2.5, the effects of the increases in hydrogen concentration under consideration on stainless steels and other non-nickel-base, non-zirconium-base RCS materials have not been fully investigated. Suggestions for addressing this issue are discussed in Section 2.4.2.3. (Low temperature crack propagation, an embrittlement issue, of nickel alloys is discussed in Chapter 7, while effects on zirconium alloys are discussed in Chapter 5.)

#### 2.3.1.6 Safety-Related System Operability

Increases in hydrogen concentration could lead to more rapid development of gas pockets in low pressure systems connected to the CVCS. These include some safety-related systems as discussed in Section 9.2.6. Additional discussion of gas pocket formation is located in Sections 9.3.1 and 9.4.3. At current hydrogen concentrations, some inoperability events have occurred, as discussed in Section 10.4.1. To address this issue, plant-specific evaluations of current programs to prevent voiding in safety-related systems should be made.

#### 2.3.1.7 RCP Seal Flow

At some plants, the allowable pressure in the VCT is limited to a relatively narrow range (e.g., 15 – 65 psig) due to RCP seal considerations. This issue is discussed in Section 9.2.7. Each plant considering a change in hydrogen concentration would need to assess the plant-specific range of allowable VCT pressures. However, the limits given above (15 – 65 psig) would not prevent operation in the range under consideration (5 – 80 cc/kg) as discussed in Section 9.4.2.

#### 2.3.1.8 Pressure Limits in Low Pressure Systems

As discussed in Section 9.2.8, pressure limits in low pressure systems (e.g., the CVCS) would need to be assessed against possible increases in hydrogen partial pressure to assure that structural limits were not challenged. However, the concentrations under consideration (up to 80 cc/kg) are not likely to challenge these limits, since the equilibrium pressure for 80 cc/kg at VCT conditions is less than a typical VCT high pressure alarm setpoint (60 psig) as discussed in Section 9.4.2.

## Conclusions and Recommendations

**2.3.2 Other Generic Issues**

Additional issues that should be addressed on a generic basis are listed in Table 2-2, which also lists the sections of this report where each topic is discussed.

**Table 2-2**  
**Other Generic Issues**

<b>Issue</b>	<b>Section Discussed</b>	<b>Action to Be Considered</b>
Effect on secondary systems	Section 9.3.3	Evaluate effect on feedwater heater efficiency Evaluate flammability of condenser offgases
Cavitation	Section 9.3.4	None
Degassing during Shutdown	Chapter 7 Section 9.3.6 Section 10.4.4	Incorporate effects on degassing times or peroxide requirements into hydrogen optimization program Develop degassing recommendations for planned and unplanned outages based on LTCP and pressurizer inventory concerns
Tritium Generation	Section 9.3.7	None
Corrosion Product Removal During Shutdown	Section 9.3.8	None
Control of Hydrogen during Water Transfers	Section 9.3.9 Section 10.3	Do not adopt a reduced hydrogen concentration program
Control of Hydrogen during Hydrogen Transients	Section 9.3.10	Do not adopt a reduced hydrogen concentration program
Resin Degradation	Section 9.3.12	Evaluate the effect of hydrogen concentration on resin degradation Evaluate the effect of hydrogen concentration on the effect of a resin ingress
Radiocobalt Behavior	Section 2.4.1.1 Section 3.4.2 Section 9.3.13	Consider a research program into solubility of mixed metal oxides
Interaction with Elevated Lithium	Section 9.3.14	None

### 2.3.3 Plant-Specific Issues

Additional issues that should be addressed on a plant-specific basis are listed in Table 2-3, which also lists the sections of this report where each topic is discussed.

**Table 2-3**  
**Plant-Specific Issues**

Issue	Section Discussed	Action to Be Considered
Gas Pocket Formation	Section 9.3.2 Section 10.4 Section 9.4.3	Review current plant-specific programs to prevent/detect gas pocket formation
Waste Gas Handling	Section 9.3.5	Evaluate effect of increased hydrogen concentration on waste gas handling systems
Flow Rates Returning to the VCT	Section 9.3.11	Evaluate flow rates returning to the VCT considering target VCT pressure under proposed hydrogen program

## 2.4 Additional Research and Analysis

The review of the current understanding of the effects of hydrogen concentration on PWSCC and plant operations has identified several issues which represent knowledge gaps. The discussion below is divided into issues which are under active investigation and issues which are not currently being addressed. Each gap is summarized, possible investigations are discussed, and the usefulness of potential new information is assessed.

### 2.4.1 Issues Currently Being Investigated

#### 2.4.1.1 Mixed Metal Oxide Solubilities

EPRI Chemistry, through the MULTEQ database committee, and the FRP are both pursuing programs to investigate the solubilities of metals from mixed oxides (e.g., nickel ferrite) as functions of temperature, pH, and hydrogen concentration. Currently, the understanding of such solubilities is somewhat limited, especially for minor oxide constituents such as cobalt and zinc. This issue is discussed in Sections 2.4, 3.5, and 3.6.

Possible routes to filling this knowledge gap include detailed solubility tests in refreshed autoclaves or flow through systems similar to those that have been performed for single metal oxides.

### *Conclusions and Recommendations*

The solubility of nickel, the chief corrosion product in PWRs that have nickel-base alloy steam generators (all currently operating U.S. PWRs), is thought to be highly dependent on the solid phase from which it is dissolving. Recent work suggests that the effects of hydrogen concentration on nickel solubility from mixed metal oxides complicate the assessment of hydrogen optimization with respect to corrosion product solubility. Similar issues may affect the solubility of zinc from mixed metal oxides and could thus affect the efficacy of zinc injection for dose reduction and PWSCC mitigation (see Section 2.4.1.2).

#### **2.4.1.2 Interaction of Hydrogen and Zinc**

As discussed in Section 12.2, zinc injection is being used for mitigation of PWSCC. The impact of increasing hydrogen on the effect of zinc on PWSCC mitigation is currently under investigation. As discussed in Section 12.2, positive, neutral, and negative interactions between increased hydrogen and zinc addition can be postulated.

In addition to on-going crack growth rate measurements, investigation of the fundamental interaction between zinc, hydrogen, and other metals could be investigated as discussed in Section 2.4.1.1.

Quantification of the interaction of hydrogen and zinc will allow utilities to evaluate the relative merits of these two mitigation strategies taken alone or together.

#### **2.4.1.3 Incorporation of Hydrogen Effects Into Comprehensive PWSCC Models**

Ongoing evaluations by the MRP have attempted to incorporate hydrogen effects into a more comprehensive model of PWSCC crack growth rates which includes material properties and heat-to-heat variability. This work is discussed in Section 4.5.5.

Prediction of PWSCC in plants is necessary for utilities to evaluate different mitigation strategies, disposition slow growing flaws, and plan repair activities. However, previous work indicates that developing a fully reliable model will be difficult and may not be practical.

### **2.4.2 Issues Not Currently Under Investigation by EPRI**

#### **2.4.2.1 Relevance of the Nickel-Nickel Oxide Transition**

Although several theories exist as to why PWSCC rates are greatest at ECPs at or near the nickel-nickel oxide transition, none has been identified as a strong candidate. This issue is discussed in Section 4.5.1.

Validation of a particular theory is likely to require very detailed microscopic investigation of the films, crack tips, and adjacent microstructures formed under different concentrations of hydrogen.

Increased understanding of the mechanism by which hydrogen concentration affects PWSCC would allow more confident extrapolation to other materials and conditions. It would also provide some insight into the interaction (or lack of interaction) between hydrogen and other mitigation strategies (e.g., zinc injection).

Additional information on this issue would also help to explain why more recent measurements of the Ni/NiO transition differ so markedly from previously widely accepted measurements.

#### 2.4.2.2 Effects of Material Condition on Mitigation by Hydrogen Optimization

Data currently available indicate that there is a significant interaction between material condition (e.g., the extent of cold work) and the effect of hydrogen on PWSCC. This is discussed in Section 4.5.2. However, this effect has not been extensively characterized. Specifically, the possible interactions between hydrogen concentration and mechanical mitigation strategies (e.g., peening) have not been addressed.

In general, bulk material conditions can be investigated using the techniques currently employed. For example, differences between X-750 HTH and X-750 AH have already been studied. However, it is not immediately evident how testing could be performed to address the issue of surface cold work since most crack growth rate tests require a macroscopic pre-crack that would penetrate below the cold worked layer.

More information on the relationship among cold work, hydrogen, and PWSCC would be useful in assessing the usefulness of multiple mitigation techniques, such as the combination of peening and optimized hydrogen concentrations.

#### 2.4.2.3 Hydrogen Effects on Other Materials

As discussed in Section 9.2.5 hydrogen embrittlement of other structural materials (stainless steels) is a concern. Although some consideration has been given to the effect of hydrogen concentrations on cracking of these materials this issue is not completely addressed by the currently available data.

This issue could be resolved by additional laboratory testing of representative materials. However, it is also possible that a more thorough review of the literature could provide enough data to address this issue.

Increased confidence that the effect of elevated hydrogen concentrations on other system materials (i.e., not zirconium or nickel alloys) is not detrimental is prudent before implementation of a significant increase in the hydrogen concentration.

#### 2.4.2.4 Compilation of Initiation and Propagation Data

Chapter 4 is a reasonable attempt to identify, compile, and analyze PWSCC initiation and propagation data on the effect of hydrogen. A comprehensive review of all possible data was beyond the scope of this report. Although the compilation of data considered was significant, a

### *Conclusions and Recommendations*

more robust effort is likely to be necessary to develop the statistical confidence in the effects of hydrogen necessary to make significant investments and to obtain the benefits of inspection relief.

A thorough evaluation of the literature data would start from the assumption that the crack growth rate model discussed in Section 4.2.2 of Chapter 4 is correct and then determine the values of the key parameters from reported crack growth rates. Comparison of results from single sources as well as comparisons between laboratories would then be used to determine the range of likely values for the parameters. Similar methods could be employed with crack initiation data, although previous work in this area suggests that such an attempt may not be useful.

An understanding of the degree of uncertainty in the factors of improvement for various changes in hydrogen concentration would allow utilities to realistically assess the expected benefits from such changes. This detailed understanding would also likely be necessary for obtaining inspection relief or dispositions based on mitigation through hydrogen optimization.

#### **2.4.2.5 Hydrogen Effects on Modern Fuel Cladding Alloys**

As discussed in Chapter 5 nearly all of the data relating to the effects of hydrogen on zirconium alloys are based on alloys that are currently in limited use in the United States. Modern alloys, M5<sup>TM</sup> and ZIRLO<sup>TM</sup>, have either not been subjected to similar testing or the results of such testing are not publicly available.

Extensive testing of historic alloys indicates very little effect of environmental hydrogen concentrations on zirconium alloy hydriding. It is likely that confirmatory testing at very high hydrogen concentrations could readily demonstrate that the same is true for modern alloys.

Fuel warranty considerations are considered to be a likely factor in delaying the implementation of changes in hydrogen concentration. Satisfactory evidence from appropriate tests that hydriding rates were not increased by higher hydrogen would satisfy many of these concerns.

#### **2.4.2.6 Hydrogen Effects in Corrosion and Corrosion Product Transport and Deposition**

Chapter 6 discusses the effects of hydrogen concentration on the deposition of corrosion products on fuel surfaces (including preliminary processes such as general corrosion, corrosion product release, and corrosion product transport). In general, the effect of hydrogen on these processes is not understood.

Efforts to develop a better understanding of corrosion product deposition are ongoing. No new avenues of investigation are immediately apparent.

Based on the high uncertainty with respect to corrosion, corrosion product transport, and deposition due to numerous other factors in addition to hydrogen, the effects of hydrogen concentration changes are not likely to be discernable in plants. To be able to reliably detect the effects of hydrogen, it will first be necessary to adequately understand and account for the effects of other factors that likely have a much larger effect.

#### 2.4.2.7 Assessment of Effects of RCS Hydrogen Concentration on LTCP

Low temperature crack propagation (LTCP) is discussed in Chapter 7. Two interrelated phenomena have been observed in laboratory testing: internal hydrogen embrittlement (IHE) and hydrogen environment embrittlement (HEE). In IHE, hydrogen dissolved in the metal (either from diffusion at high temperatures or from corrosion) results in a reduction of fracture toughness. In HEE, the same effect is caused by hydrogen from the external environment. In a plant, HEE would be accelerated by hydrogen in the coolant during cooldown. IHE would be accelerated by hydrogen in the coolant during operation.

LTCP testing on samples charged with hydrogen at high temperatures and then cooled would indicate whether IHE is significant.

If LTCP is found to be relevant to PWR conditions, the extent to which materials are susceptible to IHE versus HEE could provide input regarding shutdown management of hydrogen concentrations. It is likely that HEE could be avoided by reducing hydrogen concentrations just prior to cooldown. However, IHE would require hydrogen concentration reductions at high temperature some time prior to temperature reduction, when hydrogen can diffuse out of susceptible components. IHE might also pose risks at unplanned outages if immediate temperature reductions are required.

## 2.5 Overall Conclusions and the Path Forward

In general, the evaluations in this report suggest that operation at a moderately increased hydrogen concentration (e.g., cycle average of 50 cc/kg with a limit of 55 or 60 cc/kg to accommodate reasonable fluctuations about this set point) will provide modest but significant mitigation of PWSCC without causing problems with other plant systems and components. Additional benefits of increasing hydrogen concentrations beyond this level will have diminishing returns, based on the current understanding. Furthermore, the effect on other systems would require significantly more review to ensure confidence that adverse effects are unlikely. Operation at hydrogen concentrations below the current limit of 25 cc/kg is not recommended for the current generation of plants.

The recommended path forward regarding elevated hydrogen has two parallel groups of activities in the near term. These are as follows:

- Generic tests and analyses to address high priority items including the following:
  - Confirm that effects of hydrogen concentration on modern fuel cladding are negligible
  - Review the literature on the effect of hydrogen concentration on stainless steels

*Conclusions and Recommendations*

- Plant-specific analyses at candidate plants including the following:
  - Review safety-analyses regarding explosive gas mixtures
  - Evaluate the effect of hydrogen concentration on the adequacy of plant programs to prevent/identify gas pocket formation in safety-related systems
  - Evaluate VCT pressure limits related to RCP seals and verify that these limits do not impact the choice of hydrogen concentration within the limits under consideration (up to 80 cc/kg)
  - Evaluate pressure limits in other low pressure systems and verify that these limits do not impact the choice of hydrogen concentration within the limits under consideration (up to 80 cc/kg)

Upon completion of these tasks, the issues listed in Table 2-2 and Table 2-3 should be addressed on a generic and plant-specific basis, respectively.

# 3

## FUNDAMENTAL ELECTROCHEMISTRY

---

### 3.1 Units of Measure

Several different units of hydrogen concentration are used in this report and in the cited literature. This section discusses the bases for various conversions. Many of the conversions used are based on an assumption of ideal gas behavior. Therefore, Section 3.1.1 begins with a discussion of the likely deviations from ideal gas behavior at relevant conditions. Section 3.1.2 discusses conversion from mass based units (ppm) to volume based units (cc/kg). Section 3.1.3 discusses the use of fugacity as a measurement of hydrogen concentration.

#### 3.1.1 Ideal Gas Behavior of Hydrogen

Ideal gases are those that follow the ideal gas law, which is as follows:

$$PV = nRT \quad \text{Eq. 3-1}$$

where  $P$  is the pressure (absolute, not gauge),  $V$  is the volume of the gas,  $n$  is the number of moles ( $6.022137 \times 10^{23}$  molecules),  $T$  is the absolute temperature (e.g., on the Kelvin scale), and  $R$  is the ideal gas constant. Values for  $R$  in typical unit systems are as follows:[1]

$$\begin{aligned} R &= 8.3143 \frac{\text{kJ}}{\text{kmol} \cdot \text{K}} \\ &= 82.06 \frac{\text{atm} \cdot \text{cc}}{\text{mol} \cdot \text{K}} \\ &= 1.986 \frac{\text{Btu}}{\text{lbmol} \cdot ^\circ\text{R}} \end{aligned} \quad \text{Eq. 3-2}$$

(Note that many calculations in this report were performed using spreadsheets in which non-significant figures were retained throughout the calculation and final results were rounded to the appropriate significant figure.)

Deviations from the ideal gas law are quantified by the compressibility factor,  $z$ , which is defined as follows:

$$z = \frac{PV}{nRT} \quad \text{Eq. 3-3}$$

The law of corresponding states indicates that the compressibility factor is a function of the reduced temperature and pressure (i.e., the ratio of the temperature and pressure to the temperature and pressure at the critical point) independent of the specific gas. Deviations from ideality are largest at high pressures and low temperatures. Therefore, a bound on the ideal behavior of hydrogen may be obtained using a lower bound on temperature (25°C or 298K) and an upper bound on pressure (7 atm). Using the critical properties for hydrogen [1] the bounds on reduced pressure and temperature are as follows:

$$P_R = \frac{P}{P_C} = \frac{7 \text{ atm}}{12.8 \text{ atm}} = 0.55$$

Eq. 3-4

$$T_R = \frac{T}{T_C} = \frac{298 \text{ K}}{33.6 \text{ K}} = 8.9$$

These values give a compressibility factor of approximately 1.007 [1], which is sufficiently close to unity to justify the assumption that hydrogen behaves ideally.

### 3.1.2 Volume-Based Units (cc/kg)

Typical liquid concentrations are reported in cc/kg (standard cubic centimeters per kilogram). These units can be easily converted to alternate concentration measurements using the ideal gas law and the definition of the standard state (1 atm, 0°C) to convert from units of volume to units of mass. For example, Equation 3-5 demonstrates the conversion of cc/kg to ppb (with the approximation that most of the mass is due to water).

$$\begin{aligned} 1 \frac{\text{cc}}{\text{kg}} &= 1 \frac{\text{cc}}{\text{kg}} \frac{P}{RT} MW = 1 \frac{\text{cc}}{\text{kg}} \frac{1 \text{ atm}}{\left(82.06 \frac{\text{atm} \cdot \text{cc}}{\text{mol} \cdot \text{K}}\right) (273.15 \text{ K})} 2 \frac{\text{g}}{\text{mol}} \\ &= 8.923 \times 10^{-5} \frac{\text{g}}{\text{kg}} = 0.08923 \text{ ppm} \end{aligned}$$

Eq. 3-5

$$1 \text{ ppm} = 1 \text{ ppm} \frac{1 \frac{\text{cc}}{\text{kg}}}{0.08923 \text{ ppm}} = 11.21 \frac{\text{cc}}{\text{kg}}$$

### 3.1.3 Fugacity

For an ideal gas, the molar free energy change of an isothermal process is given by the following equation [2]:

$$\Delta \bar{G}_T = RT \ln \frac{P_2}{P_1} \quad \text{Eq. 3-6}$$

The fugacity is defined as the property which makes Equation 3-6 true for real gases, as indicated in Equation 3-7.

$$\Delta \bar{G}_T = RT \ln \frac{f_2}{f_1} \quad \text{Eq. 3-7}$$

Any measurement which uses extent of reaction to quantify concentration is a measurement of the fugacity. In some systems the fugacity may differ from a mechanically based measurement of pressure. Electrochemical based measurements of hydrogen concentration are actually measurements of fugacity, since they are measurements of the free energy (directly related to the electrical potential through Faraday's Law).

In the conditions under consideration, hydrogen is not expected to significantly react with system materials nor is its behavior expected to deviate from ideal gas behavior (see Section 3.1.1). Therefore, no significant differences are expected to exist between pressure (mass based concentration) and fugacity (chemical reactivity based concentration). Although some references report hydrogen fugacity, only pressure is used in this report and the two measures are assumed to be identical.

## 3.2 Henry's Law

It has long been observed that the concentration of a dissolved gas in aqueous solutions is linearly related to the partial pressure of the gas in the vapor phase in equilibrium with the solution as long as the following criteria are satisfied:

- The conditions are reasonably far from the critical point (374°C, 221 bar for water).
- The gas concentration in the liquid phase is low (<10,000 cc/kg) so that the activity coefficient approaches unity (i.e., the partial molar free energy is proportional to the logarithm of the concentration).
- There is a single dissolved gas species (for example, no formation of  $\text{H}^+$  and  $\text{H}_2$ ).
- The vapor phase is an ideal mixture (i.e., fugacities approach partial pressures).

Fundamental Electrochemistry

Under PWR primary coolant conditions, these criteria are satisfied and Henry's Law applies. A typical statement of Henry's Law is given in the following equation:

$$p_{hydrogen} = Hx_{hydrogen} \quad \text{Eq. 3-8}$$

where  $p_{hydrogen}$  is the partial pressure of hydrogen in the vapor phase,  $x_{hydrogen}$  is the mole fraction of hydrogen in the liquid phase, and  $H$  is the Henry's Law constant.

For consistency, a single correlation of the Henry's Law constant for hydrogen is used for all calculations in this report. The correlation used is that developed by Himmelblau [3] which was based on data collected at temperatures from 66°C to 332°C. (Additional data for other gases at temperatures from 0°C to 343°C were used in the development of trending, allowing reasonable extrapolation from the more limited temperature range of the hydrogen data.)

The correlation used to determine Henry's Law constants at various temperatures is as follows:

$$A(\log \bar{H})^2 + B\left(\frac{1}{\bar{T}}\right)^2 + C(\log \bar{H})\frac{1}{\bar{T}} + D \log \bar{H} + E\frac{1}{\bar{T}} - 1 = 0 \quad \text{Eq. 3-9}$$

where

$$\bar{H} = \frac{H}{10,000} \quad \text{Eq. 3-10}$$

and

$$\bar{T} = \frac{T}{1000} \quad \text{Eq. 3-11}$$

The temperature,  $T$ , is expressed in Kelvin and Henry's Law constant,  $H$ , is given in atm/mole fraction.

The fitting parameters in Equation 3-9 are given as follows:

$$\begin{aligned} A &= -0.1233 \\ B &= -0.1366 \\ C &= 0.02155 \\ D &= -0.2369 \\ E &= 0.8249 \end{aligned} \quad \text{Eq. 3-12}$$

The values for Henry's Law constant given by Equation 3-9 were compared to more recent measurements [4, 5], to the values given in the Primary Water Chemistry Guidelines [6], and a more recent correlation [7] to verify both the correlation given in Reference [3] and the methodology used to solve Equation 3-9. Figure 3-1 shows this comparison over the range of temperatures considered. Figure 3-2 shows a comparison of the correlation results to the high temperature data while Figure 3-3 shows a comparison to the low temperature data. In general, the Himmelblau correlation is a good fit to the data at both high and low temperatures. More physically based correlations, incorporating fugacity coefficients for water and hydrogen and the activity coefficient for the water solution, are available.[8] However, the increased accuracy of such a correlation was not necessary for the calculations performed here and the Himmelblau fit was selected for simplicity.

Note that because Henry's Law provides a linear correlation between liquid concentration and pressure, the shape of the Henry's Law constant curve is also the shape of curves of constant liquid concentration in a pressure versus temperature plot. Figure 3-4 shows several curves of constant liquid hydrogen concentration in the pressure-temperature plane.

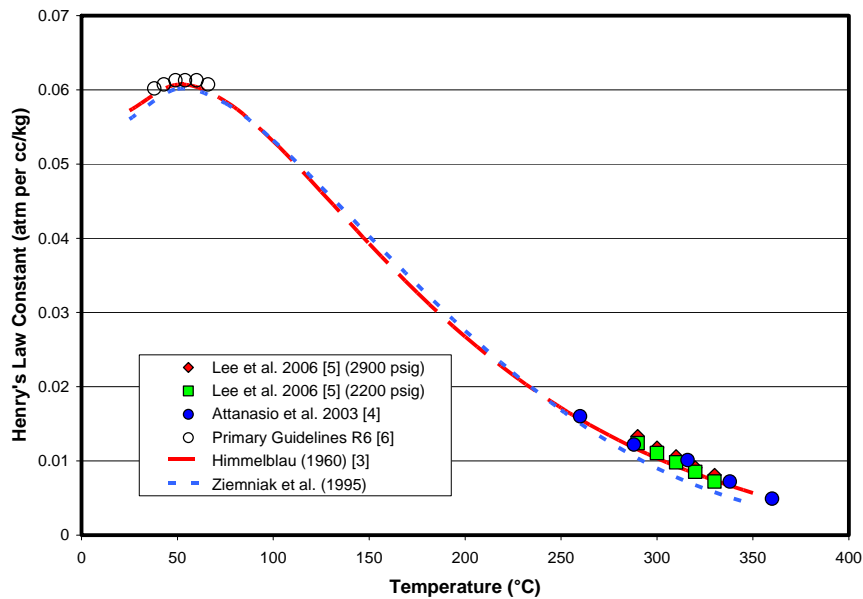


**Figure 3-1**  
**Henry's Law Constant as a Function of Temperature, Correlation Validation**

## Fundamental Electrochemistry

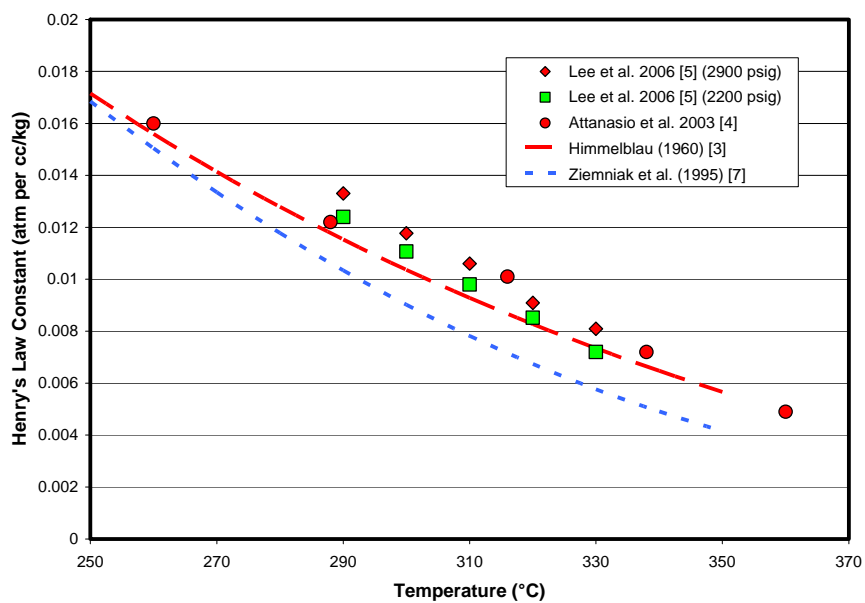


**Figure 3-2**  
High Temperature Henry's Law Constant as a Function of Temperature, Correlation Validation

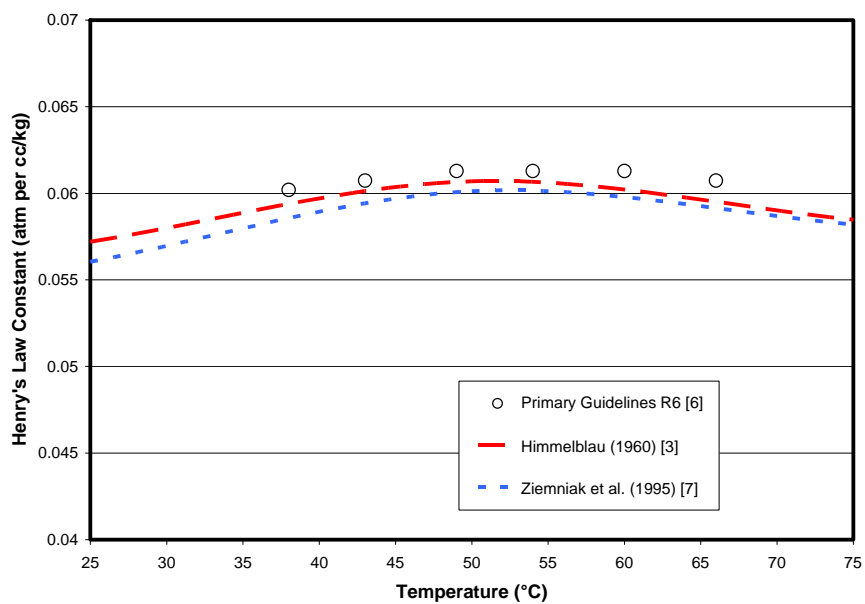


**Figure 3-3**  
Low Temperature Henry's Law Constant as a Function of Temperature, Correlation Validation

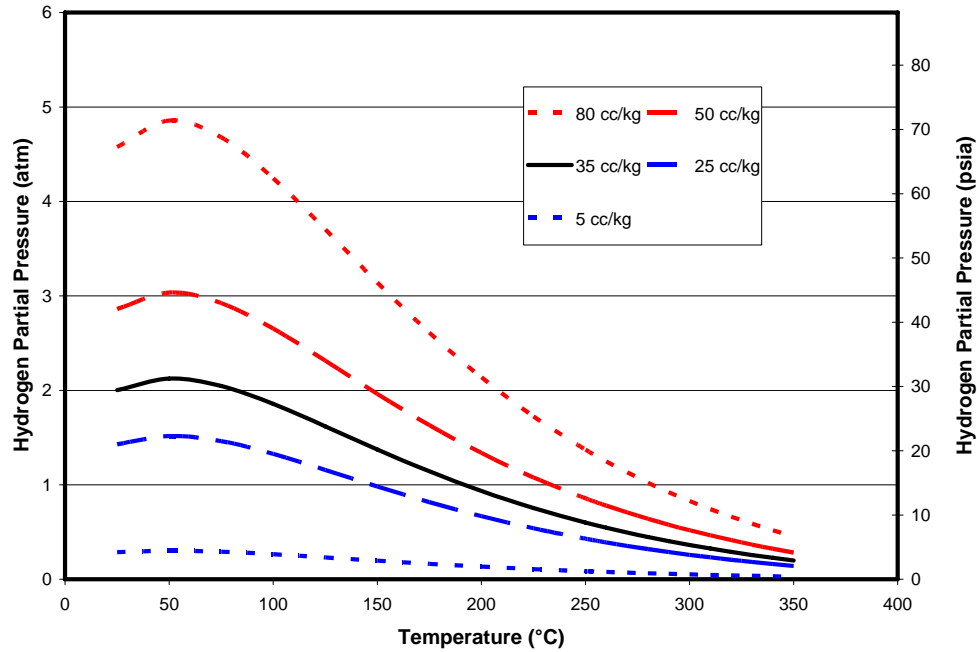


**Figure 3-4**  
Curves of Constant Liquid Hydrogen Concentration in the Pressure-Temperature Plane

### 3.3 Hydrogen Diffusion in Metal

#### 3.3.1 Basic Diffusion Model for Loss of Hydrogen Through SG Tubes

Loss of hydrogen through SG tubes has been evaluated by the industry [9] and provides useful insights regarding diffusion of hydrogen in other situations. Assessment of diffusion into other systems is the first step in assessing the impact of increased (or decreased) hydrogen concentrations on systems that are separated by solid boundaries. For example, modeling of diffusion through steam generator tubes is necessary to assess how increased hydrogen concentrations in the primary system could affect the secondary system.

The diffusion of hydrogen in nickel alloys is generally thought to follow Fick's law, which states that the diffusion mass flux ( $J$ , mol/s-m<sup>2</sup>) is proportional to the concentration gradient ( $-dC_H/dx$ , mol/m<sup>4</sup>). The proportionality constant is the diffusion coefficient ( $D_H$ , m<sup>2</sup>/s), such that the proportionality can be expressed as the following equation:

$$J = -D_H \frac{dC_H}{dx} = D_H \frac{\Delta C_H}{x_{thickness}} \quad \text{Eq. 3-13}$$

Multiplying Equation 3-13 by the transfer area,  $A$ , gives the total rate of hydrogen loss, as follows:

$$Q = D_H A \frac{\Delta C_H}{x_{thickness}} \quad \text{Eq. 3-14}$$

Note that the concentration gradient is given in terms of monatomic hydrogen. The concentration of hydrogen in the metal depends on the equilibrium between diatomic hydrogen dissolved in the liquid phase and the monatomic hydrogen dissolved in the metal. This equilibrium is generally expressed by Sievert's Law, which defines the solubility,  $S$ , in the solid phase through the following equation:

$$S = \frac{C_H}{P_{H_2}^{\frac{1}{2}}} \quad \text{Eq. 3-15}$$

Substituting Equation 3-15 into Equation 3-14 yields the following expression:

$$Q = \frac{D_H A S}{x_{thickness}} \Delta P_{H_2}^{\frac{1}{2}} = \Phi \frac{A}{x_{thickness}} \Delta P_{H_2}^{\frac{1}{2}} \quad \text{Eq. 3-16}$$

where  $\Phi$  is the product of the diffusion coefficient and the solubility, called the permeability.

The concentration of hydrogen in the liquid phase may be related to the pressure through Henry's Law, as follows:

$$P_{H_2} = H C_{H_2} \quad \text{Eq. 3-17}$$

Substituting Equation 3-17 into Equation 3-16 gives the following:

$$Q = \Phi \frac{A}{x_{thickness}} H^{\frac{1}{2}} C_{H_2}^{\frac{1}{2}} \quad \text{Eq. 3-18}$$

Equation 3-18 gives the hydrogen loss rate as a function of system geometry (transfer area,  $A$ , and tube thickness,  $x_{thickness}$ ), chemical properties (the permeability of the tubing,  $\Phi$ , and the Henry's Law constant,  $H$ , which are discussed in Section 3.3.2 and 3.2, respectively), and the concentration of hydrogen in the RCS ( $C_{H_2}$ ).

### 3.3.2 Permeability of Hydrogen in SG Tube Alloys

As indicated in Equation 3-18, the diffusion of hydrogen through the steam generator tubes depends on the permeability of the tube material,  $\Phi$ . Several researchers have investigated the permeability of Alloy 600.[10, 11, 12, 13, 14] Typically, the relationship between permeability and temperature is fit to an Arrhenius function, as follows:

$$\Phi = \Phi_0 e^{\frac{-E_{act}}{RT}} \quad \text{Eq. 3-19}$$

where  $\Phi_0$  and  $E_{act}$  are empirical constants and the temperature is expressed as the absolute temperature in K. Figure 3-5 shows the data reported in the literature, as Arrhenius curves, over the temperature range tested based on the reported values of  $\Phi_0$  and  $E_{act}$ .

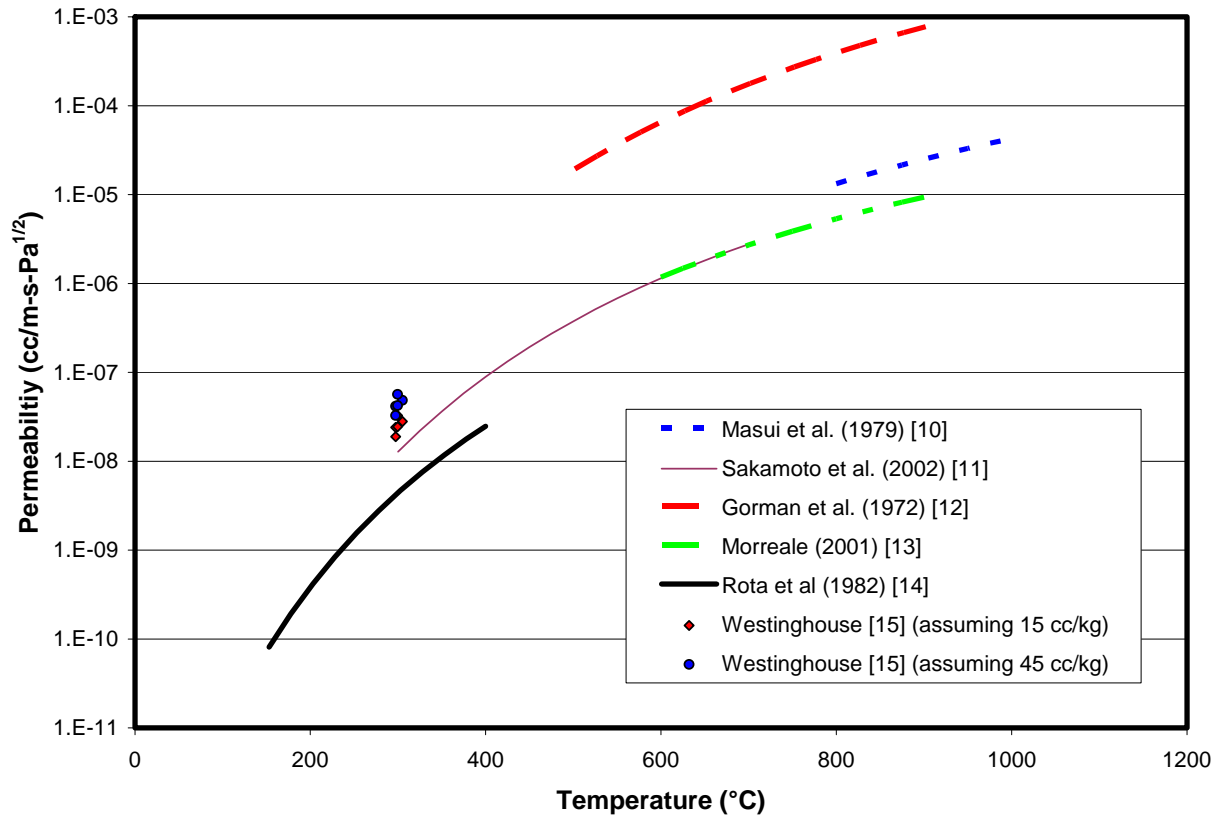


**Figure 3-5**  
Permeability as a Function of Temperature

As discussed in Section 3.3.3, conditioning of the tubes (e.g., oxidation or cold work) can significantly affect the permeability. Therefore, it would be useful to compare the permeability measured in laboratory testing with that observed in actual steam generators. Westinghouse has reported the results of secondary hydrogen monitoring with correlations to primary side hydrogen concentrations.[15] This work was completed at three plants (Prairie Island Unit 1, Ginna, and Indian Point Unit 3) with two periods of monitoring at each of two of the plants, resulting in five measurements of the permeability.

Unfortunately, the Westinghouse results are reduced to a form that assumes diatomic diffusion through the steam generator tubes. Specifically, they are expressed as a permeation constant  $K$  with units of mol/hr per cc/kg. As defined, this constant satisfies the following equation:

$$Q = KC_{H_2} \quad \text{Eq. 3-20}$$

Comparing Equation 3-20 with Equation 3-18 allows the derivation of a relationship between the Westinghouse permeation constant ( $K$ ) and the permeability ( $\Phi$ ), yielding the following:

$$\Phi = \frac{x_{thickness} KC_{H_2}^{\frac{1}{2}}}{AH^{\frac{1}{2}}} \quad \text{Eq. 3-20}$$

The hydrogen concentrations used in the Westinghouse tests are not reported, but it is reasonable to assume that they lie between 15 and 45 cc/kg. Table 3-1 gives the permeability constants reported in Reference [15] along with the plant data needed to derive a permeability per Equation 3-21. Table 3-1 also gives the permeabilities calculated per Equation 3-21 assuming hydrogen concentrations of 15 and 45 cc/kg. Note that this calculation requires a value for the Henry's Law constant,  $H$ . The values used in this calculation are those obtained through the correlation discussed in Section 3.2.

**Table 3-1**  
**Implied Permeability From Westinghouse Plant Tests [15]**

Plant	Permeation Constant K (per SG)	SG Design	T <sub>average</sub>  °C	Implied Permeability $\Phi$ (assuming 15 cc/kg)	Implied Permeability $\Phi$ (assuming 45 cc/kg)
	(g-mole/hr) / (cc/kg)			cc / m-s-Pa <sup>0.5</sup>	cc / m-s-Pa <sup>0.5</sup>
Prairie Island Unit 1	0.014	51	297.4	2.40E-08	4.16E-08
	0.011			1.89E-08	3.27E-08
Ginna	0.013	44	305.1	2.80E-08	4.86E-08
Indian Point Unit 3	0.012	44	299.7	2.45E-08	4.23E-08
	0.016			3.26E-08	5.65E-08

### 3.3.3 Sources of Variability and Uncertainty

Various material conditions can contribute to changes in the permeability, including the following:

- Cold work
- Thickness of the oxide film
- Chemical composition of grain boundaries
- Hydrogen isotope
- Surface texture

Investigations into the above factors are beyond the scope of this report. Furthermore, the differences between Alloy 600 and Alloy 690 are likely to be significant. Nevertheless, the methodology developed here should be qualitatively valid.

## 3.4 Metal — Metal Oxide Transitions

### 3.4.1 Nickel

The stable oxidation state of metal species in the primary coolant, particularly corrosion products, is currently considered to be a major factor in corrosion of materials of construction, the transport of corrosion products, the deposition of corrosion products in the core and their effects there, and the removal of corrosion products during shutdown maneuvers. As discussed extensively in Chapter 4, the nickel metal-nickel oxide transition point is of particular interest because it is believed that the stress corrosion cracking of nickel alloys and their weld metals is influenced by the proximity of this transition.

In general, transitions between stable solid phases are governed by the pH, the temperature, and the electrochemical potential. For nickel and many other metals the potential at transitions between metallic and oxide states is linearly related to the pH such that these transitions are parallel to lines of constant hydrogen concentration in a potential-pH diagram (Pourbaix diagram). Therefore, the location of the transition at a given pH is fully described by the specification of a temperature and an associated hydrogen concentration.

Figure 3-6 shows the location of the transition between nickel metal and nickel oxide stability used in this report.[16] Also shown are historic correlations [17, 18]. The correlation equation shown in Figure 3-6 forms the basis for the calculation of the peak PWSCC condition discussed in Chapter 4. Recent assessment by chemical thermodynamics experts [19] indicates that there is significant controversy regarding the adoption of the correlation shown in Figure 3-6 as an accepted description of the transition between nickel metal and nickel oxide. This is an ongoing area of analysis within EPRI (see Section 11.4).

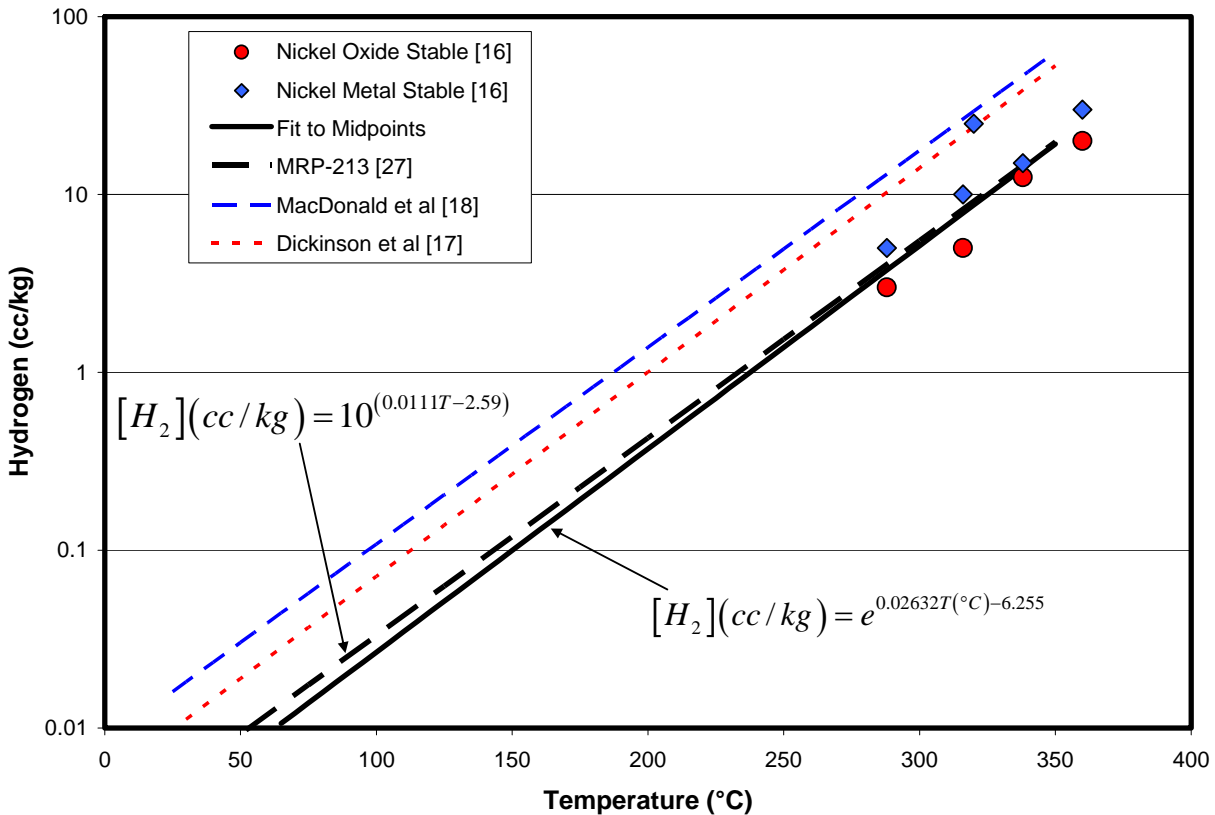


**Figure 3-6**  
**Nickel Metal – Nickel Oxide Transition: Hydrogen Concentration as a Function of Temperature**

### 3.4.2 Other Metals

In general, analyses of corrosion products from primary circuits (fuel scrapes as well as samples collected from the RCS during operation) do not indicate the presence of metal species in nickel-free phases (for example, magnetite –  $Fe_3O_4$  or zinc oxide  $ZnO$ ). Therefore, although some thermodynamic data are available regarding stable solid states of other metals, it is not evident that such data are relevant. (Solubility of other metal oxides and mixed oxides are discussed in Section 3.5 and 3.6.)

Transitions between metallic and oxide states have been measured on nickel alloys.[4, 20] These measurements indicate that transitions from oxide to metal occur on Alloy 600 surfaces at about the same hydrogen concentrations as those on nickel surfaces, indicating that the transition is dominated by the thermodynamics of nickel.

### 3.5 Nickel Solubility

The solubility of nickel in a system containing nickel and iron is governed by the complex interaction of nickel metal, nickel oxide, and non-stoichiometric nickel ferrites. This interaction is affected by the concentration of dissolved hydrogen and the temperature. Figure 3-7 shows the solubility of nickel over the range of primary temperatures at 50 cc/kg hydrogen. Figure 3-8 shows similar data for a hydrogen concentration of 25 cc/kg. Note that the values in both these figures are calculated (i.e., they are based on sets of data measured at other conditions).

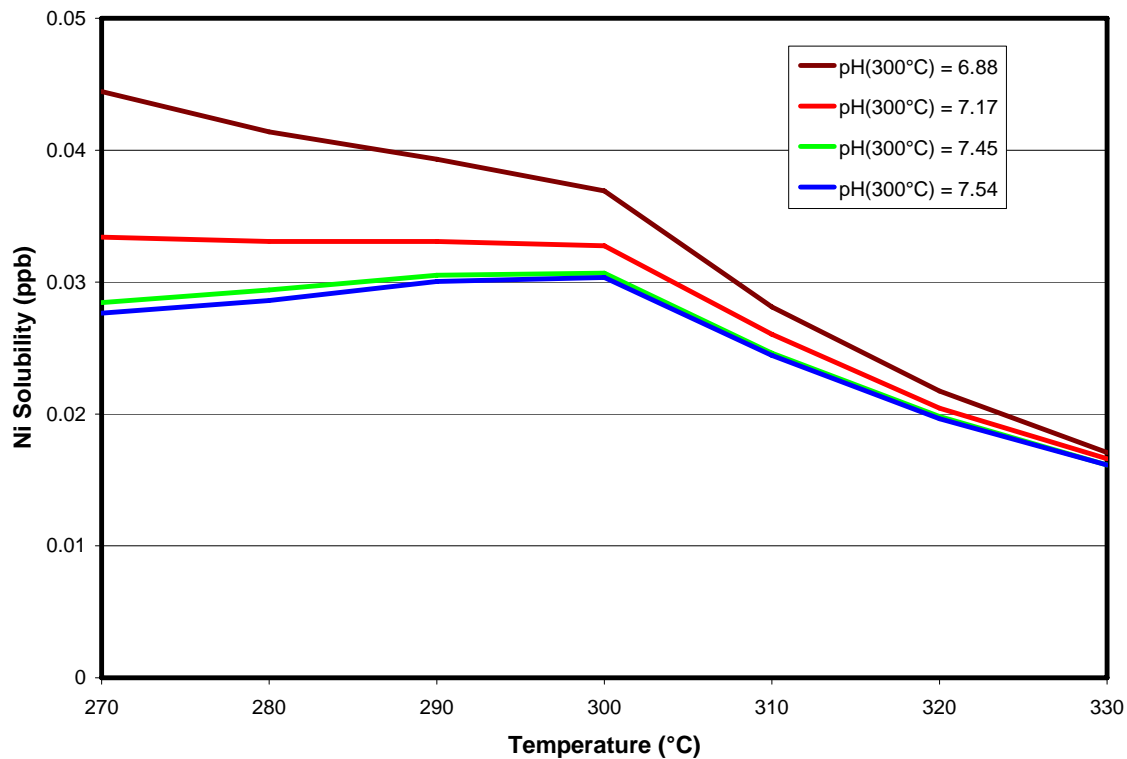


**Figure 3-7**  
**Nickel Solubility at 50 cc/kg Hydrogen [21]**

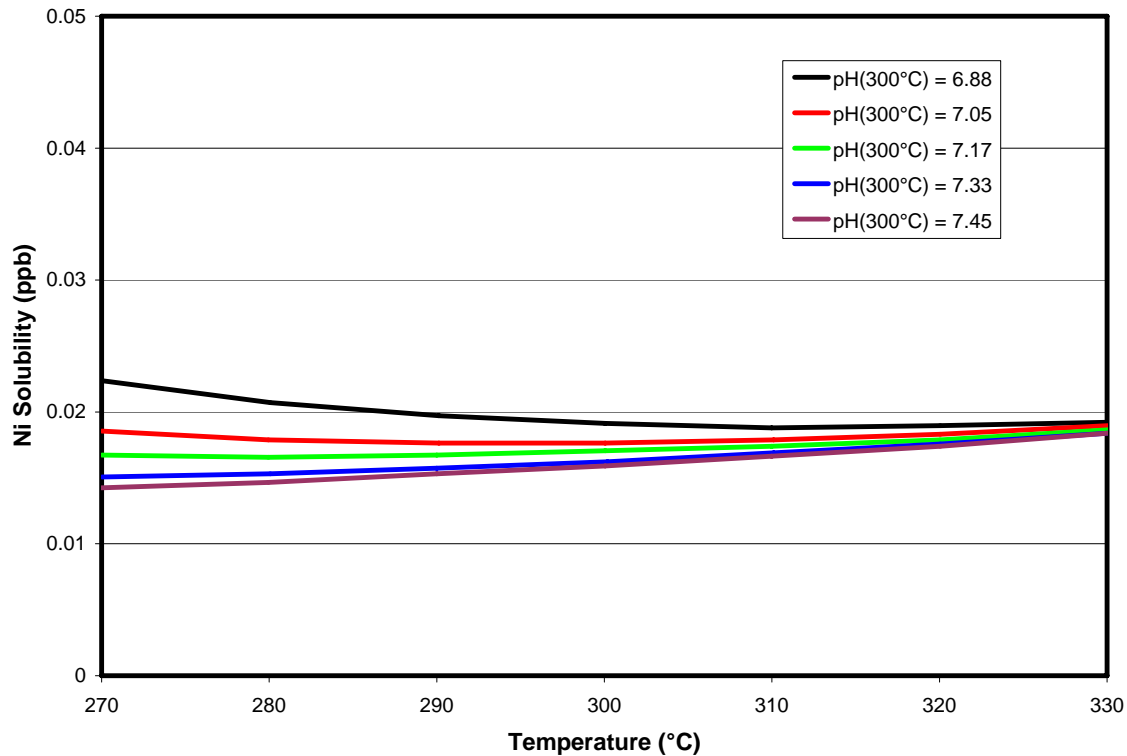


**Figure 3-8**  
**Nickel Solubility at 25 cc/kg Hydrogen [21]**

At the lower hydrogen concentration there is a discontinuity at about 300°C. This discontinuity represents the point at which the principle precipitate changes from nickel metal (at lower temperatures) to non-stoichiometric nickel ferrite (at higher temperatures). Increasing the hydrogen concentration moves the discontinuity to the right. At 50 cc/kg, the discontinuity is moved above 350°C. (Note that these specific results depend on the ratio of iron to nickel under consideration, which may not always be known.) At lower concentrations of hydrogen the discontinuity will move to the left.

Based on these evaluations, the change between nickel metal stability and nickel ferrite stability is the most significant factor in nickel solubility at operating conditions. By maintaining hydrogen above the current lower limit (25 cc/kg) nickel metal is kept stable. This results in temperature-insensitive solubilities. Increasing hydrogen is not expected to affect temperature sensitivity. However, decreasing hydrogen concentrations enough to make nickel ferrite the stable solid phase introduces a strong temperature dependence of nickel solubility.

The solubilities given in Figure 3-7 and Figure 3-8 indicate that in the nickel metal regime, increasing the hydrogen concentration lowers the solubility of nickel.

### 3.6 Iron Solubility

As discussed in Section 3.4.2, a solid phase containing only iron generally is not observed in the primary system, i.e., a magnetite phase is generally not observed. Regarding solubility from mixed metal oxides, there are some data relevant to iron solubility from nickel ferrite ( $\text{Ni}_x\text{Fe}_{3x}\text{O}_4$ ). Reference [22] concludes from the data in Figure 3-9 that the iron solubility from nickel ferrite follows a 1/3 power dependence on hydrogen concentration at high hydrogen concentrations but not at low concentrations. The data used to develop the averages given in Figure 3-9 are plotted in Figure 3-10. Also shown in this figure is the 1/3 power line given in Figure 3-9 as well as least square fits to all of the data and also to just the data at  $\geq 10$  cc/kg. The presentation of data in Figure 3-10 suggests that the data at higher hydrogen concentrations are not necessarily better correlated to a 1/3 power rule than to a 1/5 power rule that fits all of the data. Figure 3-11 shows a similar analysis of the data from Reference [22] collected at 285°C.

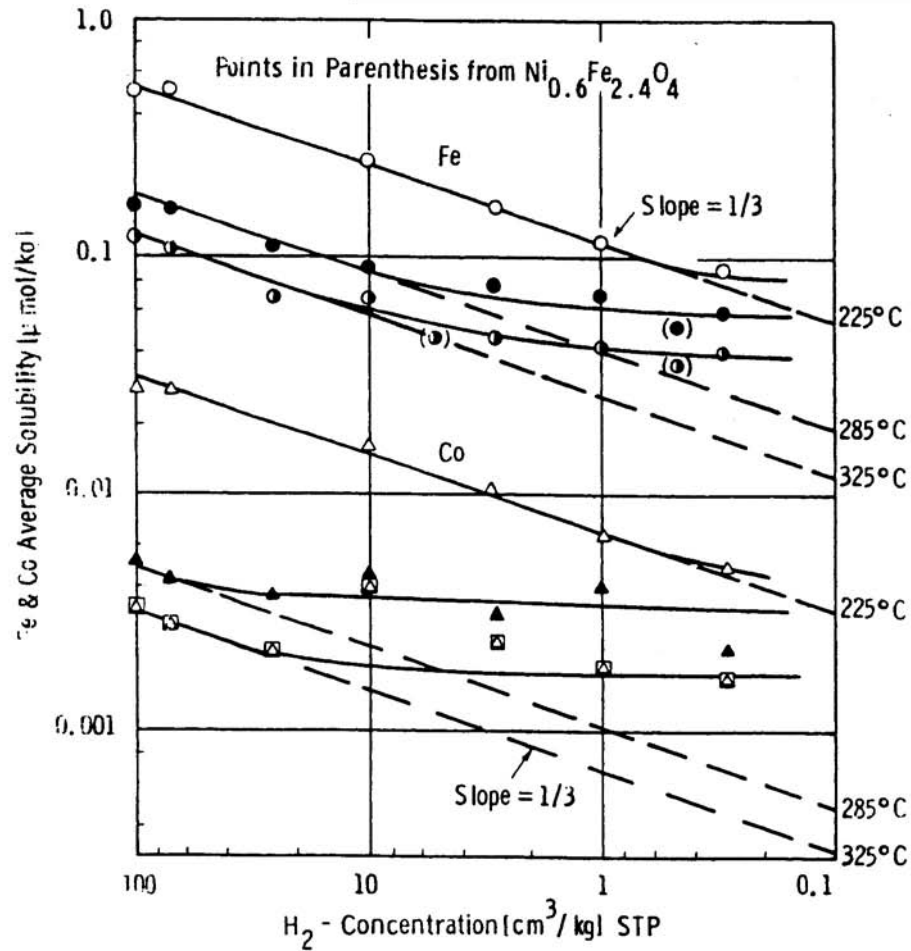
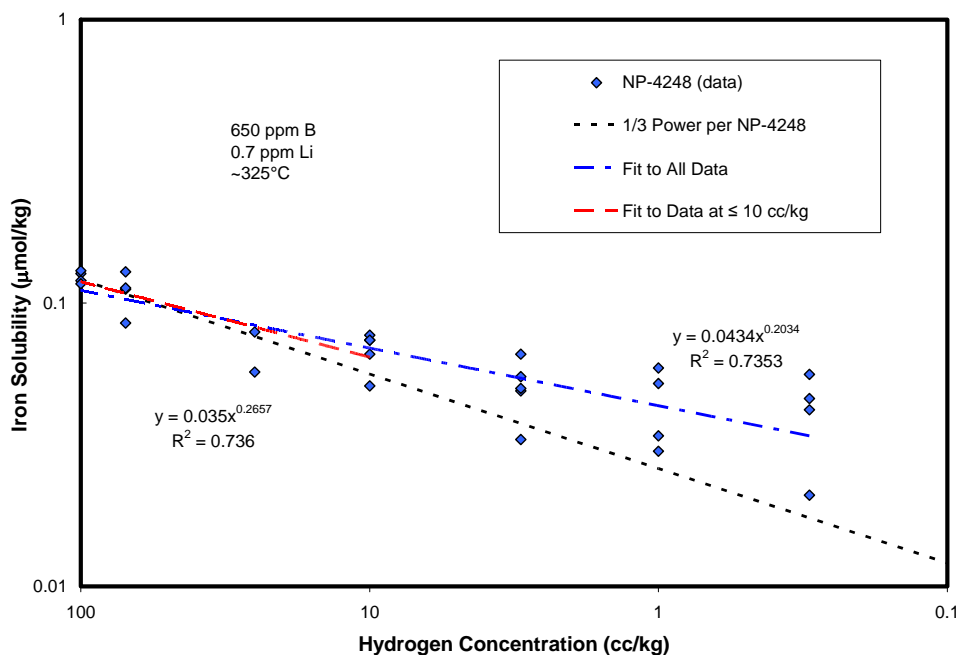


Figure 3-9. Average solubility of iron and cobalt versus hydrogen concentrations at different temperatures:

Compound	Chemistry		$[\text{H}_2]$	$\text{pH}_{25^\circ\text{C}}$
$\text{Ni}_{0.50}\text{Co}_{0.05}\text{Fe}_{2.45}\text{O}_4$	$\text{B}(\text{OH})_3$	$\text{LiOH}$	0.3 to	6.4
	0.06 M	$1.0 \times 10^{-4}$ M	100 $\text{cm}^3/\text{kg}$	

Figure 3-9  
Iron Solubility From Nickel Ferrite as a Function of Hydrogen [22]



**Figure 3-10**  
**Iron Solubility From Nickel Ferrite as a Function of Hydrogen at 325°C [22]**

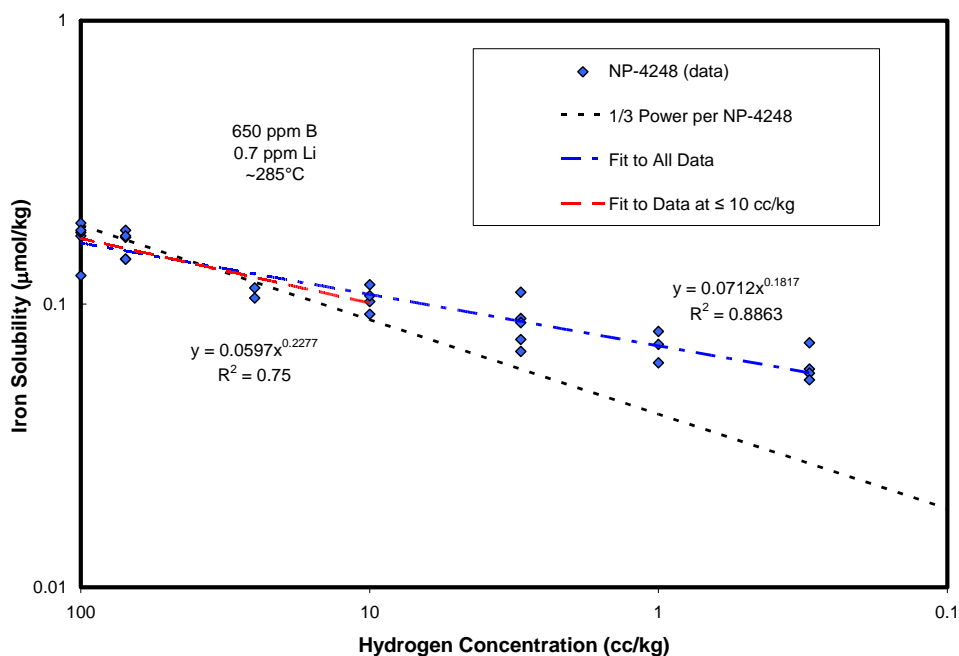


**Figure 3-11**  
**Iron Solubility From Nickel Ferrite as a Function of Hydrogen at 285°C [22]**

The data presented in Figure 3-10 and Figure 3-11 do not support the conclusion that trends in iron solubility from nickel ferrite are significantly different at high and low hydrogen concentrations. Least squares fits to the data suggest a  $1/5$  power rule dependence of the iron concentration from nickel ferrite on the hydrogen concentration. In contrast, the most recent MULTEQ database [23] suggests a  $1/2$  power rule for stoichiometric nickel ferrite ( $\text{NiFe}_2\text{O}_4$ ) and a  $2/5$  power rule for a mixed stoichiometry similar to that used in the Westinghouse testing ( $\text{Ni}_{0.5}\text{Fe}_{2.5}\text{O}_4$ ). More generally, MULTEQ would predict a dependence of  $1/z$ , where  $z$  is the number of iron atoms in the stoichiometric formula (e.g., 3 for  $\text{Fe}_3\text{O}_4$ , 2.5 for  $\text{Ni}_{0.5}\text{Fe}_{2.5}\text{O}_4$ ).

### 3.7 Simultaneous Concentrations of Oxidizers and Reducers

In most discussions of the chemical environment in the reactor coolant system, the environment is described as being either oxidizing or reducing. However, in general, both oxidizing species (hydrogen peroxide, for example) and reducing species (molecular hydrogen, for example) will be present. This is especially true during low power operation, for example, when reactor coolant pumps are started, as illustrated in Figure 3-12. During full power operation, oxidizing and reducing species are expected to co-exist even in the core, albeit in highly unbalanced concentrations.[24]

The ultimate measure of whether an environment is oxidizing or reducing is the electrochemical potential on the material of interest (or component of interest, when geometric issues like flow velocity are considered important). This potential cannot be simply related to the concentration of a single species or the excess of one species over another. For example, Figure 3-13 shows measurements of the electrochemical potential on a Type 304 stainless steel electrode at  $165^\circ\text{C}$ . [25] In this test the potential measured with excess oxygen is the same as that measured with oxygen alone. However, the potential when hydrogen is in excess but oxygen is still present is significantly greater than when hydrogen alone is present. One explanation for why this occurs is that oxygen is more reactive with the stainless steel than is hydrogen, i.e., there are kinetic barriers to reaching equilibrium.

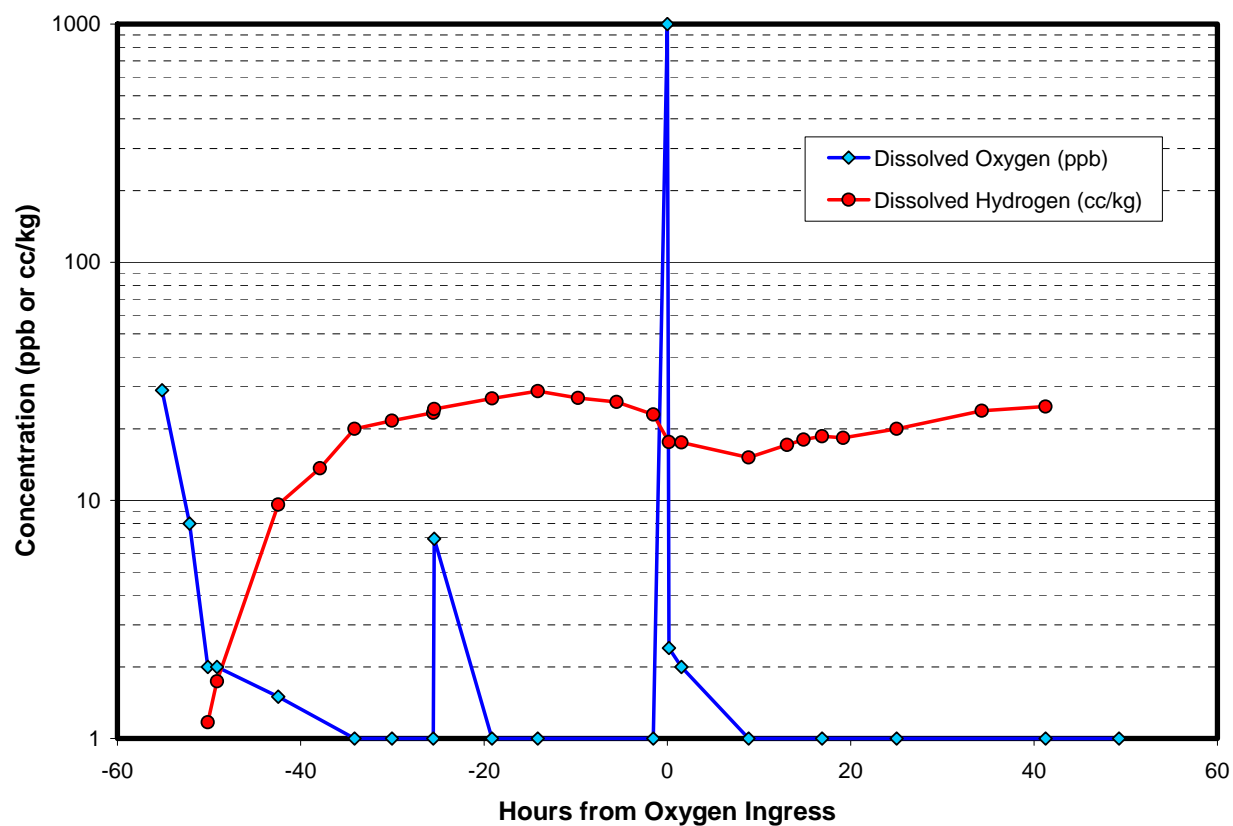


**Figure 3-12**  
**Oxygen and Hydrogen Concentrations, Callaway Startup After RF08**

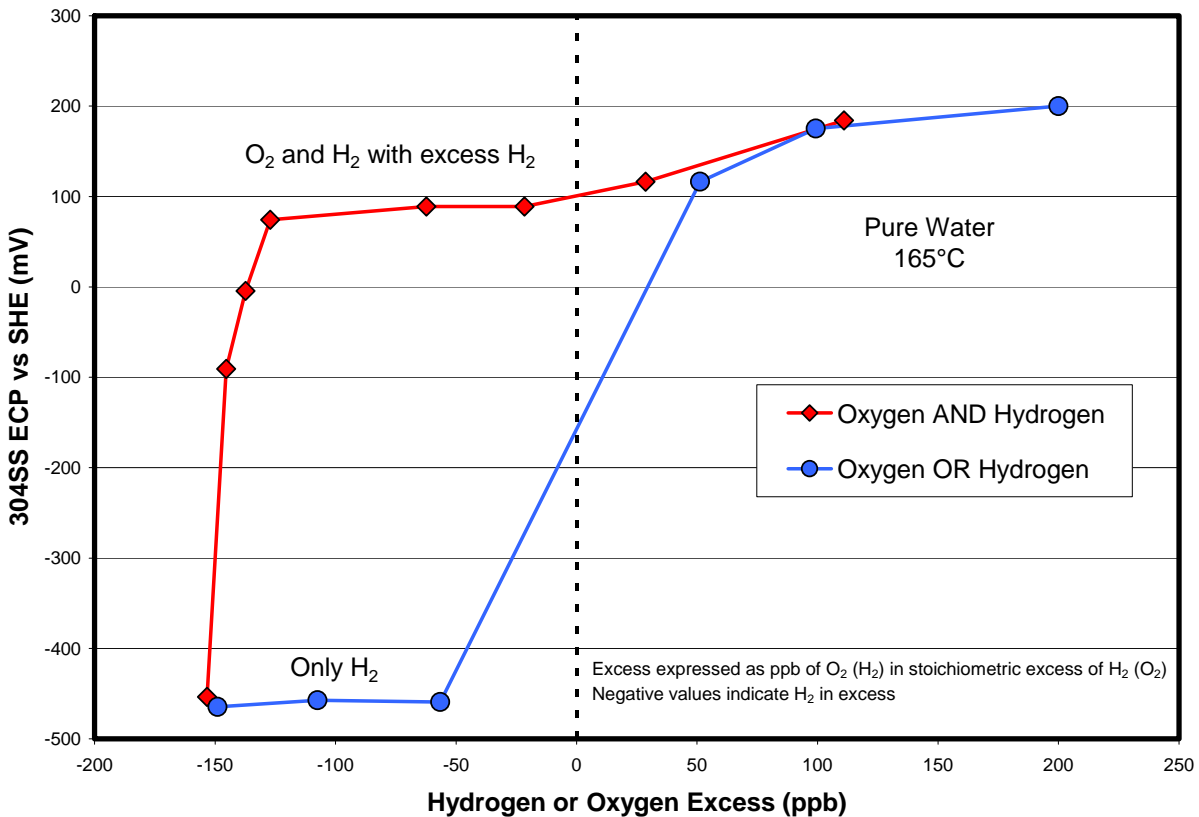


**Figure 3-13**  
ECP on SS304 in Environments Containing Oxygen, Hydrogen, or Both [25]

To accurately determine the electrochemical potential on a surface of interest, the concentrations of oxidizing and reducing species must be adjusted for their reactivity. One crude method for doing this [24] is to consider only those species which are highly reactive and to determine whether the reactive reducing species exceed the reactive oxidizing species. This method has been shown to accurately predict transitions from oxidizing to reducing conditions as measured by electrochemical potential in a test reactor loop as shown in Figure 3-14. Note that the concentrations of the highly reactive species are calculated.

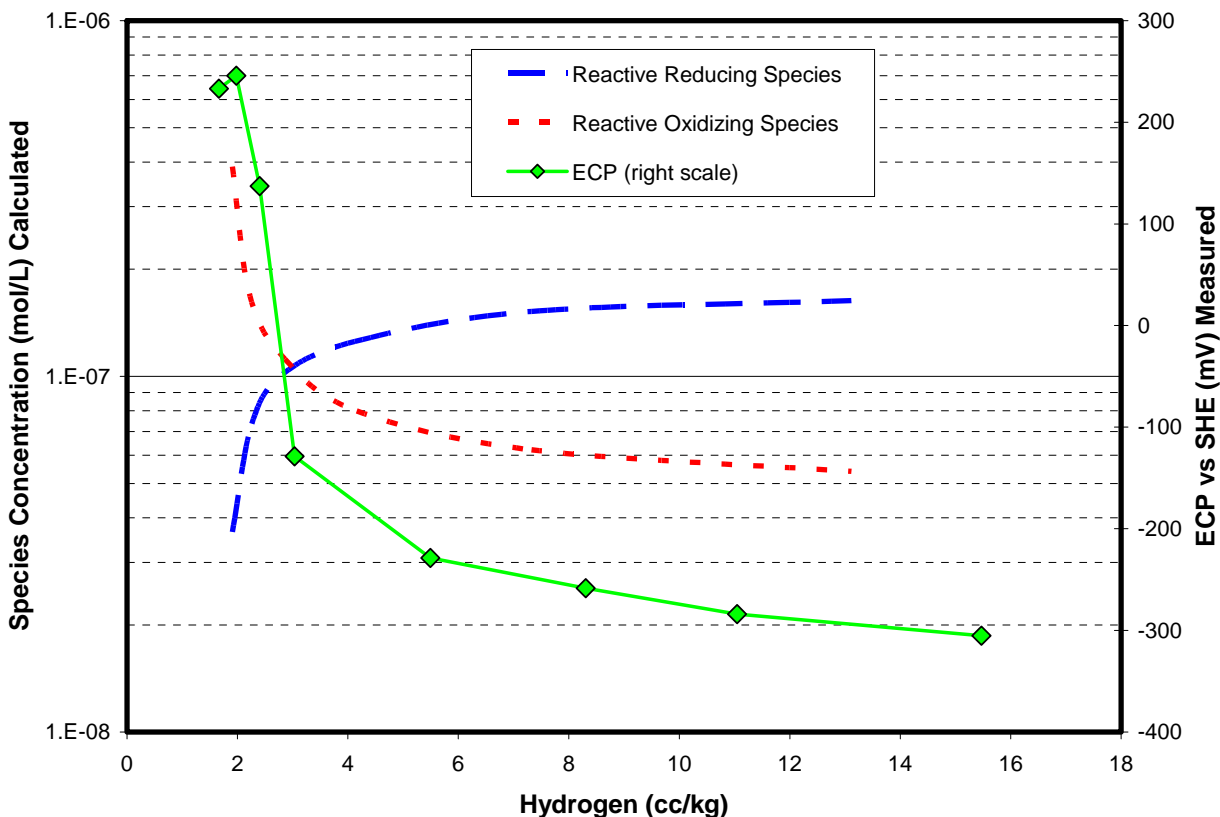


**Figure 3-14**  
**In-Pile ECP of Stainless Steel [24]**

In the out-of-core regions of the reactor coolant system, the most reactive species generated by radiolysis is expected to be hydrogen peroxide. Thus, for out-of-core components, the hydrogen peroxide concentration can be used to assess the electrochemical potential. In the core, radiation is expected to increase the rate at which all species react, and therefore excess hydrogen will be expected to maintain a reducing environment.

It is expected that nickel alloys will behave similarly to stainless steels with respect to reaction kinetics with oxidizing and reducing species (they will generally not tend to behave like noble metals which will catalyze reactions between oxygen and hydrogen, for example).[26]

### 3.8 Areas for Further Research

With respect to the fundamental issues discussed in this chapter, there appears to be little opportunity to improve the understanding of the effects of increasing hydrogen concentration in the primary system. The areas which have significant uncertainty (iron and nickel solubility from mixed oxides) are also the most difficult in which to apply such fundamental data to predictions of actual plant behavior. For example, the relationship between corrosion product transport (which can contain significant particulate content) and solubility is not well established.

*Fundamental Electrochemistry*

Nonetheless, this is an area that warrants additional study independent of hydrogen concentration optimization.

One area which could yield significant new information that would impact utility decisions is mixed metal solubility. In particular, the behavior of zinc with respect to incorporation into oxide films at various hydrogen concentrations is not at all understood. Similarly, the interaction of cobalt with hydrogen could have significant effects on plant dose rates.

# 4

## EFFECTS OF HYDROGEN CONCENTRATION ON PWSCC

---

### 4.1 Introduction

A number of organizations have studied the effect of hydrogen concentration on high-temperature cracking of nickel alloys. These studies have included measurements of the effects of hydrogen both on crack initiation and on crack growth rates. Alloys considered include Alloy 600, Alloy 690, Alloy X-750, weld metal EN82, weld metal E182/82, etc. Recently, the EPRI Materials Reliability Program (MRP) published a review of the available data.[27] The discussion in the sections below is based primarily on that review. Sections 4.2 and 4.3 discuss the experimental findings. Section 4.4 discusses factors of improvement for various changes in hydrogen concentration. Section 4.5 identifies current knowledge gaps and discusses on-going testing. Conclusions are given in Section 4.6.

### 4.2 Fundamental Observation

It has long been known that corrosion resistant materials are generally more susceptible to stress corrosion cracking in oxidizing conditions ( $\sim 100 \text{ mV}_{\text{SHE}}$  or higher at  $288^\circ\text{C}$ ). This is generally understood to arise from the generation of a potential gradient along the crack length due to the consumption of oxygen within the crack by corrosion of the freshly exposed crack faces. This potential gradient gives rise to a net flux of anions into the crack, accelerating crack growth. Such classic high potential stress corrosion cracking is one of the main reasons for operation of PWRs under reducing conditions.

However, nickel alloys demonstrate an increase in cracking susceptibility at lower potentials as shown in Figure 4-1. This is generally thought to be related to the stability of the corrosion resistant oxide film that forms on these materials. In practice, peak susceptibility has been associated with the potential of the nickel/nickel oxide transition. It has been suggested that the nickel/nickel oxide transition is important because, during cracking of nickel alloys, fresh alloy surfaces initially develop a metastable nickel oxide film.[4] Alternatively, the formation of nickel oxide could govern the extent to which protective corrosion films are depleted in nickel and enriched in chromium. An exact explanation as to why the nickel-nickel oxide transition is important is not currently available.

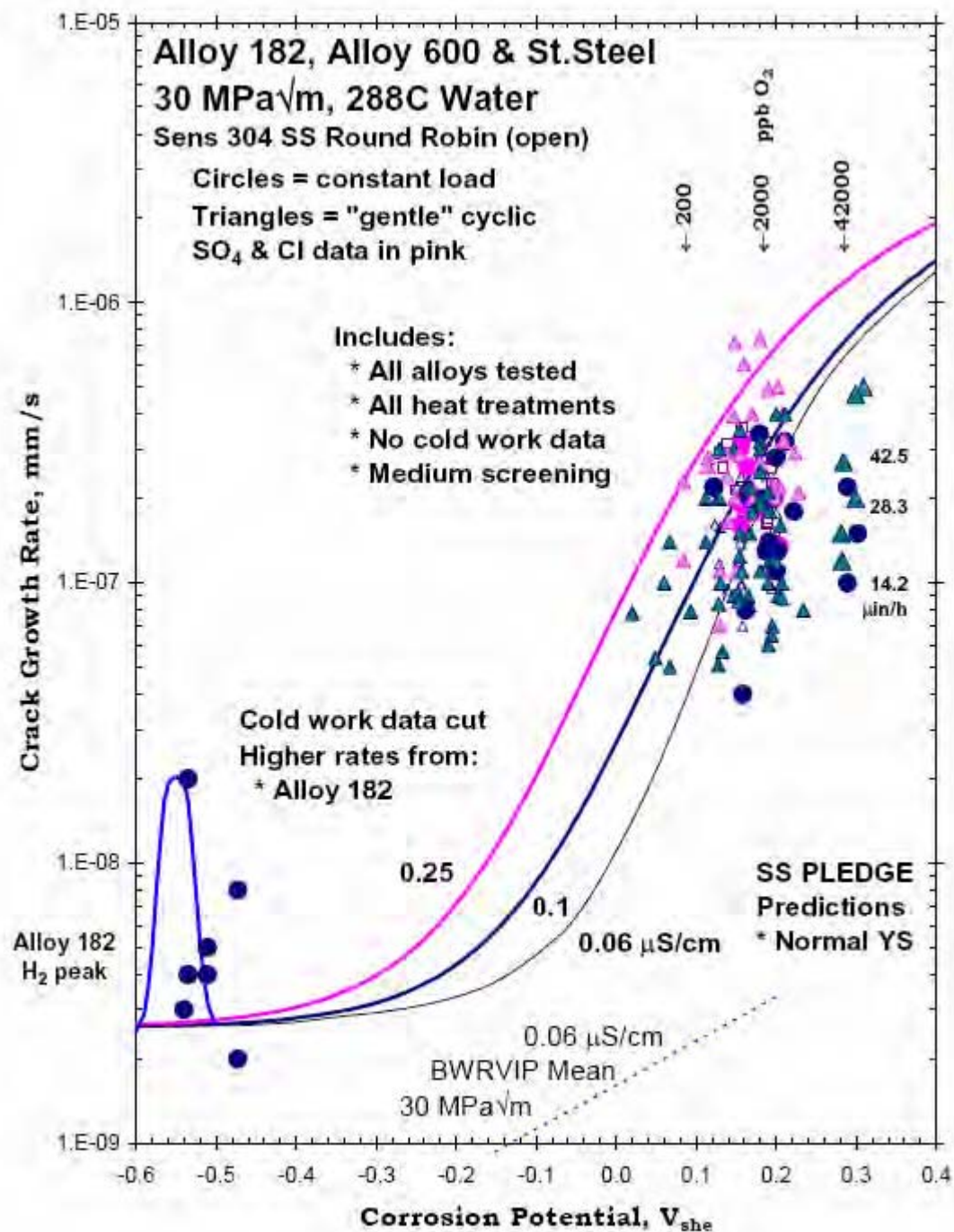


**Figure 4-1**  
**Crack Growth Rates of Corrosion Resistant Alloys Over a Wide Range of Potentials [27]**

Specific experimental observations are discussed in the next two sections. Section 4.2.1 discusses initiation data and Section 4.2.2 discusses propagation data.

## 4.2.1 PWSCC Initiation

### 4.2.1.1 Laboratory Data

The effects of chemistry parameters on PWSCC initiation have been the subject of ongoing investigations for at least the last decade.[28, 29, 30] The results of the most recent analysis [6] are shown in Figure 4-2. Note that the characteristic life is the time for approximately 63% of the population to fail and is a fitted parameter obtained by assuming that the failure distribution in a given population is described by a Weibull distribution. The analysis is based on data from testing of reverse U-bend samples (RUBs). These samples are highly stressed and cold worked, and are relatively thin-walled, so that the time to failure is close to the initiation time. Therefore, the characteristic life can be considered an inverse initiation rate.

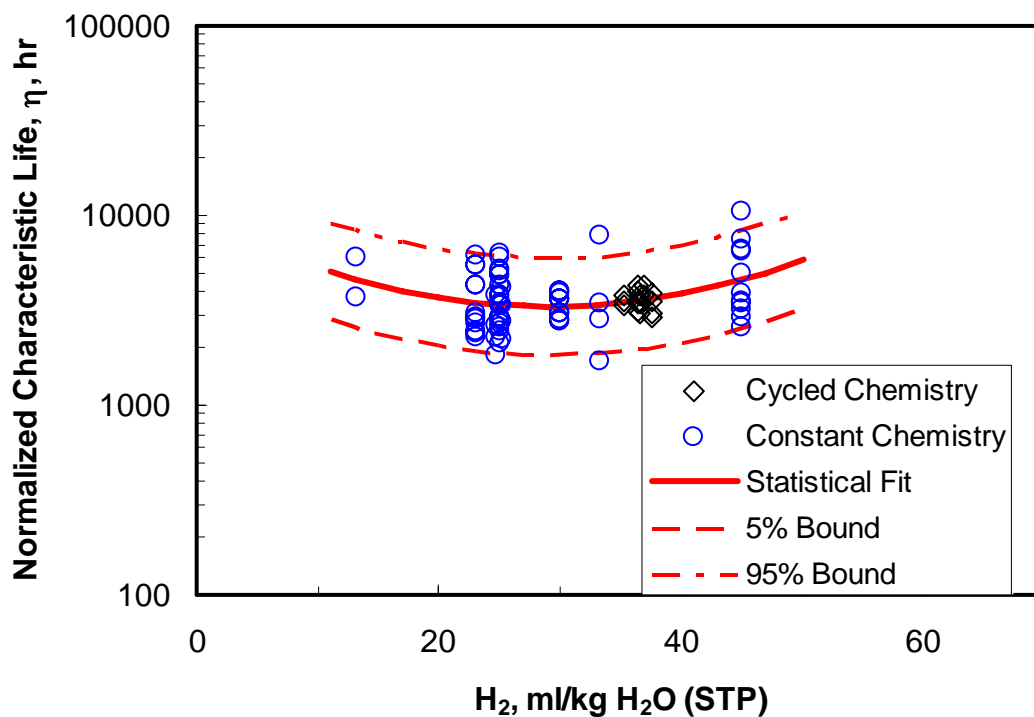


Figure 4-2  
Effect of Hydrogen Concentration on Characteristic Life [6]

The curve in Figure 4-2 labeled as “Statistical Fit” is a fitted curve assuming the following form:

$$\ln \eta = aC^2 + bC + c \quad \text{Eq. 4-1}$$

where  $C$  is the hydrogen concentration and  $a$ ,  $b$ , and  $c$  are fitted parameters. The 5% and 95% bounds are given by adjusting  $c$  such that the desired fraction of data are above the curve.

Since the trend indicated in Figure 4-2 is not derived from first principles, the high degree of scatter in the data makes it difficult to draw strong conclusions. The data indicate that it is possible that a minimum in characteristic life could be present in the range of the Ni/NiO transition, but do not provide strong evidence that such a minimum actually exists.

Other investigations have observed modest correlations between PWSCC initiation and hydrogen concentration.[31, 32, 33, 34] An example data set is shown in Figure 4-3. However, the various data sets available in the literature have not been collected and analyzed in a consistent way. As discussed in Section 4.5.6, additional compilation and analysis of these data are warranted. It should be noted that some investigators have concluded that crack initiation rates increase monotonically with hydrogen concentration.[33, 34] However, these programs have generally not collected a significant number of data at concentrations above the Ni/NiO transition.

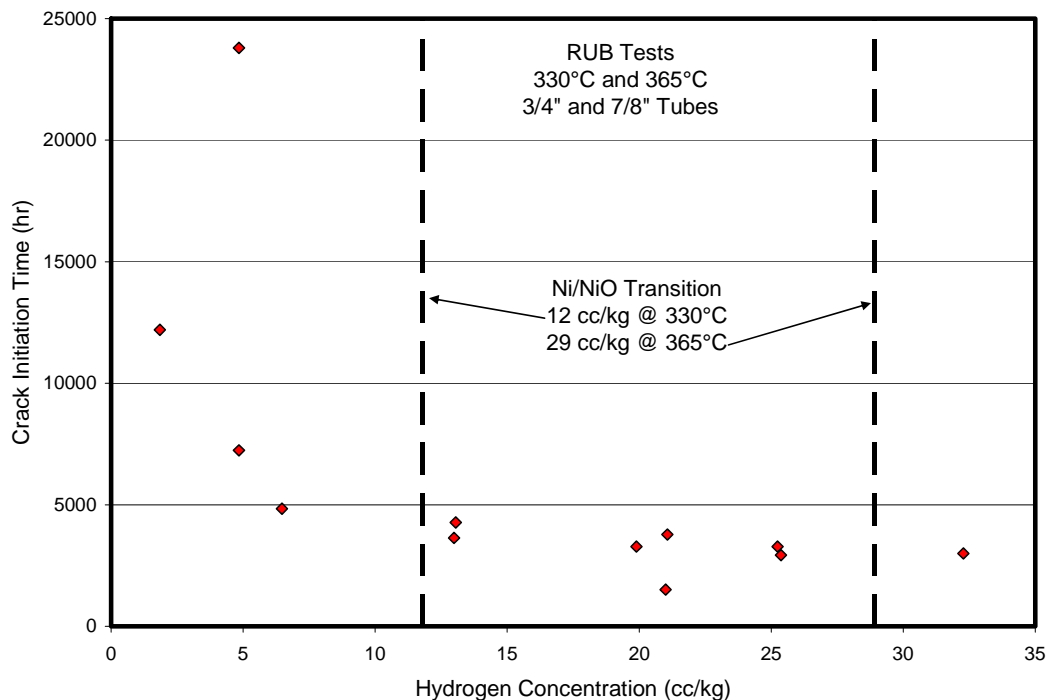


**Figure 4-3**  
**Effect of Hydrogen Concentration on Crack Initiation Time [34]**

#### 4.2.1.2 Plant Data

Plant data for roll transition PWSCC of steam generator tubes at San Onofre Unit 2, McGuire Unit 2, and Catawba Unit 1 were evaluated to determine if there were correlations between the occurrence of PWSCC and coolant hydrogen concentrations.[35] No correlations were observed. The analysis was limited by the following factors:

- Changes in material condition (due to peening) over time
- Changes in detection methods over time
- Limited changes in hydrogen concentrations

The data do not support any correlation between hydrogen and PWSCC initiation, although these limiting factors make it difficult to rule out a hydrogen effect.

#### 4.2.1.3 Conclusions Regarding Initiation

Although an effect of hydrogen concentration on PWSCC initiation rates cannot be ruled out, there appear to be no data supporting the existence of such a correlation within the hydrogen concentration range under consideration (5 – 80 cc/kg). (At concentrations below this range, there is a basis for concluding that rates decrease substantially as hydrogen concentrations are lowered below 5 cc/kg.[33, 34]) Therefore, changes in hydrogen concentration within the range under consideration are not expected to significantly influence the rate of PWSCC initiation.

### 4.2.2 PWSCC Propagation

The most significant set of crack propagation data is that generated by Morton et al. (for example, Reference [4]). This data set was generated in deaerated high purity water. A limited set of confirmatory tests in typical PWR primary water chemistry (600 ppm B as boric acid, 2.2 ppm Li as lithium hydroxide) has been reported [27] and are consistent with the high purity water results.

A typical data set for crack growth rates in Alloy 600 in deaerated water is shown in Figure 4-4. Based on data sets like these, Andresen et al. [27] reformulated the original model proposed by Attanasio et al. [4] to describe the dependence of crack growth rates on hydrogen concentrations as follows:

$$V = 1 + (P - 1)e^{-0.5 \left( \frac{\Delta\phi - \phi_{offset}}{\lambda(0.46)^{\frac{1}{P}}} \right)^2} \quad \text{Eq. 4-2}$$

with the following parameter definitions:

- $V$  is the relative crack growth rate (measured rate divided by the rate far from the nickel-nickel oxide transition)

Effects of Hydrogen Concentration on PWSCC

- $P$  is a fitted parameter describing the magnitude of the effect of hydrogen concentration (essentially the peak height in Figure 4-4, for example)
- $\Delta\phi$  is the difference in electrochemical potential between the hydrogen concentration and the nickel/nickel oxide transition
- $\lambda$  is a fitted parameter describing the rapidity with which the hydrogen effect lessens away from the nickel-nickel oxide transition (related to the peak width in Figure 4-4, for example)
- $\phi_{\text{offset}}$  is the potential difference between the peak potential (in Figure 4-4, for example) and the nickel-nickel oxide potential

Andresen et al. conclude that the available data do not indicate a significant effect from the offset parameter,  $\phi_{\text{offset}}$ , and therefore recommend the following simplified equation:

$$V = 1 + (P - 1)e^{-0.5 \left( \frac{\Delta\phi}{\lambda(0.46)^{\frac{1}{P}}} \right)^2} \quad \text{Eq. 4-3}$$

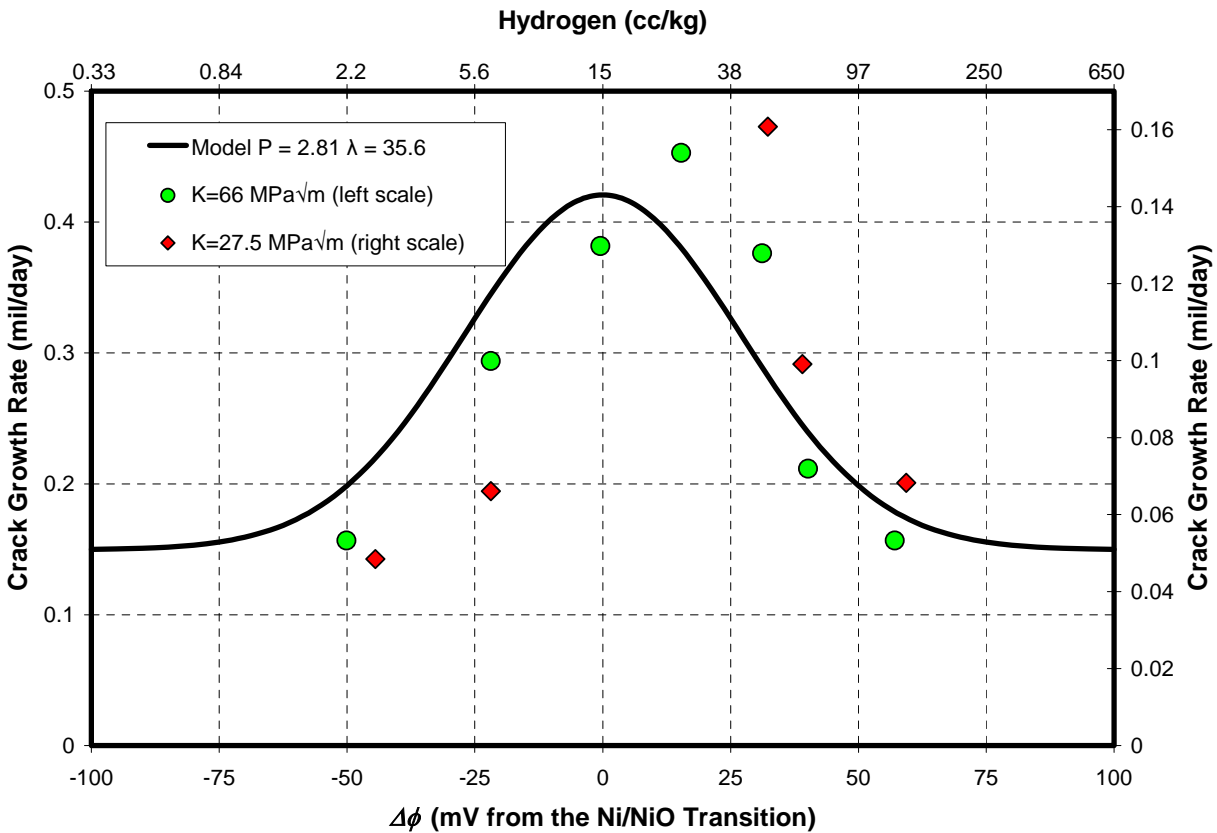


**Figure 4-4**  
Crack Growth Rates: Alloy 600, Pure Water, 338°C [36]

In Equation 4-3, the hydrogen concentration is represented by the difference in potential between that generated by the hydrogen concentration and the nickel-nickel oxide equilibrium. This relationship is expressed by the following equation:

$$\Delta\phi = 29.58 \left( \frac{T_K}{T_{ref}} \right) \log \left( \frac{[H_2]}{[H_2]_{Ni/NiO}} \right) \quad \text{Eq. 4-4}$$

with the following additional parameter definitions:

- $T_K$  is the absolute temperature
- $T_{ref}$  is the reference temperature 298.15 K (25°C)
- $[H_2]$  is the hydrogen concentration in the water
- $[H_2]_{Ni/NiO}$  is the hydrogen concentration at the nickel-nickel oxide transition at  $T_K$

Note that because the hydrogen concentration enters as a ratio, the units of measure are not relevant.

The hydrogen concentration at the nickel-nickel oxide transition is given in Reference [27] based on data from Reference [4] as follows:

$$[H_2]_{Ni/NiO} = 10^{(0.0111T_c - 2.59)} \quad \text{Eq. 4-5}$$

where  $T_c$  is the temperature in °C and the hydrogen concentration is given in cc/kg.

The usefulness of this formulation is shown in Figure 4-4, Figure 4-5, and Figure 4-6, where the same values of  $P$  and  $\lambda$  are shown with data from three independent research laboratories.

## Effects of Hydrogen Concentration on PWSCC

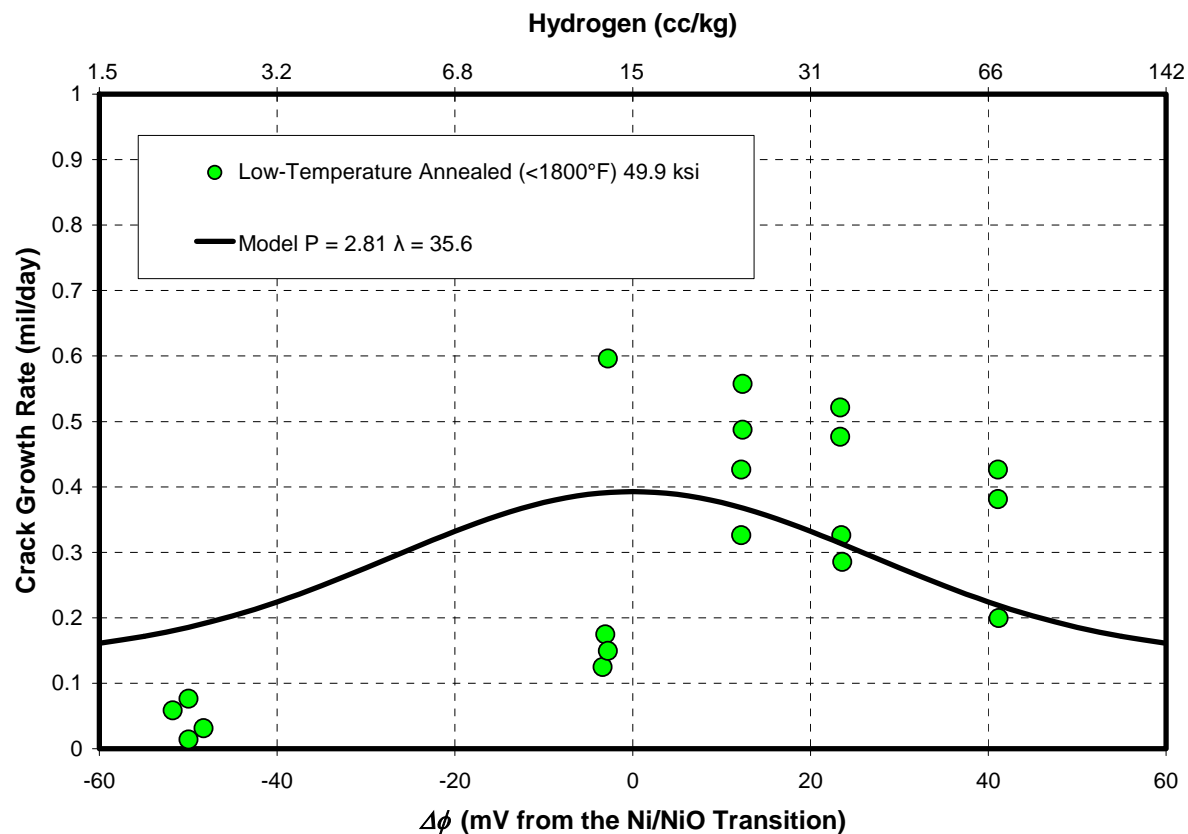


**Figure 4-5**  
Crack Growth Rates: Alloy 600, Pure Water, 338°C [37]

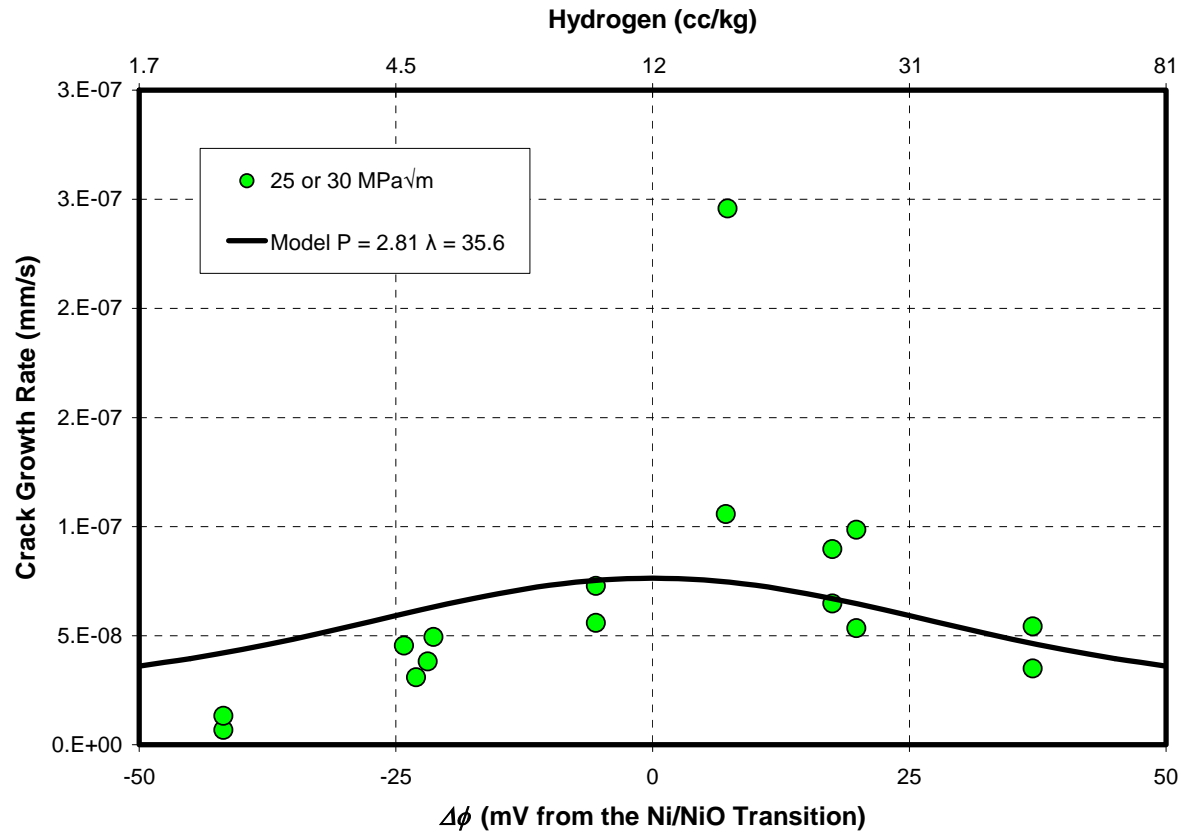


**Figure 4-6**  
Crack Growth Rates: Alloy 600, 1200 ppm B, 2.2 ppm Li, 330°C [34]

### 4.3 Specific Parameter Values

The MRP recommends the use of the values for  $P$  and  $\lambda$  (see Equation 4-3) given in Table 4-1, which are based on Reference [4]. Data typical of those from which these parameters were derived are shown in Figure 4-7, Figure 4-8, and Figure 4-9.

**Table 4-1**  
SCC Parameter Values for Various Materials [27]

Material	P	$\lambda$
EN82H	8.09	20.2
Alloy 600	2.81	35.6
Alloy X-750 HTH	4.89	20.4
Alloy X-750 AH	7.19	40.0

## Effects of Hydrogen Concentration on PWSCC

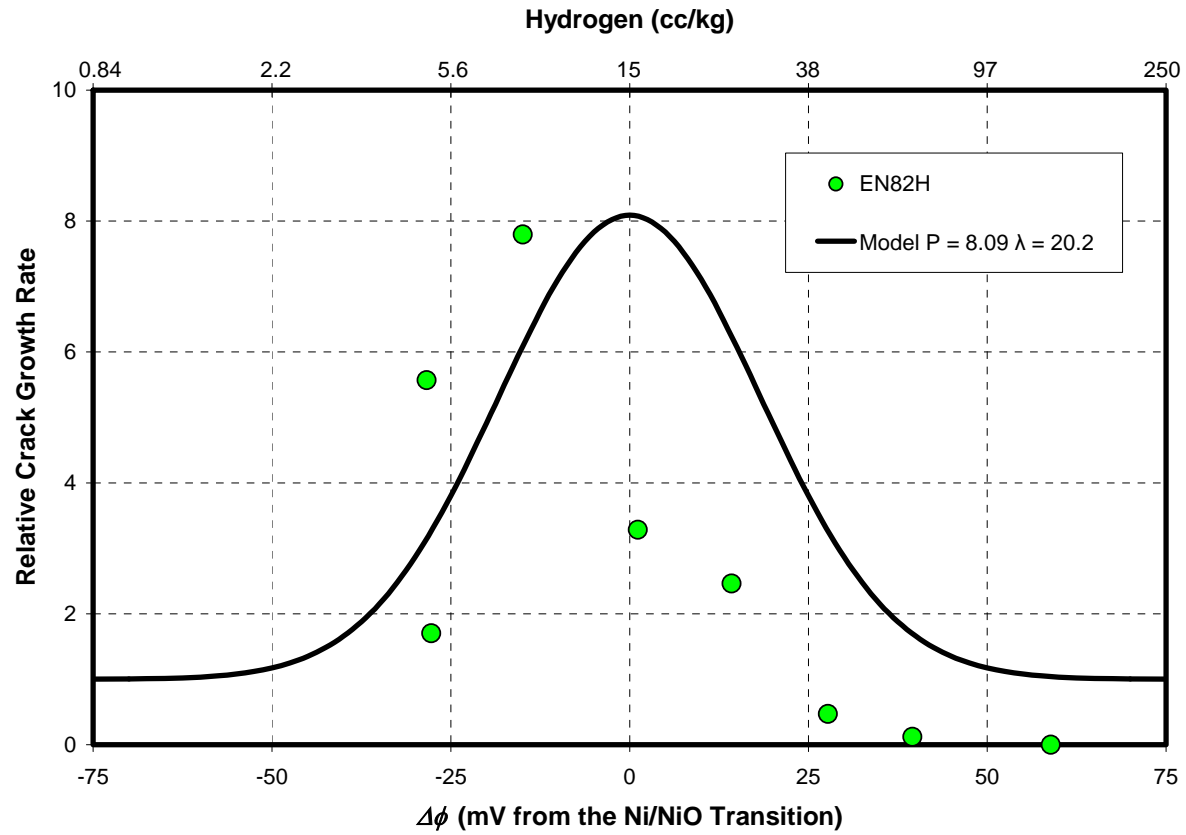
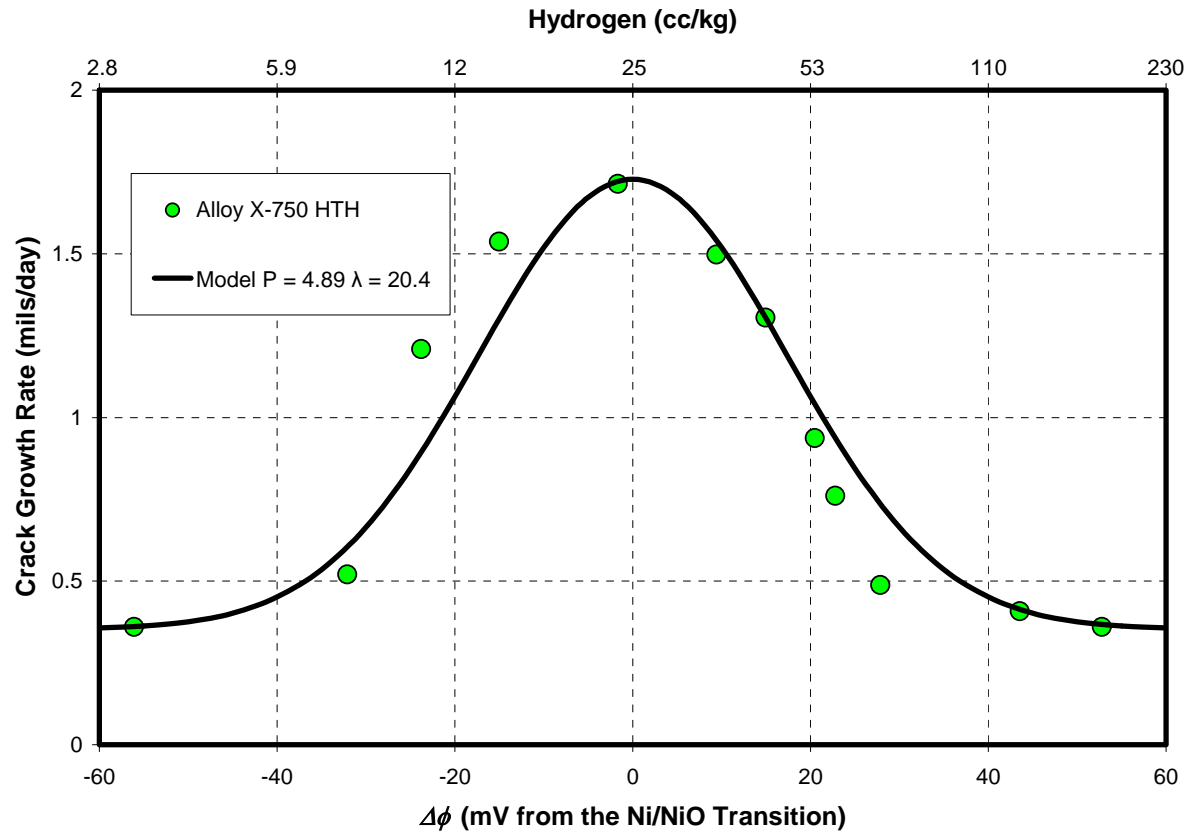
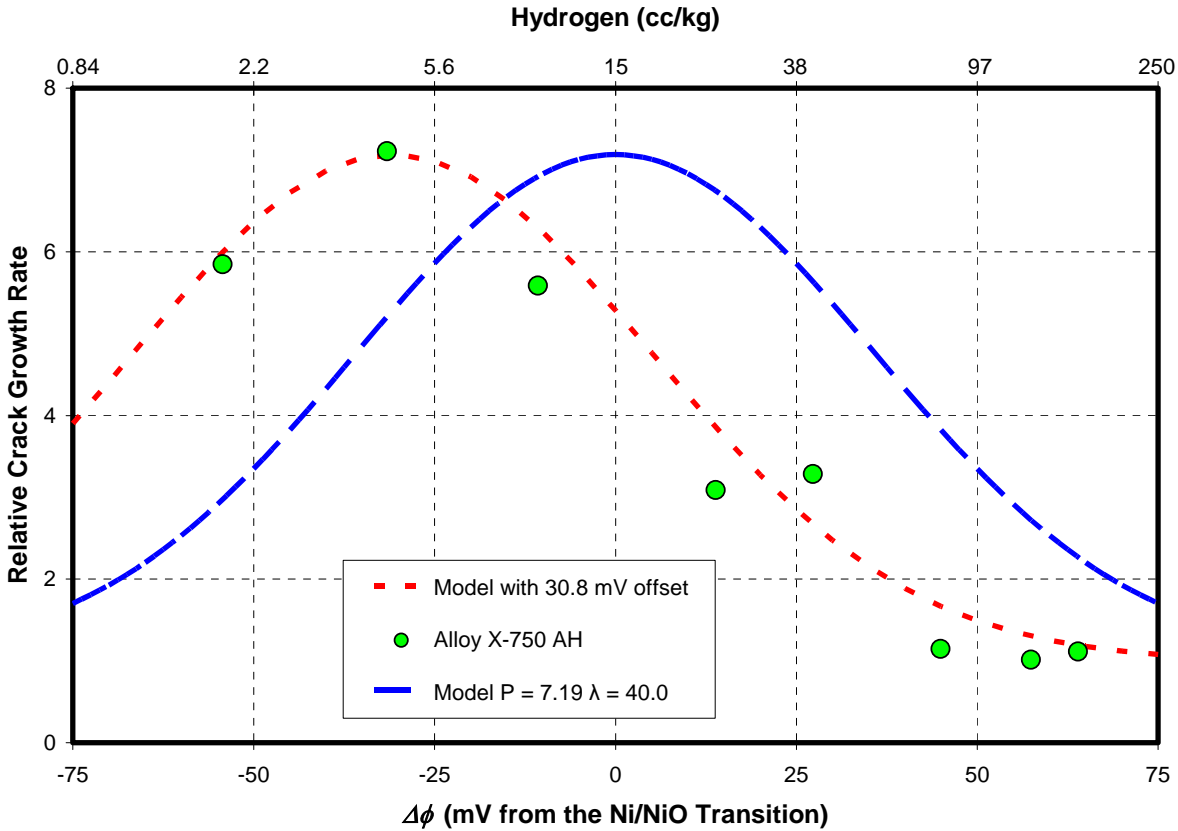


Figure 4-7  
Crack Growth Rates: Weld Metal EN82H, Pure Water, 338°C [4]



**Figure 4-8**  
Crack Growth Rates: Alloy X-750 HTH, Pure Water, 360°C [36]



**Figure 4-9**  
Crack Growth Rates: Alloy X-750 AH, Pure Water, 338°C [4]

#### 4.4 Factors of Improvement for Specific Changes

In evaluating the effects of changes in primary coolant hydrogen concentrations, it is convenient to use a *factor of improvement* (FOI). The factor of improvement for a specific change is defined by the following equation:

$$FOI = \frac{V_{old\ condition}}{V_{new\ condition}} \quad \text{Eq. 4-6}$$

( $V_{old\ condition}$  and  $V_{new\ condition}$  can be calculated using Equation 4-2 using the old and new hydrogen concentrations, respectively. Note that a statistical assessment of the uncertainty of using Equation 4-2 was not part of the scope of this review. Caution should be used in relying on the absolute quantitative values of the predictions given here. However, it is considered appropriate to use calculations based on this model for qualitative assessments, such as determination of factors of improvement.)

For illustrative purposes, it is useful to characterize the hydrogen concentration changes that will result in no increase or decrease in SCC, i.e., the changes with  $\text{FOI} = 1$ . The trivial case is one in which the hydrogen concentration is not changed, i.e.:

$$[H_2]_{\text{new}} = [H_2]_{\text{old}} \quad \text{Eq. 4-7}$$

For this trivial case the FOI is obviously unity. Examination of Equations 4-3 and 4-6 shows that a factor of improvement equal to unity is also obtained when the following condition holds:

$$\Delta\phi_{\text{new}} = -\Delta\phi_{\text{old}} \quad \text{Eq. 4-8}$$

This condition represents “crossing the hump” in the curve of growth rate versus hydrogen from a point on the up-slope to a point of equal height on the down-slope (or vice versa). Substituting Equation 4-4 into Equation 4-8 yields the following expression for conditions with  $\text{FOI} = 1$ :

$$[H_2]_{\text{new}} = \frac{[H_2]_{\text{Ni/NiO}}^2}{[H_2]_{\text{old}}} \quad \text{Eq. 4-9}$$

Plotting Equations 4-7 and 4-9 divides the plane of new and old hydrogen concentrations into four quadrants, as shown in Figure 4-10 for the pressurizer temperature of 343°C. Also shown in Figure 4-10 are representations of changes in hydrogen concentration under consideration.

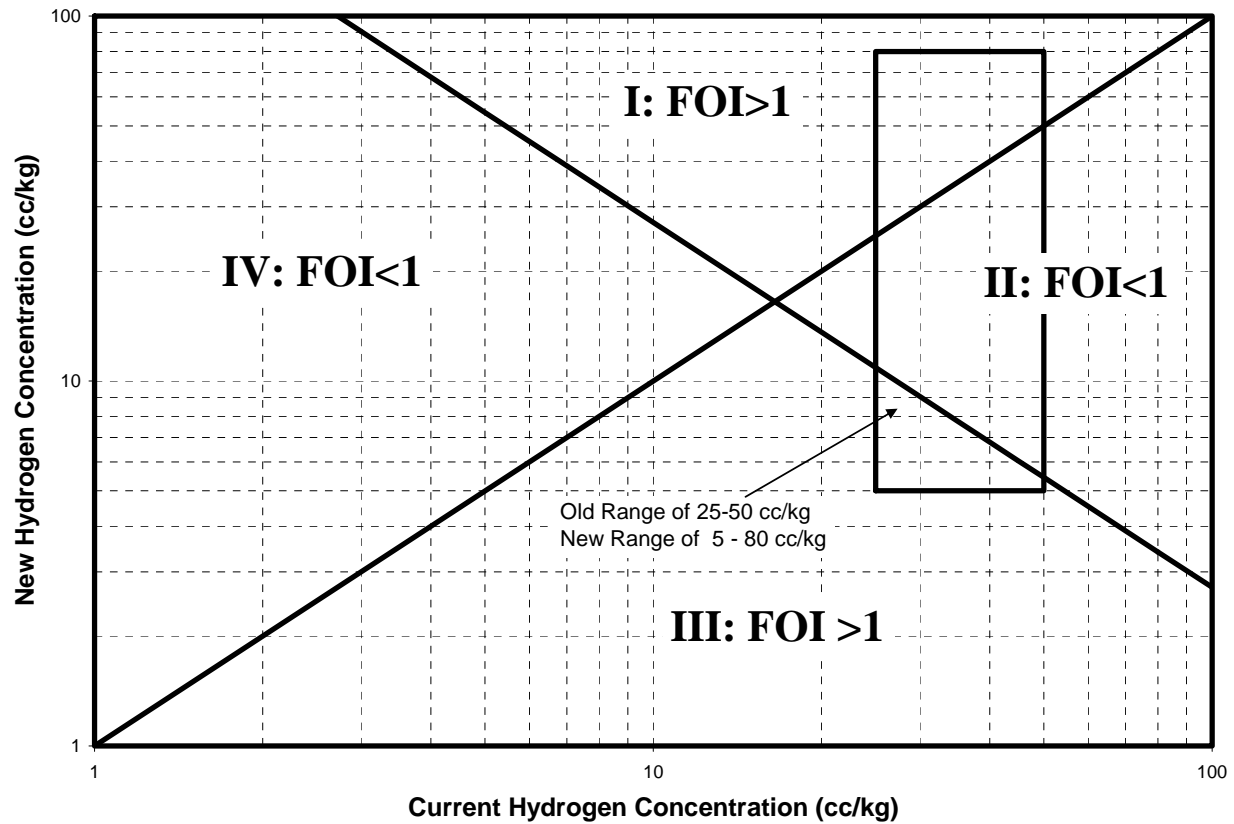


**Figure 4-10**  
**Quadrants in the New versus Old Hydrogen Concentration Plane (343°C)**

In Figure 4-10, quadrants I and IV represent increases in primary coolant hydrogen concentrations, while quadrants II and III represent decreases. The behavior of the improvement factor in each quadrant is as follows:

- Quadrant I:  $FOI > 1$ , SCC is mitigated
- Quadrant II:  $FOI < 1$ , SCC is accelerated
- Quadrant III:  $FOI > 1$ , SCC is mitigated
- Quadrant IV:  $FOI < 1$ , SCC is accelerated

Note that because Equations 4-7 and 4-9 do not contain material specific parameters, the characterization of the above quadrants is independent of material. However, the location of the line separating Quadrant I and Quadrant II from Quadrant III and Quadrant IV is dependent on the temperature, because the concentration of hydrogen corresponding to the nickel-nickel oxide transition is dependent on temperature. Plots for typical hot leg temperatures of 325°C and cold leg temperatures of 290°C are shown in Figure 4-11 and Figure 4-12.

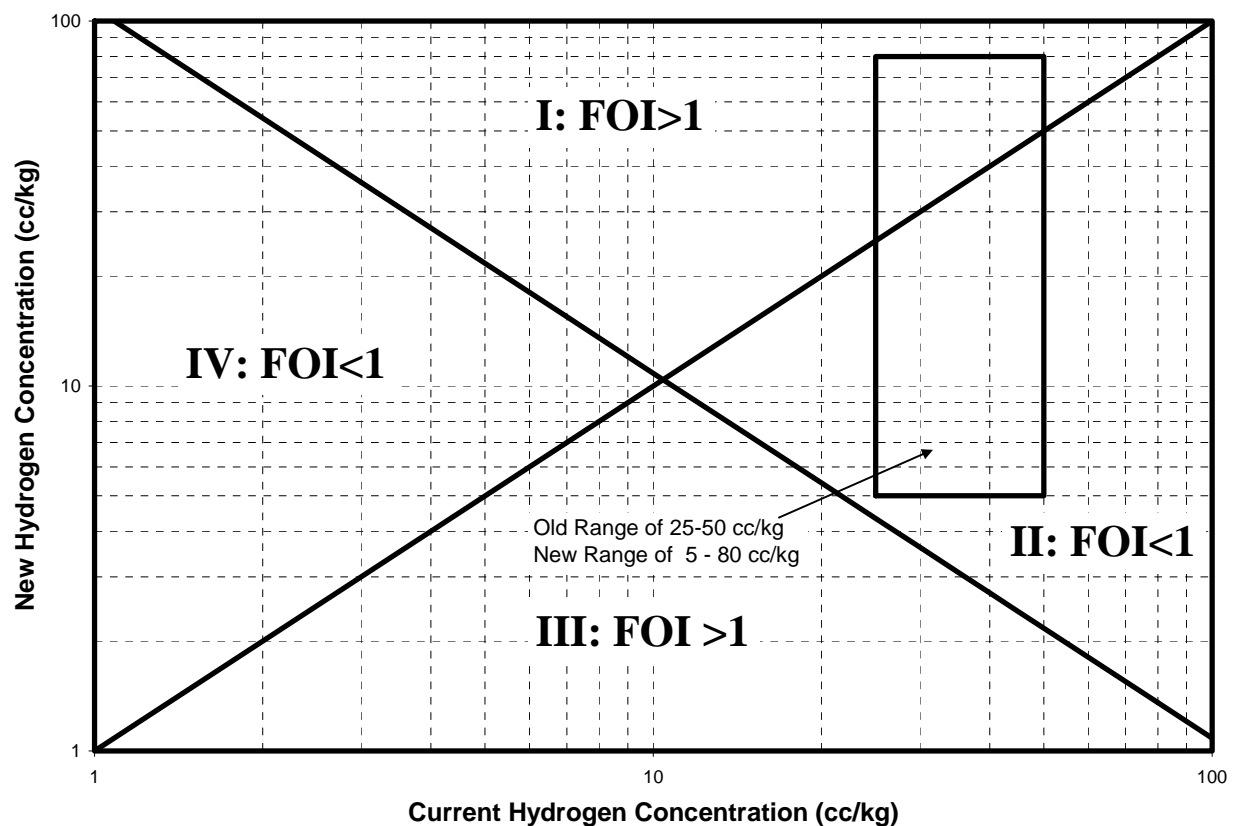


**Figure 4-11**  
**Quadrants in the New versus Old Hydrogen Concentration Plane (325°C)**

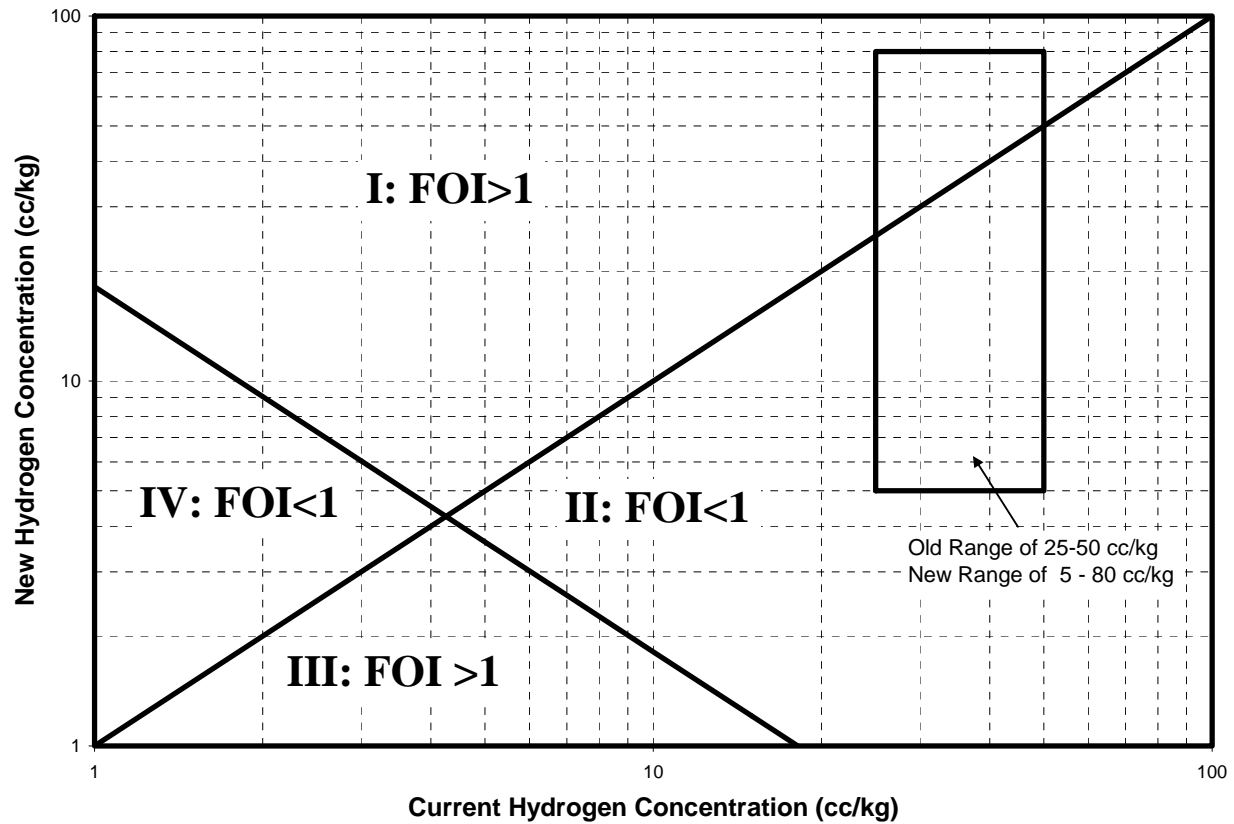


**Figure 4-12**  
**Quadrants in the New versus Old Hydrogen Concentration Plane (290°C)**

Note that the intersection of the two lines in the above figures is simply the solution obtained by combining Equations 4-7 and 4-9, which is the hydrogen concentration at the nickel-nickel oxide transition. The sliding of the intersection toward lower hydrogen concentrations corresponds to the lower hydrogen concentrations at the transition at lower temperatures. It is particularly important to note that even consideration of very low hydrogen concentrations ( $\sim 1$  cc/kg) results in factors of improvement of less than unity at 290°C. For many plants, it is likely that 5 cc/kg is the lowest possible operable concentration due to control issues, indicating (see the box in Figure 4-11) that factors of improvement for lowering hydrogen concentrations will always be less than unity (increasing SCC susceptibility) at 325°C. Figure 4-13 shows level set curves for specific factors of improvement in the new-old hydrogen plane for EN82H at 343°C. Note that the level sets for Quadrants II and IV have been omitted for clarity; they are inverses of those for Quadrants I and III, but are not of practical concern because they represent changes that increase crack growth rates. Figure 4-14 shows the data predictions plotted in linear space. Figure 4-15 through Figure 4-18 show similar predictions at 325°C and 290°C, respectively for EN82H. Note that factors of improvement in the relevant regions will be considerably less for Alloy 600 because 1) the value of  $P$  is less, indicating that the magnitude of the hydrogen effect is less and 2) because  $\lambda$  is larger, indicating that equivalent FOI can be achieved only with larger changes in hydrogen concentration.

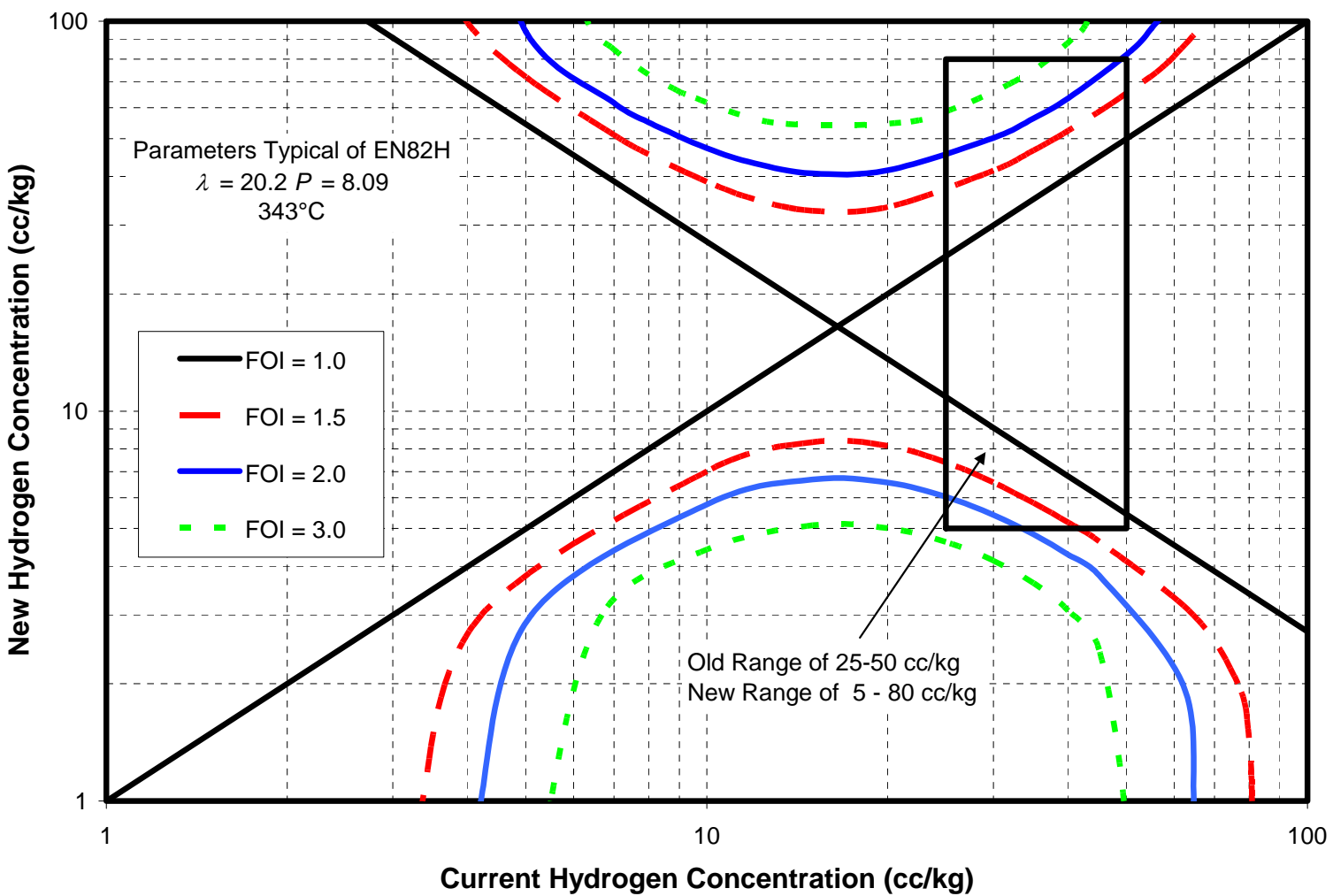


Figure 4-13  
 Factors of Improvement, EN82H, 343°C (log-log plot)

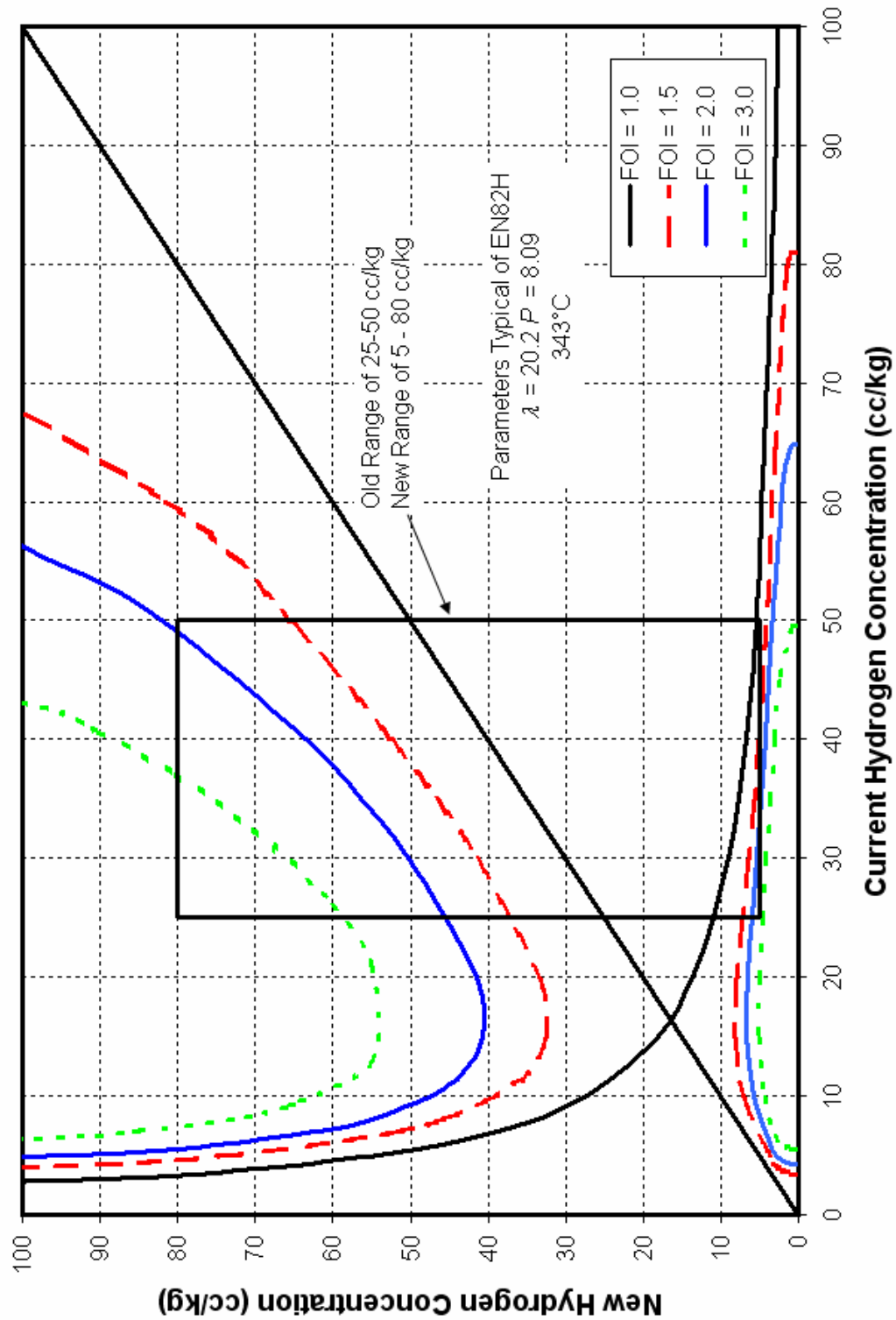


Figure 4-14  
Factors of Improvement, EN82H, 343°C (linear plot)

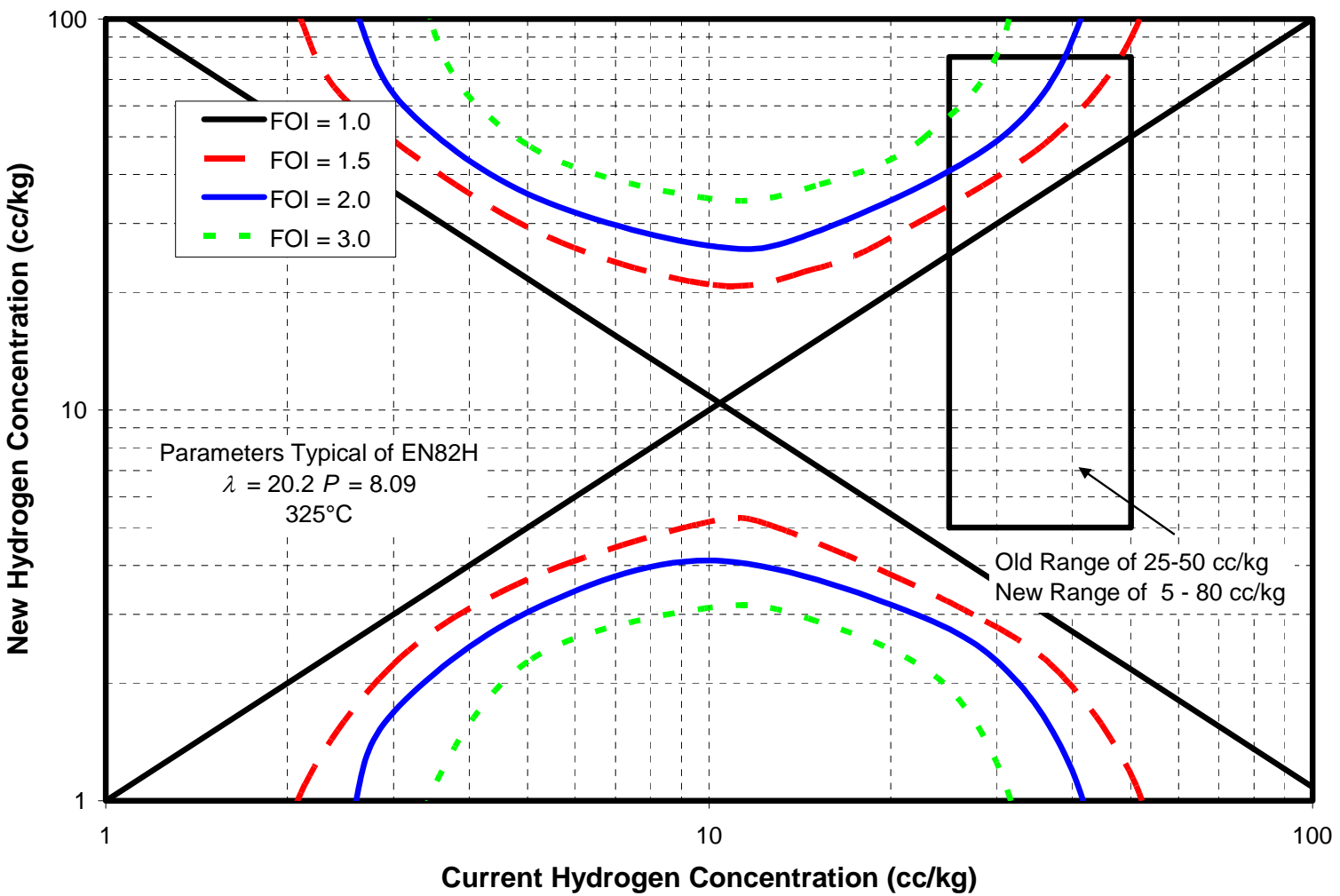


Figure 4-15  
Factors of Improvement, EN82H, 325°C (log-log plot)

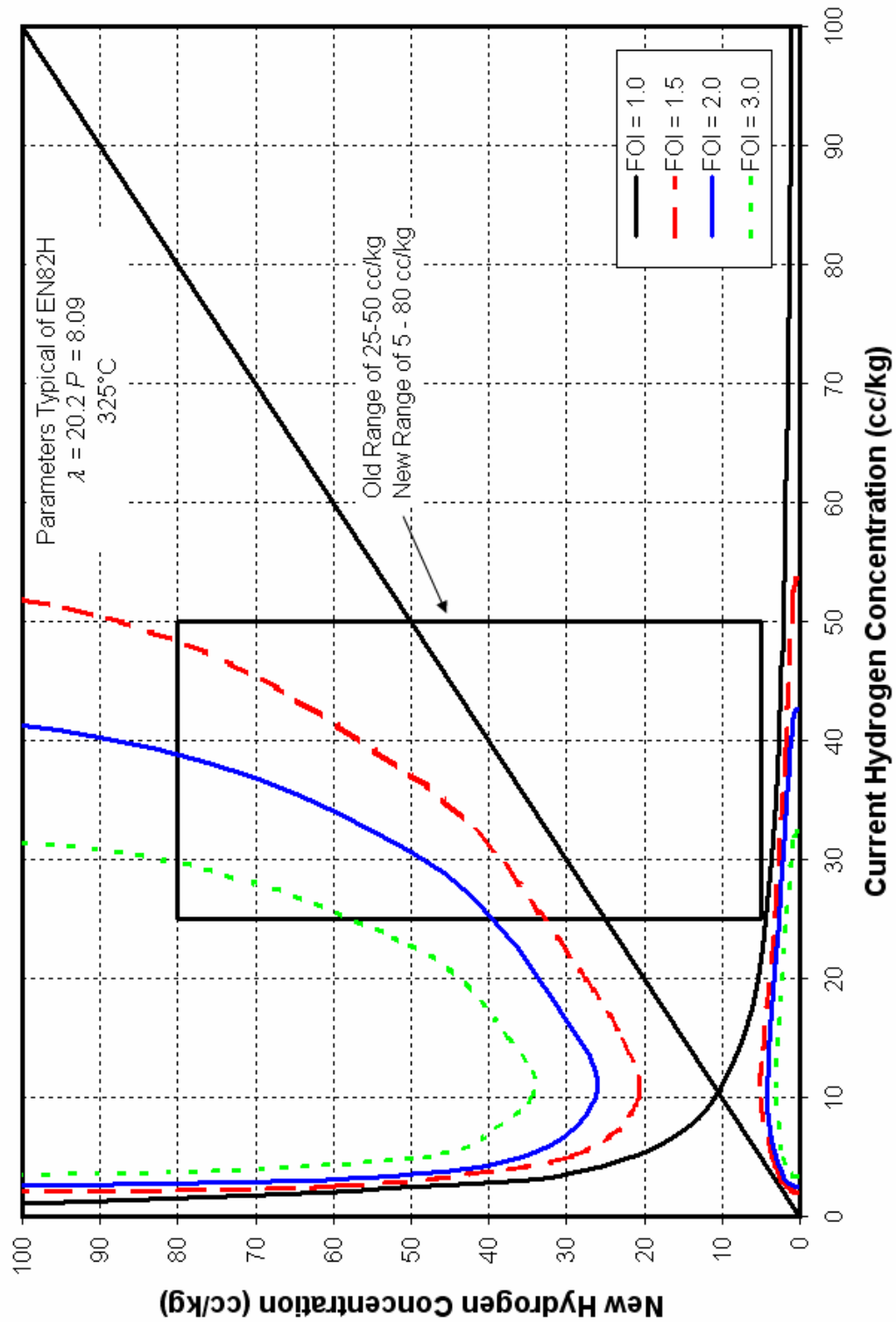


Figure 4-16  
 Factors of Improvement, EN82H, 325°C (linear plot)

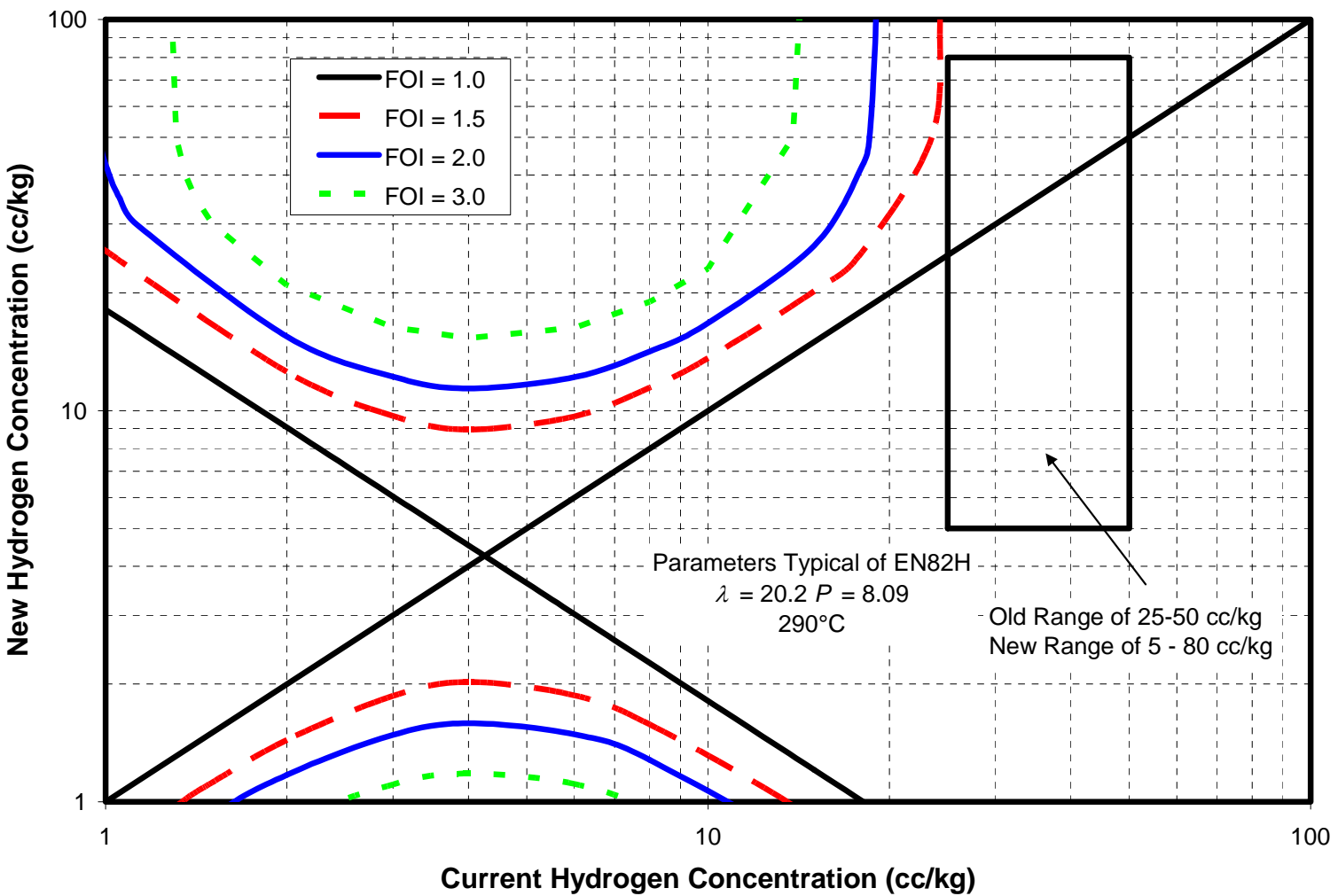


Figure 4-17  
Factors of Improvement, EN82H, 290°C (log-log plot)

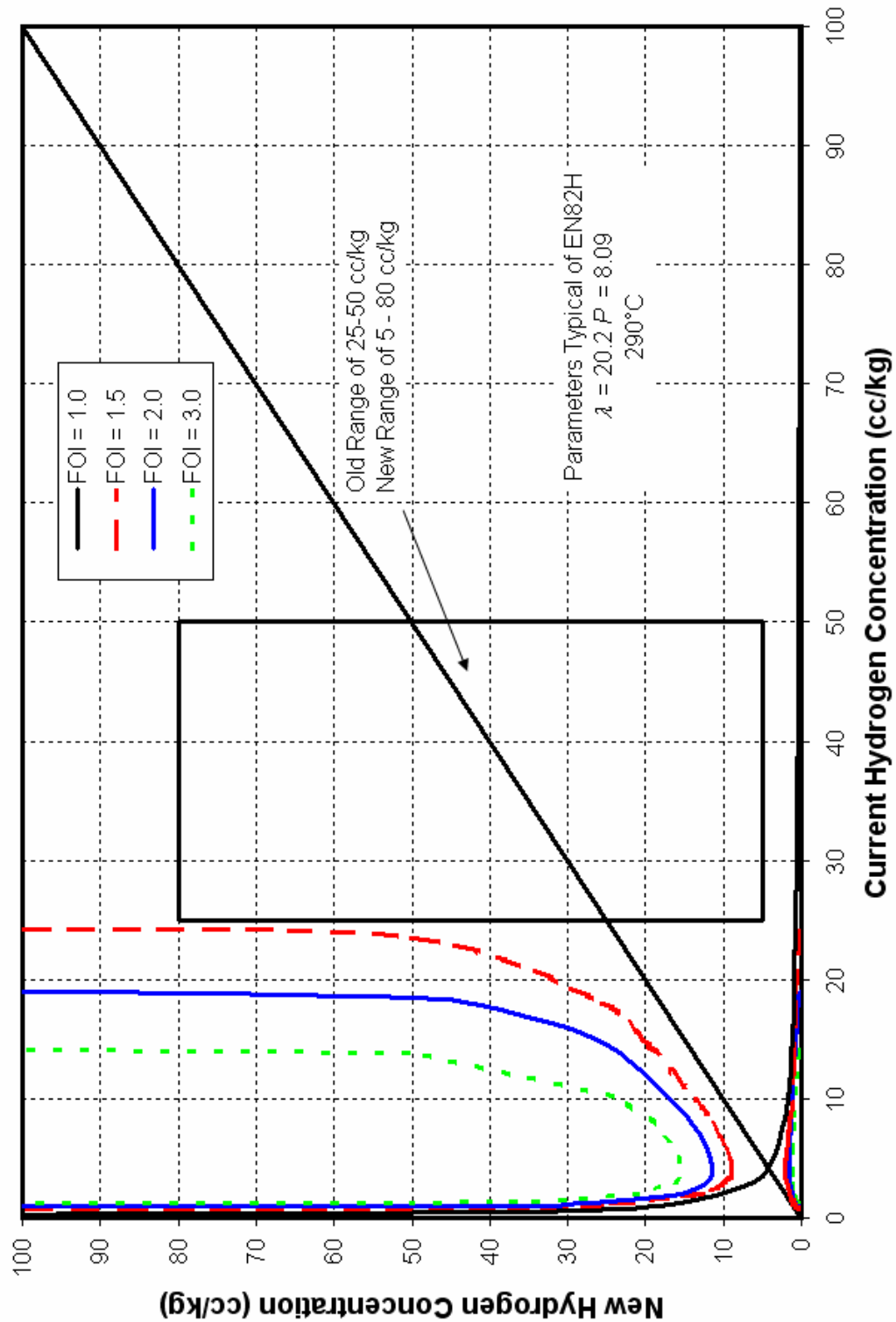


Figure 4-18  
 Factors of Improvement, EN82H, 290°C (linear plot)

An alternate method of displaying factor of improvement values is to select a reference “old” condition with which to compare changes. This has the disadvantage of being valid for only one reference concentration, but the advantage of being simpler. Figure 4-19 and Figure 4-20 show factors of improvement for EN82H relative to performance at 35 cc/kg at three different temperatures. Figure 4-21 and Figure 4-22 show similar predictions for Alloy 600.

Numerical values of factor of improvement calculated per the equations given above are given in Appendix A.

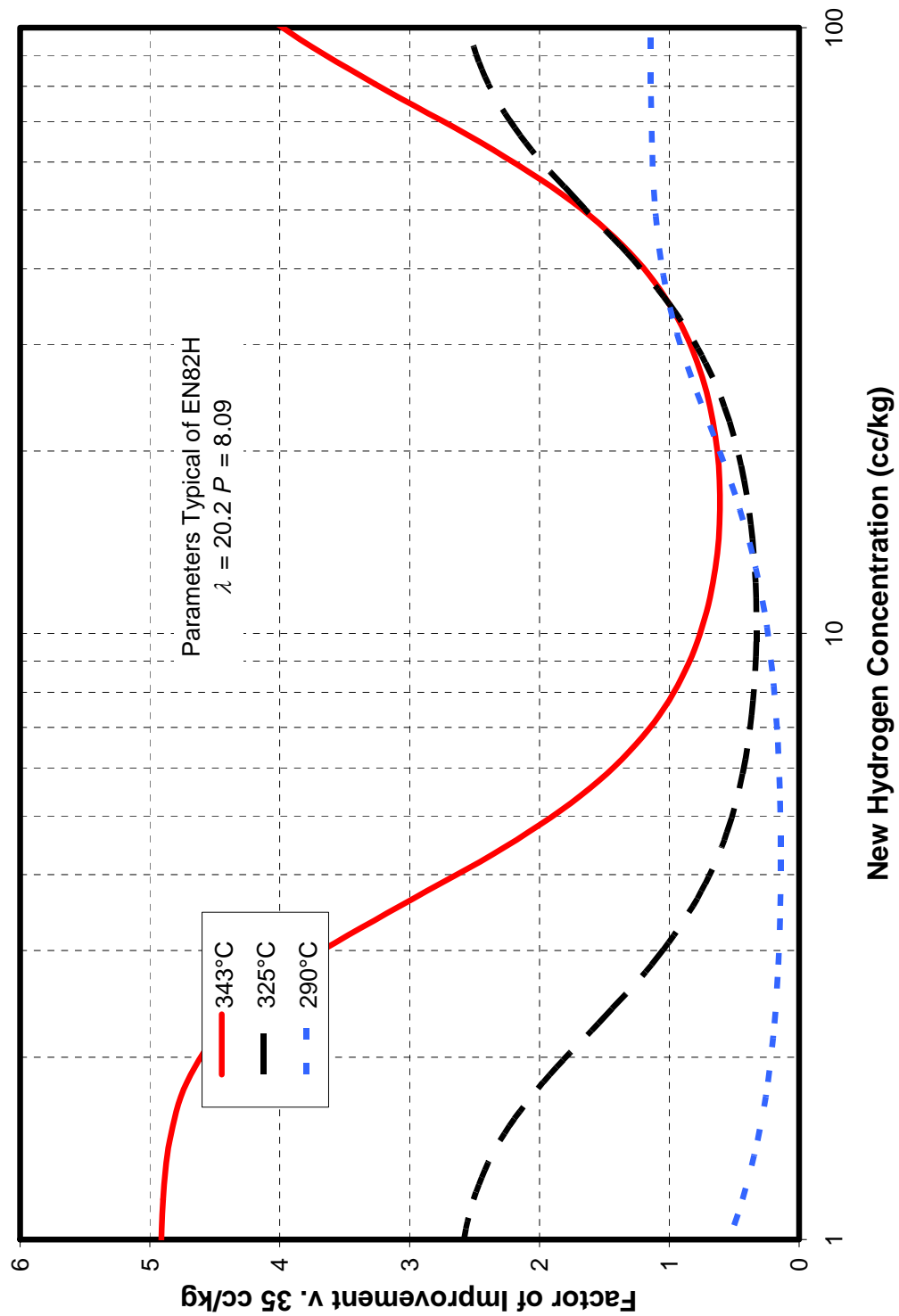


Figure 4-19  
Factors of Improvement versus 35 cc/kg, EN82H (log plot)

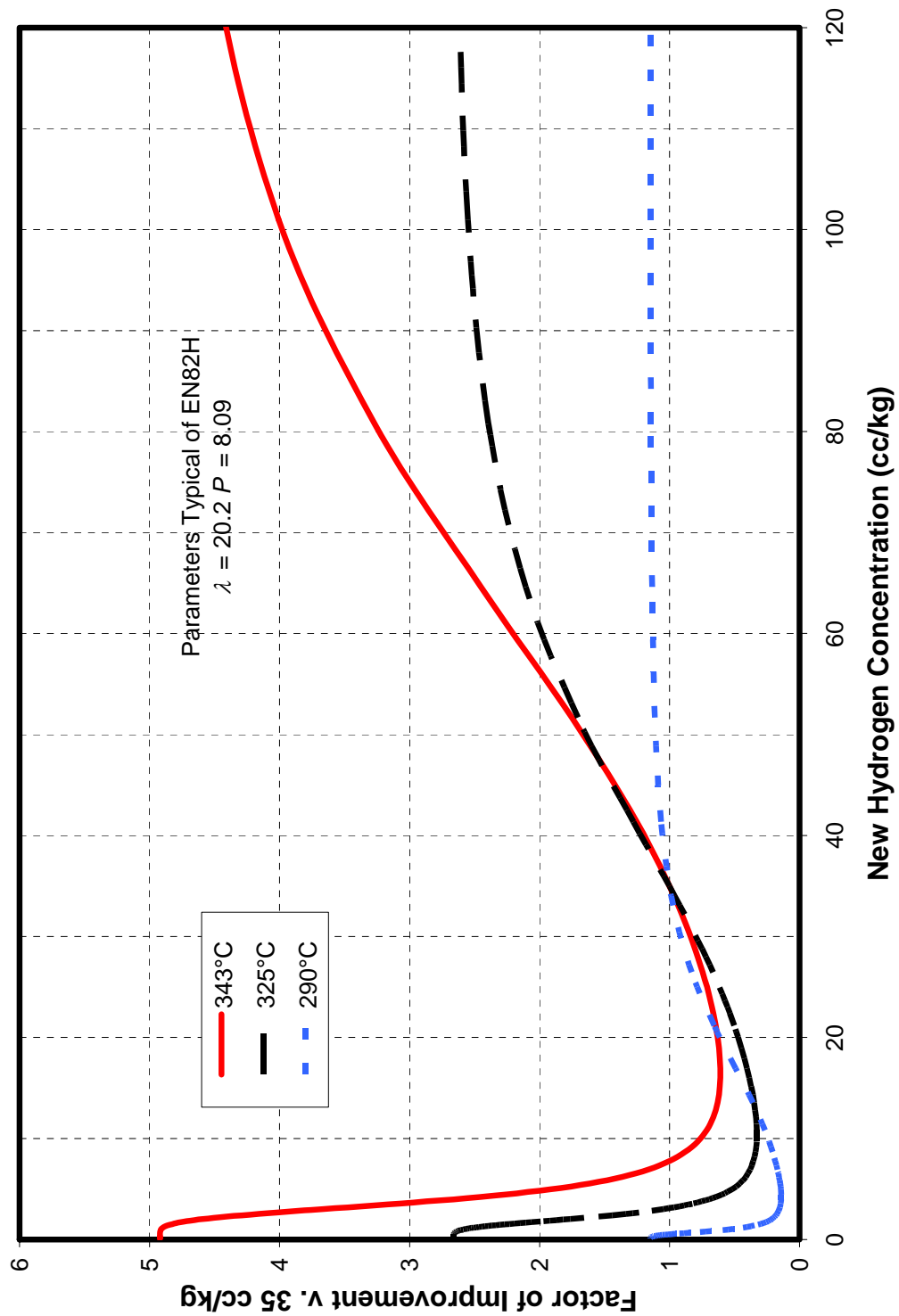


Figure 4-20  
Factors of Improvement versus 35 cc/kg, EN82H (linear plot)

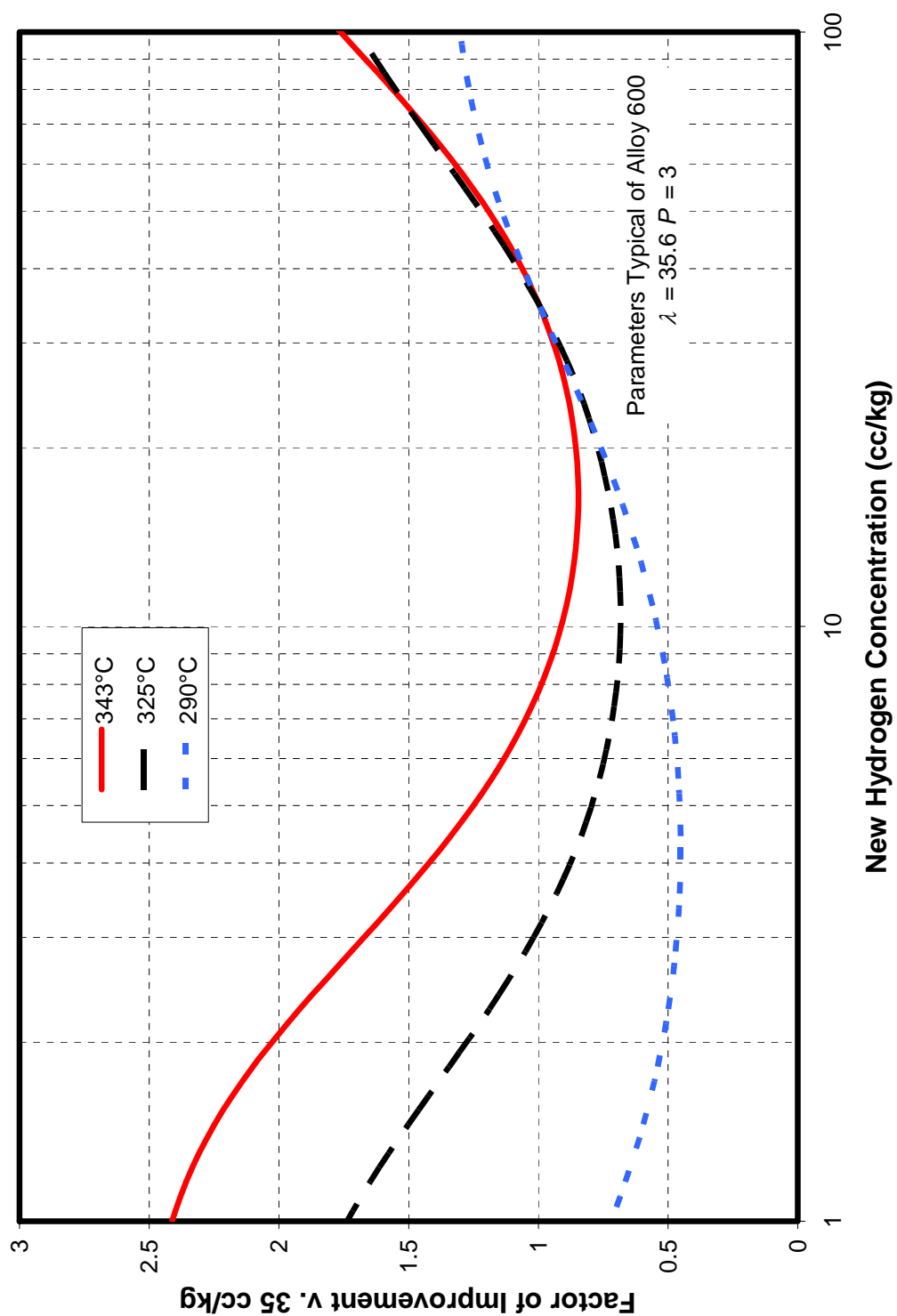


Figure 4-21  
Factors of Improvement versus 35 cc/kg, Alloy 600 (log plot)

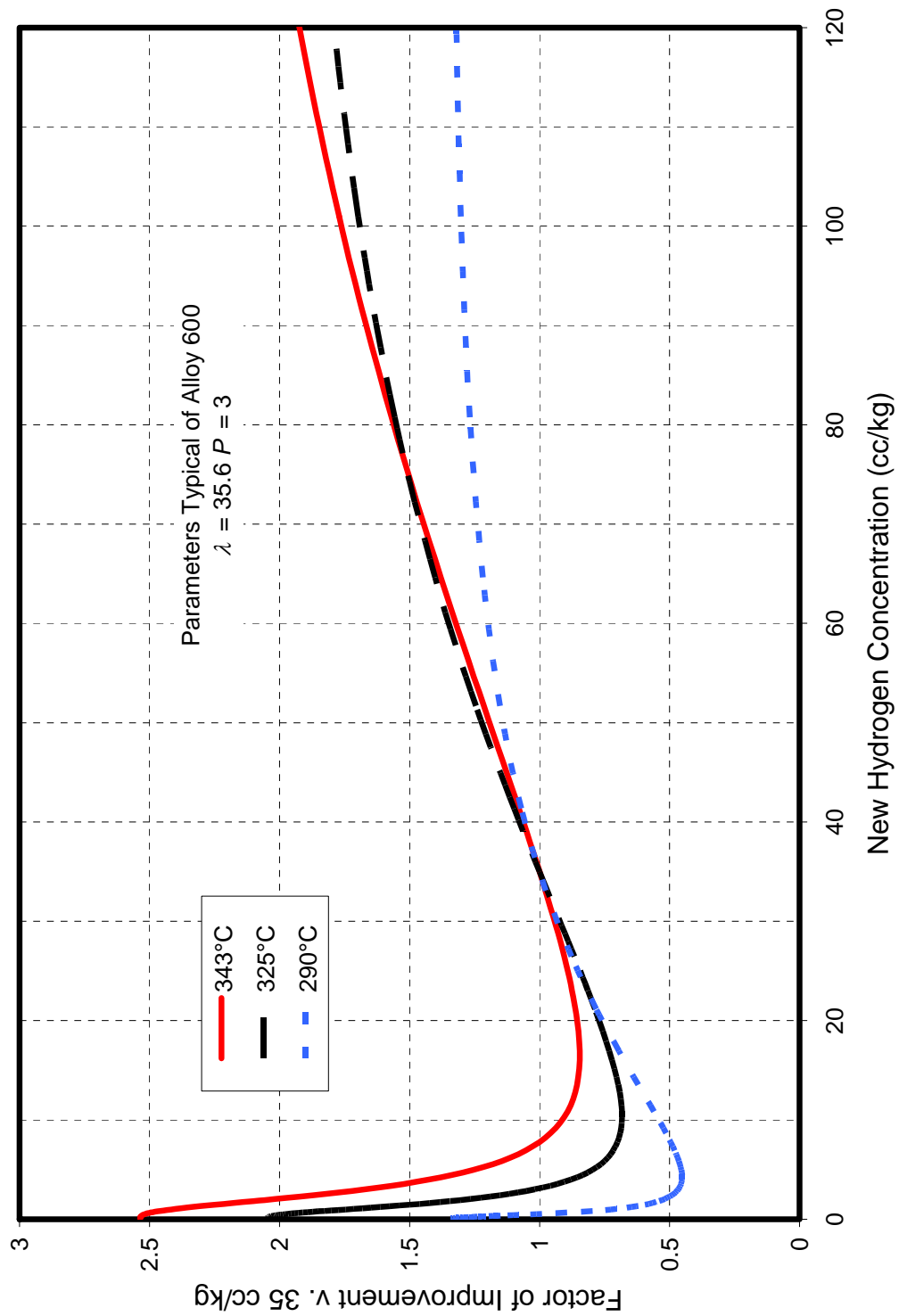


Figure 4-22  
Factors of Improvement versus 35 cc/kg, Alloy 600 (linear plot)

## **4.5 Areas for Further Research**

The following sections discuss knowledge gaps representing opportunities for increased understanding.

### **4.5.1 Relevance of the Nickel-Nickel Oxide Transition**

The exact mechanism by which the nickel-nickel oxide transition affects stress corrosion cracking is not known. Protective inner oxide films on nickel alloys are generally observed to be chromium ferrites, enriched in chromium and depleted in nickel relative to the base metal. This observation would lead to the conclusion that the formation of nickel oxide is not an important factor in the corrosion of these materials. Hypotheses for why nickel oxide might affect corrosion of nickel alloys include the following:

- The formation of a metastable nickel oxide film may be the first step in corrosion of nickel alloys.[4]
- The depletion of nickel in the protective oxide film may be governed by the formation of nickel oxide.

The determination of the mechanism by which the formation (or lack of formation) of nickel oxide is related to SCC would provide insights required to assess the applicability of the currently available observations to other alloys and to better understand the effects of heat treatment or previous passivation. These insights might also lead to a better understanding of the effect of zinc on SCC, since it is suspected that zinc also mitigates SCC of nickel alloys through modification of the protective oxide film.

### **4.5.2 Effect of Material Condition**

At least one investigation [37] has shown that cold work can reduce the improvements gained by moving to lower hydrogen concentrations. Figure 4-23 shows one data set that indicates that cold worked Alloy 600 has increasing susceptibility to SCC below the nickel-nickel oxide transition, resulting in a monotonic increase in crack growth rates with decreasing hydrogen concentrations.

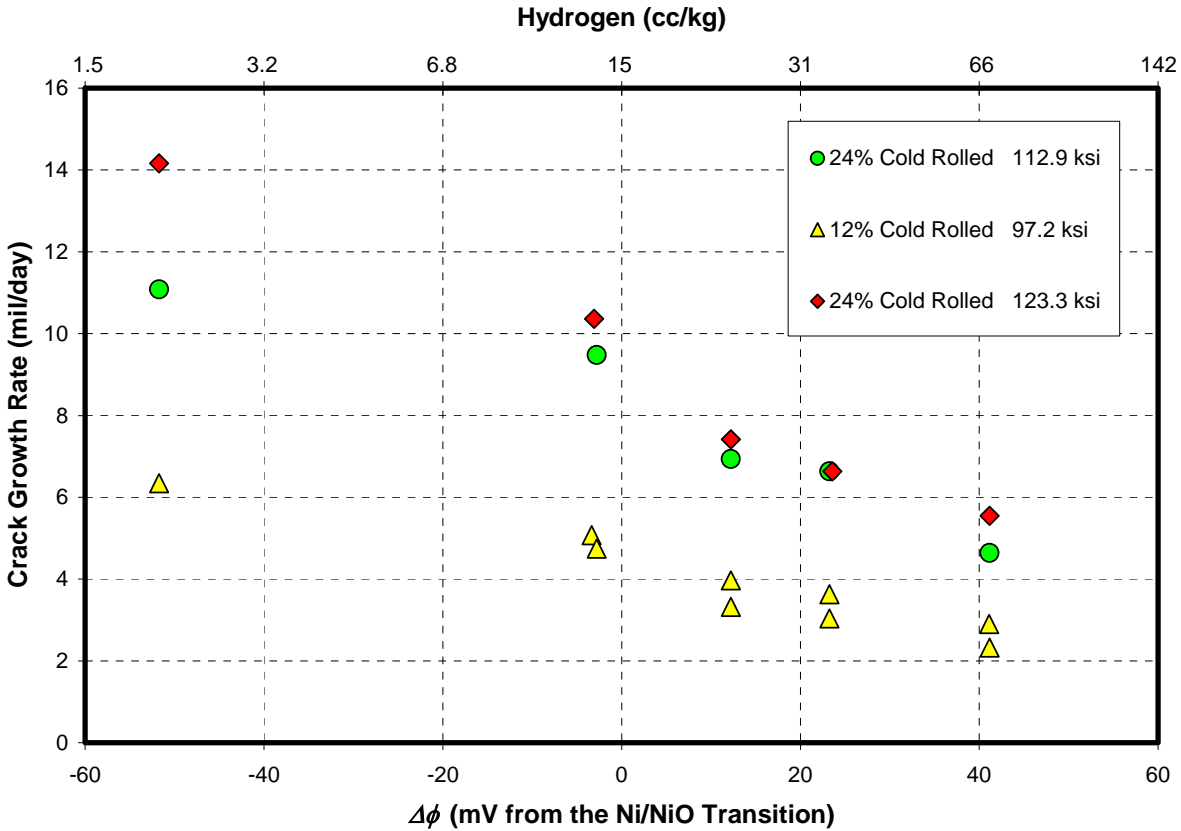


**Figure 4-23**  
**Crack Growth Rates: Alloy 600, Pure Water, 338°C [37]**

Since components to be targeted by chemical mitigation can often be cold worked (e.g., welds that have been ground) an understanding of this effect is important to assessing the actual benefits that might be obtained from moving to lower hydrogen concentrations. (Data currently available indicate that the benefit from higher hydrogen concentrations is not as strongly affected by cold work, as shown in Figure 4-23.)

#### 4.5.3 Other Alloys

In general, Alloy 690 and its weld metals have not been as thoroughly investigated as Alloy 600 and its weld metals with respect to the effects of hydrogen concentration on SCC. The limited data that are available [38] indicate that for one heat of Alloy 690, CGRs are increased at 338°C when hydrogen is increased from 23 to 50 cc/kg for stress intensities less than about 30 MPa $\sqrt{\text{m}}$ . Since many replacement components are constructed of Alloy 690, its behavior as a function of hydrogen is an important component of hydrogen optimization.

#### **4.5.4 Interaction With Zinc**

Zinc injection is currently being used as a PWSCC mitigation strategy in PWR primary systems. The possible interaction of zinc and elevated hydrogen is being explored in a current EPRI research effort (see Section 11.3). In the evaluation of elevated hydrogen concentration approaches, it is important to determine the effect of any such strategy on the mitigation of PWSCC by zinc.

#### **4.5.5 Incorporation Into More Comprehensive Models**

Numerous attempts [39, 40, 41] have been made to incorporate the hydrogen effect into a more comprehensive model of crack growth rate. These attempts have met with limited success in modeling industry databases of crack growth rate data. Nevertheless, there is significant usefulness in increasing the understanding of how hydrogen concentration relates to other factors that affect crack growth rates such as stress intensity, material properties, and temperature.

#### **4.5.6 Data Compilation**

As is evident from the discussions in Sections 4.2.1 and 4.2.2, numerous investigators have studied the initiation and propagation of PWSCC in nickel alloys. The data used in the analysis of factors of improvement in Section 4.4 have been based on those compiled in Reference [27]. However, this compilation is not complete and does not address initiation data. A comprehensive collection and analysis of all of the crack growth rate and initiation data available for these materials at varying hydrogen concentrations would provide further support of the conclusions discussed in Section 4.6.

### **4.6 Conclusions**

Based on the data available in the literature, crack growth rates in nickel alloys (and, at least qualitatively, crack initiation rates) can be reduced by optimizing hydrogen concentration in the primary coolant. Factors of improvement for a limited number of changes are given in Table 4-2. (Note that these are calculated values and that no attempt has been made to establish the correct number of significant figures for these values.)

**Table 4-2**  
**Example Factors of Improvement**

Hydrogen (cc/kg)		EN82H			Alloy 600		
New	Old	290°C	325°C	343°C	290°C	325°C	343°C
5	25	0.18	0.84	2.66	0.54	0.94	1.40
5	37.5	0.14	0.46	1.73	0.45	0.77	1.21
5	50	0.13	0.31	1.14	0.41	0.66	1.05
25	37.5	0.76	0.56	0.65	0.84	0.82	0.87
25	50	0.71	0.38	0.43	0.77	0.70	0.75
50	25	1.41	2.66	2.34	1.31	1.43	1.33
50	37.5	1.08	1.48	1.52	1.10	1.17	1.15
80	25	1.45	3.87	4.54	1.43	1.79	1.73
80	37.5	1.11	2.15	2.96	1.20	1.46	1.50
80	50	1.03	1.45	1.94	1.09	1.25	1.30

Based on the predicted factors of improvement given in Table 4-2, discussed in Section 4.4, and presented in detail in Appendix A, the following conclusions can be made:

- At high temperatures (343°C), reasonably useful factors of improvement can be achieved with relatively modest increases in the upper limit of the operating band (e.g., changing from 50 to 55 or 60 cc/kg to allow operation at 50 cc/kg). Larger increases provide larger factors of improvement.
- At intermediate temperatures (325°C), significant factors of improvement are achievable by moving from the lower end of the current operating band (25 cc/kg) to the higher end (50 cc/kg). Significant factors of improvement relative to the current upper operating limit (50 cc/kg) would require fairly large increases in hydrogen concentration (e.g., changing from 50 cc/kg to 80 cc/kg would result in a factor of improvement of  $\leq 2$ ).
- At lower temperatures (290°C), there appears to be no advantage to increasing hydrogen concentration above the current operating limits. Predictions indicate that even at the lower end of the current operating band (25 cc/kg), infinite increases in hydrogen concentration would result in factors of improvement (for EN82H) of less than 1.5 (for Alloy 600 slightly higher FOI could be realized for infinite increases, but these FOI still would not approach 2).
- Reducing hydrogen concentrations to some level greater than 5 cc/kg (i.e., adopting 5 cc/kg as a lower operating limit) would result in factors of improvement of less than unity (i.e., accelerated SCC) at low and intermediate temperatures (290°C and 325°C, respectively). At high temperatures (343°C) decreasing hydrogen concentrations provides moderate factors of improvement.

It should be noted that the discussions in this chapter, especially those regarding factors of improvement, do not address the separate effect of thermal activation of the rates of crack initiation and growth. Specifically, the discussions in this report treat factors of improvement at different temperatures with essentially equal weight. However, if thermal activation makes cracking at high temperatures more important, less weight would be given to factors of improvement at low temperatures. An evaluation that considered relative susceptibility of specific components (considering both temperature and stress intensities) is not within the scope of this report.

# 5

## EFFECTS OF ELEVATED DISSOLVED HYDROGEN ON FUEL INTEGRITY

---

### 5.1 Introduction

In support of the overall effort to explore changes in primary coolant hydrogen concentrations, EPRI's Fuel Reliability Program (FRP) commissioned a review of the effects of hydrogen concentration on fuel integrity and performance. Two independent reviews were performed by consultants formerly associated with Westinghouse (G. Sabol) and AREVA/Siemens (F. Garzarolli). These reviews were combined into a summary report [42], which formed the basis of much of the discussion in this chapter.

The FRP identified the following three mechanisms by which increases in hydrogen concentration might affect fuel integrity or performance:

- Increased hydrogen pickup, leading to hydriding and accelerated corrosion of fuel cladding alloys during operation
- Increased risk of hydriding due to “nickel windows” during startup and early operation
- Increased crud deposition, leading to accelerated corrosion and increased risk of crud induced power shifts (CIPS) also called axial offset anomaly (AOA)

The first two effects are discussed in Section 5.2. Increased CIPS risk is discussed in Chapter 6, which discusses corrosion product transport issues more generally.

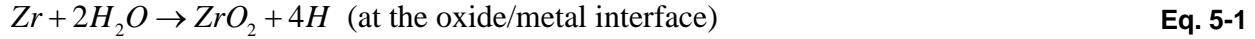
The FRP provided a recommendation regarding evaluation of the effects of increased hydrogen concentrations of fuel through laboratory and plant trials. This recommendation is discussed in Section 5.3.

In general, Reference [42] did not address the use of lower hydrogen concentrations, which is within the scope of this report. Section 5.4 discusses the possible effects on fuel from changing to lower hydrogen concentrations.

Conclusions regarding the effects of dissolved hydrogen concentration on fuel integrity and performance are given in Section 5.5.

## 5.2 Hydrogen Pickup and Hydriding

Zirconium in fuel cladding alloys is subject to the following chemical reactions when exposed to PWR environments:



Equation 5-1 represents the overall reaction responsible for typical oxidation of zirconium alloys in PWR primary systems. The mechanism of oxidation is typically thought to be oxygen vacancy diffusion, with the reaction rate limited by the rate of oxygen vacancy diffusion through the oxide layer. Equation 5-2 represents the overall reaction of zirconium hydriding. This reaction is generally thought to take place within the metal alloy (or at the metal-oxide interface), and thus requires the diffusion of hydrogen through the oxide layer. Equation 5-3 represents oxidation that might take place at the oxide/metal interface. It is discussed in Section 5.4 with regard to the possible risks of operation at low hydrogen concentrations.

Oxidation (Equation 5-1) and hydriding (Equation 5-2) are inter-related in three manners. First, the hydrogen generated in the oxidation reaction is typically the main source of hydrogen that reacts with zirconium through hydriding. Second, hydriding is generally limited by diffusion through the oxide layer, where hydrogen is much less soluble than in the metal. Thus, at least a limited amount of oxidation is required to protect against hydriding. Third, increased hydriding can lead to accelerated oxidation.[42, 48]

In this context, the main concern regarding hydrogen concentration is whether or not increased hydrogen concentrations in the reactor coolant would accelerate hydriding by increasing the concentration in the metal. This concern is generally phrased in terms of hydrogen pickup or hydrogen pickup fraction. Hydrogen pickup is the mass of hydrogen absorbed into the zirconium alloy. The pickup fraction is the ratio of the mass absorbed to the mass created by corrosion (Equation 5-1). (Some of the mass of hydrogen created by the reaction in Equation 5-1 combines to form diatomic hydrogen,  $\text{H}_2$ , which is released to the coolant.) Typically, hydrogen pickup fractions are 10-30% depending on the specific zirconium alloy. However, it is mathematically possible that the pickup fraction could exceed unity if enough hydrogen is absorbed from the coolant. The available data addressing this concern are discussed in Section 5.2.1.

Additionally, if a persistent flaw in the oxide barrier were present, increased hydrogen concentrations could lead to accelerated hydriding while such a flaw exists. This issue is discussed in Section 5.2.2.

### 5.2.1 Full Power Operation

In general, it is thought that the hydrogen that enters the zirconium alloy metal and forms hydrides is principally derived from corrosion (Equation 5-1). Data available in the literature confirm this. Figure 5-1 shows the metal hydrogen concentration of two zirconium alloys as a function of liquid hydrogen concentrations.[43] Two critical observations can be made from these data:

- The hydrogen pickup in the coolant hydrogen concentration range under consideration (e.g., up to 80 cc/kg) is only minimally increased over that which would occur in the absence of dissolved hydrogen. Note that the first two data sets in Figure 5-1 span the range 0 cc/kg to ~5000 cc/kg, nearly two orders of magnitude above the upper bound being considered.
- The hydrogen pickup as a function of coolant hydrogen concentration is strongly dependent on the specific alloy under consideration.

This last point is further supported by the slightly different behavior of a 2.5% niobium zirconium alloy, shown in Figure 5-2.[44]

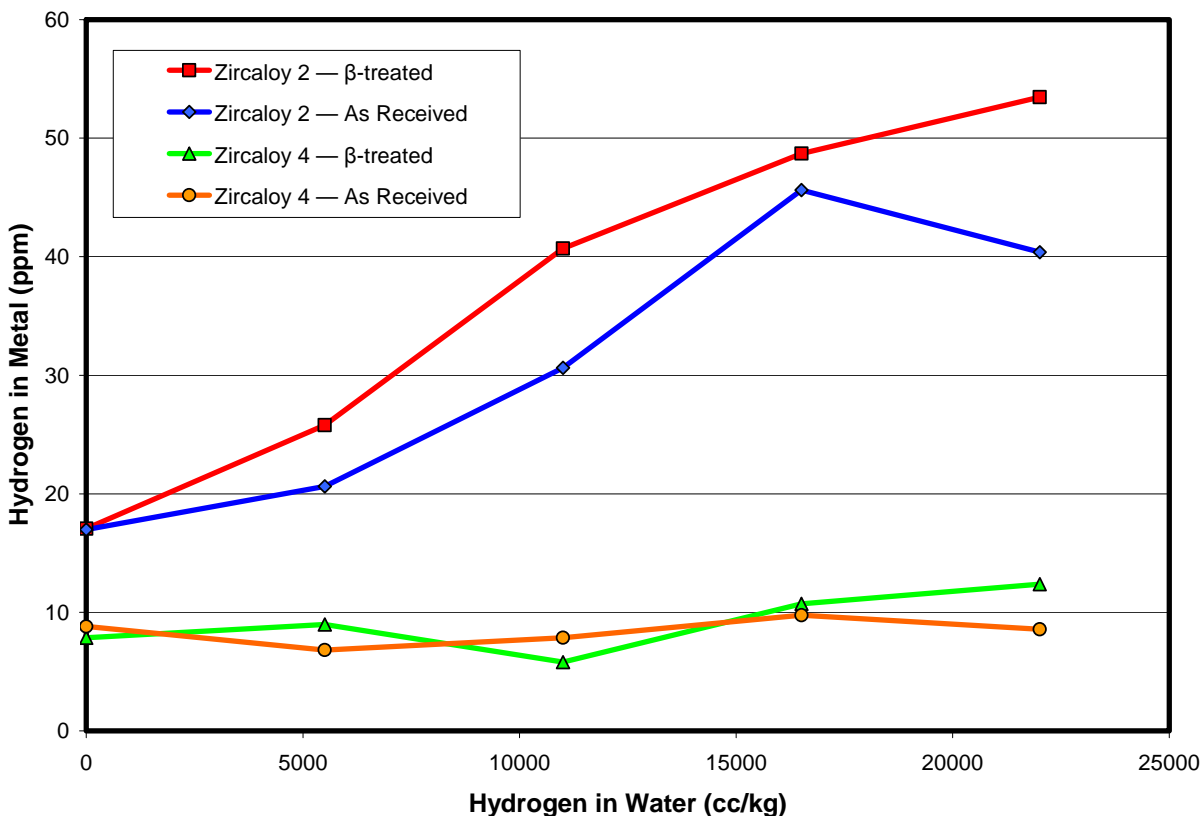


**Figure 5-1**  
**Hydrogen Pickup as a Function of Coolant Hydrogen, Zircaloy 2 and Zircaloy 4 [43]**  
**Autoclave Exposure for 14 days at 343°C**

Note that the data given in Figure 5-1 have apparently been reported in two different sources with conflicting units. This is discussed in the FRP report.[42] The values used here are based on hydrogen concentrations given in psi (which are in even 500 increments, and therefore assumed to be more likely to be the predetermined test conditions) converted to cc/kg using the Himmelblau correlation for Henry's Law constants discussed in Section 3.2. This issue in no way affects the conclusions drawn from these data, since the hydrogen concentrations are orders of magnitude above those under consideration and the differences in the two reported sources is less than a factor of two.

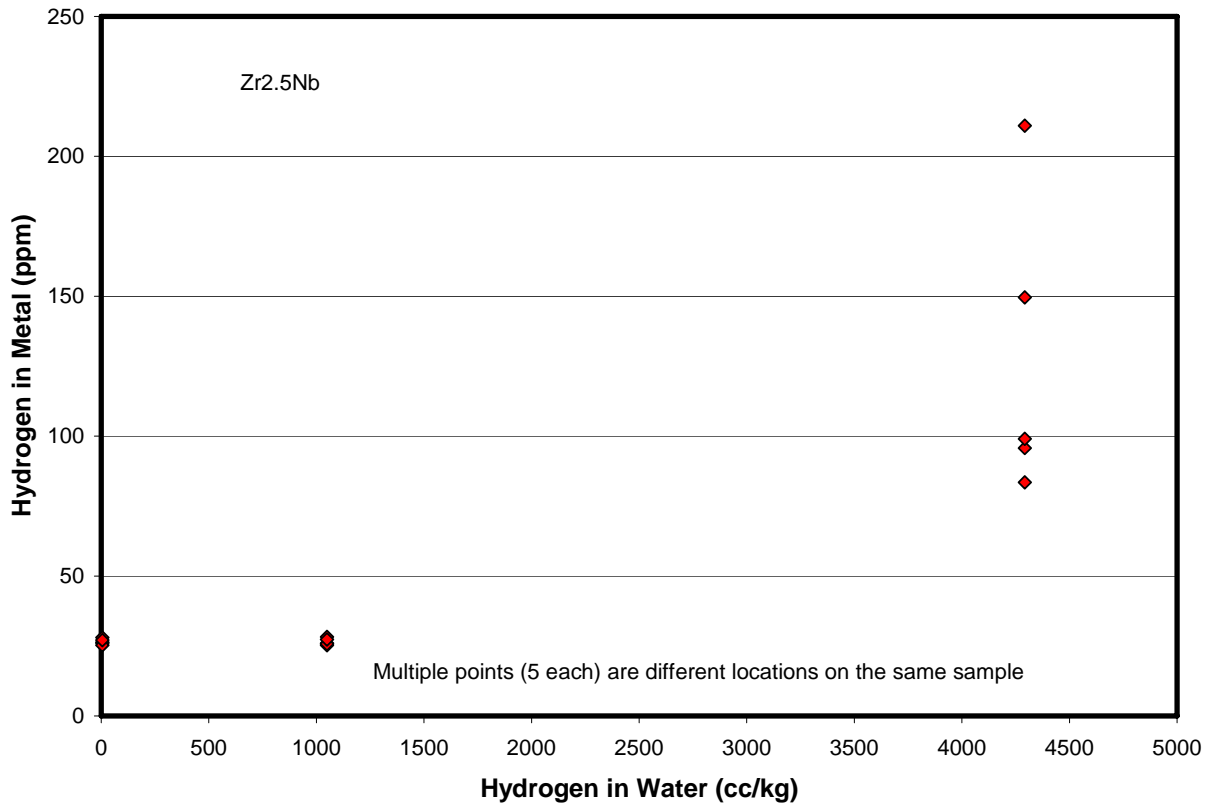


**Figure 5-2**  
**Hydrogen Pickup as a Function of Coolant Hydrogen, Zr<sub>2.5</sub>Nb [44]**  
**Autoclave Exposure at 300°C**

In the literature, there are no available hydrogen pickup data for Zr-based alloys operated in high (>50 cc/kg) RCS hydrogen conditions. There are limited hydrogen pickup fraction data for Zr-based alloys in PWRs typically operated with hydrogen concentrations in the RCS of 25-50 cc/kg hydrogen. Figure 5-4 summarizes the hydrogen pickup data from Zircaloy-2, Zircaloy-4, ZIRLO™ and M5™ available in the open literature.[42] The majority of the reported hydrogen pickup fraction data points are within 10-20%. There appears to be no correlation with coolant hydrogen concentration. However, there are gaps in the current understanding of the hydrogen pickup phenomenon and an effect of coolant hydrogen at higher concentrations cannot be ruled out.

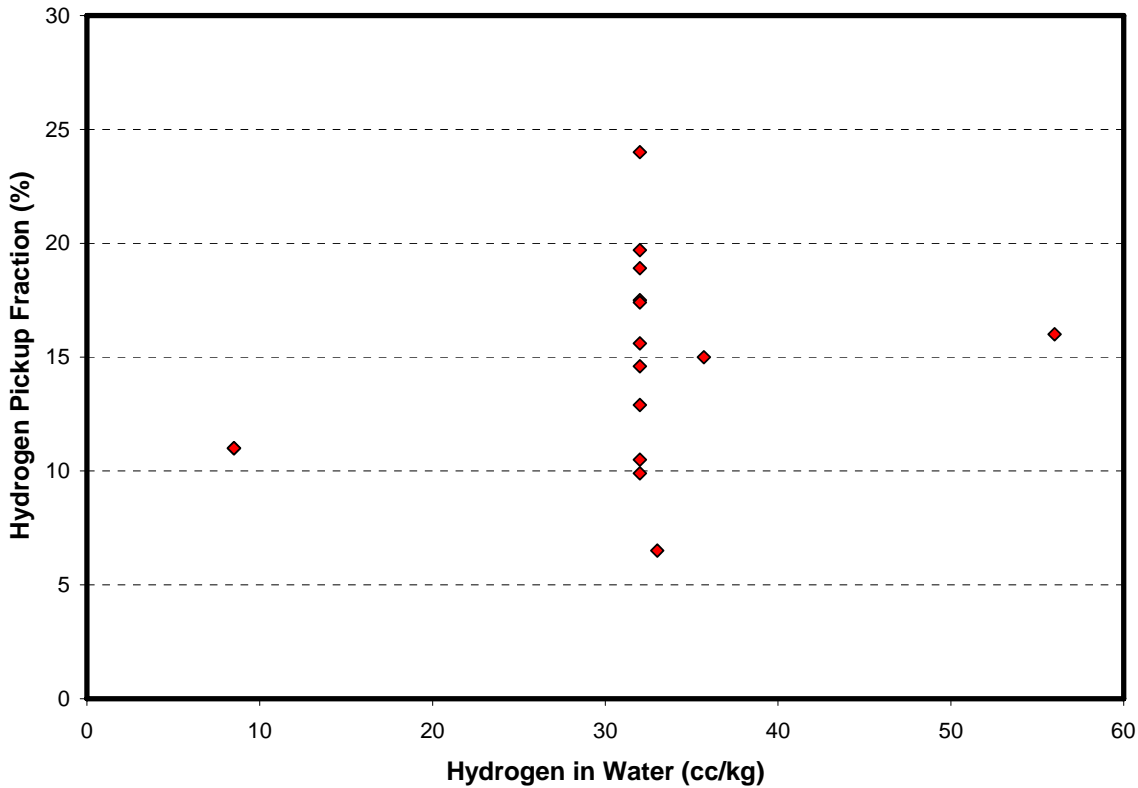


**Figure 5-3**  
**Hydrogen Pickup as a Function of Coolant Hydrogen (Discharge Fuel)**  
**(Zircaloy-2, Zircaloy-4, ZIRLO™, and M5™)**

Demanding conditions of high burnup, high duty, high coolant temperatures etc. affect hydrogen pickup properties of Zr-based alloys. Metallurgical changes occur in all alloys during service due to exposure to elevated temperature and neutron flux. These changes include dissolution of the precipitates, enrichment of the matrix in alloying elements and development of dislocation substructures. These effects, in combination with high hydrogen concentration in the metallic phase, may also affect hydrogen pickup. Until the effects of high duty are better understood, caution should be exercised in changing environmental conditions.

### 5.2.2 Startup

Historically (e.g., References [44, 45, 46]) there has been a concern that flaws in the zirconium alloy oxide could lead to rapid absorption of hydrogen, leading to accelerated hydriding. Zirconium will oxidize upon exposure to water even in the absence of dissolved oxygen in the water. The oxide coating formed by this oxidation reduces the rate of corrosion and thus the rate of release of hydrogen that can be absorbed by the metal. However, flaws in the protective oxide coating can allow water to reach the metal surface after the remainder of the surface is protected by the oxide, and thus allow continued rapid corrosion and release of hydrogen at the flaw location. For this reason, concerns have focused on the incorporation of foreign materials into

the alloy surface which would allow a flaw to persist for a significant period. Such oxide flaws, with embedded foreign materials, have generally been referred to as “windows.” Although many materials embedded in the surface might act as windows, the principal concern has been nickel and nickel alloys.

Two mechanisms have been postulated for the creation of nickel windows. These are discussed in the following paragraphs.

In the first mechanism, metallic nickel is deposited on fuel cladding by precipitation from the reactor coolant. If a previous oxide flaw exists, healing of the flaw, through further oxidation of the zirconium, is prevented by the nickel metal coating and relatively rapid diffusion of hydrogen through the nickel leads to accelerated hydriding. This mechanism has never been reported. Furthermore, it is likely that even low temperature exposure of the fuel to water will lead to the formation of a protective oxide. Laboratory tests with Zircaloy 4 indicate that over a wide range of nickel concentrations (20 ppb to 10,000 ppb) at very high hydrogen concentrations (~2500 cc/kg) accelerated hydriding was not observed unless metals with high diffusivity for hydrogen were abraded against the zirconium alloy samples.[46]

In the second mechanism, mechanical contact between the zirconium alloy and a nickel alloy leads to the embedding of nickel containing particles in the oxide. These particles bridge the existing oxide film and lead to accelerated hydriding. This mechanism has been observed both in laboratory studies [44, 45, 46] and at one plant (for multiple thimble guide tubes due to a manufacturing technique that has now been abandoned)[47]. Figure 5-4 shows an example data set [44] indicating that increases in coolant hydrogen concentration can significantly increase hydrogen pickup in zirconium alloys.

A recently reported laboratory investigation [48] has demonstrated that a combination of these two mechanisms (nickel deposition onto an embedded metal particle) can lead to significantly accelerated hydriding and that it may have been this combination of mechanisms which led to accelerated hydriding of the guide tubes at one PWR. Autoclave testing indicated that a combination of factors (all necessary, in the autoclave testing) led to hydrogen concentrations in the zirconium alloy of greater than 200 ppm (sufficient to accelerate hydriding). Specifically, the following conditions were necessary to demonstrate accelerated hydriding:

- Pre-exposure, mechanical embedding of stainless steel particles in the zirconium alloy sample (by grit blasting with a stainless steel tool, in the tests performed)
- Hydrogen concentrations above a threshold somewhere between 55 cc/kg and 110 cc/kg (accelerated hydriding was observed at some conditions at 110 cc/kg but at no conditions at 55 cc/kg)
- Nickel concentrations above a threshold somewhere between 700 and 3500 ppb (accelerated hydriding was observed at some conditions at 3500 ppb but at no conditions at 700 ppb)
- $pH_{300^{\circ}C}$  values above 6.9

Note that these criteria were found to be necessary but not sufficient for accelerated hydriding. For example, at 110 cc/kg, a nickel concentration of greater than 7,000 ppb was required to achieve conditions for accelerated hydriding. Of these criteria, only the nickel concentration is

expected to be different in PWRs relative to the autoclave tests (based on the assumption that the phenomenon is related to the total mass available for deposition, rather than the concentration).[48]

Although a conjunction of the above criteria is expected to be quite rare, the possibility of such an occurrence justifies consideration of restricting RCS hydrogen concentrations to less than 50 cc/kg, at least while nickel concentrations are elevated as typically occurs during startup.

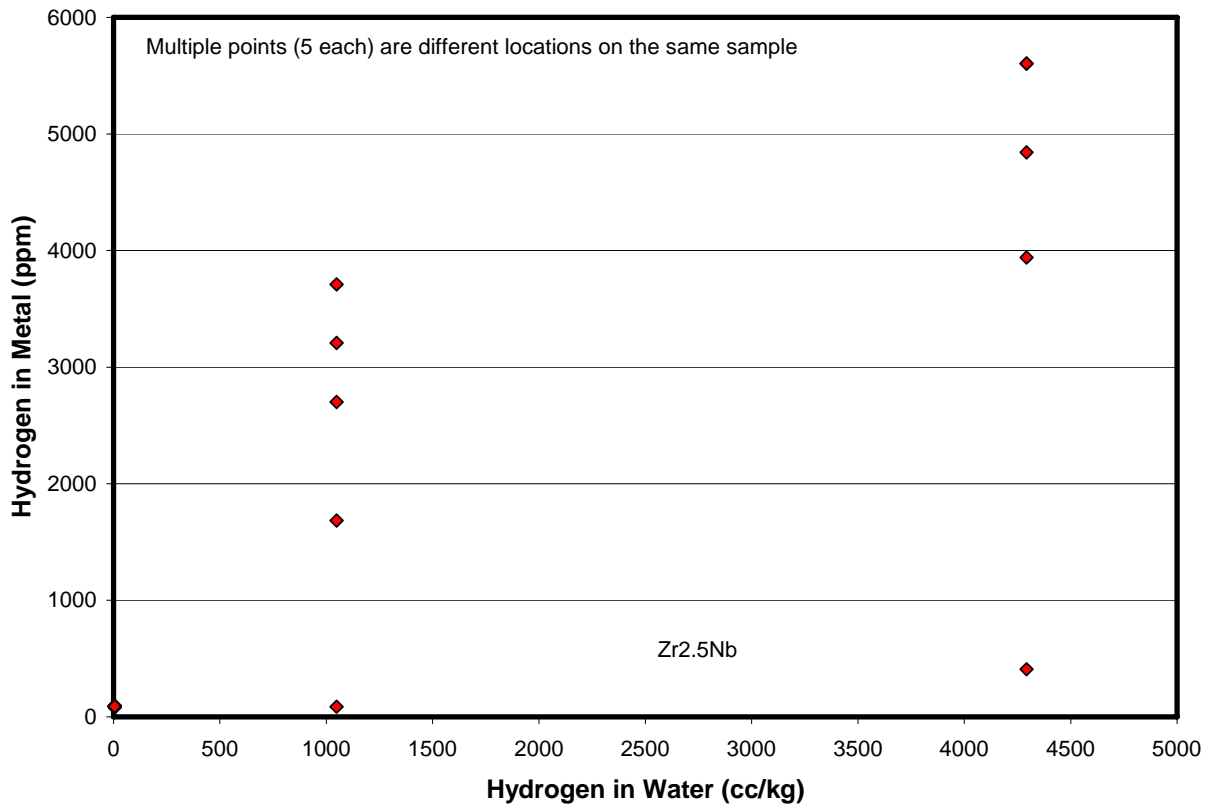


**Figure 5-4**  
**Hydrogen Pickup as a Function of Coolant Hydrogen, Zr<sub>2.5</sub>Nb [44]**  
**Autoclave Exposure at 300°C, Mechanically Embedded Nickel**

### 5.3 Recommendations of the Fuel Reliability Program

The EPRI Fuel Reliability Program recommended that a three part research program be completed prior to general approval of increasing hydrogen concentration in reactor coolant. The three tasks are as follows:

- Autoclave Testing
- In-Reactor Loop Testing
- Plant Demonstrations

Each of these tasks is summarized in the sections below, followed by an overall summary of the proposed schedule.

### **5.3.1 Autoclave Testing**

The autoclave testing is essentially a test of the effect of liquid hydrogen concentration on hydrogen pickup. The testing would generate data similar to those shown in Figure 5-1 and Figure 5-2 using current fuel cladding materials: Zircaloy-4, M5<sup>TM</sup> and ZIRLO<sup>TM</sup>. This testing would be designed only as confirmatory tests that the hydrogen pickup characteristics of current cladding materials are not substantially different from those tested in the past.

### **5.3.2 Out-Reactor Loop Testing**

This testing was conceived as a flowing autoclave test designed specifically to address the nickel window issue. Details regarding the testing are not provided in Reference [42], which recommends that the test protocols be developed by a multidiscipline team. Recently, such a team has met and recommended against conducting these tests.

### **5.3.3 In-Reactor Loop Testing**

In-reactor loop testing in a test reactor was recommended based on historic observations of discrepancies between hydrogen pickup in radiation fields and in the absence of such fields. This type of test, when properly designed to mimic PWR hydrothermal conditions, also allows confirmation that heat fluxes do not significantly influence the oxidation and hydriding characteristics of these alloys.

### **5.3.4 Plant Demonstrations**

A series of plant demonstrations followed by poolside and some hot cell fuel examinations is recommended. In the first demonstration, a modest increase in hydrogen limits is recommended (target 55 cc/kg with a limit of 60 cc/kg). Fuel examinations would include visual, oxide thickness, assembly length, and crud scrapes. It is recommended that this demonstration be performed in a plant with a moderately high, but not bounding, core duty.

If there is success at the 60 cc/kg limit in the first demonstration and there are no red flags from preliminary results from autoclave testing, a second demonstration will be performed in a high, but non-limiting fuel duty plant at 70 cc/kg (different plant than the one in first demonstration).

If there is success in the first two demonstrations, a third demonstration will be conducted in a limiting, duty plant at 60 cc/kg. Before this demonstration is begun, more information will be available from autoclave testing and in-reactor loop testing to support the higher level of hydrogen in a high duty plant.

If there is success in the previous demonstrations, a fourth demonstration will be performed in a high fuel duty plant at 70 cc/kg. Before this demonstration begins, the results of in-reactor loop test will be available.

Poolside fuel examinations after each demonstration cycle will include visual, oxide thickness and assembly length measurements (high assembly growth is an indication of high hydrogen in the thimble tubes). Crud sampling will also be performed, and effects on dose rates need to be established. Any anomalies that are observed (i.e., during 60 cc/kg program) may need to be followed by hot cell examination.

Because there are currently no means of detecting hydrogen pickup by use of poolside methods, three hot cell programs are contemplated at this time for fuel cladding and structural materials from limiting plants at 60 and 70 cc/kg. However, to expedite attainment of critical data, it is proposed that HPU data be obtained on fuel from the first plant at 60 cc/kg. These data would serve to verify acceptance and justify progression to the higher levels. Subsequent hot cell programs will verify acceptable performance in limiting duty plants at 60 and 70 cc/kg on one- and two-cycle lead fuel assemblies.

### **5.3.5 FRP Recommended Schedule**

The FRP recommended research program could begin immediately. A schedule given in terms of years and quarters from the start of the program is given in Table 5-1. As is evident, the proposed program is a long-term, multi-year study.

**Table 5-1**  
**FRP Recommended Research Program [42]**

<b>Task #</b>	<b>Test</b>	<b>Start</b>	<b>Finish</b>
1	Autoclave Testing	0Y0Q	2Y1Q
3	In-Reactor Loop Testing	0Y0Q	3Y3Q
3.1	55 cc/kg, moderately high duty demonstration	0Y0Q	3Y2Q
3.2	65 cc/kg, moderately high duty demonstration	3Y0Q	6Y2Q
3.3	55 cc/kg, limiting high duty demonstration	3Y4Q	7Y1Q
3.4	65 cc/kg, limiting high duty demonstration	5Y3Q	9Y1Q

## **5.4 Possible Effects of Low Hydrogen Concentrations**

The EPRI FRP review [42] does not address the impact of low hydrogen concentrations on fuel performance and reliability. In general, there is little information in the literature to suggest that lower hydrogen concentrations would adversely affect the fuel except through possible changes in crud transport phenomena (discussed in Chapter 6) or through the presence of oxidants generated by radiolysis (discussed in Chapter 8). With regard to oxidants, it has been suggested that newer zirconium alloys (M5<sup>TM</sup> and ZIRLO<sup>TM</sup>) may be more sensitive to low concentrations of oxidants than previous generations of cladding material (Zircaloy-4).

## **5.5 Conclusions**

In summary, although mechanisms by which increased coolant hydrogen concentrations might impact fuel performance have been postulated, there is no evidence that these mechanisms actually exist under plant conditions. Furthermore, although the data are not conclusive, there is strong evidence that coolant hydrogen concentrations do not affect the performance of zirconium alloys in PWRs. Nevertheless, based on the industry's efforts to reduce the risk of fuel failures, the FRP recommends a cautious approach to increasing coolant hydrogen concentrations.

The most significant knowledge gap with respect to the influence of coolant hydrogen concentrations on PWR fuel cladding is the absence of data on modern zirconium alloys (M5<sup>TM</sup> and ZIRLO<sup>TM</sup>). Comparison of different alloys of previous generations indicates that there can be significant differences in the effects of coolant hydrogen on hydrogen pickup, and thus hydriding. As discussed in Chapter 10, there is essentially no plant experience outside the current operating range. Thus hydrogen pickup data for fuel cladding in operating plants at elevated (>45 cc/kg) hydrogen concentrations are not available for any cladding alloy.

# 6

## EFFECT OF HYDROGEN ON CORROSION, CORROSION PRODUCT TRANSPORT, AND CORROSION PRODUCT DEPOSITION

---

### 6.1 Introduction

General corrosion of RCS materials at the internal wetted surface is not generally a concern for the structural and operational integrity of components. However, general corrosion results in the release of material from system components to the coolant. Once in the coolant, corrosion products can be distributed throughout the RCS. Of particular concern is the deposition of corrosion products on fuel cladding in the core. These deposits can contribute to crud induced power shifts (CIPS, or axial offset anomaly – AOA). They can also become activated, for example  $^{58}\text{Ni}$  (n,p)  $^{58}\text{Co}$ . Due to dynamic exchange between all surfaces in the RCS, these activated corrosion products are incorporated into all system surfaces contributing to personnel dose during outages.

Theoretically, hydrogen can affect the corrosion of system materials, the release of corrosion products from the base metal, the nature of the corrosion products in the coolant, and the deposition of corrosion products in the core. These issues are considered in the sections that follow.

### 6.2 Effect of Hydrogen on Steam Generator General Corrosion

General corrosion is not typically a significant factor in RCS component performance. Therefore, little testing has been done to quantify the effects of chemical parameters on such corrosion. What testing has been conducted has been done in relatively short tests. In preparation of this report, two literature reviews [49, 50] on corrosion of Alloy 600 were consulted. These reviews cite only one study in which the effects of hydrogen on general corrosion were investigated. The results from this study [51] are shown in Figure 6-1. Each data point in Figure 6-1 represents the average of 8 to 36 measurements on different samples. The corroded mass shown is the total (released plus adherent). These data demonstrate the difficulty of measuring general corrosion rates in short-term tests. No corrosion rate is discernable for any of the conditions. Any effect of hydrogen is hidden in the scatter.

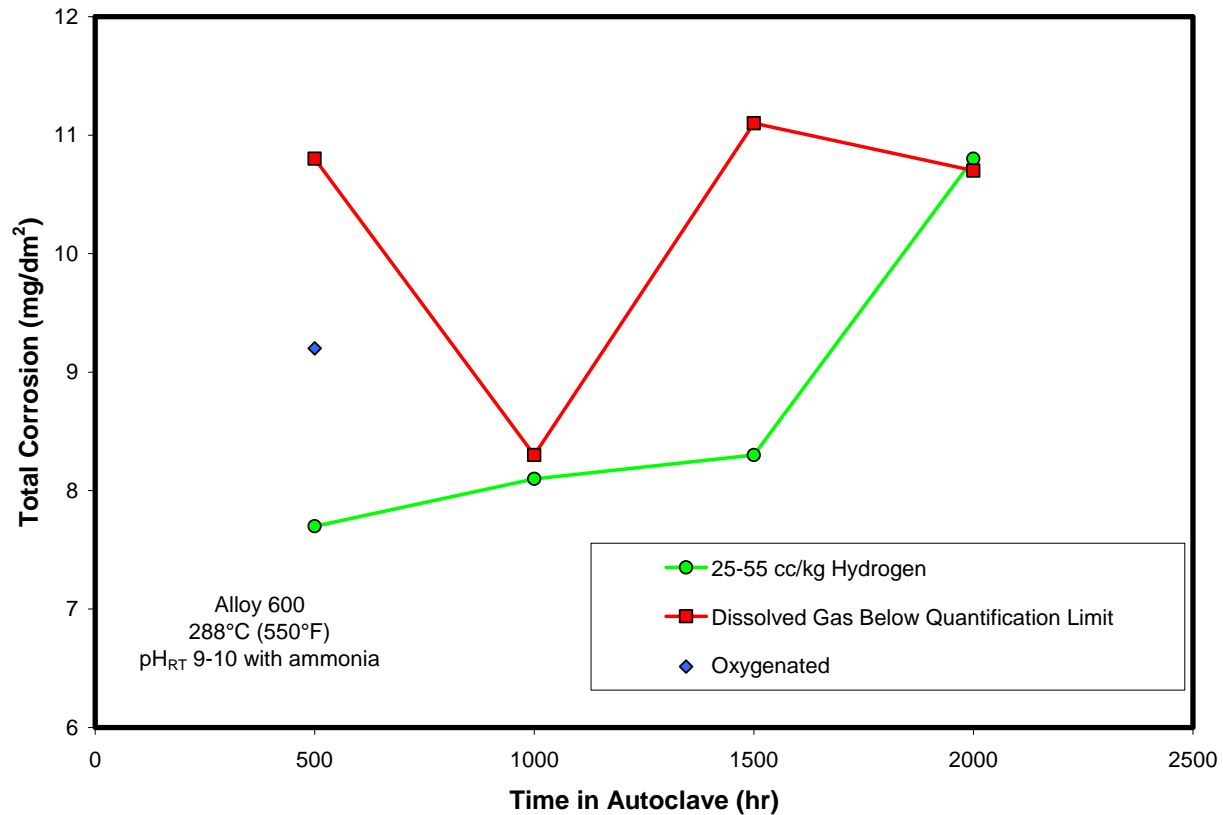


**Figure 6-1**  
**Effect of Hydrogen of General Corrosion of Alloy 600 [51]**

### 6.3 Effect of Hydrogen on Corrosion Product Release

Non-fuel surfaces exposed to the reactor coolant are generally either stainless steel or nickel alloys with significant concentrations of chromium (e.g., Alloy 600). As such, they form inner protective oxide layers enriched in chromium with an outer non-protective layer that is not as enriched in chromium. General corrosion results not only in the oxidation of the base metal, but also in the release of a fraction of the oxide into the RCS coolant.

Calculations of corrosion product release rates based on assumed oxidation rates and measurements of released mass indicate a range of release fractions (metal released as a fraction of metal oxidized). A typical distribution of measurements is shown in Figure 6-2.[49] In general, there have been no data available regarding the effect of hydrogen concentration on the release fraction in PWRs, although some work at secondary side conditions indicates that the presence of oxygen can lead to thicker films that are not as chromium enriched.[52] (The literature regarding BWR conditions has not been reviewed as part of the compilation of this report. It is considered likely that additional data may be available that has not been considered here.)

Due to the unsteady (decreasing) rate of oxidation, the corrosion film on stainless steels and nickel alloys are not expected to reach a steady state in times considered in laboratory testing (or in a single cycle at an operating PWR). Therefore, conclusions drawn from equilibrium assessments are not likely to be useful. Additionally, such calculations are not at all useful if the major release product is a particulate.

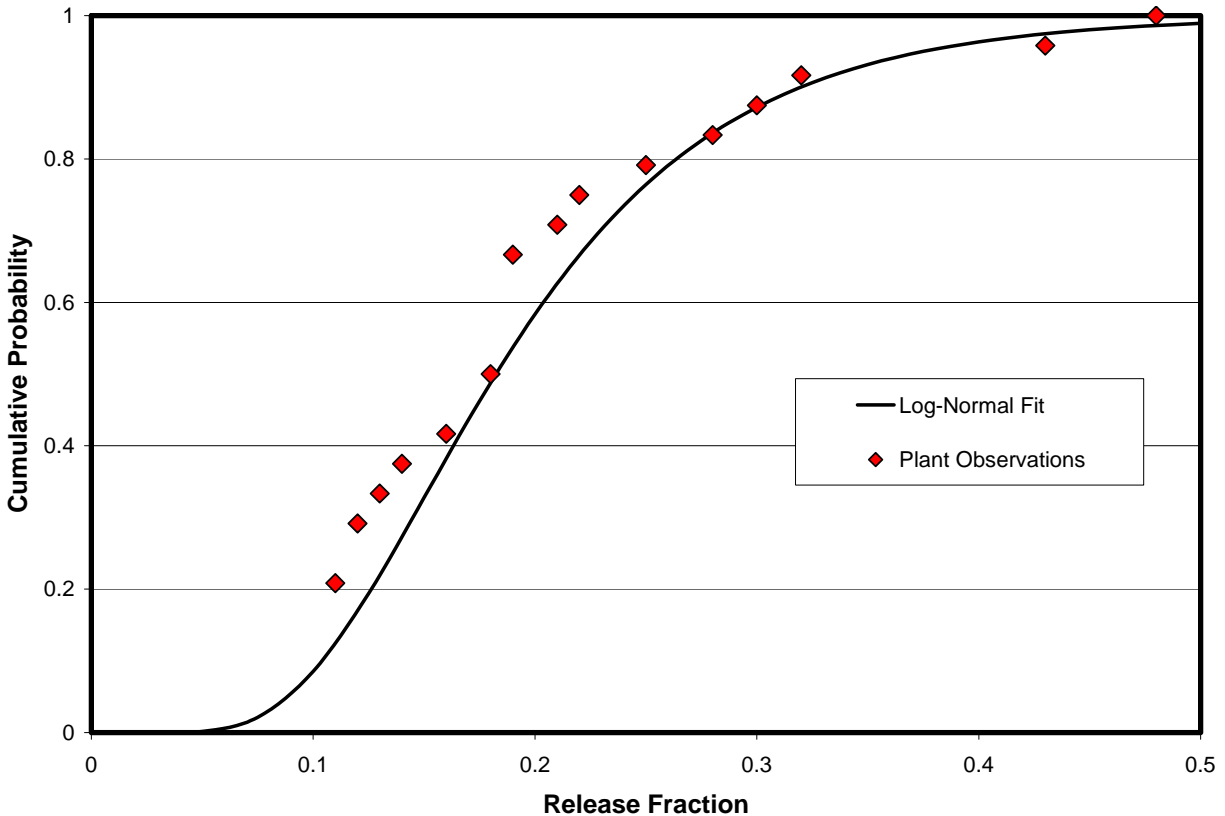


**Figure 6-2**  
**Calculated Release Fractions, Plants With Alloy 600 Tubing [49]**

Some very recent data has become available regarding the effect of hydrogen on the release rates (total rates rather than release fractions) from Alloy 690TT.[53] The effect of hydrogen concentration at 300°C is shown in Figure 6-3. Similar data taken at 325°C are given in Figure 6-4. All of these tests were conducted at 1000 ppm boron and 2 ppm lithium. The data shown indicate that there is no effect of hydrogen concentration on the release rate.

## Effect of Hydrogen on Corrosion, Corrosion Product Transport, and Corrosion Product Deposition

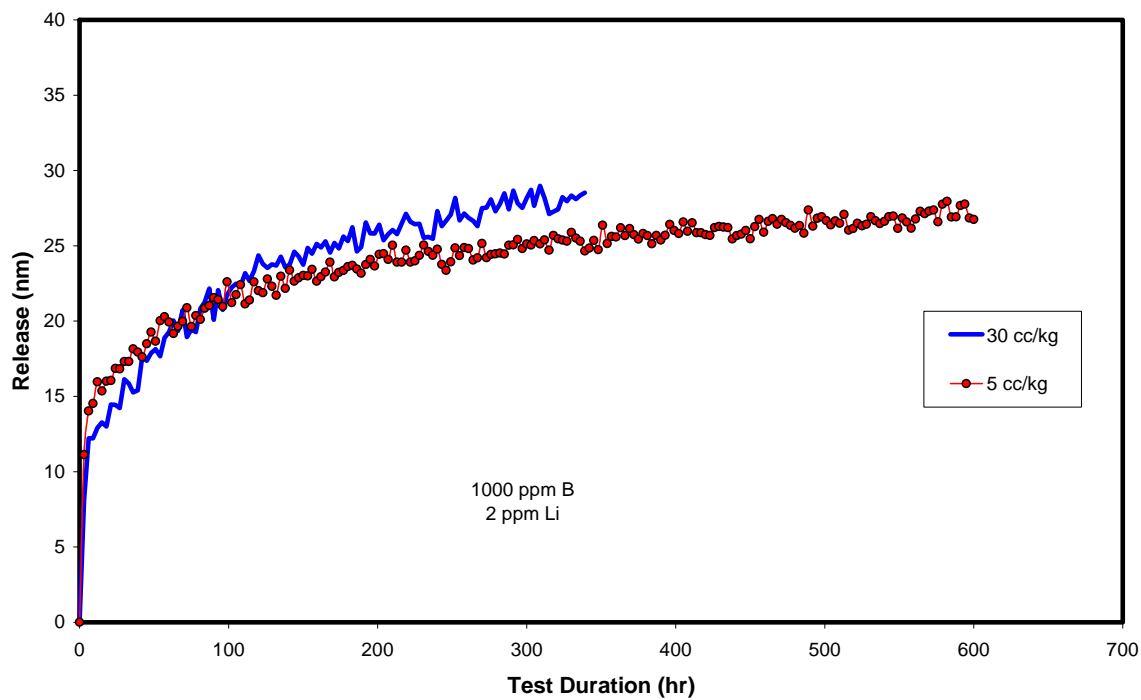


**Figure 6-3**  
Release Rate From Alloy 690TT at 300°C [53]

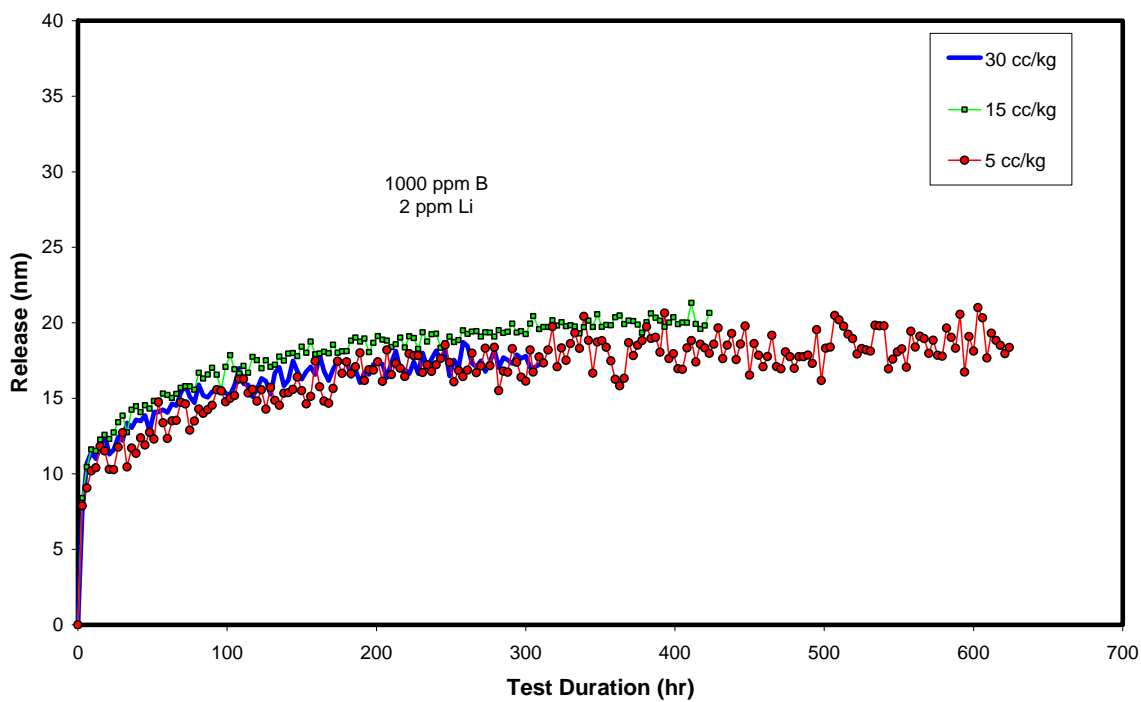


**Figure 6-4**  
Release Rate From Alloy 690TT at 325°C [53]

## 6.4 Effect of Hydrogen on Corrosion Products in the Reactor Coolant

Hydrogen concentrations in the RCS coolant are expected to influence both the morphology and the chemistry of particulates in the coolant. These issues are discussed separately in the following paragraphs.

Dissolved hydrogen has been shown to influence the morphology of the outer oxide layer on Alloy 600 exposed to primary coolant conditions.[54] Figure 6-5 shows films formed on Alloy 600 under different hydrogen concentrations at 320°C. At low hydrogen concentrations (0 and 11 cc/kg) there is a significant mass of needle-like crystals. At higher hydrogen concentrations (31 and 45 cc/kg) particles with an aspect ratio of approximately unity are formed. Additionally, as hydrogen concentration is increased from 31 cc/kg to 45 cc/kg, the average size of the crystallites decreases.

The concentration of hydrogen in the coolant is expected to change the chemical nature of the outer surface of corrosion product particulates. Specifically, as hydrogen increases the surface will become more like nickel metal than nickel oxide. This trend in surface state is expected to closely follow the Ni/NiO equilibrium curve (see Section 3.4). It should be noted that the currently accepted data set for the Ni/NiO transition is based on conversion of a surface film.[4] It has been speculated that changes in surface condition may affect the electrophoretic nature of corrosion product particles, changing the extent to which they are attracted to system surfaces.[55, 56] However, research in this area is preliminary and any conclusions that could be made would be highly speculative.

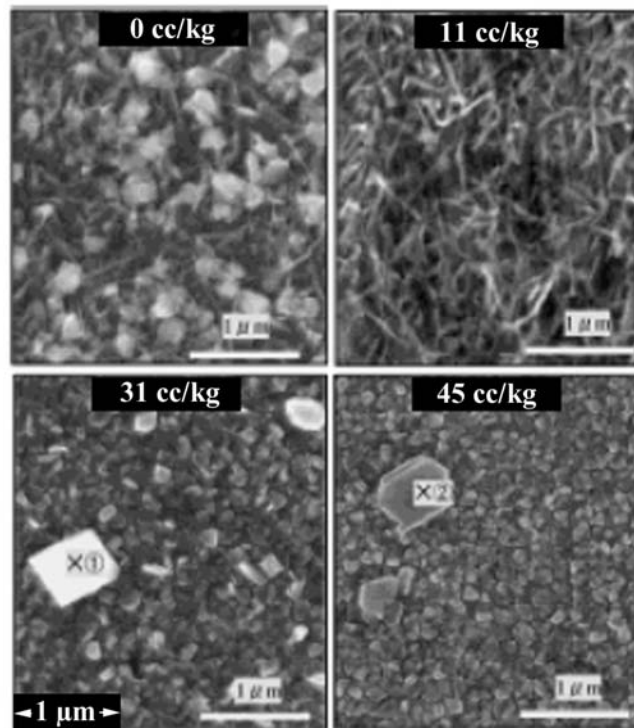


**Figure 6-5**  
**Effect of Hydrogen Concentration on Corrosion Product Morphology [54]**  
**Alloy 600, 1000 hrs, 320°C, 500 ppm B, 2.0 ppm Li**

## 6.5 Effect of Hydrogen on Deposition of Corrosion Products on Fuel Cladding

The traditional means for investigating the effects of chemistry on corrosion product deposition in the core is to evaluate changes in solubility as temperature increases. Various species have been assumed to be limiting, including magnetite, nickel ferrite, nickel metal, and nickel oxide. However, plants routinely measure RCS nickel concentrations in the range of 0.5 to 2 ppb [57, 58, 59], far above the estimated solubility limit (see Section 3.5). Therefore, it seems unlikely that deposition in the core is governed by solubility issues. With respect to hydrogen, it is unlikely that the small concentration changes under consideration would significantly affect either macroscopic or microscopic flow phenomena (e.g., mass transfer rates or wick boiling flows). However, hydrogen concentration could be expected to have a significant influence on the size and surface characteristics of corrosion product particles, as discussed in Section 6.4.

Deposition of corrosion product particles onto fuel surfaces may be governed by a number of phenomena.[60] These include the following:

- Gravitational deposition
- Inertial Deposition
- Diffusive Deposition
- Boiling Deposition
- Thermophoretic Deposition
- Electrophoretic Deposition
- Crystallization Deposition

The implications for these mechanisms of the possible effects of hydrogen on corrosion products discussed in Section 6.4 are discussed in the paragraphs below. In general, these deposition processes are described by a rate equation such as Equation 6-1 where  $n$  is the flux of corrosion products to the fuel surface,  $K$  is an overall rate constant related to various rate constants for different mechanisms (similar to an overall heat transfer coefficient with multiple modes of heat transfer), and  $\Delta C$  is a measure of the corrosion product gradient.

$$n = K \Delta C \quad \text{Eq. 6-1}$$

The effects of changes in the nature of the corrosion products on deposition rates can be assessed by examining the deposition constants for each of the mechanisms thought to be active. These are discussed below. Except as otherwise noted, the discussions are based on Reference [60].

### 6.5.1 Gravitational Deposition

Because critical core surfaces (fuel cladding) are vertical, little gravitational deposition is expected. This expectation is independent of the particulate nature.

### 6.5.2 Inertial Deposition

Inertial deposition occurs when particles are propelled toward surfaces by turbulent eddies. Larger particles have more inertia and are able to cross more streamlines than lighter particles. Inertial deposition is governed by a rate constant that is dependent on the particle size, as follows:

$$K_{inertial} = \frac{a_{inertial}}{5.23} \left( \frac{\tau_{wall}}{\rho_{liquid}} \right)^{\frac{3}{2}} \left( \frac{1}{18} \left( \frac{d_{particle}}{v_{liquid}} \right)^2 \right) e^{\frac{0.48 \rho_{particle} \tau_{wall}}{18 \rho_{liquid} \rho_{liquid}} \left( \frac{d_{particle}}{v_{liquid}} \right)^2} \quad \text{Eq. 6-2}$$

where  $a$  is a fitted constant,  $\tau_{wall}$  is the shear stress at the deposition surface,  $\rho_{liquid}$  is the liquid density,  $\rho_{particle}$  is the particle density,  $v_{liquid}$  is the kinematic viscosity of the liquid, and  $d_{particle}$  is the particle diameter. As can be seen in Equation 6-2, the deposition rate decreases monotonically with decreasing particle size. Therefore, it is expected that smaller particles will deposit more slowly by the inertial process.

### 6.5.3 Diffusive Deposition

Diffusive deposition occurs through the Brownian motion of particles which results in a net flux from regions of high concentration to regions of low concentration. The rate of diffusive deposition is governed by the following equation:

$$K_{diffusion} = \frac{a_{diffusion}}{11.9} \sqrt{\frac{\tau_{wall}}{\rho_{liquid}}} Sc^{-\frac{2}{3}} \propto d_{particle}^{-\frac{2}{3}} \quad \text{Eq. 6-3}$$

$$Sc = \frac{v_{liquid}}{D_{particle}} = \frac{v_{liquid}}{\left( \frac{\kappa T}{3\pi\mu_{liquid}d_{particle}} \right)}$$

where  $\kappa$  is the Boltzmann constant,  $T$  is the absolute temperature, and  $\mu_{liquid}$  is the liquid viscosity. From Equation 6-3 it can be seen that the diffusive deposition rate increases monotonically as the particle size decreases. Therefore, increased hydrogen concentrations, and resultant smaller particles as discussed in Section 6.4, would result in higher rates of deposition by this mechanism.

### 6.5.4 Boiling Deposition

Boiling deposition is governed by the following expression for the deposition rate constant:

$$K_{boiling} = a_{boiling} \frac{q''}{\rho_{liquid} h_{fg}} \quad \text{Eq. 6-4}$$

where  $q''$  is the heat flux and  $h_{fg}$  is the latent heat of vaporization. According to Equation 6-4, boiling deposition is governed only by the rate of coolant vaporization. Therefore, hydrogen concentration is not expected to influence boiling deposition.

### 6.5.5 Thermophoretic Deposition

Thermophoretic motion of particles is caused by temperature gradients in the liquid. Because otherwise random impacts of liquid molecules on the suspended particles have more energy on the hot side of the particle, there is a net motion of particles down the thermal gradient. When considering heated surfaces, this results in a negative deposition rate, as expressed in the following equation:

$$K_{thermophoretic} = \frac{-a_{thermo}}{3.8} \frac{q'' v_{liquid}}{(2k_{liquid} + k_{particle})T} \quad \text{Eq. 6-5}$$

where  $k_{liquid}$  and  $k_{particle}$  are the thermal conductivities of the coolant and the corrosion product particle, respectively. From Equation 6-5 it is evident that particle size does not influence the thermophoretic deposition rate.

### 6.5.6 Electrophoretic Deposition

Electrophoretic deposition is the movement of a particle to a surface due to electrical charge. The charge of a surface is typically measured in terms of zeta potential. Figure 6-6 and Figure 6-7 show possible effects of chemistry on zeta potential. When the zeta potential of the surface (stainless steel, for example) is opposite in sign from that of the particle (nickel ferrite, for example), there is an attractive force that promotes deposition.

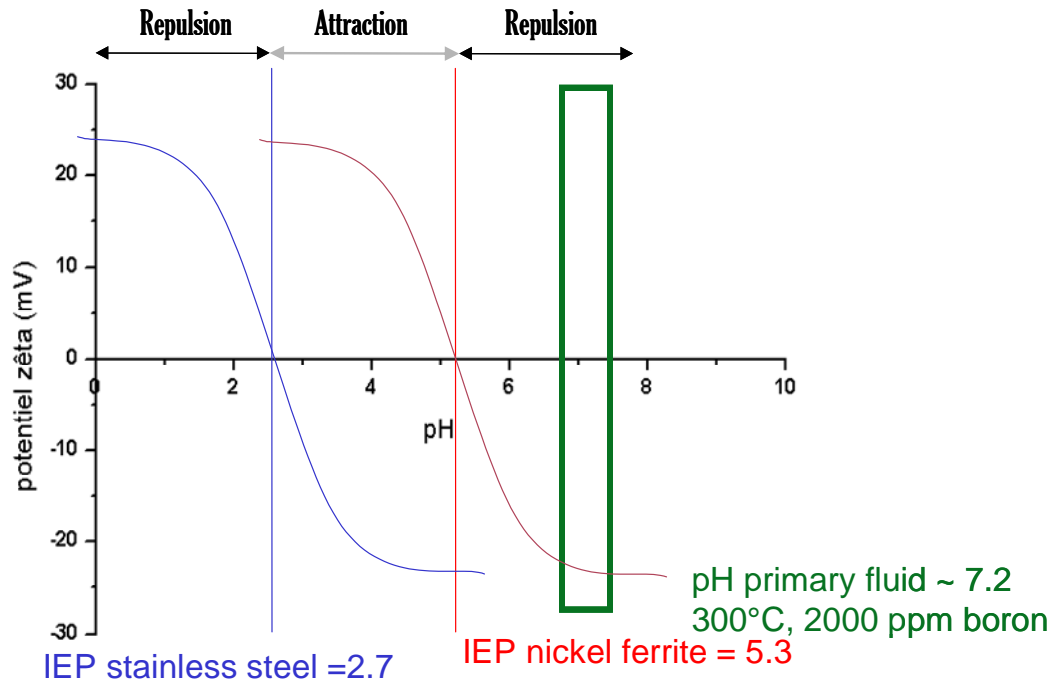


**Figure 6-6**  
Comparisons of the Zeta Potential of Stainless Steel and Nickel Ferrite, High B [55]

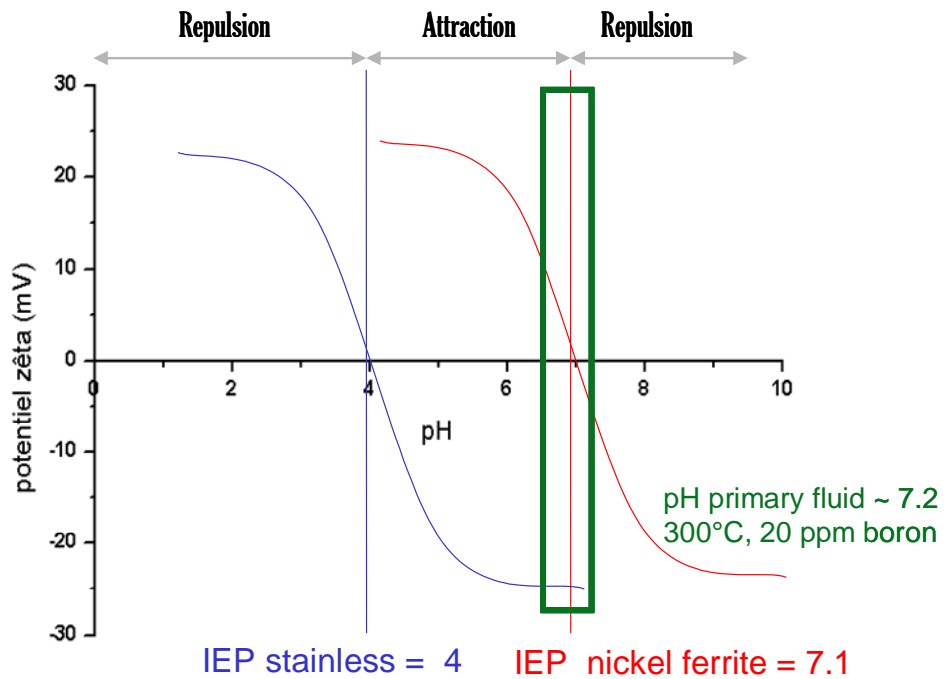


**Figure 6-7**  
Comparisons of the Zeta Potential of Stainless Steel and Nickel Ferrite, Low B [55]

Figure 6-6 and Figure 6-7 show the effect of boron concentration. Similar results might occur due to hydrogen concentration, especially if changes in hydrogen concentration cause a shift in the nature of the surface composition of corrosion product particles (for example, increasing the surface concentration of nickel metal relative to nickel oxide). However, it should be noted that such considerations are highly speculative. The effect of hydrogen on electrophoresis cannot be determined at this time.

### **6.5.7 Crystallization Deposition**

As discussed in the introduction to Section 6.5, calculated changes in solubility across the core have been the historic bases of attempts to determine optimum primary chemistry. However, it is the opinion of this author that direct precipitation is a minor factor in deposit accumulation in the core. The basis for this opinion is the numerous measurements of RCS nickel concentrations far in excess of the best estimates of solubility limits. Nevertheless, it is possible that the solubility of corrosion products does affect deposition in the core.

The solubility of corrosion products is discussed in Section 3.5 and 3.6. The significant uncertainty that exists in understanding the solubility limits of nickel and iron are discussed in those sections. However, given this uncertainty and the uncertainty in the role that soluble species might play in corrosion product transport and deposition, the following generalities are likely to hold:

- Maintaining low nickel solubility is likely to be beneficial.
- An increase in solubility with temperature is likely to be beneficial.

As shown in Figure 3-7 and Figure 3-8, increased concentrations of hydrogen are expected to make nickel metal the solubility limiting solid phase. This is expected to both reduce the overall solubility and to reduce the decrease in solubility with increasing temperature. Therefore, increasing hydrogen concentrations would be expected to be beneficial with respect to solubility-based deposition mechanisms. (As discussed in Section 3.5, if the transition between nickel metal stability and nickel ferrite stability occurs at a lower hydrogen concentration than previously believed, then the effect of hydrogen concentration is smaller. However, the overall conclusion that increased hydrogen is beneficial with respect to crystallization deposition would still be valid using alternative thermodynamic data.)

### **6.5.8 Overall Effect of Hydrogen on Deposition**

In general, the overall effect of hydrogen on deposition is largely unknown. The results of laboratory testing indicate that in the hydrogen concentration range under consideration, particle sizes could change by a factor of about 5 to 10, with smaller particles at higher concentrations. Zinc injection [61] has been observed to change particle sizes by about a factor of 100. Noticeable changes in deposition phenomena are also observed. This indicates that it is possible that corrosion product deposition could be significantly affected by changes in hydrogen concentration.

## **6.6 Conclusions**

In general, there are very few data available for assessing the effects of hydrogen concentration on corrosion product generation, release, transport, or deposition. The data that are available indicate that there may be relatively limited changes in each of these processes. At the modest changes in hydrogen concentration under consideration, these changes are expected to be small relative to the current variability and uncertainty.



# 7

## EFFECT OF HYDROGEN ON LTCP

---

### 7.1 Introduction

Low temperature crack propagation (LTCP) is a phenomenon in which hydrogen embrittlement accelerates crack growth rates at temperatures that are low relative to PWR operating temperatures. Specifically, nickel alloys and their weld metals are susceptible to rapid crack growth (on the order of one hundred millimeters per hour [62]) in the temperature range of 50°C to 150°C. This susceptibility is a function of hydrogen concentration at the crack tip which can be present due to a number of factors (e.g., generation by corrosion at the crack tip; diffusion from the water into the bulk metal at higher temperatures followed later, after cooldown, by diffusion from the bulk metal to the crack tip; and diffusion from the water into metal surfaces and then to the crack tip).

In addition to the presence of hydrogen at the crack tip, LTCP may also require stress intensities above a certain threshold. The presence of these stress intensities has not been confirmed as being realistic in actual PWR components. Therefore, the applicability of LTCP to PWR components has not been confirmed, although the possibility cannot be completely ruled out. Nevertheless, it is an area of on-going investigation that warrants some consideration in the context of selecting an optimal hydrogen concentration.

The term LTCP has been used to describe the observations from two types of test: crack growth rate tests (for example, Reference [62]) and fracture toughness tests (for example, Reference [63]). In each test, hydrogen aggravates cracking. Crack growth rates are accelerated and fracture toughness is reduced. While it is likely that these mechanisms are related, the nature of that relationship is not well understood. Most recent testing of LTCP has focused on fracture toughness testing. This type of test has the advantage of being relatively short (a few hours to a day) compared to crack growth rate testing. However, some crack growth rate tests have shown effects at stress intensities lower than those evaluated in fracture toughness testing. Therefore, caution should be used in relying upon a stress intensity threshold from fracture toughness testing to assess the likelihood of LTCP occurring in plants.[64]

In the context of optimizing hydrogen concentrations in the RCS, the following two issues must be considered:

- Would cooldown subsequent to operation at higher hydrogen concentrations “trap” sufficiently more hydrogen in the vicinity of the crack tip to increase the likelihood of LTCP during shutdown?

- Would plant shutdown (or startup) with increased hydrogen concentrations provide sufficiently more hydrogen in the vicinity of the crack tip to increase the likelihood of LTCP during shutdown (or startup)?

(These issues would tend to impact unplanned shutdowns much more severely than refueling outages due to the significant lack of flexibility to mitigate them via a planned reduction in hydrogen concentration prior to initiating a shutdown.)

In addition, with respect to the possibility of operating at lower hydrogen concentrations (either during the full cycle or at limited periods at the beginning and end of the cycle), the following additional consideration complements the two preceding issues:

- Would operating at lower hydrogen concentrations prior to shutdown cause a significant reduction in the likelihood of LTCP during shutdown?

Assessment of the relevance of LTCP to PWR components is an on-going EPRI investigation (see Section 7.3). A discussion of this relevance is outside the scope of this report. For the remainder of this chapter, the discussions assume that LTCP is relevant and consider the effects of increased (or decreased) hydrogen concentrations in the RCS.

## **7.2 Summary of Laboratory Observations**

As mentioned above, the fundamental mechanism of LTCP is believed to be the hydrogen embrittlement at the crack tip. Hydrogen can be present at the crack tip due to solid phase accumulations, leading to internal hydrogen embrittlement (IHE) or it can be present in the external phase (liquid or gas depending on the testing), leading to hydrogen environment embrittlement (HEE). It is generally accepted that these phenomena are essentially the same.[65] However, the relevant hydrogen concentrations, testing techniques, and operational considerations are different. Therefore, it is convenient to consider IHE and HEE separately.

### **7.2.1 Internal Hydrogen Embrittlement**

#### **7.2.1.1 General Mechanism**

Bulk accumulations of hydrogen can occur through two mechanisms: diffusion of environmental hydrogen into the metal and the generation of hydrogen from corrosion. Hydrogen diffusion from the environment is the only mechanism for bulk accumulation that is expected to be significantly affected by the concentration changes being considered. (Note that the relative contribution of corrosion generated hydrogen is still relatively unexamined, although one analysis of laboratory data indicates that it can be responsible for as much as one third of loss of toughness for X-750.[66])

The hydrogen concentrations typically associated with LTCP are on the order of 20-80 ppm in the metal.[65] For typical nickel alloys (e.g., X-750), this corresponds to a hydrogen fugacity of approximately 10-40 MPa at 360°C,[67] which is considerably higher than a typical PWR hydrogen concentration (40 cc/kg corresponds to about 0.05 MPa at 300°C, see Chapter 3).

However, the solubility of hydrogen in highly stressed locations may be significantly higher than values associated with bulk materials. Therefore, in evaluating the effects of hydrogen concentration increases, consideration of an absolute concentration is not feasible and the evaluations discussed here are based only on relative effects. This approach does not address the ultimate concern as to whether LTCP is relevant to actual PWR conditions, but, as noted above, resolution of the relevance issue is beyond the scope of this report.

#### 7.2.1.2 Operational Applicability

Charging of the material due to diffusion during operation is expected to be proportional to the square root of the RCS hydrogen concentration (Sievert's Law). Due to the slow diffusion of hydrogen in nickel alloys at low temperatures, this increased hydrogen is likely to be trapped in the metal during shutdown if hydrogen concentrations remain high at the end of the cycle. Therefore, this mechanism of LTCP is applicable to high-temperature elevated hydrogen concentrations in the absence of a period of low hydrogen concentrations at the end of the cycle or during the early part of the shutdown. (It is possible that for sharp crack tips the diffusion path from the point of highest stress to the water environment is short enough that hydrogen will not be trapped. However, charging may make blunt cracks more likely to propagate since the peak stresses may be further into the material where hydrogen has been trapped.[68])

Additionally, if there is a dependence of LTCP on operational hydrogen concentrations, then operation at lower concentrations would be expected to mitigate this phenomenon.

#### 7.2.1.3 Test Data

A sample of the literature on LTCP was reviewed to collect some pre-charging experimental results to evaluate the effect of hydrogen concentration. Figure 7-1, Figure 7-2, and Figure 7-3 show some results of fracture toughness measurements in experiments with hydrogen pre-charging.

## Effect of Hydrogen on LTCP

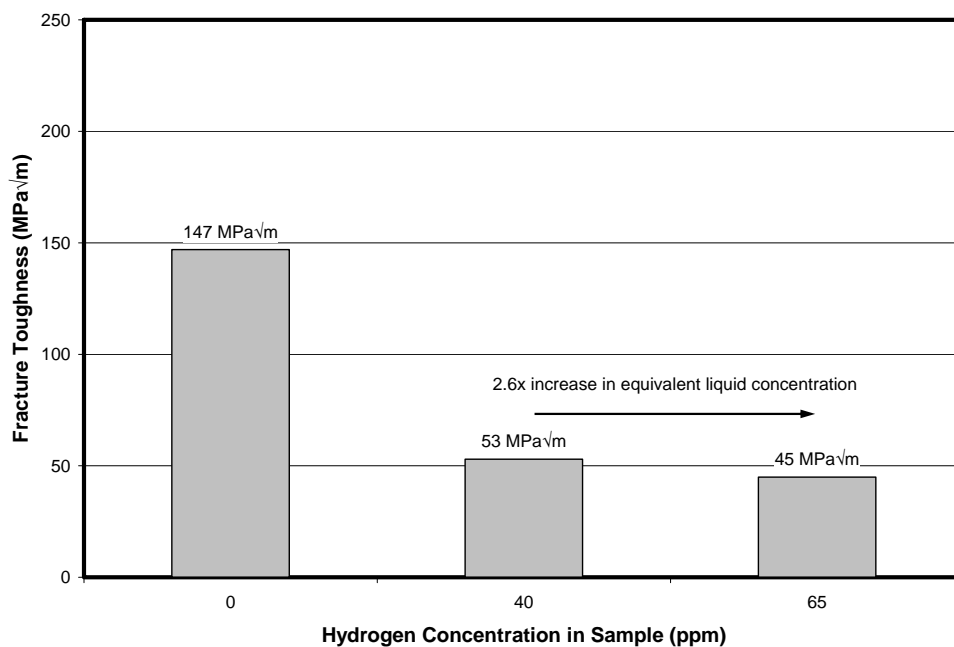


**Figure 7-1**  
Effect of Hydrogen Pre-Charging on Fracture Toughness, X-750 HTH at 25°C [65]

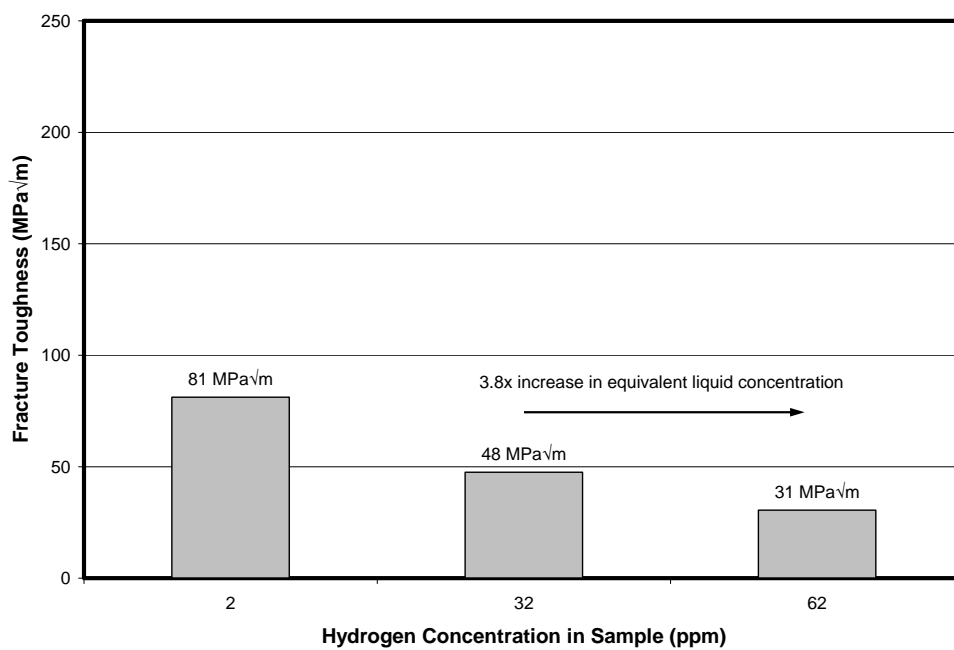


**Figure 7-2**  
Effect of Hydrogen Pre-Charging on Fracture Toughness, X-750 HTH at 93°C [68]

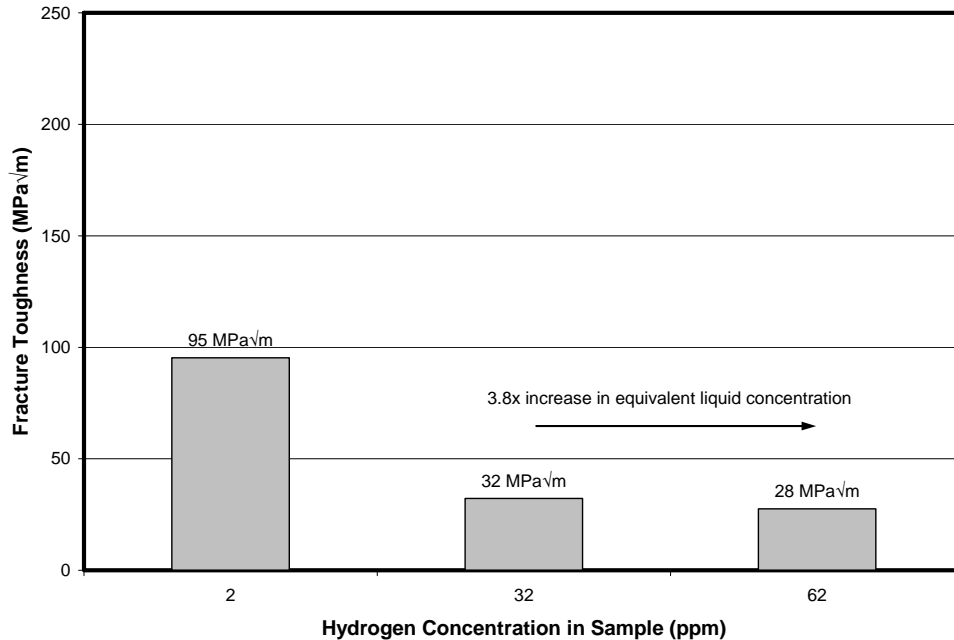


**Figure 7-3**  
**Effect of Hydrogen Pre-Charging on Fracture Toughness, X-750 BH at 93°C [68]**

The data in Figure 7-1, Figure 7-2, and Figure 7-3 show that for materials susceptible to LTCP, increased hydrogen concentrations in the bulk metal can increase that susceptibility. However, the relative increases in hydrogen concentration used to generate these data are significantly larger than the increases being considered for an elevated hydrogen program (a shift from 35 cc/kg to 80 cc/kg is a factor of 2.3x which corresponds to an equivalent increase of 1.5x in concentration in the metal).

At the current time, pre-charging tests of the more important materials (Alloys 600 and 690 and weld metals 182, 52, and 152) are not available.

## 7.2.2 Hydrogen Environment Embrittlement

### 7.2.2.1 General Mechanism

When a pre-cracked specimen of an LTCP susceptible material is exposed to water containing hydrogen, hydrogen will diffuse to the stressed location immediately ahead of the crack tip, causing hydrogen embrittlement and allowing rapid growth of the crack.

### 7.2.2.2 Operational Applicability

Hydrogen environment embrittlement is most likely to be relevant when the hydrogen present in the bulk material is too low to cause an LTCP concern. (HEE is thought to require lower hydrogen concentrations because an equivalent hydrogen mass can be transported to the crack tip

faster by liquid diffusion in the crack than by solid state diffusion in the metal.[68]) One possible scenario is that elevated hydrogen concentrations that do not charge the material enough during operations to cause IHE due to trapped hydrogen could lead to HEE if elevated hydrogen concentrations are maintained during shutdown. This is currently the principal concern regarding current operating concentrations of hydrogen.

Although HEE may be found to be a significant concern in PWRs (it has not been found to be such yet), it should not be a significant barrier to the use of elevated hydrogen concentrations during power operations since hydrogen concentrations could be lowered before shutdown. One situation in which this might not be possible is during an unscheduled shutdown with a required rapid cooldown. Current practices allow plants to significantly reduce primary system temperatures while maintaining high concentrations of hydrogen in the coolant. However, it is likely that this issue could also be addressed through procedure modifications (i.e., requiring reduction in the hydrogen concentration prior to lowering temperature) at least for the majority of unplanned outages. In some cases, rapid reductions in temperature required by technical specifications may make reductions in hydrogen concentration impossible.

### 7.2.2.3 Test Data

A selection of data from the literature is shown in Figure 7-4 through Figure 7-9. The test data indicate that the increases in hydrogen concentration under consideration (e.g., from 35 cc/kg to 80 cc/kg) significantly decrease both the fracture toughness and the tearing modulus of weld metal 182, and significantly decreases the fracture toughness of weld metal 152, but actually increase the tearing modulus of weld metal 152. These data, coupled with previously published data for weld metal 82, indicate that increases in hydrogen concentrations from 35 to 80 cc/kg in the water could significantly reduce the fracture toughness and tearing modulus of some weld materials in plants. However, this can be addressed by requiring RCS hydrogen concentrations to be decreased to low levels before the plant is fully cooled down. The length of time that a plant would operate at low levels of hydrogen would be based on susceptible components. Currently, the extent to which specific components are susceptible is not well understood.

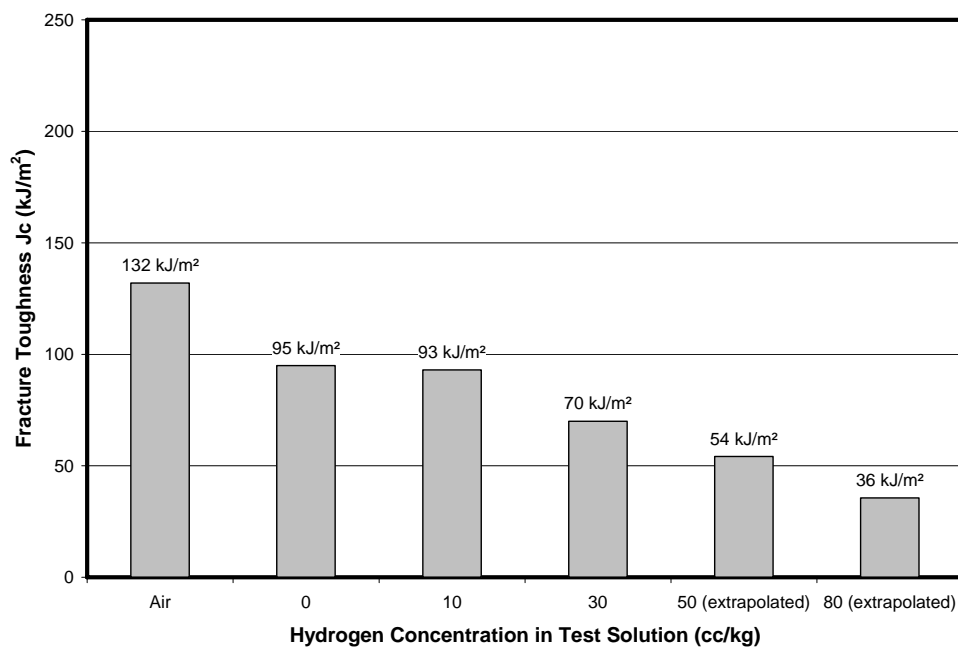


**Figure 7-4**  
Effect of Hydrogen w/o Pre-Charging on Fracture Toughness, Weld Metal 182 at 54°C [63]

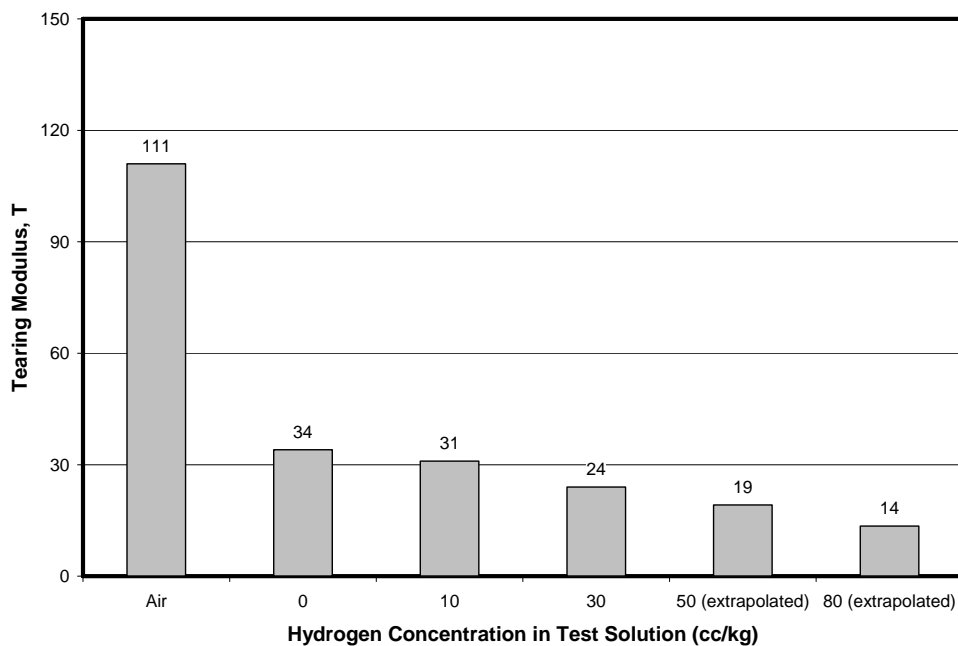


**Figure 7-5**  
Effect of Hydrogen w/o Pre-Charging on Tearing Modulus, Weld Metal 182 at 54°C [63]

Effect of Hydrogen on LTCP

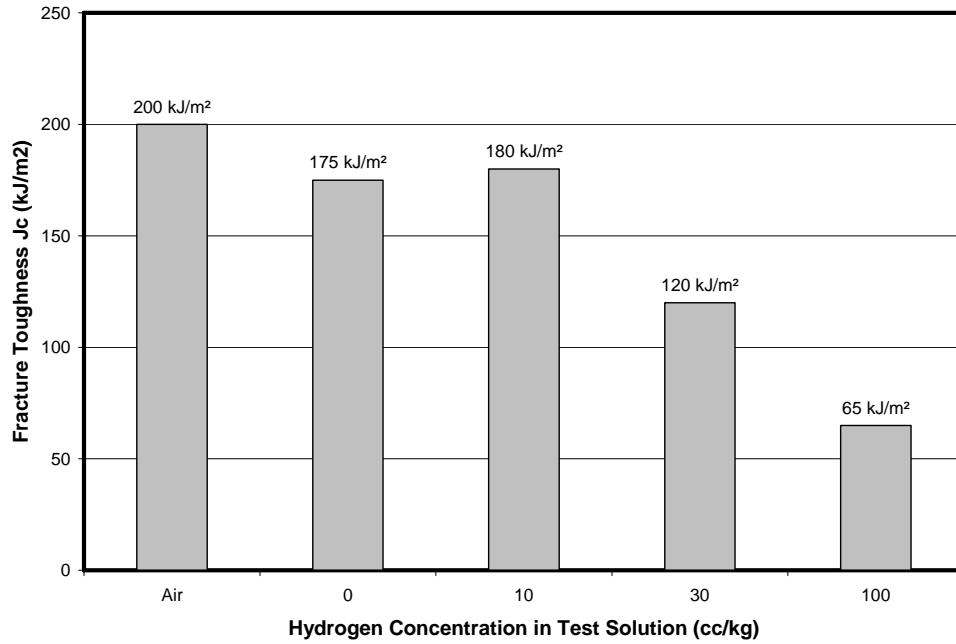


**Figure 7-6**  
Effect of Hydrogen w/o Pre-Charging on Fracture Toughness, Weld Metal 152 at 54°C [63]

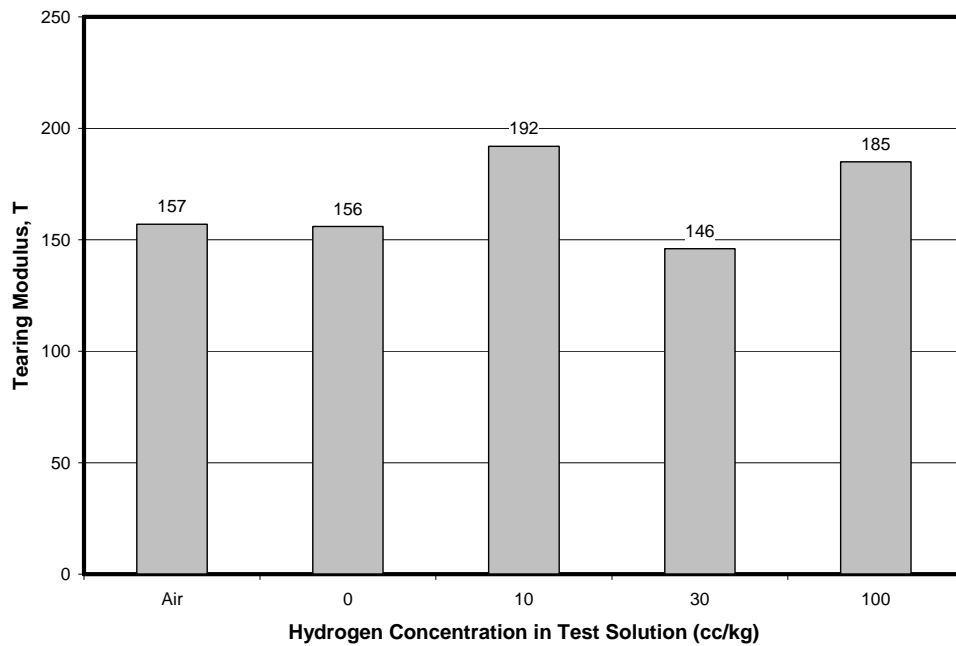


**Figure 7-7**  
Effect of Hydrogen w/o Pre-Charging on Tearing Modulus, Weld Metal 152 at 54°C [63]

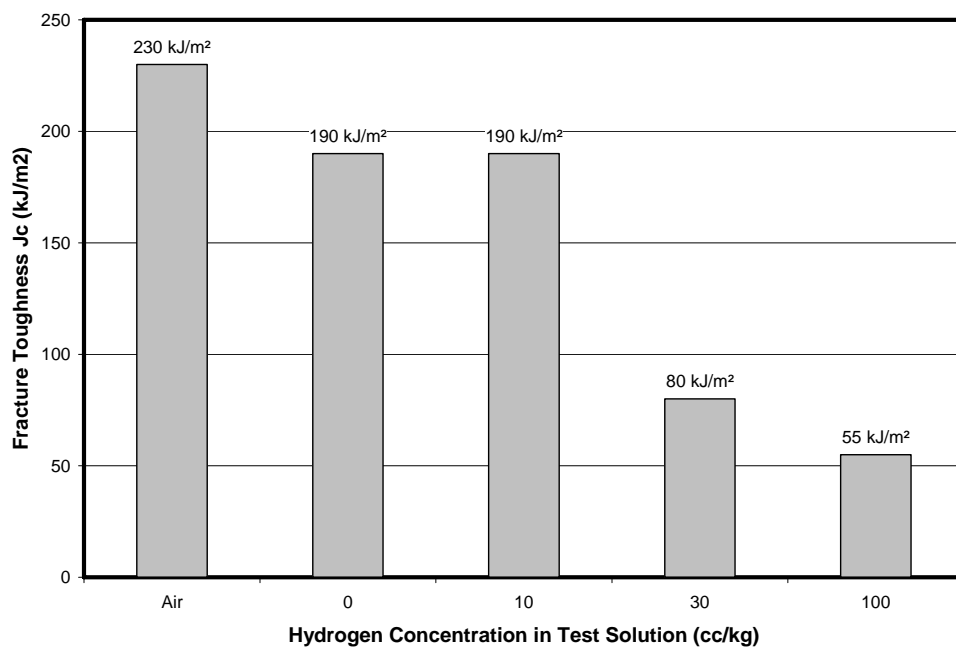


**Figure 7-8**  
Effect of Hydrogen w/o Pre-Charging on Fracture Toughness, Weld Metal 52 at 54°C [63]

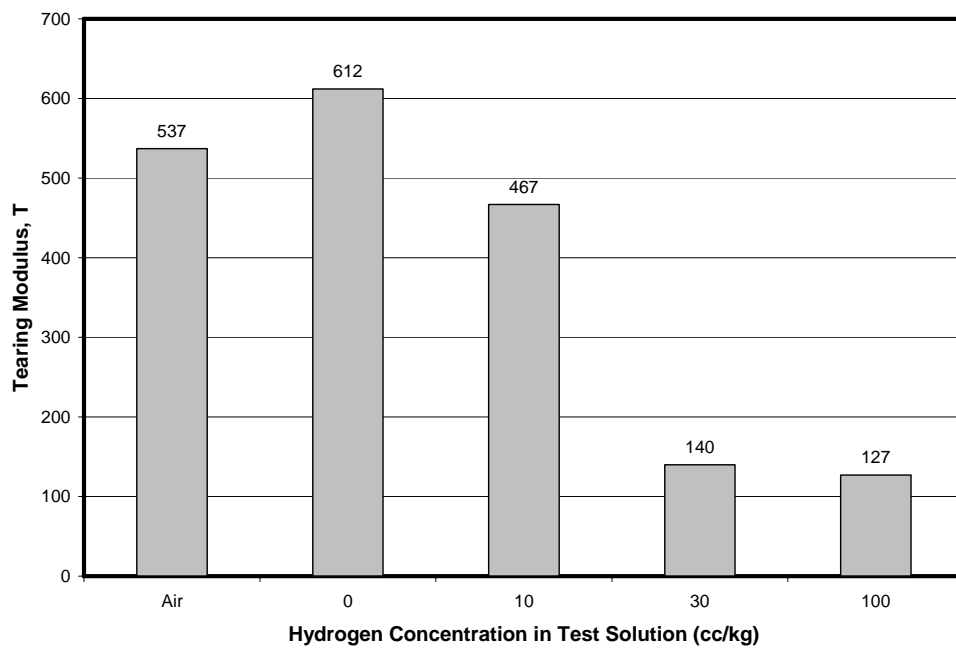


**Figure 7-9**  
Effect of Hydrogen w/o Pre-Charging on Tearing Modulus, Weld Metal 52 at 54°C [63]

### 7.3 Summary of on-Going and Future Work

EPRI is currently funding additional work on LTCP to determine if this phenomenon is relevant to PWR components. This work includes the following:

- Investigation of the effects of different loading techniques
- Investigation of the effects of stress redistribution during crack propagation

In the majority of the laboratory tests reported in the literature, the load on the specimen is generally increasing during the course of the test or the strain rate is held nominally constant. However, in a PWR component, the load is more likely to be governed either by constant displacement (i.e., a fixed strain) or by a falling stress (due to stress field relaxation as the crack grows). Therefore, additional testing under more varied loading techniques is being conducted. It is unlikely that this additional testing will affect the assessment of elevated hydrogen concentrations considered here. The results of this testing are expected to be available by the end of 2007.

A second study is investigating the effect of stress redistribution due to crack growth using advanced finite element analysis methods. The results of this project are expected to complement the first project by determining how a load in a PWR component would change with time, so that it can be determined to what extent LTCP observed in the laboratory for different loading mechanisms are applicable to PWR components.

### 7.4 Conclusions

Mills has proposed a system of classification based on fracture toughness and tearing modulus as shown in Table 7-1. The following recommendations for treatment of each class are made [69]:

- Class I: “At these toughness levels, fracture can occur at or below yield strength loadings for relatively small flaw sizes. For this class of materials, linear-elastic fracture mechanics assessments should be an integral part of design and operational analyses.”
- Class II: “Fracture control based on fracture mechanics approach should be considered, especially for materials with relatively high stress intensity limits. Elastic-plastic fracture mechanics methods may be required, particularly at the higher toughness levels.”
- Class III: “Tearing instabilities are unlikely except after gross plastic deformation. Engineering fracture mechanics evaluations are generally not required.”

**Table 7-1**  
**Mills Classification System [69]**

	<b>Class I</b>	<b>Class II</b>	<b>Class III</b>
Fracture Toughness $J_{IC}$ (kJ/m <sup>2</sup> )	< 30	30 - 150	> 150
Fracture Toughness $K_{IC}$ (MPa√m)	< 75	75 - 160	> 160
Tearing Modulus	<10	10 - 100	> 100

The conclusions and recommendations given in the following sections are based on these recommendations.

#### **7.4.1 Effect of Elevated Hydrogen on Internal Hydrogen Embrittlement**

From the data given in Figure 7-1, Figure 7-2, and Figure 7-3, it appears that increases in the bulk metal hydrogen concentration above levels that cause an initial decrease in fracture toughness do not significantly cause further reductions. The following caveats must be added to this general conclusion:

- The data on IHE (pre-charging) is relatively sparse and materials of principal interest in PWRs appear to have not been tested in this manner.
- Any effects of pre-charging can probably be eliminated for normal shutdowns by reducing hydrogen concentration in the coolant before reducing temperature. However, the possibility of rapid cooldowns during forced outages with little time for degassing needs to be considered.

#### **7.4.2 Effect of Elevated Hydrogen on Hydrogen Environment Embrittlement**

Evaluation of the data in Figure 7-4 through Figure 7-9 indicates that the increases in coolant hydrogen concentration under consideration (e.g., from 30 cc/kg to 80 cc/kg) do not result in changing classifications. There is some indication that lowering the hydrogen concentration (e.g., from 30 cc/kg to 10 cc/kg) may result in raising the material from Class II (some LTCP concern) to Class III (no LTCP concern). This indicates that reducing hydrogen concentrations before reducing temperature may provide protection against LTCP. (Note that reductions in hydrogen concentration would generally be necessary before significant reductions in temperature due to the thermal activation of diffusion. That is, lowering temperature at high hydrogen concentrations may “trap” hydrogen in the metal.)

#### **7.4.3 Recommendations for Further Analysis and Testing**

Although IHE and HEE are generally governed by the same mechanism, they involve different kinetics (diffusion lengths) which result in different effects of the hydrogen concentration. While considerable work has been done by EPRI and others to evaluate HEE, IHE should also be investigated. If PWR components are susceptible to IHE, then the extent to which the concentration of hydrogen dissolved in the materials of those components governs that susceptibility will affect end-of-cycle hydrogen strategies and strategies for dealing with rapid cooldowns following forced outages. It is therefore recommended that separate testing of the effect of IHE on the possibility of LTCP in PWR components be investigated.

## **7.5 Slow Cracking in Air at Room Temperature**

A phenomenon that may be related to LTCP but has been much less well characterized is the relatively slow (~0.5 mm/day) crack propagation in highly stressed Alloy 600MA samples in dry air at room temperature after previous exposure to high-temperature simulated primary side conditions. This cracking mode has only been reported at one laboratory.[70] Furthermore, it was not performed as part of a controlled experiment, but was simply an observation determined several weeks after completion of an experiment involving the samples. The extent to which this phenomenon is relevant to the consideration of operation at elevated hydrogen concentrations is not known. However, given the lack of confirmation despite similar exposures of other samples at numerous different laboratories, the risk of crack growth due to this mechanism is considered low.

Anecdotal evidence regarding low temperature crack propagation in plants was summarized in Reference [71]. Data from several plants (Doel 3, Doel 4, Almaraz 1, McGuire – unit unspecified) indicated that primary side crack growth rates in steam generators were more closely associated with the number of outages rather than the time at operating conditions; one possible explanation might be low temperature crack propagation, but several other mechanisms are also possible.

# 8

## HYDROGEN CONCENTRATIONS AND RADIOLYSIS

---

### 8.1 Introduction

Radiation from nuclear fuel creates chemical energy in the reactor coolant through gamma, alpha, beta, and neutron radiation interaction with the coolant. Since the principal constituent of the reactor coolant is water, essentially all of the chemical energy is created through modifications of water molecules (linear energy transfer, LET). This modification can result in new ionic species or new molecules. The chemical conversion of water by radiation is generally referred to as radiolysis. Typical species that are generated by radiolysis include the following [72]:

$H_2$	$e^-$	$H^+$	$O_2^-$
$O_2$	$H$	$OH^-$	$HO_2^-$
$H_2O_2$	$OH$	$O^-$	

Of these, only the molecular species  $H_2$ ,  $O_2$ , and  $H_2O_2$  are sufficiently stable to avoid reacting with water or other radiolysis products long enough to react with system materials. (The hydrogen and hydroxyl ions,  $H^+$  and  $OH^-$ , are of course present in small quantities in dynamic equilibrium and affect the chemical nature of the coolant as measured by the pH.)

Measurement of molecular radiolysis products in the core is nearly impossible, and nominal measurements of parameters such as electrochemical potential (ECP) combine the individual species concentrations into one measurement. Therefore, assessment of radiolysis products requires modeling. The following are the three principal inputs to radiolysis models:

- The first input is the radiation flux, including gamma, beta, alpha ( $^{10}B(n,\alpha)^7Li$ ), and neutron radiation.
- The second input is the G-values for the species generated. A G-value is defined as the number of molecules of the species generated by 100 eV of absorbed radiation. (In an alternate formulation, the W-value may be used. The W-value is the energy required to produce a single ion pair, and is inversely related to the G-value.)[73]
- The third input is a set of reaction rates for the interactions of the species listed above and water.

Combining these inputs in an appropriate manner allows the calculation of the concentrations of various species. Section 8.2 discusses calculations and their comparison to measured values for full power operation. Section 8.3 contains a similar discussion regarding reduced power or shutdown conditions.

The ultimate goal of any analysis of radiolysis products with respect to material degradation is the assessment of the electrochemical potential which results from the concentrations of the various species dissolved in the water (principally hydrogen, oxygen, and hydrogen peroxide). As discussed in Section 3.7 this assessment may be performed, in an approximate manner, by comparing the concentrations of oxidizing and reducing species. This method is used in the following assessment of modeling results from the literature.

## **8.2 Full Power Operation**

The minimum concentration of hydrogen required to suppress radiolysis in a PWR core has been the subject of continuing investigation for the last 50 years. Improvements in model inputs (from experimental data) have considerably refined predictions, making the investigation of secondary phenomena useful as other uncertainties have been reduced. Section 8.2.1 discusses the most recent understanding of the effect of hydrogen concentration on radiolysis suppression. Sections 8.2.2 through 8.2.7 discuss secondary phenomena that add refinement to the general assessment, but do not significantly affect the conclusions of that general assessment. These secondary discussions are included in this report for completeness, cataloguing the relevant phenomena that have been addressed.

### **8.2.1 Bulk Equilibrium**

A model of the type discussed in the introduction to this chapter (using G-values, rate constants, etc.) was used to predict the equilibrium hydrogen peroxide concentration in a typical PWR core (in-core) and at the outlet of the core (ex-core).[6] Modeling was performed for prototypical beginning and end of cycle chemistries. The results are shown in Figure 8-1 and Figure 8-2, for beginning and end of cycle chemistry, respectively. In both cases, the minimum hydrogen concentration required to suppress radiolysis is between 0.1 and 0.25 cc/kg. The minimum concentration to maintain an excess of reducing species (hydrogen) over oxidizing species (hydrogen peroxide), which is expected to result in a reducing environment, is also within this range, as indicated by the intersection of the curves representing hydrogen peroxide concentration and equivalent hydrogen concentration (i.e., the hydrogen concentration converted to an equivalent hydrogen peroxide concentration so that *1 eq ppm H<sub>2</sub>O<sub>2</sub>* represents the same number of moles of hydrogen as 1 ppm of hydrogen peroxide).

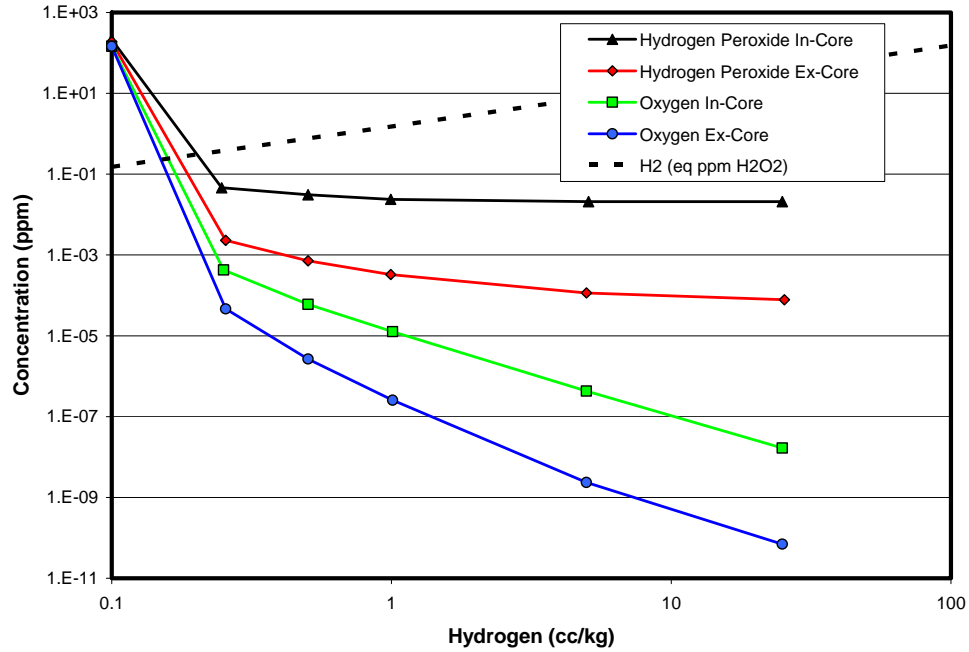


**Figure 8-1**  
Effect of Hydrogen Concentration on Oxidizing Radiolysis Product Concentration  
1800 ppm B, pH<sub>300°C</sub> = 6.9 [6]

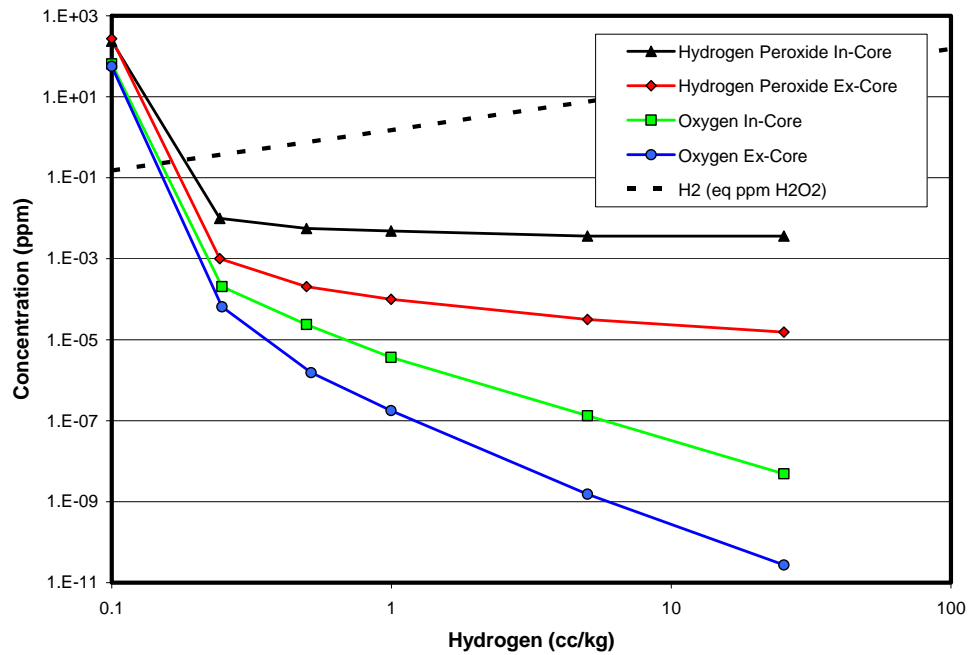


**Figure 8-2**  
Effect of Hydrogen Concentration on Oxidizing Radiolysis Product Concentration  
0 ppm B, pH<sub>300°C</sub> = 7.4 [6]

### 8.2.2 Sensitivity to Model Inputs

Reference [72] explores the sensitivity of the model used in Section 8.2.1 to changes in the basic inputs: G-values and reaction rate constants. Figure 8-3 shows the calculated results for the base model and two variations (one in G-values, the other in reaction rate constants). The results indicate that for the hydrogen concentrations under consideration, the model is robust, with all variations predicting suppression of radiolysis (and an excess of hydrogen over hydrogen peroxide, which is expected to be indicative of a reducing potential) above a hydrogen concentration of  $\sim 0.5$  cc/kg.

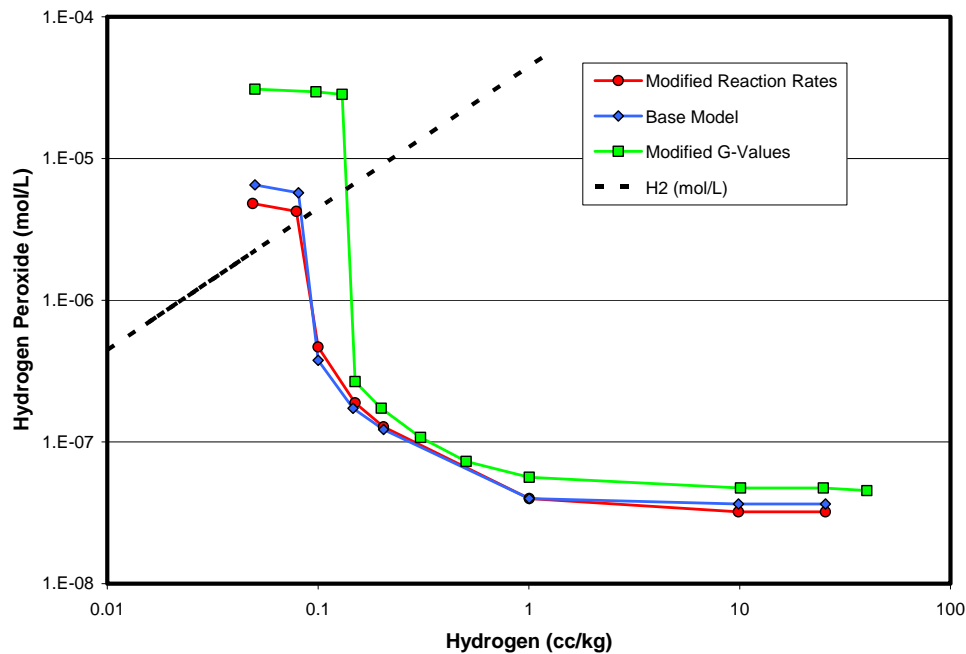


**Figure 8-3**  
Sensitivity of Radiolysis Model to Variations in Inputs [72]

### 8.2.3 Variations Along a Fuel Assembly

The local concentration of hydrogen can change along the length of a fuel assembly for a variety of reasons, including the kinetic effects of hydrolysis, changing radiation fields, and stripping of hydrogen gas by boiling. Figure 8-4 shows calculated hydrogen concentrations for a high power fuel assembly in a PWR.[74] Note that at lower concentrations of bulk hydrogen, radiolysis is not suppressed and the hydrogen concentration (along with other radiolysis products, since this hydrogen can arise only through the formation from water of the oxidizing species oxygen and hydrogen peroxide) increases along the fuel assembly. At higher bulk hydrogen concentrations, the conditions at the top of the fuel assembly are depleted in hydrogen due to boiling. However, for bulk concentrations above 0.5 cc/kg, the concentration along the assembly never falls below the concentration needed to suppress radiolysis. (Depletion due to boiling is discussed in Section 8.2.4.)

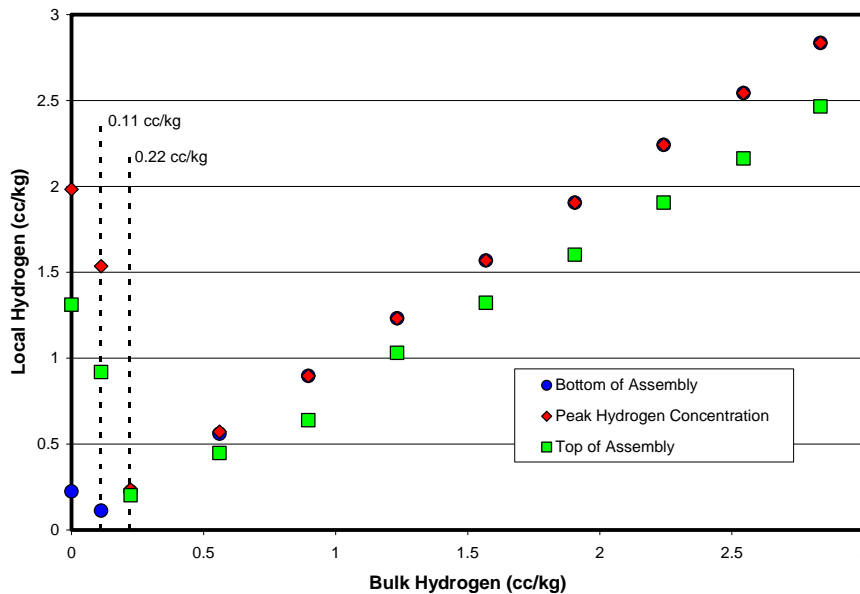


**Figure 8-4**  
**Hydrogen Concentrations Along a High Power Fuel Assembly [74]**

Note that the modeling results shown in Figure 8-4 are independent from those discussed in Section 8.2.1 and therefore provide independent confirmation that the threshold hydrogen concentration for radiolysis suppression is very low. In this modeling it was found to be between 0.11 cc/kg and 0.22 cc/kg, as indicated by the close matching between concentrations at the different locations and the bulk concentration at concentrations of 0.22 cc/kg and greater.

### 8.2.4 The Effects of Boiling

It has been speculated that boiling on the fuel cladding can lead to local depletion of hydrogen as hydrogen is transferred from the liquid bulk to the newly generated gas phase, since at equilibrium the mass/mass concentration of hydrogen is greater in the vapor phase than in the liquid phase. However, modeling of the mass transfer rates at the liquid-gas interface indicate that the depletion in hydrogen is relatively small.[72]

The model developed [72] uses the unsteady equation for hydrogen, oxygen, and hydrogen peroxide diffusion from a bubble into an essentially infinite medium with an additional term for the chemical reactions between the three species. The model predicts that over the lifetime of a bubble (1-3 ms) hydrogen is not likely to become significantly depleted in the immediate vicinity of the bubble. Furthermore, hydrogen peroxide, the major oxidizing species, is not likely to be significantly higher in concentration near the liquid-gas interface than in the bulk. Figure 8-5 shows the concentrations of hydrogen, hydrogen peroxide, and oxygen near the liquid-gas phase interface of an expanding steam bubble at 344°C when the bulk hydrogen concentration is 40 cc/kg. This figure shows that, even very close to the interface, hydrogen is not significantly depleted and hydrogen peroxide concentrations are not significantly higher than in the bulk. Note that the concentration of hydrogen is given in moles per liter so that it can be compared to the concentration of the oxidizing species on a stoichiometric basis.[72]

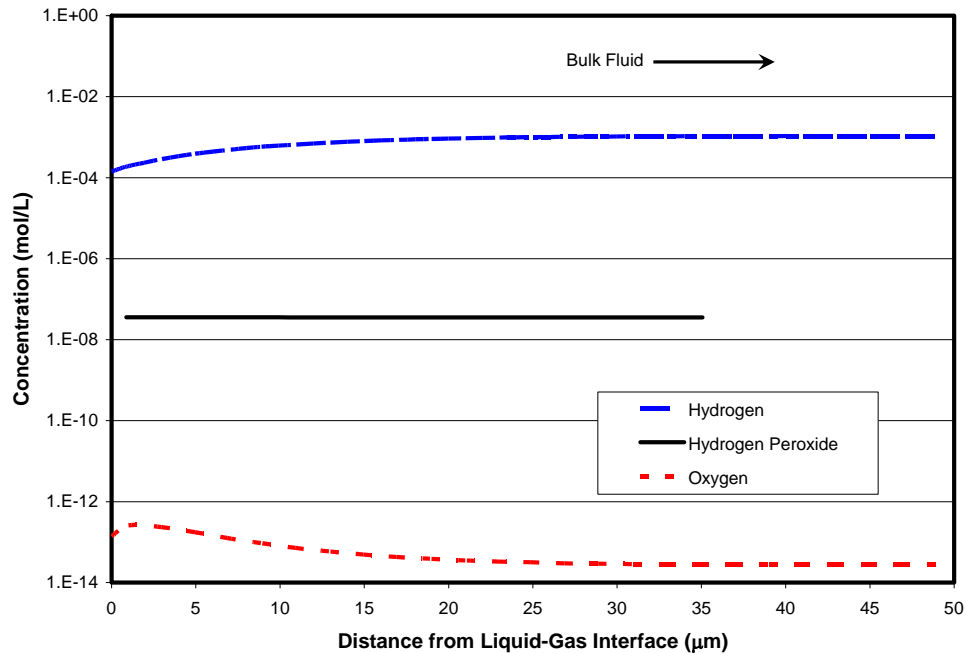


**Figure 8-5**  
 $H_2$ ,  $H_2O_2$ , and  $O_2$  Concentrations Near an Expanding Steam Bubble  
 344°C, 40 cc/kg Bulk  $H_2$  [72]

Figure 8-6 shows the effect of bulk hydrogen concentration on the depletion of hydrogen near a steam bubble surface and the resulting concentration of hydrogen peroxide. The curves show that for very low bulk hydrogen concentrations, the region near the expanding steam bubble surface may become depleted enough in hydrogen that the hydrogen peroxide concentration increases significantly near the bubble surface. However, it is important to note that 0.15 cc/kg hydrogen corresponds to about  $4 \times 10^{-6}$  mol/L hydrogen, so that even near the bubble surface the concentration of hydrogen is at least an order of magnitude higher than the hydrogen peroxide concentration.[72]

It is possible that the highly complicated geometry created by boiling in a surface deposit, with wicking of liquid through small pores and the exit of steam through large pores (chimneys), or the interaction of multiple bubbles could lead to a condition in which a vapor-liquid interface persists for extended periods (i.e., more than the 1-3 ms lifetime of a typical steam bubble). This could lead to more significant depletion of hydrogen in the liquid phase. However, such a stable interface near the cladding surface seems unlikely in the absence of contaminants which could raise the boiling point of the liquid phase. That is, the temperature gradient from the clad surface, through the deposit, and into the bulk makes a stable liquid phase at the clad surface unlikely. However, the existence of a stable liquid phase in the crud, which if depleted in hydrogen could affect the oxidation state of the deposit, is more likely. A stable liquid-vapor interface in the bulk coolant is highly unlikely. Therefore, while depletion due to boiling may be expected to affect the oxidation state of the deposits on the fuel, it is not expected to significantly change the reducing conditions (ECP) at either the clad surface or on other components susceptible to increased degradation under oxidizing conditions.

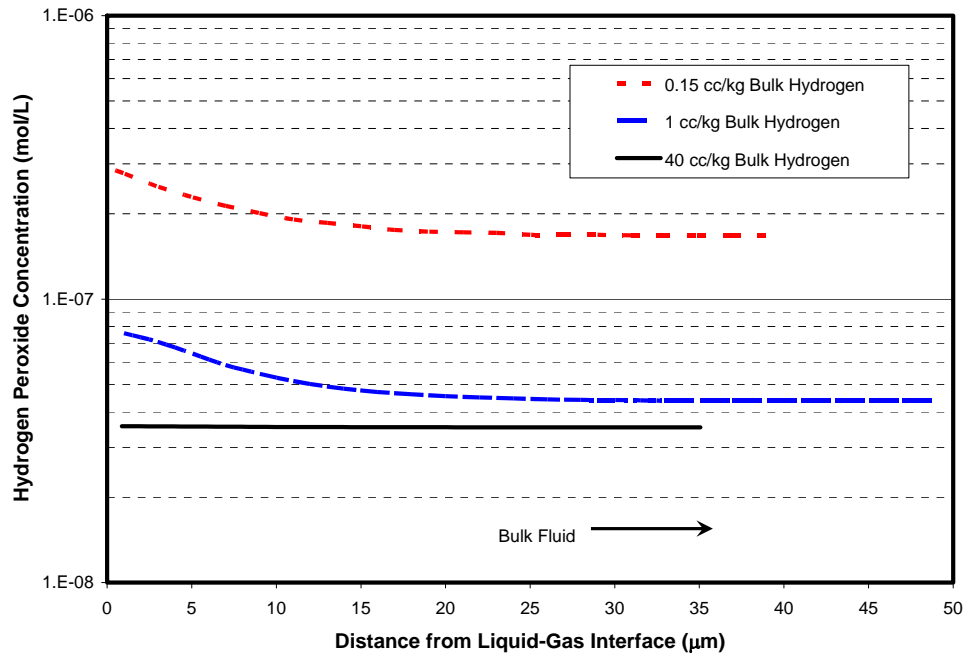


**Figure 8-6**  
**The Effect of Bulk H<sub>2</sub> on H<sub>2</sub>O<sub>2</sub> Concentrations Near an Expanding Steam Bubble (344°C)**  
**[72]**

### 8.2.5 Metal Ion Effects

Although reactions with metal ions can affect radiolysis of water, concentrations of these ions are very small in reactor coolant environments (compared, for example, to the concentrations of hydrogen under consideration). Therefore, the presence of metal ions is not expected to significantly influence the concentrations of hydrogen required to suppress radiolysis.[6]

### 8.2.6 Surface Effects

The proximity to a surface can affect radiolysis relative to the calculations for bulk equilibrium discussed in Section 8.2.1. For example, secondary electrons produced by beta irradiation of metal surfaces can contribute significantly to the formation of radiolysis products.[75] During power operation of PWRs, this effect is expected to be small when considering the threshold for production of oxidizing species because the principal mechanism for generation of oxidizing species (hydrogen peroxide) is neutron and alpha, i.e.,  $^{10}\text{B}(n,\alpha)^7\text{Li}$ , radiation.[76] The effects of beta radiation and other electron species appear to be of little importance.[72] However, at reduced power conditions when gamma radiation is more important, the effects of secondary electrons may also be important, since both of these radiations are generally [73] classified as low LET based on the energy they transfer to water. It appears that this concept has not been explored for PWR chemistries.

Surfaces can also affect the results of radiolysis by eliminating some radiolysis products through chemical reaction. During low hydrogen testing at EDF's Belleville reactor, the kinetics of hydrogen concentration changes were slower than predicted from radiolysis modeling.[77] It has been speculated that this was because conversion of corrosion products between different oxidation states consumed radiolysis products.[24] Alternatively, it is known that the principal oxidizing species formed by radiolysis, hydrogen peroxide, is subject to decomposition reactions both in bulk water and on surfaces (see, for example, Reference [78]).

### **8.2.7 Restricted Flow Areas**

In restricted flow areas such as under deposits or at support grid contact points, there is a possibility that the local hydrogen concentration is not the same as the bulk concentration. This is not expected to occur through the depletion of hydrogen by radiolysis, since, as discussed in Section 8.2.1, sufficient hydrogen is expected to be present to prevent net radiolysis. However, if hydrogen is not initially present or becomes consumed (absorption by materials of construction) radiolysis could produce oxidizing species faster than they could be removed by reaction or by diffusion out of the restricted area, resulting in a locally oxidizing environment. Although radiolysis in a crack tip has been discussed in the literature [79], comparisons of radiolysis rates with diffusion rates appear not to have been reported.

## **8.3 Reduced Power Operation**

During periods of reduced power, decreases in temperature and radiation flux combine to affect radiolysis in the core. Changes in temperature affect both the G-values for radiolysis products as well as reaction rates. Changes in the flux, both type and magnitude, affect radiolysis through reductions in energy transfer. Modeling results performed by Nexia Solutions and presented in the Primary Water Chemistry Guidelines [6] provide indications of the magnitudes of each of these effects and the degree to which the resulting radiolysis is affected by hydrogen concentration.

The effect of radiation field reductions are illustrated in Figure 8-7, which shows resulting hydrogen peroxide concentrations as a function of bulk hydrogen concentration at a flux representative of 100% power, a flux of 10% of full power gamma (with no neutron flux), and a flux of 1% of full power gamma (with no neutron flux). The lower flux cases also consider an accompanying temperature change at reduced power. These calculations indicate that if a high temperature is maintained, reductions in power will require less hydrogen to suppress radiolysis than would be required at full power.

The effects of further temperature reductions are shown in Figure 8-8. These calculations indicate that as temperature is reduced (with flux rates constant at a value typical of early shutdown values), the equilibrium concentrations of hydrogen peroxide will increase significantly. A subset of these data are plotted in Figure 8-9, which shows the equilibrium hydrogen peroxide concentration as a function of temperature for high (40 cc/kg) and low (0.1 cc/kg) dissolved hydrogen. These data indicate that there is little benefit, with respect to radiolysis suppression, in increasing hydrogen concentrations. (Note that unlike the other figures used in this chapter, the hydrogen peroxide concentration in Figure 8-9 is plotted on a linear scale.)

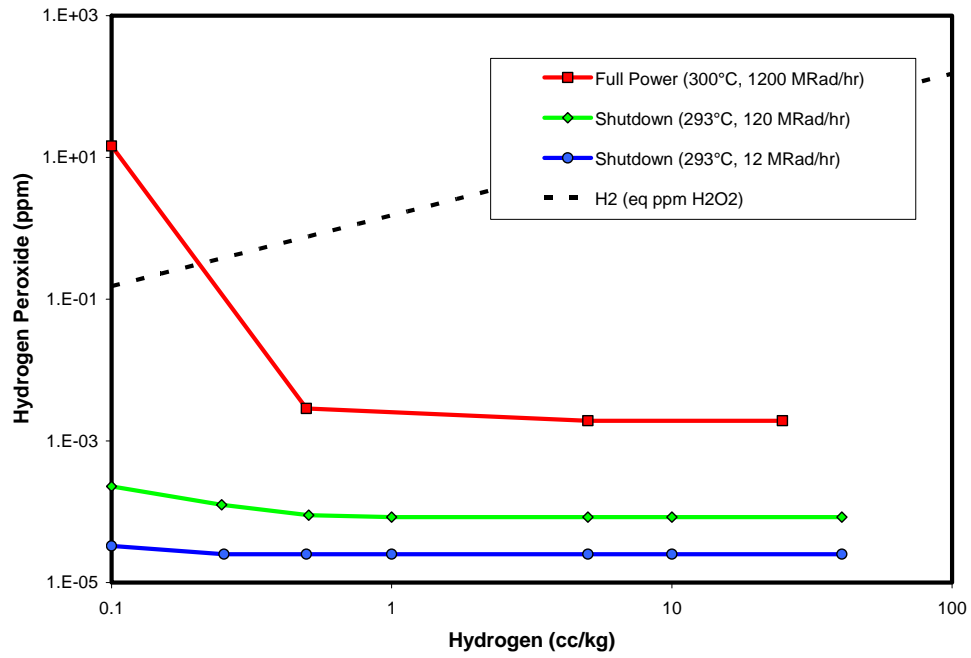


**Figure 8-7**  
The Effect of Power Reduction and Accompanying Temperature Change on Radiolysis [6]

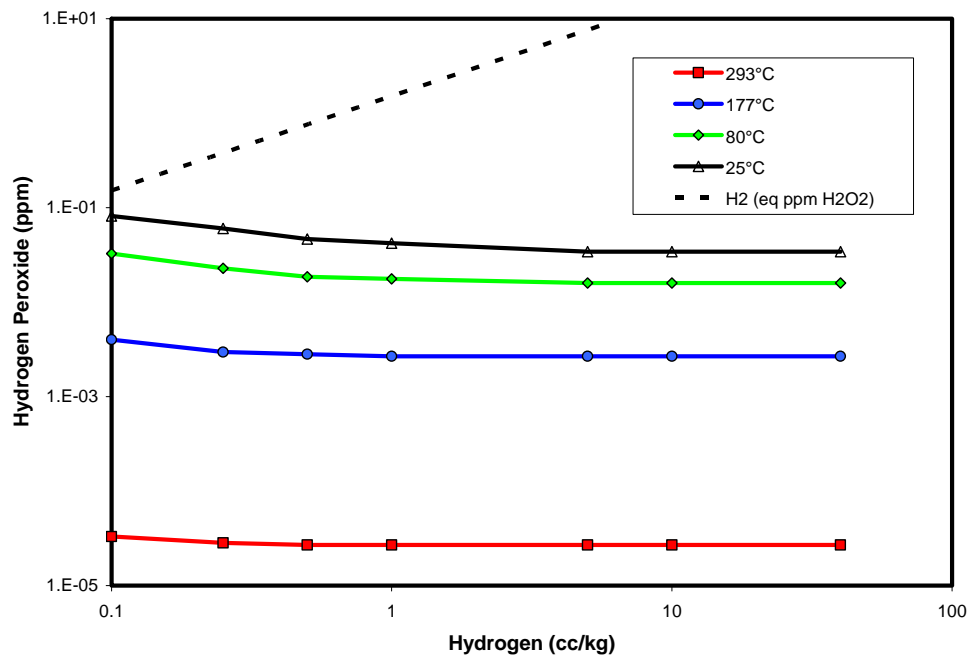


**Figure 8-8**  
The Effect of Temperature Reduction at Zero Power on Radiolysis [6]

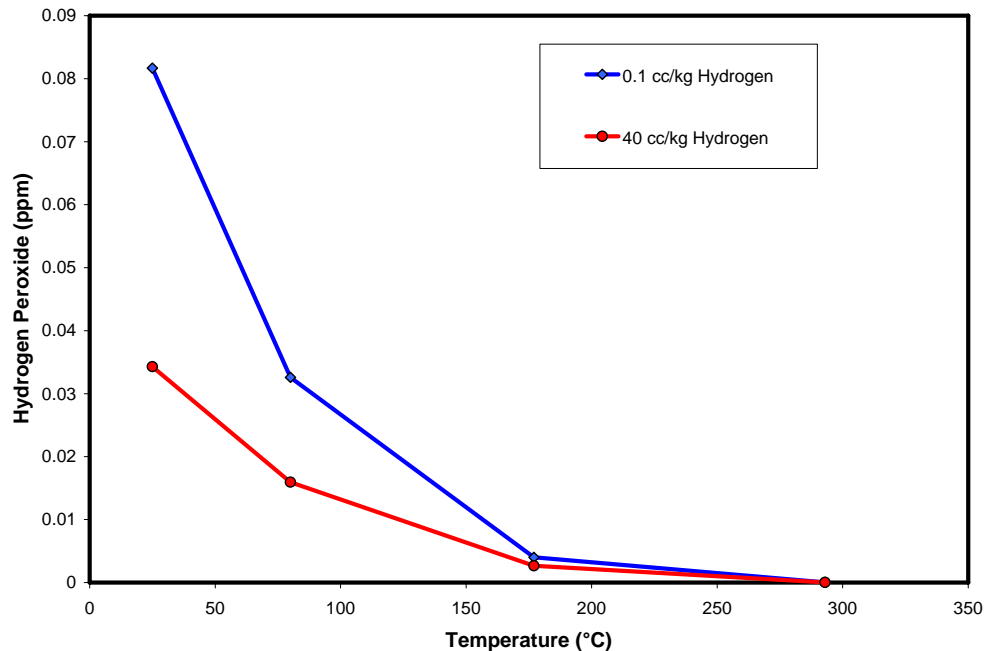


**Figure 8-9**  
**The Effect of Temperature on Radiolysis at High and Low Hydrogen Concentrations [6]**

## 8.4 Conclusions

The modeling analyses described in the previous sections lead to the following conclusions regarding the effect of dissolved hydrogen concentration on radiolysis:

- At full power, the minimum hydrogen concentration required to suppress radiolysis is less than 0.5 cc/kg.
- At reduced power, the extent of radiolysis is insensitive to hydrogen concentration in the concentration range of 0.1 - 40 cc/kg. At elevated temperatures, there is little radiolysis. As temperature decreases, radiolysis is no longer suppressed. This trend is not expected to be affected by increases in hydrogen concentration above 40 cc/kg.
- Numerous secondary factors (temperature, boiling, variations along the fuel assembly, input uncertainty) have been considered. None affect the general conclusions.

In summary, radiolysis is not significantly affected by changes in hydrogen concentration within the range being considered (5 – 80 cc/kg). Note that the analyses discussed in this chapter do not address the practical issue of whether it is possible to control dissolved hydrogen at 5 cc/kg without inadvertently lowering the concentration enough to allow radiolysis. Such practical issues are discussed in Sections 9.3 and 10.2.

# 9

## OPERATIONAL AND SAFETY ISSUES

---

### 9.1 Introduction

The purpose of this chapter is to catalogue operational and safety issues that may impede the application of elevated or reduced RCS hydrogen concentrations. The chapter is based largely on a review performed for EPRI in 2006/2007 [80]. This review included consultation with an expert panel including EPRI project managers, utility chemistry personnel, fuel and NSSS vendors, and consultants. This panel identified some issues as high priority; these are discussed in Section 9.2. Additional issues that were identified but considered lower priority are discussed in Section 9.3. Resolution of many of these issues is dependent upon a reliable understanding of hydrogen distribution throughout the RCS at various operating conditions. Modeling to address this need is discussed in Section 9.4.

This review is intended to cover all commercial PWR designs in operation in the United States. Significant differences exist between B&W (OTSG) plants and Westinghouse and CE plants. However, with respect to most of the issues discussed in this section, these differences do not affect the concerns regarding use of higher or lower hydrogen concentrations. Some major differences are as follows [81]:

- B&W plants use seal injection flow for the majority of makeup flow.
- The design pressure of a typical B&W makeup tank (the equivalent of the VCT) is 100 psig, while the design pressure of a typical Westinghouse or CE VCT is 75 psig.

The purpose of this review is to provide the technical bases for a future plant-specific evaluation (including a 50.59 safety evaluation). The technical issues discussed are generic to all plant designs, but may not include all issues which would need to be evaluated for a specific plant.

### 9.2 Priority Concerns

In general, the highest priority issues are safety related. These issues focus on material integrity and avoidance of explosive gas mixtures. Specific issues are discussed in the sections below.

#### 9.2.1 Formation of Explosive Gas Mixtures

A major consideration in the use of hydrogen is the potential for the formation of explosive gas mixtures. In general, this risk is small during normal operation. However, plant-specific safety evaluations would have to be performed before implementation of elevated hydrogen concentrations. Specific concerns that would need to be addressed are:

*Operational and Safety Issues*

- Startup conditions
- Shutdown condition (e.g., chemical degassing)
- Loss of coolant accident (LOCA) conditions

It is not possible to completely address these issues in the scope of this report. Some of these issues may be addressable on a generic basis. However, most would require a plant-specific evaluation. Generic evaluations in support of such an effort are already available.[82, 83, 84]

### **9.2.2 Effects of Hydrogen Concentration on Fuel Performance and Integrity**

Several effects of hydrogen concentration have been postulated, including the following:

- Changes in hydriding and other corrosion phenomena (Chapter 5)
- Changes in corrosion product deposition rates (Chapter 6)
- Changes in boiling rates (Section 9.4.2)
- Increases in oxidant concentrations (for decreases in hydrogen concentrations) (Chapter 8)

These issues are extensively discussed in the sections of this report noted in the above list and are not discussed further here. Although these issues pose significant concerns, they do not appear to prevent the safe application of elevated or decreased hydrogen concentrations based on current knowledge. However, additional work is needed to close existing knowledge gaps.

### **9.2.3 Avoidance of Radiolysis**

The effects of hydrogen concentration on radiolysis are thoroughly discussed in Chapter 8. There appears to be little chance of hydrogen concentration affecting radiolysis during normal operation within the range of concentrations under consideration (5 – 80 cc/kg). However, as discussed in the Primary Water Chemistry Guidelines, operation at below the current lower limit of 25 cc/kg would reduce margins against inadvertently experiencing oxidizing events during plant events (e.g., loss of letdown flow).

### **9.2.4 Acceleration of PWSCC**

As discussed in Section 4.4, some specific changes in hydrogen concentration could result in accelerated PWSCC. For lower temperature locations (325°C to 290°C) all changes to hydrogen concentrations to operate in the range of 5 – 25 cc/kg are expected to accelerate PWSCC of nickel-base alloys and weld metals (regardless of the specific material).

Since numerous susceptible components are at temperatures in this temperature range, lowering coolant hydrogen concentrations would increase the risk of pressure boundary degradation in several locations. PWSCC of components operating in this temperature range has already been observed. For these reasons, it is considered highly unlikely that decreased hydrogen concentrations can be considered desirable (or even feasible) for the current generation of plants.

### **9.2.5 Hydrogen Embrittlement**

The effects of the increases in hydrogen concentration under consideration on stainless steels and other non-nickel-base, non-zirconium-base RCS materials have not been fully considered. Hydrogen embrittlement and increased intergranular stress corrosion cracking (IGSCC) may be accelerated by increased hydrogen concentration, although the modest increases under consideration may have no effect. Hydrogen concentrations are not expected to affect crack growth rates in stainless steels [85] although there may be some limited effect [86].

### **9.2.6 Safety-Related Systems Inoperability**

As discussed in Section 10.4.1, safety-related plant systems have been found to be inoperable due to the development of gas pockets. In general, these incidents have involved the failure of a system or program designed to prevent such occurrences. The rate of gas pocket growth is expected to increase linearly with the hydrogen concentration. Therefore, the risk of safety-related system inoperability is expected to increase slightly. Review of this particular issue requires plant-specific safety evaluations.

### **9.2.7 Effect on RCP Seals and Seal Performance**

Part of the charging flow from the CVCS is diverted to the RCP seals. The portion of this flow which enters the RCS and returns to the VCT (excess seal flow) is affected by the pressure differential across the seals. Typical requirements for VCT pressure are >15 psig and <65 psig.[87] At pressures <15 psig, VCT pressure is not sufficient to prevent backflow through the seals. At >65 psig, excess seal flow will be reduced and too much seal flow will enter the RCS. Note that the lower limit of 15 psig and the upper limit of 65 psig are within the range of pressures considered in the discussion on VCT pressures (Section 9.4.2).

An additional issue affecting RCP seals is the presence of deposits in this area. Rust colored deposits, presumably hematite, have been detected on RCP seals.[6] The effects of increased hydrogen concentrations on such deposits and the subsequent consequences for RCP operability are not immediately apparent.

Due to the pressure drop across the seals, the RCP seals may be a location that is susceptible to void formation, as discussed in Section 9.3.1 and Section 9.4.3.

RCP seal materials have not been specifically evaluated for compatibility with the hydrogen concentrations under consideration. However, it is likely that compatibility with 80 cc/kg is not significantly different from compatibility with 50 cc/kg.

### **9.2.8 Pressure Limits in Low Pressure Systems**

A review of those portions of the plant that would be subject to higher pressure at elevated hydrogen concentrations will be necessary to ensure that neither structural limits nor operating capabilities will be challenged. These portions include the CVCS, VCT, boron recycle system

(BRS), recycle holdup tank (RHT), reactor coolant drain tanks, pressurizer relief tanks, reactor coolant bleed tanks, hold-up tanks, waste gas systems, and gas release tanks and piping.

RCS hydrogen concentrations are generally maintained by maintaining hydrogen in the volume control tank (VCT) vapor space at a suitable partial pressure. (Some non-US PWR designs include direct injection of hydrogen.) In order to achieve high hydrogen concentrations, the pressure must be increased. This places a physical limit on the concentration of hydrogen that may be used. This issue is discussed further in Section 9.4.2, which presents the results of VCT pressure requirement calculations.

### **9.3 Additional Issues**

Many additional issues were identified in the EPRI review.[80] Those not judged to be high priority issues are discussed here. Generally, each of these issues would need to be addressed, either generically or on a plant-specific basis, before implementation of new hydrogen concentrations. Issues that are addressed in other sections of this report (e.g., LTCP) are not discussed in this section.

#### **9.3.1 Gas Pocket Formation**

Gas pockets have formed with hydrogen concentrations under 50 cc/kg (see Section 10.4). At higher concentrations, voiding may occur at more locations and the gas pockets formed may increase in size more rapidly. A plant-specific program to evaluate which locations in the plant may become susceptible to voiding would be necessary before implementing an elevated hydrogen concentration program.

Among the critical locations where gas pockets may form is the charging pump suction. Formation of large gas volumes in this location could lead to gas binding of the pump and loss of charging flow. Evaluation of the required total pressure to prevent gas pocket formation is discussed in Section 9.4.3.

Another location which may be vulnerable to voiding is the RCP seal. Formation of voids in this location may interfere with RCP operation.

Note that gas binding is considered separately from cavitation, which is addressed in Section 9.3.3.

#### **9.3.2 Secondary Side Conditions**

Hydrogen readily diffuses through the steam generator tubes to enter the secondary side of the steam generators.[9] Due to boiling on the shell side of the steam generators, hydrogen is not expected to accumulate in the steam generators. Buildup of hydrogen in the shell side of feedwater heat exchangers also is not likely due to continuous venting of the shell sides to the condenser (the purpose of the vent is to prevent the buildup of non-condensable gases). However, if vent rates must be increased to prevent such a buildup, there could be a very minor impact on secondary side thermal performance.

An additional consideration is that the diffusion of hydrogen through the steam generator tubes is generally taken to be proportional to the square root of the liquid phase hydrogen concentration. This is due to Sievert's Law for the equilibrium between diatomic gases dissolved in water in equilibrium with monatomic gases dissolved in metals.[9]

Hydrogen that does diffuse to the secondary side will be removed in the condenser off gas. The concentration of hydrogen in this stream is expected to be very low.

The effects of RCS hydrogen on the secondary coolant system are expected to be negligible. It is likely that generic evaluations would satisfy all secondary side safety and operability concerns. One path for dispositioning secondary side effects is to note that the change in the mass diffused through the steam generators would be comparable to hydrogen ingress from primary-to-secondary leakage. Numerous plants have operated with small leaks without hydrogen related issues.

An additional consideration is the possible accumulation of hydrogen in isolated regions (i.e., blocked crevices or gaps between the tube and tubesheet that are isolated from the top of the tubesheet). Increases in primary coolant hydrogen could lead to proportional increases in the hydrogen in these hypothesized locations. It is possible that under these hypothesized conditions the hydrogen concentration could accelerate some form of outer diameter stress corrosion cracking.

### **9.3.3 Cavitation**

It has been speculated that cavitation damage may be augmented by the presence of increased dissolved hydrogen. Although there may be a higher likelihood of gas phase formation (see Section 9.4.3) cavitation damage is likely to be less if significantly higher concentrations of dissolved gasses are present. Because gas bubbles collapse in a finite time period (as opposed to steam bubbles which can collapse instantaneously) there is no shockwave, resulting in lower pulse pressures and less materials damage. Therefore, increased concentrations of hydrogen do not increase the likelihood of cavitation damage. Lower concentrations of hydrogen might increase cavitation damage in locations where cavitation already takes place. However, cavitation is not expected to be more likely with lower concentrations of hydrogen.

### **9.3.4 Waste Gas Handling**

Increases in the concentration of coolant hydrogen will have implications for waste gas handling. Hydrogen generally has a much higher concentration in the coolant than any other dissolved gas. Therefore, increases in hydrogen concentration will significantly increase waste gas volumes. The impact of this increase will be dependent on the specifics of the plant's waste gas system. If hydrogen recombiners are used in the waste handling processes, the impact will be small.

### **9.3.5 Degassing During Shutdown**

During shutdown, hydrogen must be removed from the system prior to head lift and the subsequent exposure of the coolant to containment. If mechanical degassing is used, increased concentrations of hydrogen could prolong the degassing process. If chemical degassing is used, the impact of higher hydrogen concentrations is expected to be negligible.

Increased hydrogen concentrations during operation may also affect crack propagation during shutdown, as discussed in Chapter 7.

For unplanned outages in which the RCS may not be degassed, accumulation of hydrogen in the pressurizer could cause large increases in coolant hydrogen when temperature is increased. This has led to voiding in the letdown demineralizers at one plant. (See Section 10.4.4.)

### **9.3.6 Tritium Generation**

The contribution to tritium concentrations of the  $^2\text{H}(n,\gamma)^3\text{H}$  reaction is negligible.[6] Therefore, hydrogen concentrations are not expected to influence tritium concentrations.

### **9.3.7 Corrosion Product Removal During Shutdown**

Historically, corrosion product removal during shutdown has been linked to pH and hydrogen concentrations. However, the effects of temperature, especially on nickel concentration, are more likely to dominate corrosion product release. Therefore, no effects on corrosion product releases during shutdown are expected from operating at alternative hydrogen concentrations. Additional corrosion product transport issues are discussed in Chapter 6.

### **9.3.8 Control During Water Transfers**

Many plants use aerated makeup water. The extent to which hydrogen can be controlled at low concentrations during periods when large quantities of aerated makeup water are added to the RCS would need to be evaluated before implementing a lower hydrogen concentration. Plant experience (see Section 10.3) indicates that at some plants operating much below 25 cc/kg led to oxidizing conditions even though calculations assuming the initial absence of oxygen indicate that reducing conditions would have been maintained at much lower concentrations of hydrogen (see Chapter 8).

### **9.3.9 Control During Hydrogen Transients**

At least two units have experienced a loss of letdown flow.[9] In each case, operation could continue because of the large inventory of hydrogen in the RCS. If coolant concentrations are lowered (e.g., to 5 cc/kg) this inventory would no longer be present and plants would potentially enter oxidizing conditions much sooner after loss of letdown.

### **9.3.10 Flow Rates Returning to the VCT**

In addition to excess seal flow (see Section 9.2.7) other low pressure flows (e.g., sample return or zinc injection) may return to the volume control tank (VCT). Increases in pressure in the VCT to achieve higher hydrogen concentrations could reduce these flow rates. Since sampling configurations vary significantly from plant to plant, a plant-specific evaluation would need to be performed to address this issue.

### **9.3.11 Resin Degradation**

It has been speculated that there may be an effect of hydrogen concentration on the release of sulfur compounds from demineralizer resin. This issue may warrant additional investigation. Also, the issue of whether a resin ingress would be made worse by elevated or reduced hydrogen concentrations has not been investigated.

### **9.3.12 Radiocobalt Behavior**

It is possible that changes in hydrogen concentration could affect the behavior of cobalt in the RCS, changing the manner in which it is incorporated into ex-core films where it contributes to personnel dose. Changes in hydrogen concentration could affect the stable solid phase of cobalt in a manner similar to nickel (see Section 3.4.2).

### **9.3.13 Interaction With Elevated Lithium**

In order to maintain higher coolant pH values, some units are using concentrations of lithium that exceed those qualified by prior industry experience. Elevated lithium programs have been implemented at these units with the concurrence of fuel vendors and have included augmented fuel inspections. These programs were developed for the current range of hydrogen concentrations. Although there is no indication that changes in hydrogen concentration would change the effects of increased lithium, this issue has not been addressed to date.[42]

### **9.3.14 Non-Technical Issues**

Non-technical issues, such as evaluation of warranty or technical specification requirements or modifications to operating procedures, are outside the scope of this report.

## **9.4 Distribution Modeling**

In order to quantitatively assess the effects of hydrogen concentration changes on operational and safety issues, knowledge of the distribution of hydrogen throughout the system is required. In the liquid phase, it can generally be assumed that the hydrogen concentration is constant. Small deviations from this assumption due to radiolysis in the core or diffusion through the steam generators are expected to be negligible.[9] The principal issue of concern is the

distribution of hydrogen between liquid and vapor phases. Liquid-vapor equilibria occur at the following three locations:

- In the pressurizer where a steam bubble is present during full power operations
- In the VCT where a hydrogen atmosphere is maintained to control coolant hydrogen concentration
- In low pressure regions where voiding may occur

These locations are discussed in the sections below.

#### **9.4.1 Accumulation in the Pressurizer**

During normal operation the pressurizer contains both a liquid phase and a vapor phase. At equilibrium, the mass fraction of hydrogen in the vapor phase will be significantly higher than the mass fraction in the liquid phase. Because of this, the vapor phase in the pressurizer can be a significant source of hydrogen. This is generally only an issue of importance when plant conditions are changing (for example, during shutdown). In these situations, the mass of hydrogen in the pressurizer adds “inertia” to the system and system responses can be delayed. When the exchange of mass between the pressurizer and the rest of the RCS is low (for example, at normal pressurizer spray rates) the mass of hydrogen in the vapor space can cause delayed effects. For example, it is well known that collapsing the steam bubble in the pressurizer can cause a spike in hydrogen concentration.

The effects of the hydrogen concentration changes under consideration should not have a significant impact on the nature of the accumulation of hydrogen in the pressurizer. The mass of hydrogen in the pressurizer will be linearly proportional to the concentration in the RCS.

#### **9.4.2 Required VCT Pressures**

The concentration of hydrogen in the coolant is controlled by maintaining a fixed partial pressure of hydrogen in the volume control tank (VCT). Letdown flow from the RCS is sprayed into the vapor space in the VCT rapidly achieving near-equilibrium concentrations in the liquid phase. This liquid is then returned to the RCS through the charging pumps. Thus, a coolant hydrogen concentration implies a specific VCT hydrogen partial pressure. (Deviations from equilibrium are assumed to be small. For steady state operation, this is undoubtedly valid.)

In some designs, the pressure limit on the VCT is 75 psig (6.1 atm), with an alarm at 60 psig (5.1 atm).[88] As a practical issue, air exclusion requires a slight (2 psig or 1.1 atm) over pressure in the VCT. The liquid phase hydrogen concentrations that could be achieved at these pressures for a range of temperatures are shown in Figure 9-1.

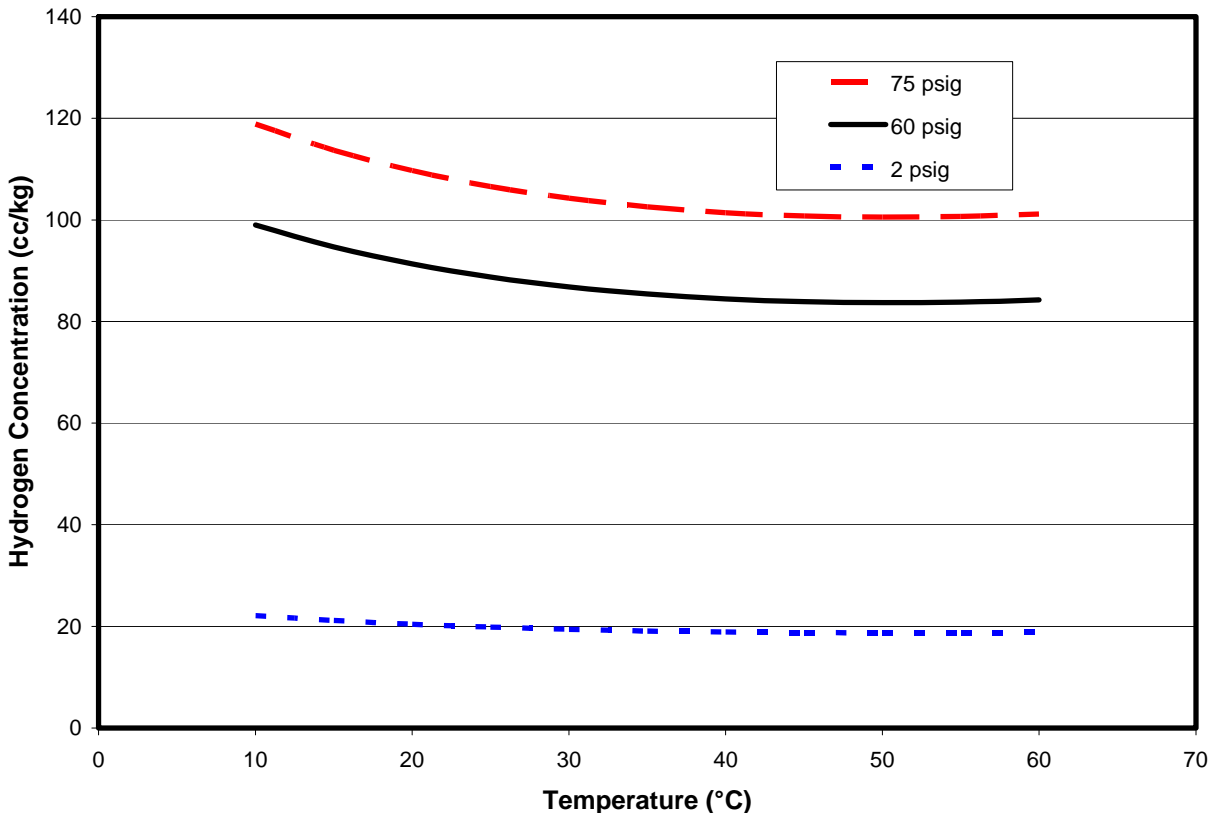


**Figure 9-1**  
**Hydrogen Concentrations Resulting From VCT Hydrogen Partial Pressures**

The calculations shown in Figure 9-1 indicate that the highest hydrogen concentrations currently under consideration (~80 cc/kg) are achievable without changes to current system configurations (including alarm levels) if a reasonably pure gas phase is maintained (steam pressures at these temperatures are not significant, i.e., they are less than 3 psi). Maintaining a reasonably pure gas phase may require additional purging of helium, since the VCT can accumulate helium. Figure 9-2 shows an alternate representation of the same calculation results. It should also be noted that significant pressure margin could be recovered if the VCT temperature were maintained at 20°C rather than 40°C.

With respect to lower hydrogen concentrations, values below 20 cc/kg would require dilution of the VCT vapor space by an inert gas in order to simultaneously achieve low hydrogen partial pressures and total pressures high enough to prevent air ingress. Selection of an acceptable diluent would need to consider radiolysis (for example, nitrogen would lead to ammonia generation in the core) and analytical issues (for example, helium can interfere with some hydrogen assays). Qualification of a specific diluent is beyond the scope of this report, although it should be noted that there has been experience with nitrogen [89] and inadvertent experience with helium [90]. With respect to helium, acceptable operation (except for approaching the dissolved hydrogen lower action level limit) has been observed with helium content in the vapor space of the VCT approaching 50%. [90] Additionally, at some plants prevention of cavitation of

the charging pumps requires about 2 psig in the VCT [91] providing a second requirement for an additional inert gas at hydrogen concentrations below 20 cc/kg.

Plant-specific verification of the range of possible pressures in the VCT would be required prior to increasing hydrogen concentrations above the current limit.

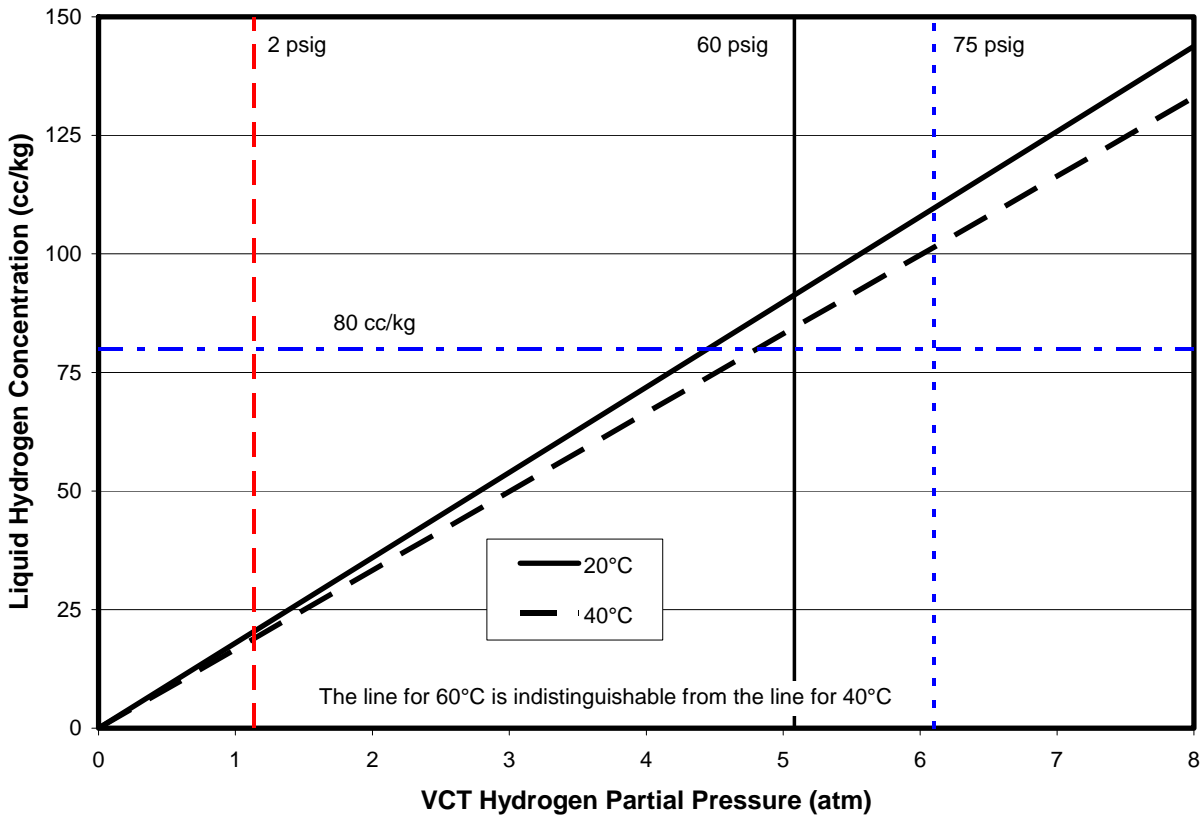


**Figure 9-2**  
VCT Partial Pressures of Hydrogen Required for Various Hydrogen Concentrations

#### 9.4.3 Effect of Hydrogen on Saturation Pressure (Voiding)

Vapor bubbles will form in the RCS and adjoining systems when the equilibrium pressure (the sum of the steam pressure and the equilibrium partial pressure of hydrogen) falls below the operating pressure. Figure 9-3 shows the calculated pressures (hydrogen, steam, and total) over the range of RCS temperatures. It is clear that at high temperatures, even with a factor of two or three increase in hydrogen concentration, the total pressure is dominated by the steam pressure. Therefore, for example, changes in hydrogen concentration are not expected to affect sub-nucleate boiling. The same calculation results are shown only for lower temperatures in Figure 9-4. At lower temperatures, the hydrogen concentration governs the pressure required to suppress voiding.

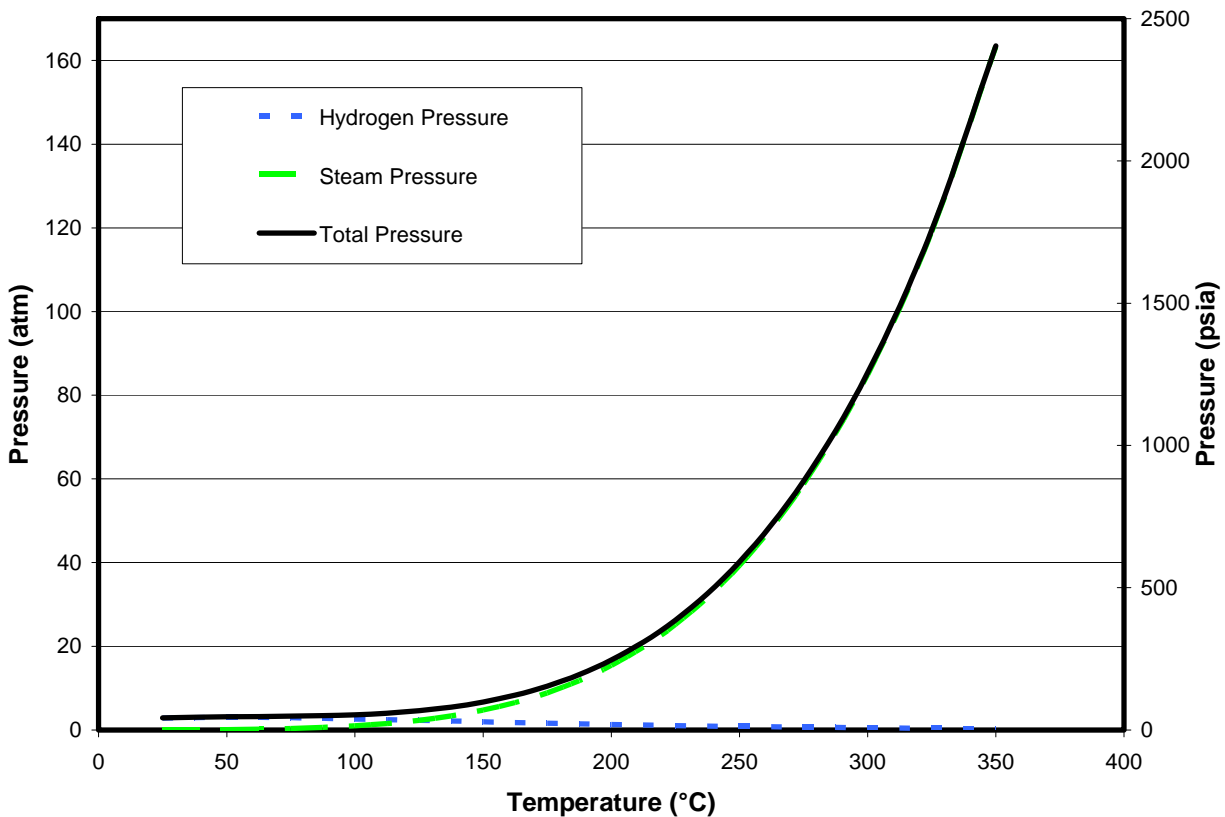


**Figure 9-3**  
**Partial Pressure of Hydrogen and Total Pressure as a Function of Temperature: 50 cc/kg**

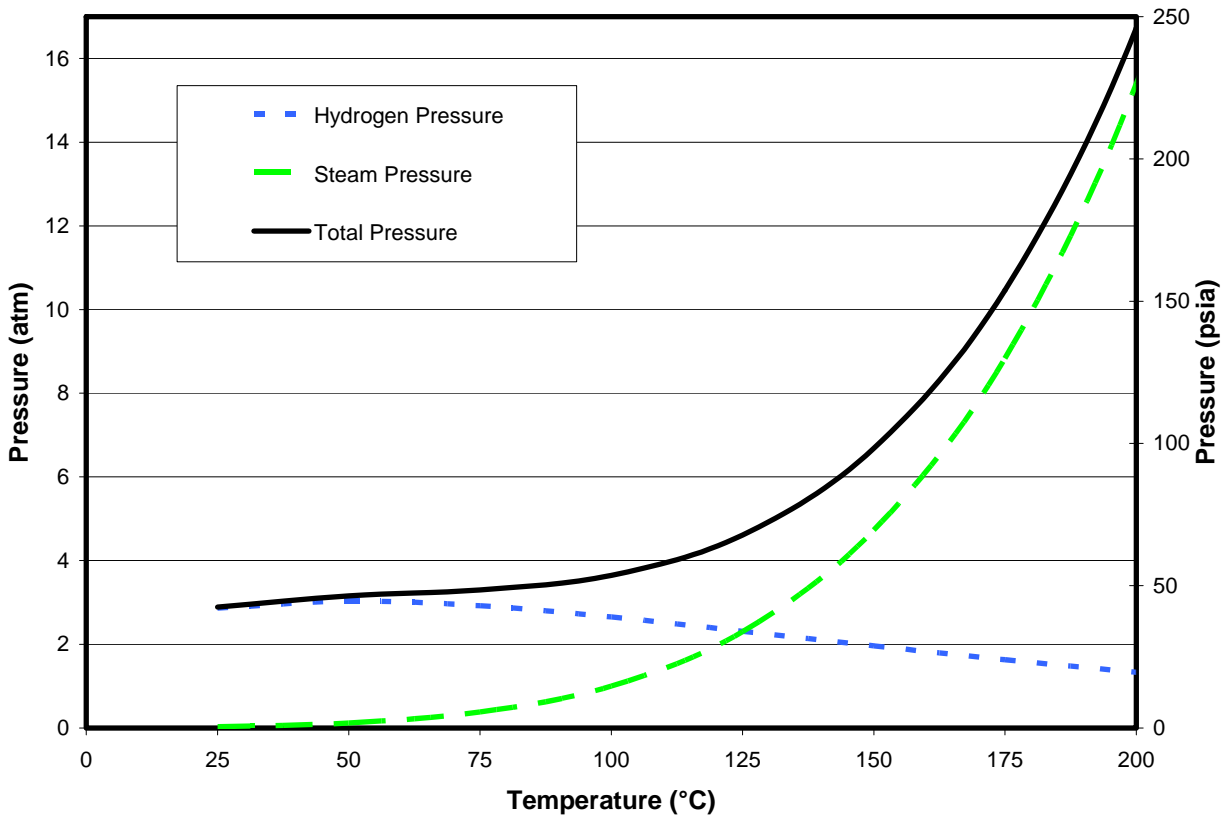


**Figure 9-4**  
**Partial Pressure of Hydrogen and Total Pressure as a Function of Temperature: 50 cc/kg**  
**Low Temperatures**

The effect on the pressure required to prevent voiding of varying hydrogen concentrations is shown in Figure 9-5. Also shown in this figure is the estimated demineralizer outlet pressure at a typical PWR.[92] As indicated in the figure, voiding is not likely to occur in the demineralizer bed or upstream unless hydrogen concentrations approach 100 cc/kg.

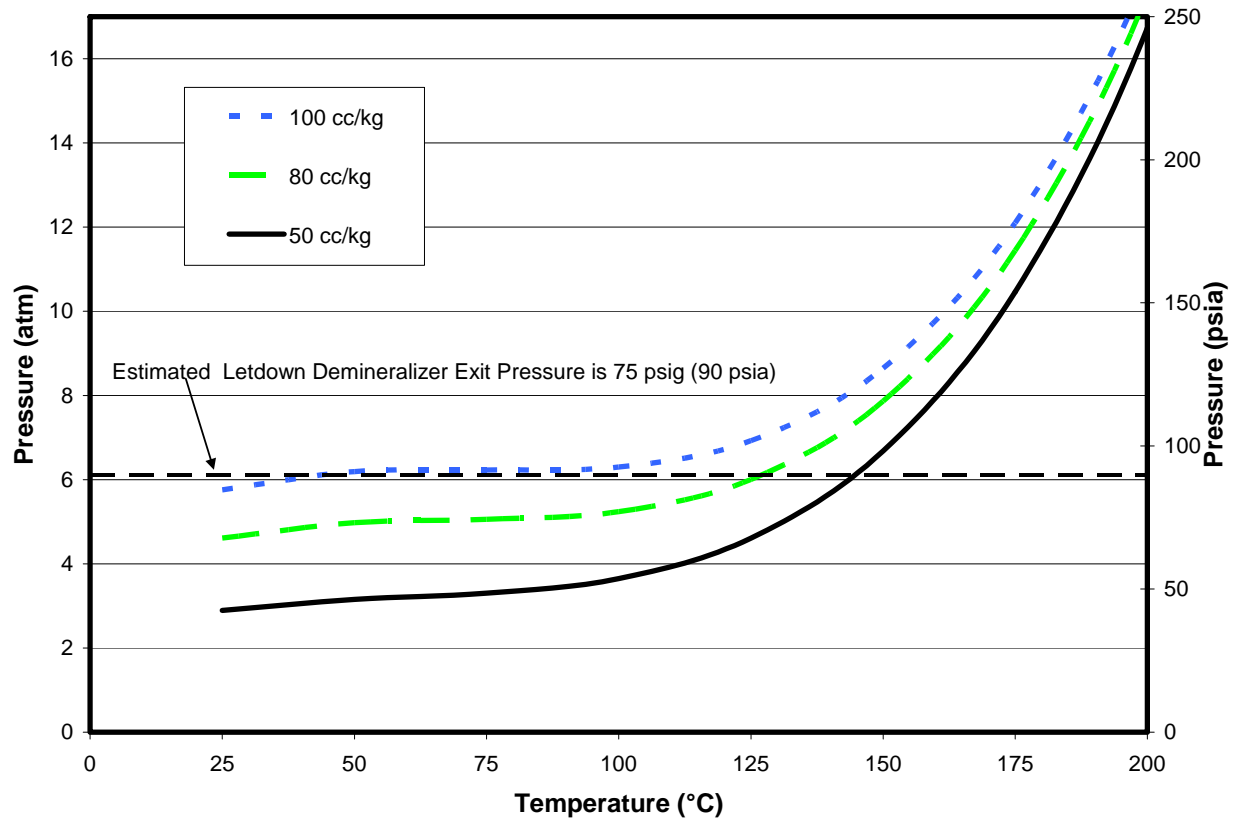


**Figure 9-5**  
**Total Pressure Required to Prevent Voiding**

A critical location where voiding might occur is the suction to the charging pumps. The pressure at this point is less than that in the VCT due to flow losses and possibly elevation changes, but depends on specific plant configuration. A plant-specific assessment of the propensity for voiding at this location should be undertaken before increasing hydrogen concentrations above the current band.

Additional consideration should be given to low pressure systems that are isolated from the CVCS by single valves. Section 10.4 discusses specific plant events in which valves have failed to contain hydrogenated water and gas pockets have formed in low pressure systems.

Control rod drive mechanism (CRDM) housings have been identified as an additional location that warrants plant-specific evaluation.[80]

## **9.5 Conclusions**

There are numerous operational and safety considerations that should be addressed on a plant-specific basis before increasing hydrogen concentrations above the current operating band (i.e., increasing above 50 cc/kg).

Changing hydrogen concentrations to levels below the current operating band presents considerable operability and safety issues. Most importantly, operation in the range of 5 - 25 cc/kg may increase the rates of PWSCC at lower temperature (below 325°C) locations.

# 10

## OPERATING EXPERIENCE

---

### 10.1 Introduction

Implementation of new chemistry regimes are often based on an incremental approach in which the boundaries of plant experience are gradually extended. This approach is based on reasonably good historic performance of PWRs and the complexity of an operating station relative to laboratory testing. Therefore, the first step in evaluating the implementation of a chemistry change such as that under consideration is a review of operating history. This chapter reviews the following three types of operating experience:

- Normal operating experience base for currently operating PWRs
- Early off-normal and test reactor experience
- Specific plant events related to hydrogen concentrations

These types of experience are reviewed in the following sections. Section 10.5 summarizes the results of these reviews.

### 10.2 Normal Operating Experience Base

Coolant hydrogen concentration is a parameter included in the FRP's Fuel Reliability Database (FRED). Figure 10-1 shows trends in hydrogen concentration from the year 2000 to the present for US plants. Figure 10-2 shows a more detailed distribution of recent cycle average concentrations for US plants. From the data shown in these figures it is evident that although there is significant operating experience in the range of 40 to 45 cc/kg, there is essentially no US experience above 45 cc/kg.

Operating Experience

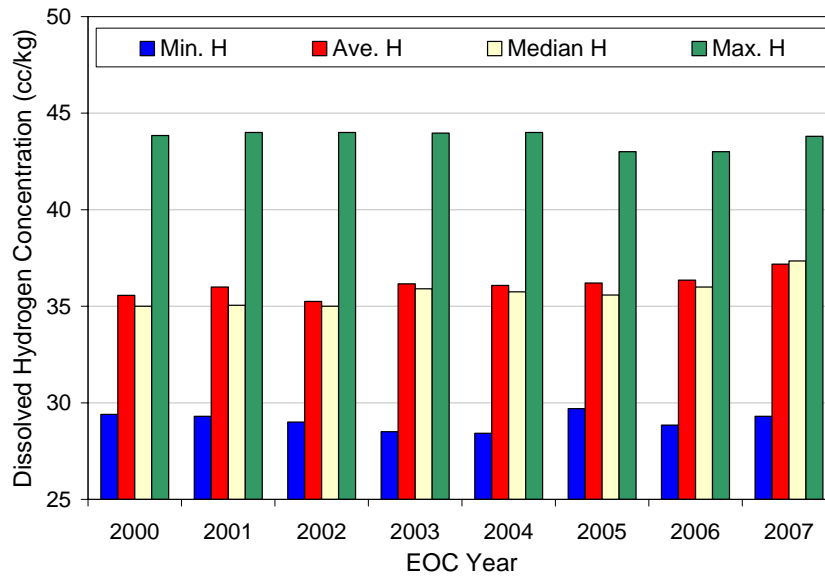


**Figure 10-1**  
**Recent Trends in Coolant Hydrogen Concentrations [93]**

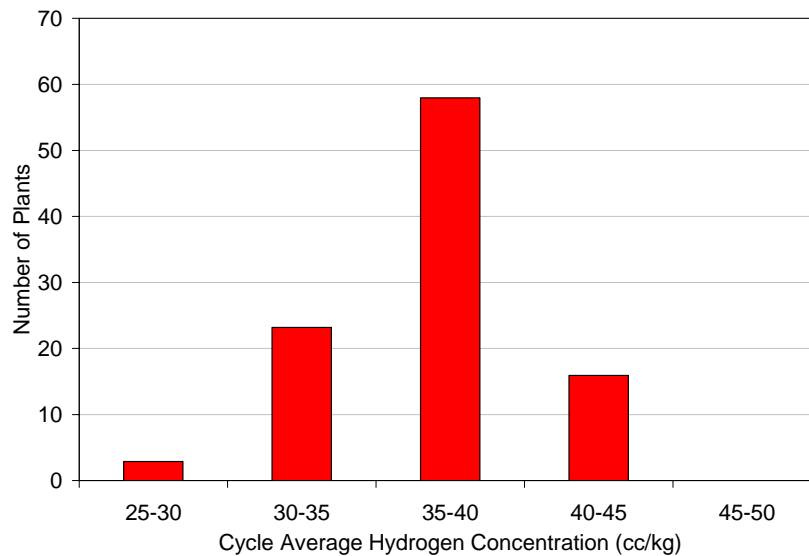


**Figure 10-2**  
**Distribution of Current Coolant Hydrogen Concentrations [93]**

A broader review [42] indicates that there has been some experience in the range of 50 to 55 cc/kg for Siemens units (1 cycle) and VVER units (2 cycles). There is no indication that any adverse effects were experienced in these cycles. However, there appears to be no significant evaluation available in the literature.

## 10.3 Early Off-Normal Operating Experience and Test Reactor Experience

Industry experience with coolant hydrogen concentrations outside the range of 25 - 45 cc/kg are largely confined to early plant experience and test reactors. A literature review of these experiences was conducted, with heavy reliance on a previous review [94] performed for EPRI. Experiences at specific plants and test facilities are discussed in the sections below. Also included in this section is a discussion of an experiment conducted at a commercial reactor (see Section 10.3.9).

### 10.3.1 Obrigheim

Obrigheim is a KWU/Siemens PWR. During its first cycle, the hydrogen concentration was 5 cc/kg. The oxygen concentration was 0.3 ppm (max).[94] No explanation is available regarding how hydrogen and oxygen were able to be present simultaneously. It is assumed that these values were either targets or cycle averages and that hydrogen and oxygen existed in the coolant at alternate times. Significant corrosion of fuel cladding was observed including failures due to clad oxidation.[94]

### 10.3.2 Belgian Reactor 3

The Belgian Reactor 3 (BR3) was a small demonstration Westinghouse PWR that started up in 1967. During cycles 4A and 4B, significant concentrations of oxygen were measured (0.05 – 0.14 ppm). Hydrogen concentrations were not measured during this period. However, subsequent to the observation of elevated oxygen, hydrogen was measured and found to be in the range of 7 - 9 cc/kg. These conditions led to significant clad corrosion and numerous fuel failures. During this period of operation, lithium concentrations were within specification.[94]

### 10.3.3 Turkey Point 4

During Cycle 4 at Turkey Point Unit 4 (1978) a crud induced power shift (CIPS, or Axial Offset Anomaly, AOA) was observed. A root cause analysis indicated that a probable contributor was operation with 15-20 cc/kg hydrogen. Standard lithium control was in use.[94]

### 10.3.4 Unidentified CE Plants

Reference [94] lists three events at unidentified Combustion Engineering (CE) plants. These are discussed in the paragraphs below.

The first incident occurred at Plant D during Cycle 1. For a period of five days, the hydrogen concentration was about 1 cc/kg, rather than the standard 15 cc/kg. No lithium was added to the coolant at this time, and lithium from  $^{10}\text{B}(n,\alpha)^7\text{Li}$  was minimal (0.04 ppm). The reduction in hydrogen concentration correlated with increased axial offset, with power production in the lower core increasing by about 10%. Upon increasing hydrogen concentrations to normal levels (15 cc/kg) some of the reactivity loss in the upper core was recovered.[94]

*Operating Experience*

During startup at Plant B, oxygen control was lost during low power testing. Oxygen concentrations were in the range of 0.1-0.2 ppm. During this time, the core pressure drop increased by approximately 25%. No lithium was present in the coolant during the transient. No crud induced power shifts (CIPS or AOA) were observed. After restoration of oxygen control, the pressure drop gradually decreased over the course of 10 weeks with lithium concentrations in the 1-2 ppm range.[94]

During Cycle 2 at Plant B, a 15% increase in core pressure drop and a crud induced power shift (CIPS or AOA) were observed. These were correlated with a period of oxygen ingress during which hydrogen in the volume control tank was maintained at 10-40 cc/kg, but the hydrogen in the coolant was on the order of 5-20 cc/kg, due to consumption by the oxygen. Lithium was within specifications (0.3-0.8 ppm) but was increased subsequent to the event to 1-2 ppm as a long-term remedy.[94]

### **10.3.5 Trojan and Beaver Valley Comparison**

Reference [94] includes a detailed comparison of Trojan Cycle 1, Trojan Cycle 2, and Beaver Valley 1 Cycle 1 with respect to chemistry control and crud formation. There are some differences in hydrogen concentration among the three cycles and some corresponding differences in crud buildup. However, general differences between the plants (the number of loops, for example) and other chemistry operating parameters (for example, differences in lithium control) make useful interpretation of these data unlikely with regard to the effects of hydrogen.

### **10.3.6 Saxton**

Saxton was a PWR test reactor operated by the Saxton Nuclear Experimental Operating Corporation, a consortium including Jersey Central Power and Light Company, New Jersey Power and Light Company, the Pennsylvania Electric Company, and the Metropolitan Edison Company. In 1963, the Saxton Technical Specifications were modified to permit operation at primary coolant hydrogen concentrations of 15 to 90 cc/kg (a change from the range 25 to 35 cc/kg). The change was motivated by control problems associated with the tighter operating range. In documentation submitted to the US Atomic Energy Commission (the precursor of the current regulatory body, the NRC), the operator indicated that operation at 15 cc/kg at other units justified the lower limit. The upper limit was justified based on loss of coolant accident (LOCA) calculations that indicated that complete venting of the primary system would not lead to explosive or flammable concentrations of hydrogen in the containment building.[95]

Secondary sources [42] indicate that the Saxton unit was operated with coolant hydrogen concentrations in the range of 30 to 112 cc/kg. However, given that the reason for increasing the range was an inability to consistently maintain a concentration in a 10 cc/kg band, it appears unlikely that the hydrogen concentration was consistent during this period. Therefore, it is unlikely that operation of the Saxton reactor contributes to the general PWR operating experience base in any useful manner.

During operation under the wider hydrogen limits, fuel failures occurred which were attributed to oxidation. However, since unusually high concentrations of silica, calcium, and magnesium were observed in the crud on fuel assemblies, it is not clear that the fuel failures could be attributed to hydrogen concentrations.[94]

### **10.3.7 Shippingport**

The Shipping Port Atomic Power Station was a demonstration reactor operated by Duquesne Light Company and designed by Westinghouse/Bettis Atomic Power Laboratory. The coolant hydrogen was controlled within a band of 10 to 60 cc/kg.[96] Given that 1) the actual operating hydrogen concentrations are not easily determined, 2) the extent to which the operating band exceeds current PWR practice is small, and 3) major design differences between the Shippingport reactor and modern PWRs, the usefulness of the coolant hydrogen operating history at Shippingport is expected to be low. Additional information was not reviewed.

### **10.3.8 Halden**

Halden is a test reactor operated for the Organization for Economic Co-operation and Development (OECD). A preliminary review of experiments conducted at Halden indicated that the effects of hydrogen concentration have not been investigated. It is possible that the in-reactor loop tests recommended by the FRP [42] could be conducted at Halden.

### **10.3.9 Belleville**

Tests were conducted at EDF's Belleville plant during which hydrogen concentrations were periodically lowered.[77] Specifically the following changes were made (during full power operation):

- At Unit 1, hydrogen was maintained between 17 cc/kg and 5.8 cc/kg for 69 hours.
- At Unit 2, hydrogen was maintained between 17 cc/kg and 3.6 cc/kg for 44 hours.

No adverse consequences were observed during this test.

## **10.4 Specific Plant Events**

A review of significant plant events related to primary coolant hydrogen concentrations was conducted. A number of specific events have been related to the concentration of dissolved gas. Specific events, or types of events, are reviewed in the sections below.

### **10.4.1 RHR/ECCS Common Piping Gas Pockets**

In many PWR designs, the residual heat removal (RHR) system and the emergency core cooling system (ECCS) share common piping. During shutdown the RHR system removes heat from the RCS that is generated by continuing radioactive decay of the fuel (residual heat). Coolant is

*Operating Experience*

taken from the RCS, passed through a heat exchanger, and returned to the RCS. During startup, the RHR system is isolated from the RCS, and the chemistry of the RCS at the time of isolation is generally maintained in the RHR throughout the power operation period.

The following sequence of events could lead to gas pockets in ECCS piping:

- Hydrogen is dissolved in the RCS while on RHR cooling.
- The RHR system is isolated.
- Depressurization of the RHR allows dissolved hydrogen to come out of solution, forming gas pockets in the RHR system piping.

Because the RHR system and the ECCS share common piping, gas pockets in the RHR system piping can lead to the ECCS being non-operational. Since the ECCS is a safety-related system, its non-operability would require a shutdown. The sequence of events described above has led to a shutdown. However, straightforward operating practices can be implemented to protect against this type of event, such as not increasing hydrogen concentrations to high levels during plant start up until the RHR system is isolated from the RCS.

#### **10.4.2 Charging Pump Gas Binding**

Typical plant designs include multiple charging pumps to inject RCS coolant from the volume control tank (VCT) into the RCS. Centrifugal pumps in this location are susceptible to gas binding if pockets of gas accumulate at the pump suction. Experience to date indicates that the rate of gas accumulation in this location is slow enough that gas binding will not occur if the pumps are in continuous operation. Additionally, typical plant designs include vent systems for this location that remove excess gases. However, in one case, this vent system has malfunctioned, leading to the development of a large gas pocket ( $\sim 0.3 \text{ m}^3$  or  $10 \text{ ft}^3$ ) while the pump was not operating. A gas pocket of this size could not be processed by the centrifugal pump and the pump became gas bound.

Note that in this incident, it was estimated that the solubility of hydrogen under these conditions was less than 50 cc/kg (45 cc/kg). Therefore this event could have occurred at hydrogen concentrations within the current operating band. However, the extent to which the hydrogen concentration was above 45 cc/kg could affect the rate at which a gas pocket large enough to bind the pump could develop. It should be noted, however, that this would require a failure of another plant system (the vent system).

Failures of the charging pump suction venting system have been attributed to the following root causes:

- Failure of the vent valve due to blockage or hydraulic lock
- Failure of a check valve

Additional plant experience indicates that operation with only a single positive displacement charging pump may make the system more vulnerable to the accumulation of a gas pocket.

### 10.4.3 Valve Failures

Valve failures have led to hydrogen ingress into systems where it is not expected, leading to the formation of gas pockets. Failed valves that have contributed to events such as these include the following:

- Charging pump vent valve
- Emergency boration header relief valve

### 10.4.4 Voiding in the Letdown Ion Exchange Beds

The ion exchange beds generate a significant pressure drop with an exit pressure close to that of the VCT. Specific plant maneuvers can result in bed pressure drops that allow the formation of gas pockets (voids) within the bed. Specifically, the following conditions have been observed to lead to such voiding:

- Diversion of letdown flow to waste (versus the VCT) can lead to voiding. This is in part due to the waste system being under vacuum in some configurations. Note that this voiding would be expected to occur at most hydrogen concentrations within the current operating band since the pressure drop between the bed outlet and the waste system is expected to be small, resulting in a very low pressure within the bed.
- At one plant, the RCS was not degassed during a mid-cycle outage. Plant temperatures were reduced with a steam bubble in the pressurizer. At the lower temperature, the partial pressure of hydrogen was increased, due to a decrease in the solubility of hydrogen. Figure 10-3 shows lines of equilibrium pressures for constant hydrogen concentrations as a function of temperature. As the temperature decreases, the equilibrium pressure needed to maintain a constant hydrogen concentration is increased. This led to the accumulation of additional hydrogen in the pressurizer during the outage. Upon startup, the temperature increased. The concentration of hydrogen in equilibrium with the pressure was then much higher (~300 cc/kg). This led to gas pocket formation in the letdown ion exchange beds. The first indication of this was increased activity on the reactor coolant filters downstream of the beds. The formation of gas pockets within the bed released particulates that had been “filtered out” by the resin bed.

A utility evaluation [92] indicated that gas voiding is expected in the ion exchange beds at a hydrogen concentration of 100-130 cc/kg. Hydrogen concentrations were measured at 120 cc/kg, but could have been higher. This measurement was made after the first observation of increased filter activity. On-line monitoring was not functioning because the concentration exceeded the meter capability of 60 cc/kg, therefore the exact peak concentration was not measured. Extrapolation of trends from continuous monitoring (below 60 cc/kg) and subsequent grab samples (after the peak), indicate that voiding probably started at about 100 cc/kg.

It should be noted that an increase in coolant hydrogen concentration during operation would be accompanied by a corresponding increase in VCT pressure, which would increase the concentration at which voiding would occur.

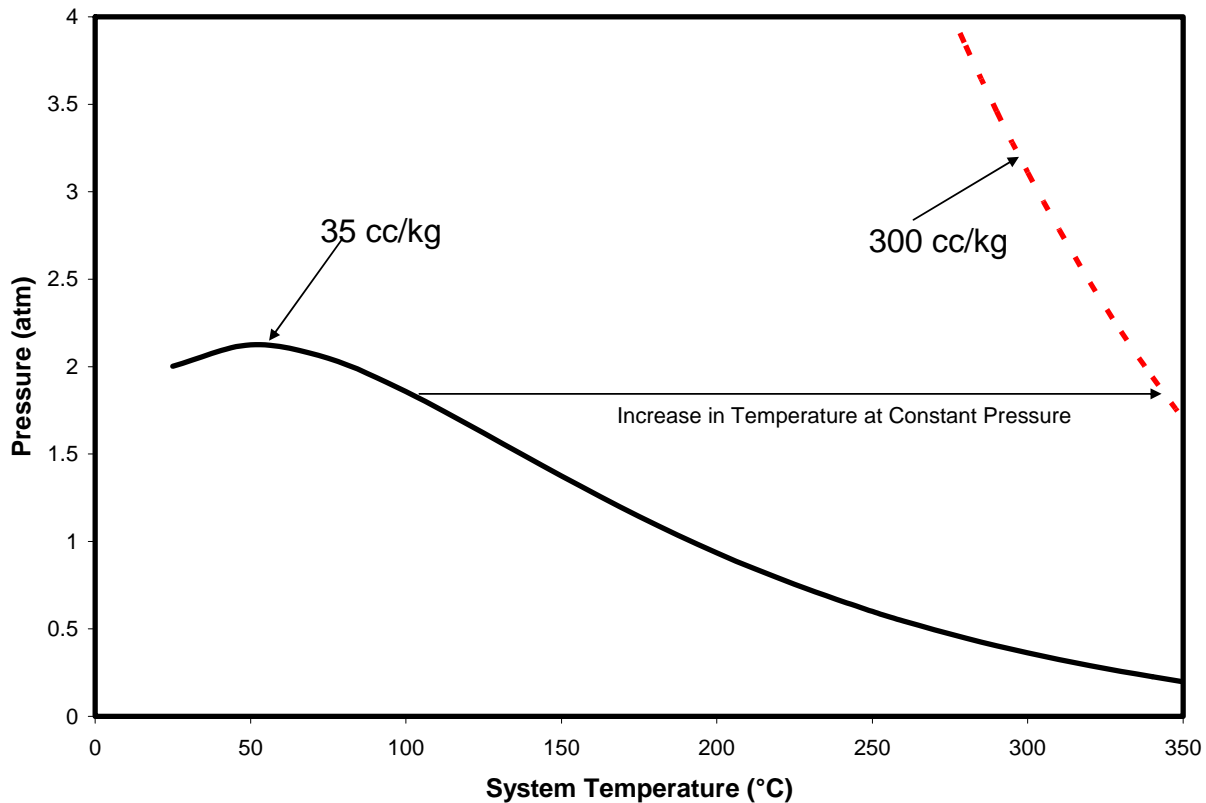


**Figure 10-3**  
**Lines of Constant Hydrogen Concentration as a Function of Temperature**

## 10.5 Conclusions

Based on a review of current plant operating experience, historic operation at early units, and specific events which have occurred at operating units, the following conclusions can be drawn:

- There is significant experience operating near the upper end of the current operating band. Operation at hydrogen concentrations of 40-45 cc/kg have not lead to any known problems at plants. However, there is essentially no documented commercial PWR experience above 45 cc/kg.
- Some early experimental stations may have operated with hydrogen concentrations above 50 cc/kg. No adverse results of such operation are known. However, data are limited and the designs of these stations are different enough from current PWRs that reliance upon these data is not warranted.
- Early operation at PWRs indicate that there can be significant corrosion product transport and deposition problems when operating at low hydrogen concentrations (nominally less than 20 cc/kg).

- Specific events at operating PWRs indicate that the formation of gas pockets in various systems can be a problem. Although there is no indication that increases in hydrogen concentration could increase the frequency of such events, it is expected that such increases would make these events worse. Specifically, gas pockets would be expected to form faster with higher concentrations of hydrogen. This effect is expected to be linear with the concentration. Therefore, modest increases in concentration would result in only modest increases in gas pocket growth rates.



# 11

## ONGOING EPRI RESEARCH

---

### 11.1 Introduction

The primary coolant hydrogen concentration is intimately related the electrochemical potential experienced by the materials in the system and therefore is one of the most important parameters affecting the behavior of metals and their oxides. In most cases, the range under consideration (5 cc/kg to 80 cc/kg) is relatively narrow compared to differences that would significantly affect material behavior. However, different concentrations in this range are thought to significantly affect the stability of various nickel phases (metal, oxide, and ferrite). Therefore, the effects of hydrogen concentration on the primary coolant system (including materials of construction, fuel cladding, and corrosion products) has been the subject of considerable EPRI research. The following sections describe research programs that are currently underway at EPRI. The descriptions are organized by EPRI program (FRP, MRP, and Chemistry).

### 11.2 Fuel Reliability Program

As discussed in Section 5.3, the Fuel Reliability Program (FRP) has developed a plan for investigating the effects of elevated hydrogen on fuel performance. In addition to this effort, the FRP is also investigating the effect of hydrogen on the stability of various nickel compounds (metal, oxide and ferrites). However, this program has to date been very preliminary and may be superseded by the collaborative MULTEQ effort discussed in Section 11.4.4.

### 11.3 Materials Reliability Program

The Materials Reliability Program has two ongoing laboratory testing programs addressing the effects of hydrogen. These programs investigate the effect of hydrogen on crack growth rates and on low-temperature crack propagation. These programs are summarized in the next two subsections.

#### 11.3.1 Crack Growth Rate Testing

The objectives of work in this area are to determine the effect of realistic changes in existing hydrogen concentration on the growth of existing PWSCC cracks, and to assess the degree of mitigation which could be achieved by changes in hydrogen concentration.

GE GRC has been conducting PWSCC growth rate chemical mitigation testing on Alloy 600 for the MRP since 2003. To date testing indicates primary water pH and Li and B content do not have a significant effect on PWSCC growth rate in Alloy 600 and its weld metals. Alloy 600 PWSCC growth rate testing so far has shown limited benefit with increased hydrogen. The task focus has recently switched to testing of Alloy 182 where a larger benefit is expected.

The current elevated hydrogen and zinc addition testing is scheduled to be completed by mid 2008. The final report documenting all testing at GE GRC will be available in late 2008.

### **11.3.2 Low-Temperature Crack Propagation**

The MRP has an on-going program to assess the applicability of LTCP of nickel-alloy components under current PWR primary system service conditions. The published laboratory results show that LTCP is not an issue for Alloy 600, but is an issue for Alloy X-750, weld metal 182/82, weld metal 152/52, and Alloy 690 (in that order of decreasing susceptibility). Another result is that the occurrence of LTCP is primarily controlled by the level of hydrogen in the water, but that stored hydrogen in the metal can act as an additional source of hydrogen contributing to the LTCP fracture toughness reduction. A 2003 MRP sponsored work confirmed results of Mills et al. tests in weld metal 82H and also showed that weld metal 182 was susceptible to this mode of propagation. An MRP study investigated the effects of applying chemical conditions closer to the shutdown conditions as well as the effects of using stress corrosion cracking (SCC) as starter cracks instead of fatigue pre-cracks on LTCP in weld metal 182. One of the key results was that fracture resistance is lower for a high temperature SCC starter crack than for a transgranular fatigue starter crack.

Since to date the LTCP issue in PWRs has been primarily investigated by focusing on the chemistry side of the problem, the current ongoing work is to determine if the issue could potentially be eliminated by investigating the stress side of the problem. In particular, if residual stress does not contribute to LTCP, then the remaining stress at low temperature would probably not be sufficient to cause LTCP. Therefore testing is being conducted on weld metal 182 in PWR environments to understand whether or not the LTCP phenomenon can occur under stress conditions different than the rising load test conditions used in the results to date; and stress analyses are being performed to determine whether or not the mechanical requirements for LTCP identified in the laboratory tests are likely to be met in any nickel-alloy components. Finally, while the previous and current testing addresses the effects of different variables on LTCP individually; it is not representative of confluence of all conditions (temperature, pressure, hydrogen level, water chemistry, stresses, rates, etc.) that occur during shutdowns conditions. Therefore additional testing is being performed to determine if the combination of some of the key shutdown variables can result in LTCP. Reports documenting results of these ongoing tasks are scheduled to be issued in 2008.

## **11.4 Chemistry**

Current research methods of quantifying the solubility of nickel, nickel oxide, and nickel ferrites may provide improved solubility data as compared to the conventional experimental methods used previously. The difficulty of quantifying the very low solubility (i.e., part-per-billion to

part-per-trillion) of these metals at PWR operating temperature has not yielded conclusive evidence about which method is optimum for application to PWR primary coolant chemistry. Thus, there is some disagreement among the experts regarding how the spectrum of relevant data should be dispositioned for use. The areas under recent review are the solubility of nickel metal in reducing environments, the required minimum hydrogen concentration for the nickel/nickel oxide transition point, and the methods for determining/estimating nickel ferrite solubilities. The following discussions highlight the issues without providing definitive recommendations, which are still under development/consideration.

In addition, the method used to calculate the nickel/nickel oxide/nickel ferrite speciation in high temperature chemistry calculators (notably MULTEQ) must be addressed. For example, Bill Lindsay [97] has noted a limitation of the MULTEQ calculation engine in that it does not allow parallel precipitation. Hence, the most stable precipitate will always form first, and may consume the constituent elements before other precipitate species may form. These issues will be discussed in future MULTEQ database committee meetings.

#### **11.4.1 Solubility of Nickel Metal in Reducing Environments**

Historically, the challenge of measuring nickel solubility at high temperatures with low electrochemical corrosion potential is that the detection limit of the instruments for ionic nickel had been above the solubility of nickel. Kunig and Sandler [22] used a flowing autoclave dissolution experiments and followed them with ion exchange columns in order to concentrate an integrated sample and measure the nickel in the acidic regenerant eluent. While this is often an effective measurement technique, there exists the possibility of introducing error by mechanisms such as particulate entrainment in the resin matrix, incomplete regeneration of the concentrator column, or background nickel contamination of the regenerant acid.

Recent work by Ziemniak, et al.[98] has measured nickel solubility using a flowing autoclave followed by ICP/MS measurements. The chemical environment was ammonia and sodium hydroxide. The instrument specifications indicate a nickel sensitivity of 7 parts per trillion (ppt); the actual minimum recordable measurement varied from as low as 10 ppt to up to 50 ppt considering the background concentration of nickel in the analytical chemicals. The experiment indicates that, while the instrumentation has the potential for measuring very low nickel concentrations, clean room environments and semiconductor grade reagent chemicals may be required for accurate solubility measurements over the entire environmental range.

#### **11.4.2 Nickel/Nickel Oxide Transition**

As discussed in Section 3.4.1, the method applied for estimating the nickel/nickel oxide transition as a function of hydrogen concentration for MULTEQ involves estimating the solubility of nickel oxide and nickel independently in autoclave experiments, and applying both solubility models in the MULTEQ engine to find at which hydrogen concentration the transition occurs.

Recent work by Attanasio et al. [4] has applied an alternative experiment that monitors the change in the electrical resistance of a nickel based electrode as a function of the hydrogen concentration. Their experimental results indicate that the method used by MULTEQ overestimates the hydrogen concentration required to maintain the nickel metal form. Future work will look at the applicability of the electrode method to aqueous chemistry calculations.

### 11.4.3 Nickel Ferrite Solubility Estimation

Measuring the formation of nickel ferrites in PWR environments is very difficult. The only known experiments that have shown nickel ferrite precipitation are the hot particle filter tests performed by the EPRI Fuel Reliability Program.[99] However, the filters in these tests were filtering coolant that had been reduced in temperature to 230°C. Additionally, this type of in-plant measurement is subject to some uncertainty as a result of any uncontrolled or unknown conditions. The experiments of Kunig and Sandler [22], Tremaine and Leblanc [100], and Lambert [101] have all used dissolution of nickel ferrite solids in flowing autoclaves and assumed thermodynamic equilibrium would yield stoichiometric quantities of nickel and iron oxide that could be used to estimate the solubility products. The thermodynamic assumptions are expected to be valid, but all experimental results have indicated a significant scatter in the data, especially when measuring the nickel metal (for the reasons noted in Section 11.4.1).

It is unknown at the publishing of this document if future work will be undertaken to explore nickel ferrite solubility via the dissolution mechanism; however, an alternate approach to estimating the solubility can be performed by measurement of the solid phase heat capacities. The methodology uses the relationship between the solubility product and the Gibb's Energy of reaction, and applies the definition of the Gibb's energy to relate to the heat capacities. The equation in the final form is as follows:

$$\ln K_T = \ln K_{298} - \frac{1}{R} \left[ \frac{1}{T} - \frac{1}{298} \right] \Delta H_{298}^0 + \frac{1}{R} \int_{298}^T \frac{\Delta C_p}{T} dT - \frac{1}{RT} \int_{298}^T \Delta C_p dT - \frac{1}{RT} \int_1^P \Delta V dP \quad \text{Eq. 11-1}$$

It may be assumed that the density change of the solid as a function of pressure is negligible. These properties can be measured from the solid phase heat capacities as a function of temperature and the tabulated heats of formation of the nickel ferrites. This method of solubility product estimation is currently being reviewed by EDF for its applicability in high temperature chemistry calculations, and a similar method has been used by the EPRI Fuel Reliability Program for deriving solubility products of nickel ferrites. At the time of this document, the MULTEQ Database Committee is currently reviewing the available precipitate models to determine which is the most applicable to PWR chemistry systems.

#### **11.4.4 Development of an EPRI Thermodynamic Model for Nickel/Nickel Oxide/Nickel Ferrite Systems**

The EPRI Fuel Reliability Program had independently developed a nickel/nickel oxide/nickel ferrite precipitation model for use in fuel clad crud deposition models. The FRP model for nickel and nickel oxide is equivalent to the MULTEQ database, Version 5.0 [23]; however, there are differences in the nickel ferrite solubility product expressions. EPRI FRP and Chemistry are currently collaborating to review the existing data and develop a common precipitate model that will be used for all EPRI chemistry simulations.



# 12

## COMPLEMENTARY MITIGATION STRATEGIES

---

### 12.1 Introduction

There are several PWSCC mitigation strategies in addition to changes in hydrogen concentration. In considering the application of hydrogen concentration changes, the relative merit of each of the strategies should be considered. Additionally, possible synergies (or cancellations) of beneficial effects should also be considered. A complete evaluation of alternative mitigation strategies is beyond the scope of this report. However, it is useful to list some of those strategies and discuss how changes in hydrogen concentration might affect them. The following sections briefly define alternate strategies and discuss possible interactions with hydrogen concentration changes.

### 12.2 Zinc Injection

Injection of zinc into the primary system is a mitigation strategy currently in use at many PWRs with a high likelihood of mitigating both PWSCC initiation and growth, as well as reducing shutdown radiation fields. This strategy involves the injection of a zinc solution into the RCS such that low concentrations (5-40 ppb) are maintained in the coolant. Zinc is generally understood to modify the oxide films formed on PWSCC susceptible materials, making them less susceptible to PWSCC initiation and, if crack growth rates are slow enough, to PWSCC growth. Details regarding zinc injection can be found in Reference [61].

Among the possible interactions between zinc and hydrogen concentration are the following:

- Changes in hydrogen concentration may slow PWSCC crack growth rates enough to allow mitigation by zinc. That is, hydrogen optimization may change cracks from fast growing cracks unaffected by zinc to slow growing cracks that will be further mitigated by zinc addition. This is a positive interaction.
- Changes in hydrogen concentration could affect the stable oxide on PWSCC susceptible materials such that zinc is no longer incorporated into oxide films in a manner that increases resistance to PWSCC. In this outcome, the positive effects of oxide modification by hydrogen would substitute for the positive effects of zinc incorporation. Whether this was a net benefit or not would depend on the relative magnitude of the benefits of zinc and hydrogen. The benefits for each strategy are difficult to quantify with accuracy.

Evaluations of the effects of zinc on PWSCC of steam generator tubes [61] indicate that zinc has mitigated PWSCC at several plants with different hydrogen concentrations. However, the differences in hydrogen concentrations at these units have been small compared to those currently under consideration.

The interaction of zinc and hydrogen is the subject of continuing research. See Section 11.3.

### **12.3 Mechanical Mitigation**

Some utilities have proposed mechanical mitigation of PWSCC by peening to place the susceptible surface in compression. The interaction of hydrogen concentration changes with this mitigation strategy has not been fully explored. However, the following cautions should be noted:

- Increases in cold work have been shown in some cases to remove the benefit of moving to lower hydrogen concentrations (as discussed in 4.5.2). The extent of the differences between surface cold work and bulk cold work with regard to this phenomenon is not well understood.
- It is possible that cold work hardening resulting from peening will increase the susceptibility of the material to hydrogen embrittlement type failures. This may be more of an issue at lower temperatures (i.e., peening could increase susceptibility to LTCP).

### **12.4 Replacement**

The ultimate mitigation strategy is replacement. There are no immediately apparent consequences of hydrogen concentration changes on component replacement assuming replacement with non-susceptible materials. However, as discussed in Section 4.5.3, some replacement materials (e.g., Alloy 690) may depend differently on hydrogen concentration than Alloy 600.

### **12.5 Conclusions**

The interaction of hydrogen concentration changes with other possible mitigation strategies has not been fully explored. Of particular interest is the impact of hydrogen concentration on the effectiveness of zinc for PWSCC mitigation.

# 13

## REFERENCES

- 
1. M.R. Lindeburg, *Chemical Engineering Reference Manual for the PE Exam, Sixth Edition*, Professional Publications, Inc., Belmont, CA, 2004.
  2. M.V. Sussman, *Elementary General Thermodynamics*, Robert E. Krieger Publishing Company, Malabar, FL, 1989.
  3. D.M. Himmelblau, "Solubilities of Inert Gases in Water," *Journal of Chemical Engineering Data* 5:1, 10, 1960.
  4. S.A. Attanasio and D.S. Morton, "Measurement of the Nickel/Nickel Oxide Transition in Ni-Cr-Fe Alloys and Updated Data and Correlations to Quantify the Effect of Aqueous Hydrogen on Primary Water SCC," *11<sup>th</sup> International Conference on Environmental Degradation of Materials in Nuclear Systems*, Stevenson WA, August 10-14, 2003.
  5. D.H. Lee, M.S. Choi, and U.C. Kim, "The Effect of Hydrogen and Li/B Concentration on the Stress Corrosion Cracking of Alloy 600 in Simulated PWR Primary Water at 330°C," *International Conference on Water Chemistry of Nuclear Reactor Systems*, Jeju Island, Korea, October 23-26, 2006.
  6. *Pressurized Water Reactor Primary Water Chemistry Guidelines: Volume 1, Revision 6*, EPRI, Palo Alto, CA: 2007. 1015018.
  7. S.E. Ziemniak, M.E. Jones, and K.E.S. Combs, "Magnetite Solubility and Phase Stability," *Journal of Solution Chemistry* 24:9, 1995.
  8. J. Alvarez, R. Crovetto, and R. Fernández-Prini, "The Dissolution of N<sub>2</sub> and H<sub>2</sub> in Water from Room Temperature to 640 K," *Ber. Bunsenges. Phys. Chem.* 92, 935, 1988.
  9. C. Marks, *Predicting Hydrogen Reductions during Loss-of-Letdown Conditions*, Memo to K. Fruzzetti, January 29, 2007. DEI M-5547-00-01, Rev. 1.
  10. K. Masui, H. Yoshida, and R. Watanabe, "Hydrogen Permeation Through Iron, Nickel, and Heat Resisting Alloys at Elevated Temperatures," *Transactions of the Iron and Steel Institute of Japan* 19, 1979. Cited in T. Takeda, "Safety Studies on Hydrogen Production System with a High Temperature Gas-Cooled Reactor," *Nuclear Engineering and Technology* 37:6, 2005.
  11. K. Sakamoto and M. Sugisaki, "Diffusion Coefficient of Tritium in Ni-Based Alloy," *International Conference on Tritium Science and Technology* 6, Tsukuba, Japan, ANS, 2001.
  12. J.K. Gorman and W.R. Nardella, "Hydrogen Permeation through Metals," *Vacuum* 12, 1962. Cited in S.A. Steward, *Review of Hydrogen Isotope Permeability through Materials*, Lawrence Livermore National Laboratory, 1983. UCRL-53441.
  13. B.D. Morreale, *Evaluation of Inorganic Hydrogen Membranes at Elevated Pressures and Temperatures*, University of Pittsburg Master's Thesis, 2001.

## References

14. E. Rota, F. Waelbroeck, P. Wienhold, and J. Winter, "Measurements of the Surface and Bulk Properties for the Interaction of Hydrogen with Inconel 600," *Journal of Nuclear Materials 111&112*, 1982. Cited in Reference [11].
15. *Hydrogen Evolution Monitoring as a Measure of Steam Generator Corrosion*, EPRI, Palo Alto, CA: 1982. NP-2650.
16. S.A. Attanasio, D.S. Morton, M.A. Ando, N.F. Panayotou, and C.D. Thompson, "Measurement of the Nickel/Nickel Oxide Phase Transition in High Temperature Hydrogenated Water Using the Contact Electric Resistance (CER) Technique," *Tenth International Conference on Environmental Degradation of Materials in Nuclear Power Systems—Water Reactors*, Lake Tahoe, NV, 2001.
17. S. Dickinson, J. Henshaw, H.E. Sims, and K. Garbett, "Some Aspects of Ni Behaviour in PWR Primary Coolant," *Water Chemistry of Nuclear Reactor Systems 8*, BNES, 2000.
18. D.D. Macdonald, *The Thermodynamics of Metal Water Systems at Elevated Temperatures, Part 4: The Nickel Water System*, 1972. AECL-4139. Cited in Reference [17].
19. W.T. Lindsay, P.R. Tremaine, and S. Dickinson, *MULTEQ Database Committee Review of Nickel/Nickel Oxide/Nickel Ferrites*, Boston, MA, September 25-26, 2007.
20. U. Ehrnsten, T. Saario, T. Laitinen, and J. Lagerstrom, "The Effect of Dissolved Hydrogen on Surface Films and EAC of Alloy 600 in PWR Primary Water," *EPRI Workshop on PWSCC of Alloy 600 in PWRs*, Daytona Beach, FL, February 25-27, 1997.
21. K. Garbett and J. Henshaw, "Optimum Primary Coolant pH for High Duty PWRs," *Presentation to the EPRI PWR Primary Water Chemistry Guidelines Revision 6 Committee*, Charlotte, NC, September 18-20, 2006.
22. *The Solubility of Simulated PWR Primary Circuit Corrosion Products*, EPRI, Palo Alto, CA: 1986. NP-4248.
23. *MULTEQ: Equilibrium of an Electrolytic Solution with Vapor-Liquid Partitioning and Precipitation—The Database*, Version 5.0. EPRI, Palo Alto, CA: 2007. 1014602.
24. H. Takiguchi, M. Sekiguchi, H. Christensen, J. Flygare, A. Molander, and M. Ullberg, "In-Pile Loop Experiment and Model Calculations for Radiolysis of PWR Primary Coolant," *Water Chemistry of Nuclear Reactor Systems 8*, 399, BNES, 2001.
25. L.W. Niedrach and W.H. Stoddard, "Corrosion Potentials and Corrosion Behavior of AISI 304 Stainless Steel in High-Temperature Water Containing Both Dissolved Hydrogen and Oxygen," *Corrosion 42:12*, 696, 1986.
26. P. Andresen (GE), email to C. Marks (DEI), February 5, 2007.
27. *Materials Reliability Program: Mitigation of PWSCC in Nickel-Based Alloys by Optimizing Hydrogen in the Primary Water (MRP-213)*. EPRI, Palo Alto, CA: 2007. 1015288.
28. *Multivariable Analysis of the Effect of Li, H<sub>2</sub>, and pH on PWR Primary Water Stress Corrosion Cracking*, EPRI, Palo Alto, CA: 1996. TR-105656.
29. *Materials Reliability Program a Model of the Effects of Li, B, and H<sub>2</sub> on Primary Water Stress Corrosion Crack Initiation in Alloy 600 (MRP-68)*, EPRI, Palo Alto, CA: 2002. 1006888.

30. *Effect of Hydrogen, pH, Lithium and Boron on Primary Water Stress Corrosion Crack Initiation in Alloy 600 for Temperatures in the Range 320 – 330°C (MRP-147)*, EPRI, Palo Alto, CA: 2005. 1012145.
31. E. Richey, D.S. Morton, and M.K. Schurman, “SCC Initiation Testing of Nickel-Based Alloys Using In-Situ Monitored Uniaxial Tensile Specimens,” *Twelfth International Conference on Environmental Degradation of Materials in Nuclear Systems—Water Reactors*, Snowbird, Utah, August 2005.
32. P.M. Scott and P. Combrade, “On the Mechanism of Stress Corrosion Crack Initiation and Growth in Alloy 600 Exposed to PWR Primary Water,” *11<sup>th</sup> International Conference on Environmental Degradation of Materials in Nuclear Systems*, Stevenson WA, August 10-14, 2003.
33. K. Dozaki, “The Influence of DH Concentration on PWSCC Initiation in Alloy 600 under Simulated PWR Primary Coolant at 320°C,” *International Workshop on Optimization of Dissolved Hydrogen Content in PWR Primary Coolant*, Tohoku University, Japan, July 18-19, 2007.
34. A. Molander, A. Jenssen, M. König, and K. Norring, “PWSCC Initiation and Crack Growth Data for Alloy 600 with Focus on Hydrogen Effects,” *International Workshop on Optimization of Dissolved Hydrogen Content in PWR Primary Coolant*, Tohoku University, Japan, July 18-19, 2007.
35. J. Gorman, “Action Item 33: Evaluate Correlations between Hydrogen Concentrations and Rate of PWSCC in SGs,” *Presentation to the EPRI PWR Primary Water Chemistry Guidelines Revision 6 Committee*, Tucson, AZ, February 6-8, 2007.
36. D.S. Morton, S.A. Attanasio, and G.Y. Young, “Primary Water SCC Understanding and Characterization through Fundamental Testing in the Vicinity of the Nickel/Nickel Oxide Phase Transition,” *10<sup>th</sup> International Conference on Environmental Degradation of Materials in Nuclear Systems*, Lake Tahoe NV, August 6-9, 2001.
37. W.C. Moshier and D.J. Paraventi, “Alloy 600 Growth Rate Testing,” *Workshop on Cold Work in Iron- and Nickel-Based Alloys*, Toronto ON, June 3-8, 2007.
38. D.J. Paraventi and W.C. Moshier, “Alloy 690 Growth Rate Testing,” *Workshop on Cold Work in Iron- and Nickel-Based Alloys*, Toronto ON, June 3-8, 2007.
39. G.A. Young, W.W. Wilkening, D.S. Morton, E. Richey, and N. Lewis, “The Mechanism and Modeling of Intergranular Stress Corrosion Cracking of Nickel-Chromium-Iron Alloys Exposed to High Purity Water,” *Twelfth International Conference on Environmental Degradation of Materials in Nuclear Reactor Systems—Water Reactors*, 2005.
40. C. Marks, G. White, and R. Jones, “Further Statistical Evaluations of MRP-55 Database of Alloy 600 PWSCC Laboratory Crack Growth Rate Data,” Presented to the *EPRI PWSCC Expert Panel Meeting*, San Diego, CA, April 27-28, 2006.
41. E.D. Eason and R. Pathania, “A Preliminary Hybrid Model of Alloy 600 Stress Corrosion Crack Propagation in PWR Primary Water Environments,” *Thirteenth International Conference on Environmental Degradation of Materials in Nuclear Reactor Systems—Water Reactors*, Whistler, British Columbia, Canada, 2007.
42. *Assessment of the Effect of Elevated Reactor Coolant Hydrogen on the Performance of PWR Zr-Based Alloys*, EPRI, Palo Alto, CA: 2006. 1013522.

## References

43. E. Hillner, *Hydrogen Absorption in Zircaloy during Aqueous Corrosion, Effect of Environment*, WAPD-TM-411 (November 1964). As cited in [42].
44. V.F. Urbanic, "Observations of Accelerated Hydriding in Zirconium Alloys," *Zirconium in the Nuclear Industry: Sixth International Symposium Sponsored by ASTM Committee B-10 on Reactive and Refractory Metals*, Vancouver, B.C., Canada, June 28 – July 1, 1982.
45. J.C. Clayton, "Out-of-Pile Nickel Alloy-Induced Accelerated Hydriding of Zircaloy Fasteners," *Zirconium in the Nuclear Industry: Sixth International Symposium Sponsored by ASTM Committee B-10 on Reactive and Refractory Metals*, Vancouver, B.C., Canada, June 28 – July 1, 1982.
46. W.E. Allmon, "Dissolved Hydrogen Issues (Actions 4 and 5)," *Presentation to the EPRI PWR Primary Water Chemistry Guidelines Revision Committee*, February 2007.
47. H. Hertweck, *Summary of the Investigations at Siemens and Modifications for Future Fabrication of Guide Tubes for RH-2, Revision A*, Siemens Work Report, 1990. Siemens B211-90-398A.
48. H. Pettersson, B. Bengtson, T. Andersson, H.-J. Sell, P.-B., Hoffmann, and F. Garzarolli, "Investigation of Increased Hydriding of Guide Tubes in Ringhals 2 during Cycle Startup," Paper 1082, *Proceedings of the 2007 International LWR Fuel Performance Meeting*, San Francisco, CA, September 30 – October 3, 2007.
49. *Impact of PWR Primary Chemistry on Corrosion Product Deposition on Fuel Cladding Surfaces*, EPRI, Palo Alto, CA: 1997. TR-108783.
50. P. Cohen, *Water Coolant Technology of Power Reactors*, American Nuclear Society, La Grange Park, IL, 1980.
51. H.R. Copson and W.E. Berry, "Qualification of Inconel for Nuclear Power Plant Applications," *Corrosion* 16:2, 123, 1960.
52. T. Sakai, S. Okabayashi, K. Aoki, K. Matsumoto, F. Nakayasu, and Y. Kishi, "A Study of the Oxide Thin Film on Alloy 600 in High Temperature Water," *Proceedings of the Fourth International Symposium on Environmental Degradation of Materials in Nuclear Power Systems—Water Reactor*, Jekyll Island, GA, August 6-10, 1989.
53. F. Cattant, "Relative Release Rate Differences, Inconel 690TT, Effects of Temperature and Hydrogen," *EDF-EPRI Data Exchange*, 2007.
54. T. Terachi, N. Totsuka, T. Yamada, T. Nakagawa, H. Deguchi, M. Horiuchi, and M. Oshitani, "Influence of Dissolved Hydrogen on Structure of Oxide Film on Alloy 600 Formed in Primary Water of Pressurized Water Reactors," *Journal of Nuclear Science and Technology* 40:7, 509, 2003.
55. D. Hussey, "Effects of Boron on Zeta Potential," *Presentation to the EPRI PWR Primary Water Chemistry Guidelines Revision 6 Committee*, Tucson, AZ, February 6-8, 2007.
56. M. M. Barale, *Etude du Comportement des Particules Colloïdales dans les Conditions Physico-Chimiques du Circuit Primaire des Réacteurs à Eau sous Pression*, Doctoral Thesis, University Paris 6, 2006.
57. A. Sanchez, N. Doncel, G. Rubio, and J.L. Gago, "1<sup>st</sup> Cycle Experience of Zinc Injection in Ascó II and Vandellos II NPP," *EPRI Zinc Workshop*, Washington, DC, August 23, 2007.

58. D.E. Adams and W.A. Clontz, "TVA PWR Zinc Injection Strategy," *EPRI Zinc Workshop*, Washington, DC, August 23, 2007.
59. G. Gary, "Callaway Plant Zinc Experience Update," *EPRI Zinc Workshop*, Washington, DC, August 23, 2007.
60. *Prevention of Flow Restrictions in Generator Stator Water Cooling Circuits*, EPRI, Palo Alto, CA: 2002. 1006684.
61. *Pressurized Water Reactor Primary Water Zinc Application Guidelines*, EPRI, Palo Alto, CA: 2006. 1013420.
62. C.A. Grove and L.D. Petzold, "Mechanisms of Stress-Corrosion Cracking of Alloy X-750 in High-Purity Water," *Conference Proceedings of the International Conference on Corrosion of Nickel-Base Alloys*, Cincinnati, OH, October 23-25, 1984.
63. J. Peng, A. Demma, A. McIlree, and P.J. King, "Effects of Dissolved Hydrogen and Hydrogen Peroxide on the Fracture Resistance of Weld Metals 182, 52, and 152 in Simulated PWR Shutdown Environment," *Thirteenth International Conference on Environmental Degradation of Materials in Nuclear Systems—Water Reactors*, Whistler, BC, Canada, 2007.
64. P. Andresen (GE), e-mail to C. Marks (DEI), October 25, 2007.
65. D.M. Symons, "A Comparison of Internal Hydrogen Embrittlement and Hydrogen Environment Embrittlement of X-750," *Engineering Fracture Mechanics* 68, 751, 2001.
66. M.M. Hall, Jr. and D.M. Symons, "Hydrogen Embrittlement Mechanism for Low Potential Stress Corrosion Cracking of Nickel Base Alloys," *Proceedings: 2000 EPRI Workshop on PWSCC of Alloy 600 in PWRs (PWRRP-27)*, EPRI, Palo Alto, CA: 2000. 1000873.
67. D.M. Symons, "The Effect of Hydrogen on the Fracture Toughness of Alloy X-750 at Elevated Temperatures," *Journal of Nuclear Materials* 265, 225, 1999.
68. W.J. Mills, M.R. Lebo, and J.J. Kearns, "Hydrogen Embrittlement, Grain Boundary Segregation, and Stress Corrosion Cracking of Alloy X-750 in Low- and High-Temperature Water," *Metallurgical and Materials Transactions A* 30A, 1579, 1999.
69. W.J. Mills and C.M. Brown, "Fracture Behavior of Nickel-Based Alloys in Water," *Ninth International Symposium on Environmental Degradation of Materials in Nuclear Power Systems—Water Reactors*, 167, TMS, 1999.
70. Z. Xia, W.-K. Lai, and Z. Szklarska-Smialowska, "Aftereffects Produced in Alloy 600 by Exposure to Lithiated High-Temperature Water," *Corrosion* 47:3, 173, 1991.
71. J. Stubbe and P. Hernalsteen, "Is Corrosion Dependent on the Duration of In-Service Cycle?" *Proceedings of the International Symposium Fontevraud III: Contribution of Materials Investigation to the Resolution of Problems Encountered in Pressurized Water Reactors*, September 12-16, 1994.
72. S. Dickinson, J. Henshaw, A. Tuson, and H.E. Sims, "Radiolysis Effects in Sub-Cooled Nucleate Boiling," *Chimie 2002, Water Chemistry of Nuclear Reactor Systems, April 22-26, 2002*, Avignon, France.
73. A. Mozumder, *Fundamentals of Radiation Chemistry*, Academic Press, New York, NY, 1999.

## References

74. K. Lundgren, H. Wijkström, and G. Wikmark, "Recent Development in the LwrChem Radiolysis Code," *International Conference on Water Chemistry of Nuclear Reactor Systems*, San Francisco, CA, October 11-14, 2004.
75. E. Ibe, A. Watanabe, Y. Wada, and M. Takahashi, "Water Radiolysis Near Metal Surfaces and Relevant Phenomena in Nuclear Reactor Systems," *Water Chemistry of Nuclear Reactor Systems* 6, 73, BNES, 1992.
76. H.E. Sims, "Radiolysis Effects at Shutdown," *Whitepaper prepared to the EPRI PWR Primary Water Chemistry Guidelines Revision 6 Committee*, 2007.
77. C. Brun, A. Long, P. Saurin, M.C. Thiry, and N. Lacoudre, "Radiolysis Studies at Belleville (PWR 1300) Water Chemistry with Low Hydrogen Concentration," *Chemistry in Water Reactors: Operating Experience and New Developments*, 73, Nice France, April 24-27, 1994.
78. D. Hiroishi and K. Ishigure, "Poster 12. Homogeneous and Heterogeneous Decomposition of Hydrogen Peroxide in High-Temperature Water," *Water Chemistry of Nuclear Reactor Systems* 5, BNES, 1989.
79. T. Satoh, S. Uchida, and Y. Satoh, "Water Radiolysis in a Crack Tip Under Gamma Ray Irradiation," *Chimie 2002, Water Chemistry of Nuclear Reactor Systems, April 22-26, 2002*, Avignon, France.
80. *Evaluations for PWR Hydrogen Management Assessment*, BWC, Draft, June 6, 2007.
81. E.J. Grove and R.J. Travis, *Effect of Aging on the PWR Chemical and Volume Control System*, NRC, Washington, DC, 1995. NUREG/CR-5954. BNL-NUREG-52410.
82. A.L. Camp, J.C. Cummings, M.P. Sherman, C.F. Kupiec, R.J. Healy, J.S. Caplan, J.R. Sandhop, and J.H. Saunders, *Light Water Reactor Hydrogen Manual*, Sandia National Laboratories, Albuquerque, NM, 1983. NUREG/CR-2726 R3. SAND82-1137 R3.
83. A.L. Berlad, M. Sibulkin, and C.H. Yang, *Hydrogen Combustion Characteristics Related to Reactor Accidents*, Brookhaven National Laboratory, Upton, NY, 1983. NUREG/CR-2475. BNL-NUREG-51492.
84. P.D. Randolph, L. Isaacson, A.L. Ayers, F.Y. Tsang, and C.M. McCullagh, *Control of Explosive Mixtures in PWR Waste Gas Systems*, EG&G Idaho, Inc., Idaho Falls, ID, 1985. NUREG/CR-3237. EGG-2251.
85. P. Andresen (GE), email to C. Libby (EPRI), June 12, 2007.
86. E. Herms, O. Raquet, F. Vaillant, and T. Couvant, "SCC of Cold-Worked Austenitic Stainless Steels in PWR Conditions," *Workshop on Cold Work in Iron- and Nickel-Based Alloys*, Toronto ON, June 3-8, 2007.
87. *RCPI, RCP Seal Package*, Rev. 2., ComEd Company, November 20, 1997. (For training purposes only.).
88. N. Vitale (Westinghouse), email to C. Marks (DEI), September 18, 2007.
89. H. Ichige, "Study on Optimization of Concentration Band for Dissolved Hydrogen in PWR Coolant," *6<sup>th</sup> International Workshop on LWR Coolant Radiolysis and Electrochemistry*, Jeju Island, Korea, October 27, 2006. Acited in Reference [80].
90. D.E. Adams, "Estimation of RCS Helium Production Rate," via email from D. Adams (TVA) to C. Marks (DEI), September 19, 2007.

91. F. Cattant (EDF), e-mail to C. Libby (EPRI), October 8, 2007.
92. *Problem Investigation Process Catawba Nuclear Station*, C-98-03142, Duke Energy, 1998.
93. EPRI FRP Fuel Reliability Database (FRED).
94. *Corrosion-Product Buildup on LWR Fuel Rods*, EPRI, Palo Alto, CA: 1985. NP-3789.
95. *Change Request No. 9*, Saxton Nuclear Experimental Corporation, Docket No. 50.146, License DPR-4, October 1963.
96. J.C. Clayton, D.A. Gorscak, K.D. Richardson, and W.R. Campbell, "End-of-Life Corrosion and Hydriding Performance of Zircaloy Components in the Shippingport Light Water Breeder Reactor," *Proceedings of the Fourth International Symposium on Environmental Degradation of Materials in Nuclear Power Systems—Water Reactor*, Jekyll Island, GA, August 6-10, 1989.
97. W.T. Lindsay, *MULTEQ Database Committee Review of Nickel/Nickel Oxide/Nickel Ferrites*, Boston, MA, September 25-26, 2007.
98. S.E. Ziemniak, P.A. Guilmette, R.A. Turcotte, and H.M. Tunison, *Oxidative Dissolution of Nickel Metal in Hydrogenated Hydrothermal Solutions*, Lockheed Martin Corporation, Schenectady, NY, 2007. LM-07K020.
99. *Evaluation of Fuel Clad Corrosion Product Deposits and Circulating Corrosion Products in Pressurized Water Reactors*, EPRI, Palo Alto, CA: 2004. 1009951.
100. P.R. Tremaine and J.C. LeBlanc, "The Solubility of Nickel Oxide and Hydrolysis of  $\text{Ni}^{2+}$  in water to 573 K," *J. Chem. Thermodynamics* 12, 521, 1980.
101. I. Lambert and J. Lecomte, P. Beslu, and F. Joyer, "Corrosion Product Solubility in the PWR Primary Coolant," *Water Chemistry for Nuclear Reactor Systems 4*, BNES, 1986.



# A

## TABULATED FACTORS OF IMPROVEMENT

The purpose of this appendix is to provide tabular values of the calculated factors of improvement (FOI) for changes in hydrogen concentration. The methodology of Section 4.4 is used along with the parameter values given in Table 4-1.

Each table gives a numerical factor of improvement for changes from a current hydrogen concentration (listed in the top header) to a new hydrogen concentration (listed in the left-most column). In each block, three improvement factors are listed. These are the temperature specific FOI, for 290°C, 325°C, and 343°C from top to bottom. The following illustration demonstrates the use of the tables for a change from 35 cc/kg to 70 cc/kg:

		Current Hydrogen Concentration (cc/kg)					
		25	30	35	40	45	50
New Hydrogen Concentration (cc/kg)							
	70			1.14 2.22 2.74	FOI @ 290°C FOI @ 325°C FOI @ 343°C		

Figure A-1  
Use of FOI Tables

*Tabulated Factors of Improvement*

Entries in the tables below are colored red if the FOI is less than unity. As discussed in Section 4.4, the FOI is the ratio of the old crack growth rate to the new crack growth rate and higher values are more advantageous. Values less than unity represent faster crack growth rates at the new condition.

No attempt has been made to determine the appropriate resolution (number of significant figures) for these values. Two decimal places are retained to facilitate qualitative comparison (i.e., identification of trends).

With respect to Table A-7 and Table A-8 for Alloy X-750 AH, it should be noted that the offset (i.e., the distance of the peak crack growth rate from the nickel metal nickel oxide transition) may be significantly different from zero (see Figure 4-9). However, these tables were generated assuming a zero offset.

**Table A-1**  
**Factors of Improvement for EN82H (Part 1)**

		Current Hydrogen Concentration (cc/kg)					
		25	30	35	40	45	50
New Hydrogen Concentration (cc/kg)	5	0.18	0.16	0.14	0.14	0.13	0.13
		0.84	0.65	0.52	0.42	0.36	0.31
		2.66	2.26	1.89	1.59	1.34	1.14
	10	0.31	0.26	0.24	0.23	0.22	0.22
		0.54	0.41	0.33	0.27	0.23	0.20
		1.07	0.91	0.76	0.64	0.54	0.46
	15	0.53	0.45	0.41	0.39	0.38	0.37
		0.60	0.46	0.37	0.30	0.26	0.23
		0.86	0.73	0.61	0.51	0.43	0.37
	20	0.78	0.67	0.61	0.58	0.56	0.55
		0.76	0.59	0.47	0.39	0.33	0.29
		0.88	0.75	0.63	0.53	0.44	0.38
	25	1.00	0.86	0.79	0.75	0.72	0.71
		1.00	0.77	0.62	0.51	0.43	0.38
		1.00	0.85	0.71	0.60	0.50	0.43
	30	1.16	1.00	0.91	0.87	0.84	0.83
		1.29	1.00	0.80	0.65	0.55	0.49
		1.18	1.00	0.84	0.70	0.59	0.50
	35	1.27	1.09	1.00	0.95	0.92	0.90
		1.62	1.26	1.00	0.82	0.70	0.61
		1.41	1.19	1.00	0.84	0.71	0.60
	40	1.34	1.15	1.05	1.00	0.97	0.95
		1.98	1.53	1.22	1.00	0.85	0.74
		1.68	1.43	1.19	1.00	0.84	0.72

## Tabulated Factors of Improvement

**Table A-2**  
**Factors of Improvement for EN82H (Part 2)**

		Current Hydrogen Concentration (cc/kg)					
		25	30	35	40	45	50
New Hydrogen Concentration (cc/kg)	45	1.38	1.19	1.09	1.03	1.00	0.98
		2.33	1.80	1.43	1.18	1.00	0.88
		1.99	1.69	1.42	1.19	1.00	0.85
	50	1.41	1.21	1.11	1.05	1.02	1.00
		2.66	2.06	1.64	1.35	1.14	1.00
		2.34	1.99	1.66	1.39	1.17	1.00
	55	1.42	1.22	1.12	1.06	1.03	1.01
		2.96	2.29	1.82	1.50	1.27	1.11
		2.71	2.30	1.93	1.61	1.36	1.16
	60	1.44	1.23	1.13	1.07	1.04	1.02
		3.22	2.49	1.98	1.63	1.38	1.21
		3.09	2.63	2.20	1.84	1.55	1.32
	65	1.44	1.24	1.13	1.08	1.04	1.02
		3.44	2.66	2.11	1.74	1.47	1.29
		3.47	2.95	2.47	2.07	1.74	1.49
	70	1.45	1.24	1.14	1.08	1.05	1.03
		3.61	2.80	2.22	1.83	1.55	1.36
		3.85	3.27	2.74	2.29	1.93	1.65
	75	1.45	1.25	1.14	1.08	1.05	1.03
		3.76	2.91	2.31	1.90	1.61	1.41
		4.21	3.58	3.00	2.51	2.11	1.80
	80	1.45	1.25	1.14	1.08	1.05	1.03
		3.87	3.00	2.38	1.96	1.66	1.45
		4.54	3.86	3.23	2.71	2.28	1.94

**Table A-3**  
**Factors of Improvement for Alloy 600 (Part 1)**

		Current Hydrogen Concentration (cc/kg)					
		25	30	35	40	45	50
New Hydrogen Concentration (cc/kg)	5	0.54	0.50	0.47	0.44	0.43	0.41
		0.94	0.86	0.80	0.74	0.70	0.66
		1.40	1.32	1.24	1.17	1.11	1.05
	10	0.64	0.59	0.55	0.53	0.51	0.49
		0.81	0.74	0.69	0.64	0.60	0.57
		1.02	0.97	0.91	0.86	0.81	0.77
	15	0.77	0.71	0.67	0.63	0.61	0.59
		0.84	0.77	0.71	0.66	0.62	0.59
		0.95	0.90	0.85	0.80	0.75	0.71
	20	0.89	0.82	0.77	0.73	0.71	0.68
		0.91	0.84	0.77	0.72	0.68	0.64
		0.96	0.91	0.86	0.81	0.76	0.72
	25	1.00	0.92	0.86	0.82	0.79	0.77
		1.00	0.92	0.85	0.79	0.74	0.70
		1.00	0.95	0.89	0.84	0.79	0.75
	30	1.09	1.00	0.94	0.89	0.86	0.83
		1.09	1.00	0.92	0.86	0.81	0.76
		1.06	1.00	0.94	0.89	0.84	0.79
	35	1.16	1.07	1.00	0.95	0.92	0.89
		1.18	1.08	1.00	0.93	0.87	0.83
		1.12	1.06	1.00	0.94	0.89	0.84
	40	1.22	1.12	1.05	1.00	0.96	0.93
		1.27	1.16	1.07	1.00	0.94	0.89
		1.19	1.13	1.06	1.00	0.94	0.89

## Tabulated Factors of Improvement

**Table A-4**  
**Factors of Improvement for Alloy 600 (Part 2)**

		Current Hydrogen Concentration (cc/kg)					
		25	30	35	40	45	50
New Hydrogen Concentration (cc/kg)	45	1.27	1.16	1.09	1.04	1.00	0.97
		1.35	1.24	1.15	1.07	1.00	0.95
		1.26	1.19	1.13	1.06	1.00	0.95
	50	1.31	1.20	1.13	1.07	1.03	1.00
		1.43	1.31	1.21	1.13	1.06	1.00
		1.33	1.26	1.19	1.12	1.06	1.00
	55	1.34	1.23	1.15	1.10	1.06	1.02
		1.50	1.38	1.27	1.19	1.11	1.05
		1.40	1.33	1.25	1.18	1.11	1.05
	60	1.36	1.25	1.18	1.12	1.08	1.04
		1.57	1.44	1.33	1.24	1.16	1.10
		1.47	1.39	1.31	1.24	1.17	1.11
	65	1.39	1.27	1.19	1.14	1.09	1.06
		1.63	1.50	1.38	1.29	1.21	1.14
		1.54	1.46	1.37	1.29	1.22	1.16
	70	1.40	1.29	1.21	1.15	1.11	1.07
		1.69	1.55	1.43	1.33	1.25	1.18
		1.61	1.52	1.43	1.35	1.27	1.20
	75	1.42	1.30	1.22	1.16	1.12	1.09
		1.74	1.60	1.47	1.37	1.29	1.22
		1.67	1.58	1.49	1.40	1.32	1.25
	80	1.43	1.31	1.23	1.17	1.13	1.09
		1.79	1.64	1.51	1.41	1.32	1.25
		1.73	1.64	1.54	1.45	1.37	1.30

**Table A-5**  
**Factors of Improvement for Alloy X-750 HTH (Part 1)**

		Current Hydrogen Concentration (cc/kg)					
		25	30	35	40	45	50
New Hydrogen Concentration (cc/kg)	5	0.25	0.23	0.22	0.21	0.21	0.21
		0.85	0.68	0.56	0.49	0.43	0.40
		2.40	2.05	1.73	1.47	1.27	1.11
	10	0.41	0.38	0.36	0.35	0.35	0.35
		0.55	0.44	0.36	0.31	0.28	0.26
		1.07	0.91	0.77	0.66	0.56	0.49
	15	0.65	0.60	0.57	0.56	0.56	0.55
		0.61	0.49	0.41	0.35	0.31	0.29
		0.86	0.74	0.62	0.53	0.45	0.40
	20	0.86	0.79	0.76	0.75	0.74	0.73
		0.78	0.62	0.52	0.45	0.40	0.37
		0.88	0.75	0.64	0.54	0.47	0.41
	25	1.00	0.92	0.89	0.87	0.86	0.85
		1.00	0.80	0.66	0.57	0.51	0.47
		1.00	0.85	0.72	0.61	0.53	0.46
	30	1.08	1.00	0.96	0.94	0.93	0.92
		1.25	1.00	0.83	0.72	0.64	0.59
		1.17	1.00	0.85	0.72	0.62	0.54
	35	1.13	1.04	1.00	0.98	0.97	0.96
		1.51	1.20	1.00	0.86	0.77	0.71
		1.39	1.18	1.00	0.85	0.73	0.64
	40	1.15	1.06	1.02	1.00	0.99	0.98
		1.75	1.39	1.16	1.00	0.89	0.82
		1.63	1.39	1.18	1.00	0.86	0.75

## Tabulated Factors of Improvement

**Table A-6**  
**Factors of Improvement for Alloy X-750 HTH (Part 2)**

		Current Hydrogen Concentration (cc/kg)					
		25	30	35	40	45	50
New Hydrogen Concentration (cc/kg)	45	1.16	1.08	1.03	1.01	1.00	0.99
		1.95	1.56	1.30	1.12	1.00	0.92
		1.90	1.62	1.37	1.16	1.00	0.88
	50	1.17	1.08	1.04	1.02	1.01	1.00
		2.12	1.70	1.41	1.22	1.09	1.00
		2.17	1.85	1.56	1.33	1.14	1.00
	55	1.18	1.09	1.05	1.02	1.01	1.00
		2.26	1.80	1.50	1.29	1.16	1.06
		2.43	2.07	1.75	1.49	1.28	1.12
	60	1.18	1.09	1.05	1.03	1.01	1.01
		2.36	1.89	1.57	1.35	1.21	1.11
		2.68	2.29	1.93	1.64	1.41	1.24
	65	1.18	1.09	1.05	1.03	1.01	1.01
		2.44	1.95	1.62	1.40	1.25	1.15
		2.91	2.48	2.10	1.78	1.54	1.34
	70	1.18	1.09	1.05	1.03	1.02	1.01
		2.50	1.99	1.66	1.43	1.28	1.18
		3.12	2.66	2.25	1.91	1.64	1.44
	75	1.18	1.09	1.05	1.03	1.02	1.01
		2.54	2.03	1.69	1.45	1.30	1.20
		3.29	2.81	2.37	2.02	1.74	1.52
	80	1.18	1.09	1.05	1.03	1.02	1.01
		2.57	2.06	1.71	1.47	1.32	1.21
		3.44	2.94	2.48	2.11	1.82	1.59

**Table A-7**  
**Factors of Improvement for Alloy X-750 AH (Part 1)**

		Current Hydrogen Concentration (cc/kg)					
		25	30	35	40	45	50
New Hydrogen Concentration (cc/kg)	5	0.56	0.50	0.45	0.41	0.38	0.36
		0.95	0.88	0.82	0.76	0.71	0.67
		1.33	1.27	1.21	1.15	1.10	1.04
	10	0.65	0.58	0.52	0.48	0.44	0.41
		0.85	0.78	0.73	0.68	0.64	0.60
		1.02	0.98	0.93	0.88	0.84	0.80
	15	0.76	0.68	0.61	0.56	0.52	0.48
		0.87	0.81	0.75	0.70	0.65	0.61
		0.96	0.92	0.88	0.84	0.79	0.76
	20	0.88	0.78	0.71	0.65	0.60	0.56
		0.93	0.86	0.80	0.75	0.70	0.65
		0.97	0.93	0.88	0.84	0.80	0.76
	25	1.00	0.89	0.81	0.74	0.68	0.63
		1.00	0.93	0.86	0.80	0.75	0.70
		1.00	0.96	0.91	0.87	0.83	0.79
	30	1.12	1.00	0.90	0.83	0.76	0.71
		1.08	1.00	0.93	0.87	0.81	0.76
		1.04	1.00	0.95	0.91	0.86	0.82
	35	1.24	1.11	1.00	0.91	0.84	0.78
		1.16	1.08	1.00	0.93	0.87	0.82
		1.10	1.05	1.00	0.95	0.90	0.86
	40	1.36	1.21	1.09	1.00	0.92	0.86
		1.25	1.16	1.07	1.00	0.94	0.88
		1.15	1.10	1.05	1.00	0.95	0.90

## Tabulated Factors of Improvement

**Table A-8**  
**Factors of Improvement for Alloy X-750 AH (Part 2)**

		Current Hydrogen Concentration (cc/kg)					
		25	30	35	40	45	50
New Hydrogen Concentration (cc/kg)	45	1.47	1.31	1.19	1.08	1.00	0.93
		1.33	1.24	1.15	1.07	1.00	0.94
		1.21	1.16	1.11	1.05	1.00	0.95
	50	1.58	1.41	1.27	1.16	1.07	1.00
		1.42	1.32	1.22	1.14	1.07	1.00
		1.27	1.22	1.16	1.11	1.05	1.00
	55	1.69	1.50	1.36	1.24	1.15	1.07
		1.51	1.40	1.30	1.21	1.13	1.06
		1.34	1.28	1.22	1.16	1.10	1.05
	60	1.79	1.60	1.44	1.32	1.22	1.13
		1.60	1.48	1.38	1.28	1.20	1.12
		1.40	1.34	1.28	1.22	1.16	1.10
	65	1.89	1.68	1.52	1.39	1.28	1.19
		1.68	1.56	1.45	1.35	1.26	1.19
		1.47	1.41	1.34	1.28	1.21	1.15
	70	1.98	1.77	1.60	1.46	1.35	1.25
		1.77	1.64	1.53	1.42	1.33	1.25
		1.54	1.47	1.40	1.33	1.27	1.21
	75	2.07	1.85	1.67	1.53	1.41	1.31
		1.86	1.73	1.60	1.49	1.40	1.31
		1.60	1.54	1.46	1.39	1.32	1.26
	80	2.16	1.92	1.74	1.59	1.47	1.36
		1.95	1.81	1.68	1.56	1.46	1.37
		1.67	1.60	1.53	1.45	1.38	1.31



## **Export Control Restrictions**

Access to and use of EPRI Intellectual Property is granted with the specific understanding and requirement that responsibility for ensuring full compliance with all applicable U.S. and foreign export laws and regulations is being undertaken by you and your company. This includes an obligation to ensure that any individual receiving access hereunder who is not a U.S. citizen or permanent U.S. resident is permitted access under applicable U.S. and foreign export laws and regulations. In the event you are uncertain whether you or your company may lawfully obtain access to this EPRI Intellectual Property, you acknowledge that it is your obligation to consult with your company's legal counsel to determine whether this access is lawful. Although EPRI may make available on a case-by-case basis an informal assessment of the applicable U.S. export classification for specific EPRI Intellectual Property, you and your company acknowledge that this assessment is solely for informational purposes and not for reliance purposes. You and your company acknowledge that it is still the obligation of you and your company to make your own assessment of the applicable U.S. export classification and ensure compliance accordingly. You and your company understand and acknowledge your obligations to make a prompt report to EPRI and the appropriate authorities regarding any access to or use of EPRI Intellectual Property hereunder that may be in violation of applicable U.S. or foreign export laws or regulations.


**The Electric Power Research Institute (EPRI)**, with major locations in Palo Alto, California; Charlotte, North Carolina; and Knoxville, Tennessee, was established in 1973 as an independent, nonprofit center for public interest energy and environmental research. EPRI brings together members, participants, the Institute's scientists and engineers, and other leading experts to work collaboratively on solutions to the challenges of electric power. These solutions span nearly every area of electricity generation, delivery, and use, including health, safety, and environment. EPRI's members represent over 90% of the electricity generated in the United States. International participation represents nearly 15% of EPRI's total research, development, and demonstration program.

Together...Shaping the Future of Electricity

## **Program:**

Nuclear Power

© 2007 Electric Power Research Institute (EPRI), Inc. All rights reserved. Electric Power Research Institute, EPRI, and TOGETHER...SHAPING THE FUTURE OF ELECTRICITY are registered service marks of the Electric Power Research Institute, Inc.

 Printed on recycled paper in the United States of America

1015017

## **Electric Power Research Institute**

3420 Hillview Avenue, Palo Alto, California 94304-1338 • PO Box 10412, Palo Alto, California 94303-0813 USA  
800.313.3774 • 650.855.2121 • [askepri@epri.com](mailto:askepri@epri.com) • [www.epri.com](http://www.epri.com)